Little Ice Age Climate in the Western Tropical Atlantic Inferred from Coral Geochemical Proxies

by

Alice Elizabeth Alpert

Sc.B., Brown University, 2009

Submitted in partial fulfillment of the requirements for the degree of

Doctor of Philosophy

at the

MASSACHUSETTS INSTITUTE OF TECHNOLOGY

and the

WOODS HOLE OCEANOGRAPHIC INSTITUTION

September, 2016

Author Signature redacted

Joint Program in Oceanography/Applied Ocean Science and Engineering

Massachusetts Institute of Technology and Woods Hole Oceanographic Institution

July 22, 2016

Certified by Signature redacted

Anne L. Cohen

Associate Scientist, Department of Geology and Geophysics, WHOI

Thesis Co-Supervisor

Certified by Signature redacted

Glenn A. Gaetani

Associate Scientist, Department of Geology and Geophysics, WHOI

Thesis Co-Supervisor

Certified by Signature redacted

Delia W. Oppo

Senior Scientist, Department of Geology and Geophysics, WHOI

Thesis Co-Supervisor

Accepted by Signature redacted

Timothy L. Gove

Professor of Earth, Atmospheric, and Planetary Sciences, MIT

Chairman, Joint Committee for Marine Geology and Geophysics

Little Ice Age Climate in the Western Tropical Atlantic inferred from coral geochemical proxies

by

Alice Elizabeth Alpert

Abstract

Paleoclimate archives place the short instrumental record of climate variability in a longer temporal context and allow better understanding of the rate, nature and extent by which anthropogenic warming will impact natural and human systems. The ocean is a key component of the climate system and records of past ocean variability are thus essential for characterizing natural variability and quantifying climate sensitivity to radiative forcing. Coral skeletons are high-resolution archives of tropical sea surface temperatures (SSTs), but inconsistencies call the accuracy of existing coral proxy records into question.

In this thesis, I first quantify the errors associated with the traditional coral thermometer, Sr/Ca, by comparing *in situ* logged SST with Sr/Ca-derived SST in four corals on the same reef. I show that intercolony disparities in mean Sr/Ca, amplitude of variability, and trend are not due to differences in water temperature, but rather to "vital effects" that result in a ± 2° C uncertainty on reconstructed SST.

I then expand, refine, and test a new paleothermometer, Sr-U, across multiple coral species and through time. I show that Sr-U captures spatial SST variability with an uncertainty of ± 0.6° C. When applied to two corals outside of the calibration, Sr-U accurately captures the mean SST and the 20th century trend in the Western Tropical Atlantic.

Finally, I apply Sr-U to a coral from the Little Ice Age (LIA) to address uncertainties in the magnitude of western tropical Atlantic cooling during a 95-year period spanning 1465-1560. Results suggest the region was 1.1° C±0.6°C cooler than the 1958-1988 mean, but within error of early 20th century SST at this site. Critically, several periods of warmth, equivalent to the 1958-1988 mean, occurred during a solar minimum that is widely believed to have been a cool period of the LIA. My results indicate that Sr/Ca exaggerates the actual cooling by almost 3 °C. My record demonstrates the value of Sr-U and highlights the need for continuous accurate SST records to better constrain the amplitude, drivers, and mechanisms of LIA tropical climate change.

Thesis Co-Supervisor: Dr. Anne L. Cohen
Title: Associate Scientist, Department of Geology and Geophysics, WHOI
Thesis Co-Supervisor: Dr. Glenn A. Gaetani
Title: Associate Scientist, Department of Geology and Geophysics, WHOI
Thesis Co-Supervisor: Dr. Delia W. Oppo
Title: Senior Scientist, Department of Geology and Geophysics, WHOI

Acknowledgements

Science is a team effort, especially when samples are collected in the field. My PhD could not have happened without the generosity of time and expertise of countless people and many funding sources.

First and foremost I would like to thank my thesis co-supervisors Anne Cohen, Glenn Gaetani, and Delia Oppo. I accepted their invitation to the world of corals, and it was a magical ride. While helping me producing excellent science, they never missed a moment to teach me and rarely told me the answer to anything that I could have figured out myself. Beyond the late nights of correspondence, back and forth plots, and careful editing, I thank them for their restraint in letting me make and learn from my own mistakes. My committee members David McGee and Caroline Ummenhofer provided steady guidance and feedback on my thesis as it slowly and then quickly progressed. I thank them for thoughtful questions and suggestions.

A substantial monetary investment is required to produce a single PhD, and I would like to acknowledge the National Science Foundation's Graduate Research Fellowship Program for funding three years of my education. NSF grants OCE-0926986 to Anne Cohen and Delia Oppo, OCE-1031971to Anne Cohen, OCE-1338320 to Glenn Gaetani and Anne Cohen supported portions of my research, fieldwork, and stipend. WHOI's Ocean Exploration Institute funded the last year of my stipend. WHOI's Access to the Sea Program and the Bermuda Biological Station for Research Fund funded fieldwork. WHOI's Ocean Ventures Fund provided me the experience of writing a scientific proposal and funds for sample analysis. Presenting my research at conferences and interacting with other scientists resulted in rapid strides in my scientific development, and I am grateful to research grants as well as travel grants from WHOI's Academic Programs Office and the MIT Graduate Student Council for funding my conference travel expenses.

I am lucky to have been a member of the Cohen lab. Our science requires teamwork in assisting with others' fieldwork and with sharing technical experience back in the lab. My lab mates have been a consistent source of discussion and assistance, and always made me feel part of an intellectual community. Thank you Hannah Barkley, Tom DeCarlo, Liz Drenkard, Pat Lohmann, Nathan Mollica, Kathryn Pietro, and Hanny Rivera.

My coauthors and collaborators were a source of fresh ideas and crucial data, often unavailable anywhere else. I would like to thank Rusty Brainard, Jamie Gove, and Chip Young of NOAA's Coral Reef Ecosystem Program, Amos Winter and Edwin Hernandez-Delgado of the University of Puerto Rico, Meagan

Gonneea of USGS, and Mark Vermeij of CARMABI. The geochemical data collected for this thesis owes its existence in part to spectacular technicians including Scot Birdwhistel, Jurek Bluszstajn, Louis Kerr, and Gretchen Swarr. Thank you for your flexibility and tireless commitment to excellence.

Many WHOI scientists and postdocs spent valuable time to teach and guide me along the twisting PhD path. Thank you Jenny Arbuzweski, Jake Gebbie, Karl Helfrich, Denner Huang, Kris Karnauskas, and Andy Solow, among others. I heartily thank Ed O'Brien of the WHOI scientific diving program for introducing me to the wonderland under the waves and ensuring my safety in the field. Much of my fieldwork took place aboard Sea Dragon operated by Pangaea Explorations, and I have Emily Penn and Ron Ritter, as well as Captains Dale Selvam and Eric Loss, and many hard working crew members to thank for providing unparalleled access to the field, all under the thrill of sail power.

WHOI's Academic Programs Office and the EAPS Education Office have been incredibly supportive in every way. I must be content that I cannot know all the hard work they do to make Joint Program students' lives charmed. Thank you so very much Roberta Allard, Linda Cannata, Valerie Caron, Lea Fraser, Tricia Gebbie, Michelle McCafferty, Vicki McKenna, Libby Pike of G&G, Ronni Schwartz, Meg Tivey, Julia Westwater, and Jim Yoder, among others.

Lastly I cannot thank my family and friends enough for their love and acceptance of me as I did a very hard thing. Although you always provided solace and encouragement during tough times, the laughs and adventures we've had together were always the best support. My fiancé Edgar, love of my life, I cannot wait to begin our new life together. We have been through so much and it was all worth it, my marshmallow. My parents David and Elizabeth have selflessly encouraged me to spread my wings and fly far away from my native California. My sister Emily brings the sun with her and comforts me with the knowledge that there is another person in the world who looks just like me. My uncle Tom has been an inspiration to use technical expertise to make the world a better place.

My friends in the Joint Program are the best I have ever made. You helped me flourish and taught me invaluable lessons about patience, love, and time. I found my tribe, and I can only imagine all the wonderful memories we have yet to make together.

Contents

Chapter 1

Introduction

1.1 Climate change

Mean global temperature in 2015 was the warmest since modern instrumental records began in 1880 [*Tollefson*, 2016], and the first few months of 2016 indicate that it will be still warmer. This year follows a trend of globally averaged surface air temperature (SAT) warming by an estimated 0.85 °C since 1880 [*Hartmann et al.*, 2013] (Figure 1-1). Observations show that the global ocean has taken up more than 90% of additional energy accumulated in the earth system between 1971 and 2010 [*Rhein et al.*, 2013]. Warming since 1950 can only be explained by including the effects of increased atmospheric energy flux, or radiative forcing, due to increased atmospheric carbon dioxide (CO_2) from anthropogenic fossil fuel burning, cement production, and land use changes [*Bindoff et al.*, 2013].

Anthropogenic emissions continue to rise, and further warming of the earth's surface has the potential to change precipitation patterns and increase sea level, affecting billions of people throughout the world. In order to accurately estimate the amount of future warming due to human activity, we must understand the relationship between climate forcing and the response of global temperature, or "climate sensitivity" [*Collins et al.*, 2013]. A climate forcing is a process that changes Earth's energy balance. For example the intensity of incoming solar radiation, Total Solar Irradiance (TSI), fluctuates naturally with higher TSI associated with more energy reaching the earth's surface, leading to warming [*Myhre et al.*, 2013]. Sulfate aerosols injected into the atmosphere by volcanic eruptions scatter incoming radiation, generally resulting in surface temperature cooling [*Robock*, 2000]. CO_2 and other greenhouse gases (GHGs) trap outgoing longwave radiation and reemit it. When GHG concentrations change due to natural or anthropogenic causes, the earth's surface temperature shifts to remain in energy balance (i.e. Boltzman's law of blackbody radiation). A common method to estimate climate sensitivity is to run simulations using global climate models (GCMs) over the 20^{th} century and into the future. By these methods estimates of the response to a doubling of atmospheric CO_2, range from 1.5 to 4.5 $^{\circ}$C globally averaged warming [*Collins et al.*, 2013]. The large degree of uncertainty is due to the limitations of GCMs in capturing the dynamics of the climate system and the short duration of reliable instrumental temperatures [*Kiehl*, 2007; *Deser et al.*, 2010a].

In addition to broad responses to external forcings, global and regional temperature is characterized by changes on interannual to multidecadal scales. Much of this variability can be described by climate modes or oscillations. For example El Nino Southern Oscillation (ENSO) is an interannual oscillatory phenomenon in the Pacific Ocean leading to a distinctive pattern of SST anomalies [*Rasmusson and Carpenter*, 1982] with major impacts on global precipitation patterns and fisheries [*Trenberth et al.*, 1998; *McPhaden et al.*, 2006]. The Atlantic Multidecadal Oscillation (AMO), a pattern of SST anomalies in the North Atlantic varying on multidecadal timescales [*Schlesinger and Ramankutty*, 1994; *Enfield et al.*, 2001], significantly affects climate throughout the Atlantic basin [*Sutton and Hodson*, 2005; *Zhang and Delworth*, 2006]. While there is evidence that these climate modes arise from processes internal to the climate system, their behavior may be influenced by external forcing as well [*Timmermann et al.*, 1999; *Knudsen et al.*, 2014; *Ting et al.*, 2014].

Characterizing and distinguishing the contributions of internal and external, anthropogenic and natural forcings to interannual and multidecadal variability is key for anticipating future climate changes. However it is challenging given the limited length of observational datasets [*Deser et al.*, 2010b; *Johns et al.*, 2011; *Solomon et al.*, 2011].

1.2 Paleoclimatology

Paleoclimate records, natural archives of environmental conditions on timescales longer than the instrumental record, are powerful tools to better understand climate sensitivity and temperature variability. Air bubbles in ice cores, the composition of cave deposits, the width of tree rings, and the chemical, physical, and biological attributes of lake and ocean sediments all preserve information about climate in the past [*Masson-Delmotte et al.*, 2013]. While these quantities are not necessarily meaningful in themselves they are indicators, or "proxies" of past climate. With accurate age control and understanding of the relationship between a proxy and the conditions it reflects, we can reconstruct records of temperature, rainfall, atmospheric composition, sea level, wind speed, ocean currents, volcanic eruptions, and ecosystem type, among others. For example, paleoclimate archives of oxygen isotopes, temperature, and glacial extent have evoked a narrative of great changes associated with glacial-interglacial cycles [*Imbrie et al.*, 1992; *Jouzel et al.*, 2007; *Clark et al.*, 2009]. Records of temperature response to forcing in the past can better constrain climate sensitivity by capturing the impact of feedbacks within the earth system that operate on longer timescales than the instrumental record [*Hegerl et al.*, 2006; *Schmittner et al.*, 2011]. They also have the potential to characterize multidecadal variability and examine its response to external forcings such as TSI and volcanism [*Otterå et al.*, 2010; *Knudsen et al.*, 2011].

Information about ocean temperatures is an essential piece of the paleoclimate puzzle because the global ocean plays a large role in the climate system both in its shaping of and response to global temperature changes. Ocean circulation distributes heat around the globe and has a profound affect on global and regional climate patterns [*Rahmstorf*, 2002]. The slow, integrated response of the ocean to climate forcing also makes it diagnostic of global change in the past [*Rhein et al.*, 2013]. The high heat content, ocean-atmosphere coupling, and potential for large variations make the tropical oceans a particularly important part of the climate system [*Gill and Rasmusson*, 1983; *Newman et al.*, 2003]. Changes in ocean temperature, salinity, and current patterns over many millions of years have been reconstructed using the composition of ocean sediments and the microfossils contained in them. However these techniques rarely provide the temporal resolution needed to investigate questions relating to multidecadal or shorter period variability.

1.3 Coral paleoceanography

The skeletons of long-lived, massive coral colonies have the potential to produce high-resolution records of past tropical ocean temperatures [*Gagan et al.*, 2000; *DeLong et al.*, 2014; *Linsley et al.*, 2015]. The thin layer of living coral tissue continually precipitates an aragonite ($CaCO_3$) skeleton allowing the coral colony to grow upward and preserve its older skeleton below [*Cohen and McConnaughey*, 2003]. Large coral colonies can live for hundreds of years and provide continuous paleoceanographic records at subannual resolution defined by annual density band couplets. Analyses of skeletal extension rate, minor elements, stable isotope ratios, and radioisotopes can reveal information regarding water temperature, salinity, terrestrial runoff, and oceanic upwelling [*Gagan et al.*, 2000].

Geochemical coral proxies take advantage of corals' biologically mediated calcification of their aragonite skeletons from seawater [*Gaetani and Cohen*, 2006; *Gagnon et al.*, 2012]. The coral polyp transports seawater into a calcifying space through vacuoles or paracellular transport [*Cohen and McConnaughey*, 2003] and precipitates aragonite from the calcifying fluid contained in the calcifying space [*Gaetani and Cohen*, 2006; *Sinclair et al.*, 2006; *Gagnon et al.*, 2007]. While aragonite is composed almost entirely of $CaCO_3$, some minor elements (e.g., Sr, Mg, U) are incorporated as well. The model described above identifies two major controls on the abundance of minor elements in coral aragonite: Rayleigh fractionation and temperature. The concentration of a given minor element in the precipitated aragonite will differ from that in the calcifying fluid and can be described over time by the Rayleigh distillation equation [*Rayleigh*, 1896]. Through the distillation process Sr/Ca has an inverse relationship with the degree of Rayleigh fractionation. Rayleigh fractionation appears to vary among coral colonies at a single site and in individuals on subannual scales [*Gaetani et al.*, 2011]. The second control on minor element abundance is the influence of temperature on the rate of incorporation of minor elements into the coral aragonite skeleton [*Gaetani and Cohen*, 2006]. This rate varies from element to element but for Sr/Ca leads to an inverse correlation with temperature.

Temperature has been shown to account for only ~ 25% of Sr/Ca variability measured in corals [*Cohen and Thorrold*, 2007], with the remainder likely related to "vital effects" associated with individual colony differences in the biological mediation of the calcification process. Nonetheless the Sr/Ca paleothermometer has been used to investigate changes in mean SST, variability on interannual scales such as ENSO, and changes in seasonal temperature cycles [*Hetzinger et al.*, 2010; *Kilbourne et al.*, 2010; *Wu et al.*, 2014; *Tierney et al.*, 2015]. However, inter-colony results can be inconsistent and questions remain regarding "vital effects" on the abundance of minor elements in coral skeleton [*Cohen et al.*, 2006; *Cohen and Thorrold*, 2007; *Cohen and Gaetani*, 2010].

DeCarlo et al. [2016] proposed a new coral thermometer, Sr-U that uses both Sr/Ca and U/Ca. Sr-U is conceptually based upon a forward biomineralization model that correctly predicts the concentrations of skeleton Sr/Ca and U/Ca [*DeCarlo et al.,* 2015]. While coral skeleton Sr/Ca is sensitive to both temperature and Rayleigh fractionation, coral skeleton U/Ca is sensitive only to Rayleigh fractionation through changes in calcifying fluid carbonate ion concentration ($[CO_3^{2-}]$). Thus the observed positive correlation between coral skeleton Sr/Ca and U/Ca at a single temperature is produced by Rayleigh fractionation [*DeCarlo et al.* 2016]. Among different corals, different Sr/Ca values corresponding to a single benchmark U/Ca ratio are expected to reflect different temperatures. The "Sr-U" value for an individual coral is defined as the Sr/Ca at a U/Ca benchmark value of 1.1umol/mol according to the regression of a skeleton Sr/Ca on U/Ca for a single coral.

DeCarlo et al. [2016] showed that Sr-U values in a set of 14 modern *Porites spp.* corals from the Pacific Ocean and Red Sea are highly correlated to mean annual water temperature. They derived an expression relating Sr-U to temperature with an uncertainty of 0.5 °C. *DeCarlo et al.* [2016] tested the theoretical basis of Sr-U using the boron isotope ($\delta^{11}B$) proxy for pH in the calcifying fluid. They confirmed that $\delta^{11}B$ and U/Ca in several corals with differing Sr/Ca is consistent with vital effects on Sr/Ca due to calcifying fluid [CO_3^{2-}]. This technique appears to be applicable across coral colonies and may potentially eliminate the need for a coral-specific modern calibration. Uncertainties surrounding Sr/Ca and Sr-U-derived SSTs must be resolved before coral-based SST reconstructions can be interpreted confidently.

1.4 Thesis objectives

In this thesis I use coral geochemical proxies to accurately reconstruct past sea surface temperature (SST). I document trends and variability of tropical SST on timescales ranging from interannual to centennial and evaluate the response of SST to climate forcings. I tackle this in three steps. First, in chapter 2, I examine the most commonly used coral paleothermometer, Sr/Ca [*Smith et al.*, 1979; *Beck et al.*, 1992]. I attempt to reconstruct SST at a site in the central equatorial Pacific, a region that plays a key role in the ENSO phenomenon and in global carbon and heat budgets but whose response to climate change is poorly understood in simulations and observations [*Deser et al.*, 2010a; *Nurhati et al.*, 2011]. However I find inconsistencies in Sr/Ca mean, sensitivity to SST, and trend between individual coral colonies. Using *in situ* temperature data I determine that the inconsistencies cannot be explained by temperature differences and instead attribute them to "vital effects." I characterize the resulting uncertainty of Sr/Ca-derived SST at this site and find that its magnitude prohibits reconstructing ENSO events or the centennial trend of SST. This chapter was published as "Comparison of equatorial Pacific sea surface temperature variability and trends with Sr/Ca records from multiple corals" in 2016 in *Paleoceanography.*

Next, in chapter 3, I expand, refine, and test the calibration of a new coral thermometer, Sr-U, that combines Sr/Ca and U/Ca ratios in coral skeletal aragonite to control for the effects of Rayleigh fractionation on Sr/Ca. I expand an initial spatial calibration of *Porites spp.* corals from the Pacific Ocean calibration [*DeCarlo et al.*, 2016] to include four additional coral genera in the Pacific and Atlantic Oceans and show that Sr-U accurately captures spatial SST variability. I apply the modified SrU-SST calibration to two longer coral cores from Puerto Rico and show that Sr-U replicates well between the two cores and is able to capture the mean SST, trend, and multidecadal variability well over the 20th century. This chapter has been submitted to *Paleoceanography* as "20th century warming of the tropical Atlantic captured by Sr-U paleothermometry."

Lastly in chapter 4, I apply the Sr-U to SST calibration from chapter 3 to reconstruct SST at Puerto Rico during a cool period known as the Little Ice Age (LIA, ~1400-1850CE). The LIA is the most recent episode of centennial scale climate change [*Masson-Delmotte et al.*, 2013]. As the climate forcings volcanism and TSI are reasonably well known, the LIA is an excellent time period to examine the response of tropical SSTs to these known forcings [*Jones and Mann*, 2004; *Schleussner and Feulner*, 2013; *McGregor et al.*, 2015; *Tierney et al.*, 2015]. High latitude cooling has been constrained to 1-2 °C [*Overpeck et al.*, 1997; *Marcott et al.*, 2013] but previous Sr/Ca derived estimates of LIA cooling from this region range from 0 to 5 °C [*Haase-Schramm et al.*, 2003; *Saenger et al.*, 2008; *Kilbourne et al.*, 2010; *DeLong et al.*, 2014]. The cold end of these estimates implies greater climate sensitivity in the tropics than at high latitudes, conflicting with evidence from both simulations [*Holland and Bitz*, 2003; *Landrum et al.*, 2013] and 20th century observations [*Pithan and Mauritsen*, 2014].

Using Sr-U paleothermometry I find that over the period 1465-1560 the region was 1.1° C±0.6°C cooler than the 1958-1988 mean, but within error of early 20th century SST at this site. Critically, several periods of warmth, equivalent to the 1958-1988 mean, occurred during a solar minimum that is widely believed to have been a cool period of the LIA. My record spans only part of the LIA, the coldest time period of which may vary spatially. For example, several high latitude records from Northern Europe suggest that the later 18th century may have been a particularly cold period [*Denton and Karlen*, 1973]. Longer and more continuous records are required to assess spatial heterogeneity in the timing of LIA cooling. This chapter will be submitted shortly to *Geophysical Research Letters* as "Modest Little Ice Age cooling in the Western Tropical Atlantic."

This thesis contributes to the field of coral paleoceanography by improving the coral paleotemperature proxy methodology and applying it to reveal information about SST and the climate in the past.

1.5 Figure

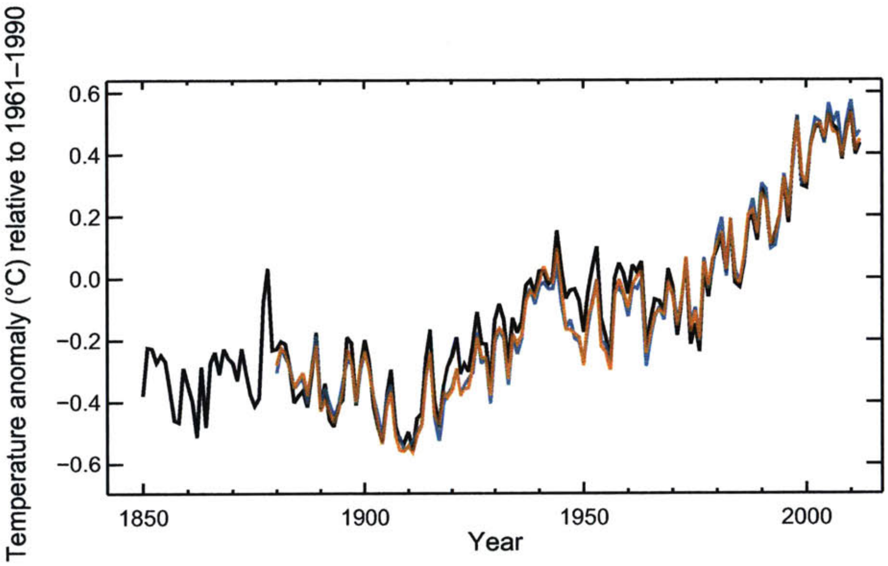

Figure 1-1: Observed globally averaged combined land and ocean surface temperature anomaly 1850-2012, adapted from *Stocker et al.*, [2013].

1.6 References

Beck, J. W., R. L. Edwards, E. Ito, F. W. Taylor, J. Recy, F. Rougerie, P. Joannot, and C. Henin (1992), Sea-surface temperature from coral skeletal strontium/calcium ratios, *Science*, *257*(5070), 644-647

Bindoff, N. L., P. A. Stott, M. AchutaRao, M. R. Allen, N. Gillett, D. Gutzler, K. Hansingo, G. Hegerl, Y. Hu, and S. Jain (2013), Detection and attribution of climate change: from global to regional, *In: Climate Change 2013: The Physical Science*

Basis. Contribution of Working Group I to the Fifth Assessment Report of the Intergovernmental Panel on Climate Change, Cambridge University Press, Cambridge, United Kingdom and New York, NY, USA, pp. 867–952, doi:10.1017/CBO9781107415324.022

Clark, P. U., A. S. Dyke, J. D. Shakun, A. E. Carlson, J. Clark, B. Wohlfarth, J. X. Mitrovica, S. W. Hostetler, and A. M. McCabe (2009), The last glacial maximum, *science*, *325*(5941), 710-714

Cohen, A., and T. McConnaughey (2003), Geochemical Perspectives on Coral Mineralization, *In: Dove, P.M., Weiner, S., de Yoreo, J.J. (Eds.), Biomineralization. : Rev. Mineral. Geochem., vol. 54. Mineral. Soc. of Am, Washington, D. C.*, 151-187

Cohen, A., and S. R. Thorrold (2007), Recovery of temperature records from slow-growing corals by fine scale sampling of skeletons, *Geophysical Research Letters*, *34*(17). doi:10.1029/2007GL030967.

Cohen, A., and G. Gaetani (2010), Ion partitioning and the geochemistry of coral skeletons: solving the mystery of the vital effect, *EMU Notes in Mineralogy*, *11*, 377-397

Cohen, A., G. A. Gaetani, T. Lundälv, B. H. Corliss, and R. Y. George (2006), Compositional variability in a cold-water scleractinian, Lophelia pertusa: New insights into "vital effects", *Geochemistry, Geophysics, Geosystems*, *7*(12). doi:10.1029/2006GC001354.

Collins, M., et al. (2013), Long-term Climate Change: Projections, Commitments and Irreversibility, *In: Climate Change 2013: The Physical Science Basis. Contribution of Working Group I to the Fifth Assessment Report of the Intergovernmental Panel on Climate Change.* Cambridge University Press, Cambridge, United Kingdom and New York, NY, USA, pp. 1029–1136, doi:10.1017/CBO9781107415324.024

DeCarlo, T. M., G. A. Gaetani, A. L. Cohen, G. L. Foster, A. E. Alpert, and J. Stewart (2016), Coral Sr-U Thermometry, *Paleoceanography*

DeLong, K. L., J. A. Flannery, R. Z. Poore, T. M. Quinn, C. R. Maupin, K. Lin, and C. C. Shen (2014), A reconstruction of sea surface temperature variability in the southeastern Gulf of Mexico from 1734–2008 CE using cross-dated Sr/Ca records from the coral Siderastrea siderea, *Paleoceanography*, *29*(5). doi:10.1002/2013PA002524.

Denton, George H., and Wibjörn Karlén. "Holocene climatic variations—their pattern and possible cause." *Quaternary Research* 3.2 (1973): 155IN1175-174IN2205.

Deser, C., A. S. Phillips, and M. A. Alexander (2010a), Twentieth century tropical sea surface temperature trends revisited, *Geophysical Research Letters*, *37*(10). doi:10.1029/2010GL043321.

Deser, C., M. A. Alexander, S.-P. Xie, and A. S. Phillips (2010b), Sea surface temperature variability: Patterns and mechanisms, *Annual Review of Marine Science*, *2*, 115-143

Enfield, D. B., A. M. Mestas-Nuñez, and P. J. Trimble (2001), The Atlantic multidecadal oscillation and its relation to rainfall and river flows in the continental US, *Geophysical Research Letters*, *28*(10), 2077-2080

Gaetani, G. A., and A. L. Cohen (2006), Element partitioning during precipitation of aragonite from seawater: a framework for understanding paleoproxies, *Geochimica et Cosmochimica Acta*, *70*(18), 4617-4634

Gaetani, G. A., A. L. Cohen, Z. Wang, and J. Crusius (2011), Rayleigh-based, multi-element coral thermometry: A biomineralization approach to developing climate proxies, *Geochimica et Cosmochimica Acta*, *75*(7), 1920-1932

Gagan, M. K., L. K. Ayliffe, J. W. Beck, J. E. Cole, E. R. M. Druffel, R. B. Dunbar, and D. P. Schrag (2000), New views of tropical paleoclimates from corals, *Quaternary Science Reviews*, *19*(1–5), 45-64. doi:10.1016/s0277-3791(99)00054-2.

Gagnon, A. C., J. F. Adkins, and J. Erez (2012), Seawater transport during coral biomineralization, *Earth and Planetary Science Letters*, *329*, 150-161

Gagnon, A. C., J. F. Adkins, D. P. Fernandez, and L. F. Robinson (2007), Sr/Ca and Mg/Ca vital effects correlated with skeletal architecture in a scleractinian deep-sea coral and the role of Rayleigh fractionation, *Earth and Planetary Science Letters*, *261*(1), 280-295

Gill, A., and E. M. Rasmusson (1983), The 1982–83 climate anomaly in the equatorial Pacific

Haase-Schramm, A., F. Böhm, A. Eisenhauer, W. C. Dullo, M. M. Joachimski, B. Hansen, and J. Reitner (2003), Sr/Ca ratios and oxygen isotopes from sclerosponges: Temperature history of the Caribbean mixed layer and thermocline during the Little Ice Age, *Paleoceanography*, *18*(3). doi:10.1029/2002PA000830.

Hartmann, D., A. Klein Tank, M. Rusicucci, L. Alexander, B. Broenniman, Y. Charabi, F. Dentener, E. Dlugokencky, D. Easterling, and A. Kaplan (2013), Observations: atmosphere and surface, *In: Climate Change 2013: The Physical Science Basis. Contribution of Working Group I to the Fifth Assessment Report of the Intergovernmental Panel on Climate Change,* Cambridge University Press, Cambridge, United Kingdom and New York, NY, USA, pp. 159–254, doi:10.1017/CBO9781107415324.008.

Hegerl, G. C., T. J. Crowley, W. T. Hyde, and D. J. Frame (2006), Climate sensitivity constrained by temperature reconstructions over the past seven centuries, *Nature*, *440*(7087), 1029-1032

Hetzinger, S., M. Pfeiffer, W.-C. Dullo, D. Garbe-Schönberg, and J. Halfar (2010), Rapid 20th century warming in the Caribbean and impact of remote forcing on climate in the northern tropical Atlantic as recorded in a Guadeloupe coral, *Palaeogeography, Palaeoclimatology, Palaeoecology*, *296*(1), 111-124

Holland, M. M., and C. M. Bitz (2003), Polar amplification of climate change in coupled models, *Climate Dynamics*, *21*(3-4), 221-232

Imbrie, J., E. Boyle, S. Clemens, A. Duffy, W. Howard, G. Kukla, J. Kutzbach, D. Martinson, A. McIntyre, and A. Mix (1992), On the structure and origin of major glaciation cycles 1. Linear responses to Milankovitch forcing, *Paleoceanography*, *7*(6), 701-738

Johns, W. E., M. O. Baringer, L. Beal, S. Cunningham, T. Kanzow, H. L. Bryden, J. Hirschi, J. Marotzke, C. Meinen, and B. Shaw (2011), Continuous, array-based estimates of Atlantic Ocean heat transport at 26.5 N, *Journal of Climate*, *24*(10), 2429-2449

Jones, P. D., and M. E. Mann (2004), Climate over past millennia, *Reviews of Geophysics*, *42*(2)

Jouzel, J., V. Masson-Delmotte, O. Cattani, G. Dreyfus, S. Falourd, G. Hoffmann, B. Minster, J. Nouet, J.-M. Barnola, and J. Chappellaz (2007), Orbital and millennial Antarctic climate variability over the past 800,000 years, *science*, *317*(5839), 793-796

Kiehl, J. T. (2007), Twentieth century climate model response and climate sensitivity, *Geophysical Research Letters*, *34*(22)

Kilbourne, K., T. Quinn, R. Webb, T. Guilderson, J. Nyberg, and A. Winter (2010), Coral windows onto seasonal climate variability in the northern

Caribbean since 1479, *Geochemistry, Geophysics, Geosystems*, *11*(10). doi:10.1029/2010GC003171.

Knudsen, M. F., M.-S. Seidenkrantz, B. H. Jacobsen, and A. Kuijpers (2011), Tracking the Atlantic Multidecadal Oscillation through the last 8,000 years, *Nature Communications*, *2*, 178

Knudsen, M. F., B. H. Jacobsen, M.-S. Seidenkrantz, and J. Olsen (2014), Evidence for external forcing of the Atlantic Multidecadal Oscillation since termination of the Little Ice Age, *Nature communications*, *5*

Landrum, L., B. L. Otto-Bliesner, E. R. Wahl, A. Conley, P. J. Lawrence, N. Rosenbloom, and H. Teng (2013), Last millennium climate and its variability in CCSM4, *Journal of Climate*, *26*(4), 1085-1111

Linsley, B. K., H. C. Wu, E. P. Dassié, and D. P. Schrag (2015), Decadal Changes in South Pacific Sea Surface Temperatures and the Relationship to the Pacific Decadal Oscillation and Upper Ocean Heat Content, *Geophys. Res. Lett.* doi:10.1002/2015GL063045.

Marcott, S. A., J. D. Shakun, P. U. Clark, and A. C. Mix (2013), A reconstruction of regional and global temperature for the past 11,300 years, *science*, *339*(6124), 1198-1201

Masson-Delmotte, V., M. Schulz, A. Abe-Ouchi, J. Beer, A. Ganopolski, J. González Rouco, E. Jansen, K. Lambeck, J. Luterbacher, and T. Naish (2013), Information from paleoclimate archives, *In: Climate Change 2013: The Physical Science Basis. Contribution of Working Group I to the Fifth Assessment Report of the Intergovernmental Panel on Climate Change,*Cambridge University Press, Cambridge, United Kingdom and New York, NY, USA, pp. 383–464, doi:10.1017/CBO9781107415324.013.

McGregor, H. V., M. N. Evans, H. Goosse, G. Leduc, B. Martrat, J. A. Addison, P. G. Mortyn, D. W. Oppo, M.-S. Seidenkrantz, and M.-A. Sicre (2015), Robust global ocean cooling trend for the pre-industrial Common Era, *Nature Geoscience*

McPhaden, M. J., S. E. Zebiak, and M. H. Glantz (2006), ENSO as an Integrating Concept in Earth Science, *Science*, *314*(5806), 1740-1745. doi:10.1126/science.1132588.

Myhre, G., D. Shindell, F. Bréon, W. Collins, J. Fuglestvedt, J. Huang, D. Koch, J. Lamarque, D. Lee, and B. Mendoza (2013), Anthropogenic and natural radiative forcing, *In: Climate Change 2013: The Physical Science Basis. Contribution of Working Group I to the Fifth Assessment Report of the Intergovernmental Panel on Climate Change* Cambridge University Press, Cambridge, United Kingdom and New York,
NY, USA, pp. 659–740, doi:10.1017/ CBO9781107415324.018

Newman, M., G. P. Compo, and M. A. Alexander (2003), ENSO-forced variability of the Pacific decadal oscillation, *Journal of Climate*, *16*(23), 3853-3857

Nurhati, I. S., K. M. Cobb, and E. Di Lorenzo (2011), Decadal-scale SST and salinity variations in the central tropical Pacific: Signatures of natural and anthropogenic climate change, *Journal of Climate*, *24*(13), 3294-3308

Otterå, O. H., M. Bentsen, H. Drange, and L. Suo (2010), External forcing as a metronome for Atlantic multidecadal variability, *Nature Geoscience*, *3*(10), 688-694

Overpeck, J., K. Hughen, D. Hardy, R. Bradley, R. Case, M. Douglas, B. Finney, K. Gajewski, G. Jacoby, and A. Jennings (1997), Arctic environmental change of the last four centuries, *Science*, *278*(5341), 1251-1256

Pithan, F., and T. Mauritsen (2014), Arctic amplification dominated by temperature feedbacks in contemporary climate models, *Nature Geosci*, *7*(3), 181-184. doi:10.1038/ngeo2071.

Rahmstorf, S. (2002), Ocean circulation and climate during the past 120,000 years, *Nature*, *419*(6903), 207-214

Rasmusson, E. M., and T. H. Carpenter (1982), Variations in tropical sea surface temperature and surface wind fields associated with the Southern Oscillation/El Niño, *Monthly Weather Review*, *110*(5), 354-384

Rayleigh, L. (1896), L. Theoretical considerations respecting the separation of gases by diffusion and similar processes, *The London, Edinburgh, and Dublin Philosophical Magazine and Journal of Science*, *42*(259), 493-498

Rhein, M. a., S. Rintoul, S. Aoki, E. Campos, D. Chambers, R. Feely, S. Gulev, G. Johnson, S. Josey, and A. Kostianoy (2013), Observations: ocean, *In: Climate Change 2013: The Physical Science Basis. Contribution of Working Group I to the Fifth Assessment Report of the Intergovernmental Panel on Climate Change*, Cambridge University Press, Cambridge, United Kingdom and New York, NY, USA, pp. 255–316, doi:10.1017/CBO9781107415324.010.

Robock, A. (2000), Volcanic eruptions and climate, *Reviews of Geophysics*, *38*(2), 191-219

Saenger, C., A. L. Cohen, D. W. Oppo, and D. Hubbard (2008), Interpreting sea surface temperature from strontium/calcium ratios in Montastrea corals: Link with growth rate and implications for proxy reconstructions, *Paleoceanography*, *23*(3). doi:10.1029/2007PA001572.

Schlesinger, M. E., and N. Ramankutty (1994), An oscillation in the global climate system of period 65-70 years, *Nature*, *367*(6465), 723-726

Schleussner, C., and G. Feulner (2013), A volcanically triggered regime shift in the subpolar North Atlantic Ocean as a possible origin of the Little Ice Age, *Clim. Past*, *9*(3), 1321-1330

Schmittner, A., N. M. Urban, J. D. Shakun, N. M. Mahowald, P. U. Clark, P. J. Bartlein, A. C. Mix, and A. Rosell-Melé (2011), Climate sensitivity estimated from temperature reconstructions of the Last Glacial Maximum, *Science*, *334*(6061), 1385-1388

Sinclair, D. J., B. Williams, and M. Risk (2006), A biological origin for climate signals in corals—Trace element "vital effects" are ubiquitous in Scleractinian coral skeletons, *Geophysical Research Letters*, *33*(17). doi:10.1029/2006GL027183.

Smith, S., R. Buddemeier, R. Redalje, and J. Houck (1979), Strontium-calcium thermometry in coral skeletons, *Science*, *204*(4391), 404-407

Solomon, A., L. Goddard, A. Kumar, J. Carton, C. Deser, I. Fukumori, A. M. Greene, G. Hegerl, B. Kirtman, and Y. Kushnir (2011), Distinguishing the roles of natural and anthropogenically forced decadal climate variability: implications for prediction, *Bulletin of the American Meteorological Society*, *92*(2), 141

Stocker, T. F., D. Qin, G.-K. Plattner, M. Tignor, S. K. Allen, J. Boschung, A. Nauels, Y. Xia, V. Bex, and P. M. e. Midgley (2013), Summary for Policymakers, *In: Climate Change 2013: The Physical Science Basis. Contribution of Working Group I to the Fifth Assessment Report of the Intergovernmental Panel on Climate Change. Cambridge University Press, Cambridge, United Kingdom and New York, NY, USA*, 1 – 30. doi:10.1017/CBO9781107415324.004.

Sutton, R. T., and D. L. Hodson (2005), Atlantic Ocean forcing of North American and European summer climate, *Science*, *309*(5731), 115-118

Tierney, J. E., N. J. Abram, K. J. Anchukaitis, M. N. Evans, C. Giry, K. H. Kilbourne, C. P. Saenger, H. C. Wu, and J. Zinke (2015), Tropical sea surface temperatures for the past four centuries reconstructed from coral archives, *Paleoceanography*, *30*(3), 226-252

Timmermann, A., J. Oberhuber, A. Bacher, M. Esch, M. Latif, and E. Roeckner (1999), Increased El Niño frequency in a climate model forced by future greenhouse warming, *Nature*, *398*(6729), 694-697

Ting, M., Y. Kushnir, and C. Li (2014), North Atlantic multidecadal SST oscillation: External forcing versus internal variability, *Journal of Marine Systems*, *133*, 27-38

Tollefson, J. (2016), 2015 declared the hottest year on record, *Nature*, *529*(7587), 450-450

Trenberth, K. E., G. W. Branstator, D. Karoly, A. Kumar, N. C. Lau, and C. Ropelewski (1998), Progress during TOGA in understanding and modeling global teleconnections associated with tropical sea surface temperatures, *Journal of Geophysical Research: Oceans*, *103*(C7), 14291-14324

Wu, H. C., M. Moreau, B. K. Linsley, D. P. Schrag, and T. Corrège (2014), Investigation of sea surface temperature changes from replicated coral Sr/Ca variations in the eastern equatorial Pacific (Clipperton Atoll) since 1874, *Palaeogeography, Palaeoclimatology, Palaeoecology*, *412*, 208-222

Zhang, R., and T. L. Delworth (2006), Impact of Atlantic multidecadal oscillations on India/Sahel rainfall and Atlantic hurricanes, *Geophysical Research Letters*, *33*(17)

Chapter 2

Comparison of equatorial Pacific sea surface variability and trends with Sr/Ca records from multiple corals[1]

2.1 Abstract

Coral Sr/Ca is widely used to reconstruct past ocean temperatures. However, some studies report different Sr/Ca-temperature relationships for conspecifics on the same reef, with profound implications for interpretation of reconstructed temperatures. We assess whether these differences are attributable to small-scale oceanographic variability or "vital effects" associated with coral calcification and quantify the effect of intercolony differences on temperature estimates and uncertainties. Sr/Ca records from four massive *Porites* colonies growing on the east and west sides of Jarvis Island, central equatorial Pacific, were compared with *in situ* logger temperatures spanning 2002–2012. In general, Sr/Ca captured the occurrence of interannual sea surface temperature events but their amplitude was not consistently recorded by any of the corals. No long-term trend was identified in the instrumental data, yet Sr/Ca of one coral implied a statistically significant cooling trend while that of its neighbor implied a warming trend. Slopes of Sr/Ca-temperature regressions from the four different colonies were within error, but offsets in mean Sr/Ca rendered the regressions statistically distinct. Assuming that these relationships represent the full range of Sr/Ca-temperature calibrations in Jarvis *Porites*, we assessed how well Sr/Ca of a nonliving coral with an unknown Sr/Ca-temperature relationship can constrain

[1] Published as: Alice E. Alpert, Anne L. Cohen, Delia W. Oppo, Thomas M. DeCarlo, Jamison M. Gove, and Charles W. Young, 2016. Comparison of equatorial Pacific sea surface temperature variability and trends with Sr/Ca records from multiple corals. *Paleoceanography,* 31. This article was originally published at http://onlinelibrary.wiley.com/doi/10.1002/2015PA002897/pdf, and is reprinted as published with permission granted in the original copyright agreement.

past temperatures. Our results indicate that standard error of prediction methods underestimate the actual error as we could not reliably reconstruct the amplitude or frequency of El Niño–Southern Oscillation events as large as ± 2°C. Our results underscore the importance of characterizing the full range of temperature-Sr/Ca relationships at each study site to estimate true error.

2.2 Introduction

Precise and accurate sea surface temperature (SST) estimates are critical for extending the instrumental record in the tropical Pacific and for separating internal climate variability from long-term trends. Instrumental reconstructions extending back to the mid nineteenth century [e.g., Smith et al., 2008] rely on sparse observational sampling both in space and in time and are unreliable prior to 1950 in some places [*Vecchi et al.*, 2008; *Deser et al.*, 2010; *Tokinaga et al.*, 2012]. For example, the estimated trend in the central equatorial Pacific over the twentieth century from three different SST data products ranges from +0.36°C per century to +0.74°C per century [*Nurhati et al.*, 2011]. Identifying the true rate of warming is important for estimating the sensitivity of Pacific SST to global warming, as well as for understanding the full impact of tropical Pacific SSTs on recent and future global temperatures and climate [*DiNezio et al.*, 2009].

Annually banded tropical corals have potential to provide continuous seasonally resolved records of ocean variability and trends over the last several centuries and, with application of accurate dating techniques, even further back in time using data extracted from nonliving colonies. Coral Sr/Ca is currently the most widely used coral paleothermometer [*Smith et al.*, 1979; *Beck et al.*, 1992] and is based on the generally negative correlation over seasonal cycles between skeletal Sr/Ca and the temperature of the water in which the coral grew. While the goal of many studies has been to reconstruct SSTs during the preinstrumental era (e.g., *Kuhnert et al.*, [2005]; *Goodkin et al.*, [2008]; *Kilbourne et al.*, [2008]; *Hetzinger et al.*, [2010]; *DeLong et al.*, [2012, 2014]), several recent applications attempt to resolve inconsistencies in twentieth century SST variability and trends among the different SST data products or where instrumental coverage is sparse (e.g., *Nurhati et al.*, [2011]; *Carilli et al.*, [2014]; *Linsley et al.*, [2015]), applications that require both accurate and precise reconstructed temperatures.

Despite their widespread use, potential sources of uncertainty exist in paleotemperature records derived from coral Sr/Ca. Within a single coral colony, offsets in mean Sr/Ca occur along different growth axes [*de Villiers et al.*, 1994; *Alibert and McCulloch*, 1997; *DeLong et al.,* 2007], and experimental culture studies have shown that the Sr/Ca of corals responds to changes in seawater pH and light, even when temperature is constant [*Reynaud et al.*, 2004; *Cohen et al.*, 2009; *Gagnon et al.*, 2012]. Nutrients and possibly gender have also been shown to affect the Sr/Ca of corals [*Atkinson et al.*, 1995; *Carricart-Ganivet et al.*, 2013]. Many of these discrepancies have been attributed to "vital effects," the result of processes that occur during coral biomineralization (skeletal growth).

The recognition of vital effects has led to the application of targeted sampling strategies intended to minimize their impact (e.g., *DeLong et al.*, [2013]). Yet despite careful, targeted sampling strategies, inconsistencies remain. For example, offsets in mean Sr/Ca of neighboring colonies collected on the same reef have been observed, as have differences in the Sr/Ca sensitivity to temperature [*Goodkin et al.*, 2005; *Linsley et al.*, 2006; *Saenger et al.*, 2008; *Cahyarini et al.*, 2009; *Pfeiffer et al.*, 2009]. *Grove et* al. [2013] reported different long-term SST trends derived from Sr/Ca of two *Porites* corals on a Madagascar reef, with one suggesting warming and one suggesting cooling. *Carilli et al.* [2014]

reported a cooling trend in corals from the central tropical Pacific over a time period when satellite SSTs showed a clear warming trend. Also in the tropical Pacific, *Nurhati et al.* [2011] reported decadal-scale variability in a Sr/Ca-based coral SST record that was not observed in the instrumental SST record from the region. Such inconsistencies between coral Sr/Ca-derived SST and instrumental SST have sometimes been attributed to uncertainties in the instrumental record or to real SST variability within the reefal system (e.g., *Pfeiffer et al.*, [2009]). These are valid concerns. First, there are significant uncertainties and biases in the early part of the instrumental record due mainly to a lack of standardization in the way the measurements were made (e.g., *Rayner et al.*, [2006], *Kennedy et al.*, [2011]). In areas where data coverage is sparse there are inconsistencies in data even after 1950 [*Casey and Cornillon*, 1999]. Second, many reefal environments are morphologically complex and SST gradients can exist between exposed barrier environments and more sheltered back reefs and lagoons where large *Porites* often grow [*Linsley et al.*, 2004]. Therefore, differences in Sr/Ca-derived SST records from coral colonies sampled on the same reef may reflect real differences that are not resolved by satellite or Voluntary Observing Ships data.

Despite these issues, the origin of the observed inconsistencies between Sr/Ca-derived SST and instrumental SST, whether vital effects, real oceanographic variability, or errors in the instrumental SST record, has never been directly addressed. As a result, the ability of coral Sr/Ca to return reliable SST variations and trends over a relatively small temperature range remains in question.

We generated Sr/Ca records from *Porites* corals collected on Jarvis, a small (4.5 km^2), island in the central equatorial Pacific (159°59'W, 0°22'S) fringed by a submerged coral reef. Jarvis Island is situated in the path of the

Equatorial Undercurrent (EUC), a subsurface (20–400 m) current that brings cool water along the equator from the western to the eastern Pacific [*Philander*, 1973; *Wyrtki and Kilonsky*, 1984]. The EUC upwells when it encounters Jarvis, creating a patch of cooler surface water on the west side of the island [Gove et al., 2006]. EUC strength and upwelling at Jarvis are affected by El Niño–Southern Oscillation (ENSO). El Niño events are associated with a weaker EUC, reduced upwelling, and warming [*Firing et al.*, 1983; *Gove et al.*, 2006]. The converse is true during La Niña events. Temperature loggers deployed at several stations and depths across the reef provide nearly a decade of *in situ* temperature data that enable quantification of the cross-island difference, the response of island SST to interannual variability driven by ENSO, and the global warming trend.

Analysis of coral skeletons collected on each side of the island offers an opportunity to assess the ability of coral Sr/Ca to resolve the cross-island temperature gradient and to capture the frequency and amplitude of ENSO events, as well as any longer-term trend. Our data show that temperature estimates derived from Sr/Ca of four Jarvis corals are associated with large uncertainties and that they do not consistently record either the ENSO events or the long-term trend indicated by the logger data. We conclude that inconsistencies among the Jarvis coral Sr/Ca records do not reflect actual SST variability around the island and that absolute SSTs, decadal trends, and records of interannual variability reconstructed using coral Sr/Ca ratios must be interpreted with caution.

2.3 Material and Methods

In April 2010, and May and September 2012, five skeletal cores were collected from two live coral colonies (*Porites lobata*) on each of the east and west sides of Jarvis Island (Figure 2-1). Using pneumatic drills, cores W037 (April 2010) and W497 (September 2012) were collected from a single colony on the west side at 13 m depth, and core W490 was collected from the west side (September 2012) approximately 80 m away at 8 m depth. On the east side of the island, core E016 was collected in May 2012 at 5 m depth. Core E500 was collected in September 2012 approximately 300 m away, also at 5 m depth.

Sea-Bird Electronics (SBE) 39 Temperature Recorder loggers deployed on both sides of the island by NOAA's Coral Reef Ecosystems Program of the Pacific Islands Fisheries Science Center (Figure 2-1) recorded temperature every 30 min. The drift of the SBE recorders is 0.0002°C per month and the precision is ± 0.002°C. We averaged the logger data into monthly bins. We constructed a composite west side temperature record using data from three loggers: W022 (7 m) and W013 (11 m), within 75 m of both west side corals, and W001 (15 m), located 1400 m from both corals (Figures 2-1 and A1-1 in the supporting information). When data exist from multiple loggers over the same time period, the values are averaged; the mean difference between concurrent values is only 0.26°C. The east side record is composed of records from loggers E006 (2004–2010, 13 m) and E020 (2010–2012, 10 m) at the same location within 1100 m of both corals (Figures 2-1 and 2-2). As logger E020 essentially replaced logger E006, there is no overlapping period for the two east side logger records. However, a composite logger record is not needed because both east side logger records closely match contemporaneous monthly optimal interpolation SSTs (OISSTs v.2) [Reynolds et al., 2002] (see section 2.3) for a 1° × 1° grid box centered on Jarvis Island. The OISST analysis combines *in situ* and satellite

SSTs and is adjusted for biases. Weekly resolution fields are linearly interpolated to daily resolution and then averaged over each month. We use this relatively coarse resolution data product to test whether temperatures at Jarvis Island are representative of regional surface conditions.

The 30mm diameter coral cores were scanned using a Siemens volume zoom spiral computerized tomography (CT) scanner at the Woods Hole Oceanographic Institution (WHOI) following methods described in *DeCarlo et al.* [2015] (Figure A1-2). Cores were slabbed to 2 mm thickness and ultrasonicated in deionized water to remove coral dust. The 50–80μg coral powder was milled at 1mm intervals in a continuous sampling transect using a Minicraft MB170 drill with a 1mm diameter diamond bit. Counts of ^{88}Sr and ^{48}Ca were collected on two single-collector Element 2 inductively coupled plasma mass spectrometers at WHOI. Sr/Ca ratios were determined by calibration to published standards derived from coral skeleton (JCp-1) [*Okai et al.*, 2002; *Hathorne et al.*, 2013a], fish otoliths (FEBS-1 [*Sturgeon et al.*, 2005] and National Institute for Environmental Studies (NIES) [*Yoshinaga et al.*, 2000]), and limestone (National Bureau of Standards (NBS)-19) [*Fernandez et al.*, 2011]. The R^2 values between measured $^{88}Sr/^{48}Ca$ counts and published molar Sr/Ca ratios were typically >0.999. The JCp-1 standard has a Sr/Ca ratio (8.838 ± 0.042 mmol/mol) similar to our coral samples (8.8–9.7 mmol/mol), whereas Sr/Ca ratios of FEBS-1, NIES, and NBS-19 are all less than 3 mmol/mol. As a result, our calibration curves for Sr/Ca determinations are controlled mainly by the JCp-1 standard. Repeated measurements of an in-house secondary coral standard indicate an external precision of ± 0.035 mmol/mol (1σ, n = 140, 0.4% relative) and were stable throughout our study. Our uncertainty estimates take this analytical precision into account through our calculation of the standard error of prediction. To evaluate the accuracy of our method and facilitate comparison to Sr/Ca ratios measured in other laboratories, we measured the Sr/Ca ratio of JCp-1 by calibration to an independent set of standards. Single-element standards (High-Purity Standards) were mixed to simulate coral skeleton (40 ppm Ca and variable concentrations of Mg, Sr, Ba, and U). Three aliquots of JCp-1 powder were dissolved, and each was measured in duplicate by calibrating to the simulated coral standards (calibration curve $R^2 > 0.9999$). We measured the Sr/Ca ratio of JCp-1 as 8.870 ± 0.028 mmol/mol, which is within uncertainty of the mean, and within the range of precision, reported from JCp-1 analyses conducted in 21 different laboratories [*Hathorne et al.*, 2013a].

Sr/Ca of overlapping time periods of cores W037 and W497, drilled from the same colony, were combined into a single record, hereafter referred to as W037 (Figure A1-4). The period of 1996–2010.3 derives from core W037 and 2010.3-2012.2 derives from core W497. Annual density bands visible in 3-D CT scans of the cores were used to construct a first-order chronology with an estimated error of ± 1 year. Using Arand software [*Howell et al.*, 2006], we fine-tuned the Sr/Ca variability to the *in situ* temperature variations (e.g., *Guilderson et al.*, [2004]). Note that this method maximizes the correlation between Sr/Ca and temperature. The average adjustment of the band-based chronology was < 1 month for cores W497, W037, and E500 and 4 months for W490 and E016. The maximum adjustment of any point was 8 months.

2.4 Results

2.4.1 Logger and OISSTs

The mean and variance of both east side logger records E006 and E020 are statistically indistinguishable from those of contemporaneous monthly satellite-derived OISST for a 1° × 1° grid box centered on Jarvis Island (two-sample t test; $r = 0.99$, $p = 0.34$, and $n = 67$ and $r = 0.98$, $p = 0.60$, and $n = 12$, respectively), indicating that temperatures on the east side are uniform and reflect regional SSTs. The mean (27.17°C) and variance (1.53°C) of the combined east side logger record are also statistically indistinguishable from OISST (mean 27.41°C and variance 1.44°C; $p = 0.44$, $n = 75$), and their correlation coefficient is high ($r = 0.99$). Furthermore, the mean difference between contemporaneous monthly resolved values is only 0.24°C. By contrast, the mean (26.49°C) and variance (2.31°C) of the west side composite logger record are statistically different from those of OISST over the same period ($p < 0.05$, $n = 75$), and the correlation coefficient is lower ($r = 0.91$). While the relatively large (1° × 1°) OISST grid box cannot resolve these differences due to their small spatial scale, the logger data indicate that corals on the west side of Jarvis experienced significantly colder mean temperatures (26.49°C) than their counterparts on the east side (27.17°C, $p < 0.05$, $n = 75$).

Interannual temperature variabilities on both sides of the island are dominated by ENSO (Figure 2-2). The cross-island temperature gradient is most pronounced during La Niña, when west side temperatures are up to 1°C cooler than they are on the east side (e.g., the peak month of the 2010–2011 La Niña; Figure 2-2). This reflects the increase in the strength of the EUC and consequently, EUC upwelling on the west side of Jarvis during La Niña events [*Gove et al.*, 2006]. OISST and logger records reveal a significant decade-long (2002–2012) cooling trend determined by the ordinary least squares (OLS) regression method (-0.204 ± 0.130°C/yr, $p<0.05$; Table 2-4), consistent with an equatorial Pacific cooling trend reported by *Kosaka and Xie* [2013]. However, over the full period covered by the longest coral records (1997–2012), there is no significant trend in the OISST (Table 2-2).

2.4.2 Sr/Ca coral records

Over the period common to all corals (2007–2012), mean Sr/Ca values of each colony are statistically different from one another, with the exception of one west side (W037) and one east side (E016) coral ($p > 0.99$; Table 2-1). Corals E500 and E016, both growing on the east (warmer) side of the island, have lowest (warmest) and highest (coolest) mean Sr/Ca, respectively.

Trends in the Sr/Ca records do not follow expected patterns and in some cases, contradict each other. Over the full length of the records (1997–2012), Sr/Ca of one east side coral (E016) shows a statistically significant increase, implying cooling, whereas Sr/Ca of the other (E500) shows a statistically significant decrease, implying warming (Figure 2-2 and Table 2-2). Over the length of the logger records (2002–2012), Sr/Ca of E016 and W037 suggest cooling, consistent with the logger records, but that of E500 does not (Figure 2-2 and Table 2-3).

2.4.3 Sr/Ca-temperature regressions

We used the OLS regression method to assess how the Sr/Ca time series generated for each individual coral captured recorded temperature variability through time. Monthly interpolated Sr/Ca from all four cores were regressed onto *in situ* temperature for the period of 2004–2012, over which loggers recorded *in situ* temperatures on both sides of the island (Figure 2-3a and Table 2-4). Slopes range from -0.03 ± 0.01 to -0.09 ± 0.01 (mmol/mol/°C), within the range of values reported in *Corrège* [2006].

Analysis of variance (ANOVA) performed between Sr/Ca and logger temperature regressions identified statistically different slopes (95% confidence level) among most combinations of coral pairs ($p<0.05$; Table 2-1). However, the slopes of W490 and E500 versus temperature are different at the 90% confidence level and of W037 and E016 are the same at the 99% confidence level. Sr/Ca-temperature correlation coefficients range from -0.58 ($n = 65$, $p < 0.05$) in core W490 to -0.84 ($n = 95$, $p < 0.05$) in core W037, which are comparable with those generated for *Porites* corals at other tropical Pacific sites [*Cahyarini et al.*, 2009; *Nurhati et al.*, 2011; *Carilli et al.*, 2014]. Regressing Sr/Ca onto OISST rather than logger temperature yielded similar results (Figure 2-3b), with slopes all significantly different except for W037 versus E016. Sr/Ca-SST correlation coefficients range from -0.47 ($n = 65$, $p < 0.05$) in core W490 to -0.81 ($n = 98$, $p < 0.05$) in core E016. Slopes of the regression of Sr/Ca on OISST and of the regression of Sr/Ca on logger temperatures are statistically identical for each coral ($p < 0.05$; Table 2-1).

2.4.4 Temperature-Sr/Ca regressions

In order to use Sr/Ca to estimate temperatures, we regressed logger temperature on Sr/Ca. Except for W037 versus E500, the regressions are not within error of each other (Figure 2-4), although an ANOVA showed statistically indistinguishable slopes of the regressions ($p < 0.05$; Table 2-1). Correlation coefficients are identical to those reported above in section 2.3.3. We calculated the standard error of prediction of temperature $SE(\hat{T})$ for a single derived temperature estimate using the following expression from *Brownlee* [1965]:

$$SE(\hat{T}) = \hat{\sigma}\sqrt{\left[\frac{1}{n} + \frac{\left(Sr/Ca - \overline{Sr/Ca}\right)^2}{\widehat{\beta_1}^2 \sum_{j=1}^{n}(T_j - \bar{T})^2} + 1\right]} \qquad \text{(Eq. 2-1)}$$

where $\hat{\sigma}$ is the standard deviation of the estimated temperature values, $\widehat{\beta_1}$ is the estimated slope of the regression, n is the number of samples, overbars indicate time series means, T_j is the temperature measured at all times j, 1 to n. This statistic is not a propagation of error; rather, it estimates the error on temperature derived from a Sr/Ca ratio of the same coral from which the regression was derived. Standard errors of prediction for logger temperature regressions on Sr/Ca range from 0.7°C in E016 to 1.21°C in W490 (Table 2-1). Regressing OISST on Sr/Ca yielded similar results (Table 2-1), and slopes of the regression of Sr/Ca on OISST and of the regression of Sr/Ca on logger temperatures are statistically identical for each coral ($p<0.05$; Table 2-1). However, equation (2-1) represents only the error of prediction internal to a particular coral record (i.e., the calibration equation is applied to the same coral with which it was developed). When temperature reconstructions are performed using multiple corals, equation (2-1) drastically underestimates the true error as a result of varia- tions in Sr/Ca-temperature relationships among corals (section 2.4.2.1 below).

2.5 Discussion

2.5.1 Vital effects or real oceanographic variability

Analysis of the Sr/Ca records generated from contemporaneous *Porites* corals sampled from the west and east sides of Jarvis Island reveal inconsistencies that cannot be attributed to island-scale oceanographic variability. The mean Sr/Ca of E016 is 0.13 mmol/mol higher than that of E500 growing adjacent to it over the same time period. At the Sr/Ca-temperature sensitivities of these corals (Table 2-1), this difference represents 1.4–2.2°C. At Jarvis, such a large temperature difference is unlikely, given that the corals are both located on the east side of the island, at the same depth, in unsheltered locations, and east side logger records are each statistically identical to satellite temperature indicating the homogeneity of the temperature field bathing the corals there. Similarly, the 0.10 mmol/mol difference in mean Sr/Ca between the corals on the west side suggests a temperature difference of 1.1–3.3°C. However, the standard deviation of absolute differences in temperatures from multiple *in situ* loggers deployed on the west side is 0.07°C and the distance between the loggers is an order of magnitude greater than the distance between the corals.

Moreover, mean Sr/Ca of corals occupying the west, and thus the cooler, side of the island are not consistently higher than those of corals occupying the east side of the island, as would be predicted from the generally inverse relationship between Sr/Ca and temperature. Together these observations exclude the possibility that the Sr/Ca differences among corals are due to micro-oceanographic heterogeneity and point toward vital effects as a source of the inconsistencies.

2.5.2 Evaluation of Sr/Ca-derived temperature records from non-living corals

Like our study, previous studies have reported offsets in mean Sr/Ca translating to 1–4°C [*Goodkin et al.*, 2005; *Linsley et al.*, 2006; *Saenger et al.*, 2008; *Cahyarini et al.*, 2009; *Pfeiffer et al.*, 2009; *Wu et al.,* 2014] from multiple corals from the same genus and the same reef or island. Our attribution of the offsets we find to vital effects poses a problem for interpretation of long-term temperature records from multiple, nonoverlapping nonliving corals [*Guilderson et al.*, 1994; *McCulloch et al.*, 1996; *Beck et al.*, 1997; *Gagan et al.*, 1998; *Hughen et al.*, 1999; *Abram et al.*, 2009; *Kilbourne et al.*, 2010; *Toth et al.*, 2015]. For example, if E016 was a nonliving coral and E500 was a modern coral, we could erroneously infer that there had been a 1.4–2.2°C increase in mean temperature at this site, when in fact, we have shown that the difference in Sr/Ca is not due to temperature.

Like ours, other studies have found statistically distinct regression slopes of Sr/Ca on temperature [*Saenger et al.*, 2008; *Cahyarini et al.*, 2009; *Pfeiffer et al.*, 2009]. Here we use several approaches to further investigate the implications of such differences in mean Sr/Ca and regression slopes for temperatures reconstructed from nonliving corals.

2.5.2.1 Stacking records

Several studies present a Sr/Ca "stack" or "master" record constructed by averaging concurrent Sr/Ca values from multiple cores and regressing temperature on the stacked Sr/Ca. This has been applied in cases when the regression slopes of multiple corals were distinct [*Linsley et al.*, 2006; *Cahyarini et al.*, 2009; *Pfeiffer et al.*, 2009; *Wu et al.*, 2014], as well as another in which multiple corals had regression slopes within error and no offsets [*DeLong et al.*, 2007]. We replicated this method to create an averaged stack of Sr/Ca from all four corals over the time covered by all coral records (2007–2012) and regressed OISSTs onto this stack (Figure 2-5 and Table 2-1). The mean error of prediction of the stack regression is 0.779 ± 0.006°C (1σ, n = 260; Table 2-1), calculated following *Brownlee* [1965].

To simulate the application of this regression to a single coral with unknown temperature-Sr/Ca relationship (i.e., a nonliving coral that is analyzed to extend the record back in time), we applied the stack regression to each of the four Sr/Ca records generated in this study (Figure 2-6). We assume that our living corals have captured the full range of possible temperature-Sr/Ca relationships at this site. Using the same stack regression however, the different corals suggest different temperature histories, including inconsistencies that are exaggerated during cold (La Niña) events. For example, corals E500 and W490 do not record the strong cooling during the 2007–2008 La Niña and the derived 2010 cooling is smaller in these corals than that suggested by E016 and W037. Coral W490 shows warming during the 2012 cooling. Corals E016 and W037 register large cool events in 2007–2008, 2010, and 2012, although they disagree on the magnitude of the 2008 cooling. Using only one of these records, we might draw erroneous conclusions with respect to the amplitude or frequency of large cold events at this site. Differences also exist among the colonies in the estimated temperature and amplitude of warm events, although they are not as large as the discrepancies during cool events.

Inconsistencies between coral records extend beyond amplitude of variability. As expected from the differences in mean Sr/Ca, the mean SSTs derived from the stack regression for the four corals are not all within standard error of one another: 27.7 ± 0.1°C (n=65), 27.3 ± 0.1°C (n=65), 26.3 ± 0.2°C (n=65), and 27.3 ± 0.1°C (n = 65), for corals E500, W490, W037, and E016, respectively, with differences among sites inconsistent with their growth temperatures.

Long-term trends in reconstructed SST are also inconsistent. Over the period covered by all three corals (1998–2012), the trends in W037, E016, and OISST are positive and statistically indistinguishable from one another (Figure 2-6). However, the trend in estimated temperatures for E500 is cooling and statistically distinct. Similar discrepancies are seen in a record from Butaritari [*Carilli et al.*, 2014], where the post-1976 Sr/Ca-derived trend is cooling, when the instrument-based data indicate warming [*Karnauskas et al.*, 2015], and in two Sr/Ca records from the same site in Madagascar [*Grove et al.*, 2013] having opposite trends. These observations imply that coral Sr/Ca may suggest temperature trends opposite to those actually experienced. Thus, interpretations of long-term trends derived from coral Sr/Ca should be viewed cautiously, and any implied trend should be replicated in several corals.

The large spread in Sr/Ca-derived temperatures and the often nonoverlapping error of the derived temperatures indicate that the standard error of prediction for the stack underestimates the true error of applying this calibration to a nonliving coral or any coral with an unknown SST-Sr/Ca relationship. The departures of the Sr/Ca-temperature points of each of the individual corals have a systematic relation- ship with SST; the departures from the stack regression are correlated, rather than randomly distributed. For example, since the regression from E016 lies above the stacked regression (Figure 2-5), the estimates from coral E016 are largely too cool, while the estimates from E500, lying below the stack regression, are largely too warm. A more realistic estimate of the potential range of temperatures takes the difference between the concurrent maximum and minimum temperature estimates from the four corals, including the error bars constructed using one standard error of prediction (Figure 2-6, bottom, gray curve). This approach yields an average range on temperatures derived from Sr/Ca of 3.8 $\pm$ 1.0°C (1σ, n=65), with the largest values at low temperatures (for example, 6.4°C at an OISST of 25.1°C; Figure 2-6, bottom, gray curve) and smallest values at high temperatures (for example, 2.2°C at an OISST of 28.5°C; Figure 2-6, bottom, gray curve).

2.5.2.2 "Global" regression

Given the uncertainties of applying a regression based on stacked Sr/Ca, another approach is to combine all Sr/Ca values from the four colonies in a single global regression. In contrast to the stack regression in which we averaged concurrent Sr/Ca values from all four corals for a single data set of 65 points, in the global regression we used all 359 original data points (for 2004–2012) employed in the logger-based regressions for all four corals (Figure 2-4). We then regressed the corresponding logger temperatures on these Sr/Ca values (Figure 2-7 and Table 2-1). As with the stack regression, we applied this global regression to each of the four Sr/Ca records as if they were from nonliving corals with unknown relationship to temperature (Figure 2-8). The average standard error of prediction is 1.023 $\pm$ 0.003°C (1σ, n = 316; Table 2-1) calculated according to *Brownlee* [1965]. The results of this method are similar to those using the stack; there is little consensus among the corals on the amplitude of large warm and cold events, with the uncertainty especially large during cold events. Depending on which coral was selected from the set of corals and analyzed for Sr/Ca, the results could indicate strong ENSO-driven interannual variability (E016 or

W037) or virtually none (W490).

Similar to the results of the stack regression, the mean temperature predictions among corals are not within standard error of each other and differences among sites are inconsistent with their growth temperatures. Trend results are the same as for the stack regression (Figure 2-8) and are not sensitive to the period over which the trends are calculated.

Like the estimates based on the stack regression, the standard error of prediction for the global regression underestimates the true range of temperatures resulting from the application of this calibration to a coral with an unknown SST-Sr/Ca relationship, which we estimate is 3.8 ± 0.8°C (1σ, $n = 65$) calculated the same way as for the stack regression.

2.5.2.3 Application of all individual regressions

We investigated one additional method for estimating temperatures and associated errors for a Sr/Ca record from a nonliving coral from Jarvis, applying all regressions to each single Sr/Ca record. The range of estimates is graphically represented by the difference between the maximum and minimum temperatures for a given Sr/Ca value, based on any of the four regressions on logger temperatures (Figure 2-4), and their associated estimates, as discussed below.

We applied all regressions to each coral and took the maximum and minimum temperatures returned by the four regressions as the maximum and minimum temperature estimates for that time point. To account for the errors of prediction of the regressions, we added the standard error of prediction of the regression used to construct the maximum estimate (W490, 1.21°C) to the initial maximum estimate and subtracted the standard error of prediction of the regression used to construct the minimum estimate (E016, 0.74°C) to the initial minimum estimate. The temperatures between the resulting maximum and minimum estimates for each coral indicate the range of potential temperatures estimated by that coral (Figure 2-9), and these average 3.7 ± 0.7°C (1σ, n = 78). Although the range of estimated temperatures includes the OISST estimate for most of all four records, the spread in the derived temperatures is so large that even temperature excursions that are ± 2°C from the mean could not be reliably identified using a Sr/Ca record from a single coral (Figure 2-9).

2.6 Conclusions and Outlook

SST records from corals in the tropical Pacific such as those at Jarvis Island have the potential to help answer critical questions about the global climate system and its response to anthropogenic increases in greenhouse gases. In general, SST derived from Sr/Ca captured the occurrence of interannual SST events but the amplitude of these events was not consistently recorded by any of the corals (Figure A1-5). The slopes of the regressions of temperature on Sr/Ca are within error for all four different corals (Figure 2-4); however, mean offsets in Sr/Ca, equivalent to 1.1–3.3°C, between corals experiencing the same temperatures (Table 2-1) imply that the regressions of temperature on Sr/Ca are not within error. Therefore, deriving a temperature-Sr/Ca relationship from a coral collected live and applying it to another coral has the potential to introduce errors as large as 4°C or more (e.g., Figure 2-9), comparable to errors found in a compilation of 18 corals [Moreau et al., 2015]. The large uncertainty when any regression is applied to a single coral of unknown temperature-Sr/Ca relationship compromises the utility of Sr/Ca to estimate the amplitude and frequency of ± 2°C temperature oscillations with any confidence.

Calibrating a stack of all four Sr/Ca records against temperature (Figure 2-5) or combining all coral data into a global regression (Figure 2-7) yields inconsistent SST estimates when applied to individual corals (Figures 2-6 and 2-8). Standard error of prediction based on the expression in *Brownlee* [1965] underestimates the potential errors, based on the ranges of temperature estimates using these methods, by a factor of more than 2.

While the magnitude of the resulting uncertainty is problematic for absolute temperature estimates based on Sr/Ca from nonliving corals, it is also troublesome for determining the amplitude of temperature variability from nonliving corals. Even if the mean is removed, differences in the slope of the Sr/Ca-temperature relationship will result in different amplitudes of variability.

Finally, Sr/Ca trends from different corals living at the same time in the same water temperature are of opposite sign, implying that extreme caution must also be exercised in using a calibration based on a coral collected live to estimate recent or preinstrumental temperature trends.

Our results indicate that temperature estimates derived from coral Sr/Ca must be accompanied by realistic errors that can only be estimated by characterizing the distribution of potential Sr/Ca-SST relationships at the study site. Coral skeleton Li/Mg ratios are potentially a more robust temperature proxy [*Montagna et al.*, 2014], yet unexplained deviations between Li/Mg and temperature remain [*Hathorne et al.*, 2013b]; it is essential to further expand this and other methods to take into account vital effects.

2.7 Acknowledgments

We are grateful to Pat Lohmann (WHOI) and Liz Drenkard (Rutgers) for field assistance, the entire crew of Seadragon for getting us out to Jarvis and to Emily Penn and Ron Ritter of Pangaea Exploration; Kathryn Pietro (WHOI) and Scot Birdwhistell (WHOI) for lab assistance; Andrew Solow (WHOI) and Olivier Marchal (WHOI) for assistance with statistics and insightful discussions. We thank two anonymous reviewers for their thoughtful and helpful suggestions. This study was supported by an NSF Graduate Research Fellowship to A.A. and by NSF-OCE-0926986 and NSF-OCE-1031971. The authors declare no competing financial interest. The coral Sr/Ca data used in this paper is included in a supplementary dataset available online and will be archived at http://www.ncdc.noaa.gov/data- access/paleoclimatology-data/datasets.

2.8 References

Atkinson M. J., B. Carlson, and G.L. Crow (1995), Coral growth in high-nutrient, low-pH seawater: a case study of corals cultured at the Waikiki Aquarium, Honolulu, Hawaii, *Coral Reefs, 14*:215–223.

Abram, N. J., H. V. McGregor, M. K. Gagan, W. S. Hantoro, and B. W. Suwargadi (2009), Oscillations in the southern extent of the Indo-Pacific Warm Pool during the mid-Holocene, *Quaternary Science Reviews*, *28*(25), 2794-2803.

Alibert, C., and M. T. McCulloch (1997), Strontium/calcium ratios in modern Porites corals from the Great Barrier Reef as a proxy for sea surface temperature: Calibration of the thermometer and monitoring of ENSO, *Paleoceanography*, *12*(3), 345-363. doi:10.1029/97PA00318.

Beck, J. W., R. L. Edwards, E. Ito, F. W. Taylor, J. Recy, F. Rougerie, P. Joannot, and C. Henin (1992), Sea-surface temperature from coral skeletal strontium/calcium ratios, *Science*, *257*(5070), 644-647.

Beck, J. W., J. Récy, F. Taylor, R. L. Edwards, and G. Cabioch (1997), Abrupt changes in early Holocene tropical sea surface temperature derived from coral records, *Nature*, *385*(6618), 705-707.

Brownlee, K. A. (1965), *Statistical theory and methodology in science and engineering*, Wiley New York.

Cahyarini, S. Y., M. Pfeiffer, and W.-C. Dullo (2009), Improving SST reconstructions from coral Sr/Ca records: multiple corals from Tahiti (French Polynesia), *International Journal of Earth Sciences*, *98*(1), 31-40.

Carricart-Ganivet, J. P., L. F. Vasquez-Bedoya, N. Cabanillas-Teran, and P. Blanchon, (2013), Gender-related differences in the apparent timing of skeletal density bands in the reef-building coral Siderastrea siderea, *Coral Reefs, 32*(3) 769-777.

Carilli, J. E., H. V. McGregor, J. J. Gaudry, S. D. Donner, M. K. Gagan, S. Stevenson, H. Wong, and D. Fink (2014), Equatorial Pacific coral geochemical records show recent weakening of the Walker Circulation, *Paleoceanography*, *29*(11), 1031-1045. doi:10.1002/2014PA002683.

Casey, K. S., and P. Cornillon (1999), A comparison of satellite and in situ-based sea surface temperature climatologies, *Journal of Climate*, *12*(6), 1848-1863.

Cohen, A., D. C. McCorkle, S. de Putron, G. A. Gaetani, and K. A. Rose (2009), Morphological and compositional changes in the skeletons of new coral recruits reared in acidified seawater: Insights into the biomineralization response to ocean acidification, *Geochemistry, Geophysics, Geosystems*, *10*(7). doi:10.1002/ggge.20095.

Corrège, T. (2006), Sea surface temperature and salinity reconstruction from coral geochemical tracers, *Palaeogeography, Palaeoclimatology, Palaeoecology*, *232*(2–4), 408-428. doi:10.1016/j.palaeo.2005.10.014.

de Villiers, S., G. T. Shen, and B. K. Nelson (1994), The SrCa-temperature relationship in coralline aragonite: Influence of variability in (SrCa) seawater and skeletal growth parameters, *Geochimica et Cosmochimica Acta*, *58*(1), 197-208.

DeCarlo, T. M., A. L. Cohen, H. C. Barkley, Q. Cobban, C. Young, K. E. Shamberger, R. E. Brainard, and Y. Golbuu (2015), Coral macrobioerosion is accelerated by ocean acidification and nutrients, *Geology*, *43*(1), 7-10.

DeLong, K. L., T. M. Quinn, and F. W. Taylor (2007), Reconstructing twentieth-century sea surface temperature variability in the southwest Pacific: A replication study using multiple coral Sr/Ca records from New Caledonia, *Paleoceanography*, *22*(4). doi:10.1029/2007PA001444.

DeLong, K. L., T. M. Quinn, F. W. Taylor, K. Lin, and C.-C. Shen (2012), Sea surface temperature variability in the southwest tropical Pacific since AD 1649, *Nature Climate Change*, *2*(11), 799-804.

DeLong, K. L., T. M. Quinn, F. W. Taylor, C.-C. Shen, and K. Lin (2013), Improving coral-base paleoclimate reconstructions by replicating 350years of coral Sr/Ca variations, *Palaeogeography, Palaeoclimatology, Palaeoecology*, *373*, 6-24.

DeLong, K. L., J. A. Flannery, R. Z. Poore, T. M. Quinn, C. R. Maupin, K. Lin, and C. C. Shen (2014), A reconstruction of sea surface temperature variability in the southeastern Gulf of Mexico from 1734–2008 CE using cross-dated Sr/Ca records from the coral Siderastrea siderea, *Paleoceanography*, *29*(5). doi:10.1002/2013PA002524.

Deser, C., M. A. Alexander, S.-P. Xie, and A. S. Phillips (2010), Sea surface temperature variability: Patterns and mechanisms, *Annual Review of Marine Science*, *2*, 115-143.

DiNezio, P. N., A. C. Clement, G. A. Vecchi, B. J. Soden, B. P. Kirtman, and S.-K. Lee (2009), Climate response of the equatorial Pacific to global warming, *Journal of Climate*, 22(18), 4873-4892.

Fernandez, D. P., A. C. Gagnon, and J. F. Adkins (2011), An isotope dilution ICP-MS method for the determination of Mg/Ca and Sr/Ca ratios in calcium carbonate *Geostandards and Geoanalytical Research, 35*(1) 23-37.

Firing, E., R. Lukas, J. Sadler, and K. Wyrtki (1983), Equatorial undercurrent disappears during 1982–1983 El Niño, *Science*, 222(4628), 1121-1123.

Gagan, M. K., L. K. Ayliffe, D. Hopley, J. A. Cali, G. E. Mortimer, J. Chappell, M. T. McCulloch, and M. J. Head (1998), Temperature and surface-ocean water balance of the mid-Holocene tropical western Pacific, *Science*, *279*(5353), 1014-1018.

Gagnon, A. C., J. F. Adkins, and J. Erez (2012), Seawater transport during coral biomineralization, *Earth and Planetary Science Letters*, *329*, 150-161.

Goodkin, N. F., K. A. Hughen, A. L. Cohen, and S. R. Smith (2005), Record of Little Ice Age sea surface temperatures at Bermuda using a growth-dependent calibration of coral Sr/Ca, *Paleoceanography*, *20*(4). doi:10.1029/2005PA001140.

Goodkin, N. F., K. A. Hughen, W. B. Curry, S. C. Doney, and D. R. Ostermann (2008), Sea surface temperature and salinity variability at Bermuda during the end of the Little Ice Age, *Paleoceanography*, *23*(3). doi:10.1029/2007PA001532.

Gove, J. M., M. A. Merrifield, and R. E. Brainard (2006), Temporal variability of current-driven upwelling at Jarvis Island, *Journal of Geophysical Research: Oceans (1978nard (*, 111(C12), doi:10.1029/2005JC003161.

Grove, C. A., S. Kasper, J. Zinke, M. Pfeiffer, D. Garbe-Schönberg, and G. J. A. Brummer (2013), Confounding effects of coral growth and high SST variability on skeletal Sr/Ca: implications for coral paleothermometry, *Geochemistry, Geophysics, Geosystems*, *14*(4), 1277-1293. doi:10.1002/ggge.20095.

Guilderson, T. P., R. G. Fairbanks, and J. L. Rubenstone (1994), Tropical temperature variations since 20,000 years ago: modulating interhemispheric climate change, *Science*, *263*(5147), 663-665.

Guilderson, T., D. Schrag, and M. Cane (2004), Surface water mixing in the Solomon Sea as documented by a high-resolution coral 14C record, *Journal of Climate*, *17*(5), 1147-1156.

Hathorne, E. C., A. Gagnon, T. Felis, J. Adkins, R. Asami, W. Boer, N. Caillon, D. Case, K. M. Cobb, and E. Douville (2013a), Inter-laboratory study for coral Sr/Ca and other element/Ca ratio measurements, *Geochemistry, Geophysics, Geosystems*, *14*(9), 3730-3750, doi:10.1002/ggge.20230.

Hathorne, E. C., T. Felis, A. Suzuki, H. Kawahata, and G. Cabioch (2013b), Lithium in the aragonite skeletons of massive Porites corals: A new tool to reconstruct tropical sea surface temperatures, *Paleoceanography*, *28*(1), 143-152, doi: 10.1029/2012PA002311.

Hetzinger, S., M. Pfeiffer, W.-C. Dullo, D. Garbe-Schönberg, and J. Halfar (2010), Rapid 20th century warming in the Caribbean and impact of remote forcing on climate in the northern tropical Atlantic as recorded in a Guadeloupe coral, *Palaeogeography, Palaeoclimatology, Palaeoecology*, *296*(1), 111-124

Howell, P., N. Pisias, J. Ballance, J. Baughman, and L. Ochs (2006), Arand time-series analysis software, *Brown University, Providence RI.*

Hughen, K. A., D. P. Schrag, S. B. Jacobsen, and W. Hantoro (1999), El Nino during the last interglacial period recorded by a fossil coral from Indonesia, *Geophysical Research Letters*, *26*(20), 3129-3132. doi:10.1029/1999GL006062.

Karnauskas, K. B., A. L. Cohen, and E. J. Drenkard (2015), Comment on "Equatorial Pacific coral geochemical records show recent weakening of the Walker Circulation" by J. Carilli et al, *Paleoceanography*, 2014PA002753. doi:10.1002/2014PA002753.

Kennedy, J., N. Rayner, R. Smith, D. Parker, and M. Saunby (2011), Reassessing biases and other uncertainties in sea surface temperature observations measured in situ since 1850: 2. Biases and homogenization, *Journal of Geophysical Research: Atmospheres (1984–2012)*, *116*(D14). doi:10.1029/2010JD015220.

Kilbourne, K., T. Quinn, R. Webb, T. Guilderson, J. Nyberg, and A. Winter (2008), Paleoclimate proxy perspective on Caribbean climate since the year 1751: Evidence of cooler temperatures and multidecadal variability, *Paleoceanography*, *23*(3), doi:10.1029/2008PA001598.

Kilbourne, K., T. Quinn, R. Webb, T. Guilderson, J. Nyberg, and A. Winter (2010), Coral windows onto seasonal climate variability in the northern Caribbean since 1479, *Geochemistry, Geophysics, Geosystems*, *11*(10). doi:10.1029/2010GC003171.

Kosaka, Y., and S.-P. Xie (2013), Recent global-warming hiatus tied to equatorial Pacific surface cooling, *Nature*, *501*(7467), 403-407.

Kuhnert, H., T. Crüger, and J. Pätzold (2005), NAO signature in a Bermuda coral Sr/Ca record, *Geochemistry, Geophysics, Geosystems*, *6*(4), doi:10.1029/2010GC003344.

Linsley, B., G. Wellington, D. Schrag, L. Ren, M. Salinger, and A. Tudhope (2004), Geochemical evidence from corals for changes in the amplitude and spatial pattern of South Pacific interdecadal climate variability over the last 300 years, *Climate Dynamics*, *22*(1), 1-11.

Linsley, B. K., A. Kaplan, Y. Gouriou, J. Salinger, P. B. Demenocal, G. M. Wellington, and S. S. Howe (2006), Tracking the extent of the South Pacific Convergence Zone since the early 1600s, *Geochemistry, Geophysics, Geosystems*, *7*(5), doi:10.1029/2005GC001115.

Linsley, B. K., H. C. Wu, E. P. Dassié, and D. P. Schrag (2015), Decadal Changes in South Pacific Sea Surface Temperatures and the Relationship to the Pacific Decadal Oscillation and Upper Ocean Heat Content, *Geophysical Research Letters, 42*, doi:10.1002/2015GL063045.

McCulloch, M., G. Mortimer, T. Esat, L. Xianhua, B. Pillans, and J. Chappell (1996), High resolution windows into early Holocene climate: SrCa coral records from the Huon Peninsula, *Earth and Planetary Science Letters*, *138*(1), 169-178.

Montagna, P., M. McCulloch, E. Douville, M. L. Correa, J. Trotter, R. Rodolfo-Metalpa, D. Dissard, C. Ferrier-Pages, N. Frank, and A. Freiwald (2014), Li/Mg systematics in scleractinian corals: Calibration of the thermometer, *Geochimica et Cosmochimica Acta*, *132*, 288-310.

Moreau, M., T. Corrège, E. Dassié, and F. Le Cornec (2015), Evidence for the non-influence of salinity variability on the Porites coral Sr/Ca palaeothermometer, *Climate of the Past*, *11*(3), 523-532.

Nurhati, I. S., K. M. Cobb, and E. Di Lorenzo (2011), Decadal-scale SST and salinity variations in the central tropical Pacific: Signatures of natural and anthropogenic climate change, *Journal of Climate*, *24*(13), 3294-3308.

Okai, T., A. Suzuki, S. Terashima, M. Inoue, M. Nohara, H. Kawahata, and N. Imai (2004), Collaborative analysis of GSJ/AIST geochemical reference materials JCp-1 (Coral) and JCt-1 (Giant Clam), *Chikyukagaku (Geochemistry), 38*, 281–286.

Pfeiffer, M., W.-C. Dullo, J. Zinke, and D. Garbe-Schönberg (2009), Three monthly coral Sr/Ca records from the Chagos Archipelago covering the period of 1950–1995 AD: reproducibility and implications for quantitative reconstructions of sea surface temperature variations, *International Journal of Earth Sciences*, *98*(1), 53-66.

Philander, S. (1973), Equatorial undercurrent: Measurements and theories, *Reviews of Geophysics*, *11*(3), 513-570.

Rayner, N., P. Brohan, D. Parker, C. Folland, J. Kennedy, M. Vanicek, T. Ansell, and S. Tett (2006), Improved analyses of changes and uncertainties in sea surface temperature measured in situ since the mid-nineteenth century: the HadSST2 dataset, *Journal of Climate*, *19*(3), 446-469.

Reynaud, S., C. Ferrier-Pagès, F. Boisson, D. Allemand, and R. G. Fairbanks, (2004) Effect of light and temperature on calcification and strontium uptake in the scleractinian coral Acropora verweyi, *Marine Ecology Progress Series*, *279*, 105-112.

Reynolds, R. W., N. A. Rayner, T. M. Smith, D. C. Stokes, and W. Wang (2002), An improved in situ and satellite SST analysis for climate, *Journal of Climate*, *15*(13), 1609-1625.

Saenger, C., A. L. Cohen, D. W. Oppo, and D. Hubbard (2008), Interpreting sea surface temperature from strontium/calcium ratios in Montastrea corals: Link with growth rate and implications for proxy reconstructions, *Paleoceanography*, *23*(3). doi:10.1029/2007PA001572.

Smith, S., R. Buddemeier, R. Redalje, and J. Houck (1979), Strontium-calcium thermometry in coral skeletons, *Science*, *204*(4391), 404-407.

Smith, T. M., R. W. Reynolds, T. C. Peterson, and J. Lawrimore (2008), Improvements to NOAA's historical merged land-ocean surface temperature analysis (1880-2006), *Journal of Climate*, 21(10), 2283-2296.

Sturgeon, R. E., S. N. Willie, L. Yang, R. Greenberg, R. O. Spatz, Z. Chen, C.

Scriver, V. Clancy, J. W. Lam, and S. Thorrold (2005), Certification of a fish otolith reference material in support of quality assurance for trace element analysis, *Journal of Analytical Atomic Spectrometry*, *20*(10), 1067–1071.

Tokinaga, H., S.-P. Xie, C. Deser, Y. Kosaka, and Y. M. Okumura (2012), Slowdown of the Walker circulation driven by tropical Indo-Pacific warming, *Nature*, *491*(7424), 439-443.

Toth, L. T., R. B. Aronson, K. M. Cobb, H. Cheng, R. L. Edwards, P. R. Grothe, and H. R. Sayani (2015), Climatic and biotic thresholds of coral-reef shutdown, *Nature Climate Change*, *5*, 369-374.

Vecchi, G. A., A. Clement, and B. J. Soden (2008), Examining the tropical Pacific's response to global warming, *Eos, Transactions American Geophysical Union*, *89*(9), 81-83.

Wu, H. C., M. Moreau, B. K. Linsley, D. P. Schrag, and T. Corrège (2014), Investigation of sea surface temperature changes from replicated coral Sr/Ca variations in the eastern equatorial Pacific (Clipperton Atoll) since 1874, *Palaeogeography, Palaeoclimatology, Palaeoecology*, *412*, 208-222.

Wyrtki, K., and B. Kilonsky (1984), Mean water and current structure during the Hawaii-to-Tahiti shuttle experiment, *Journal of Physical Oceanography*, *14*(2), 242-254.

Yoshinaga, J., A. Nakama, M. Morita, and J. S. Edmonds (2000), Fish otolith reference material for quality assurance of chemical analyses, *Marine Chemistry*, *69*(1), 91-97.

2.9 Figures and tables

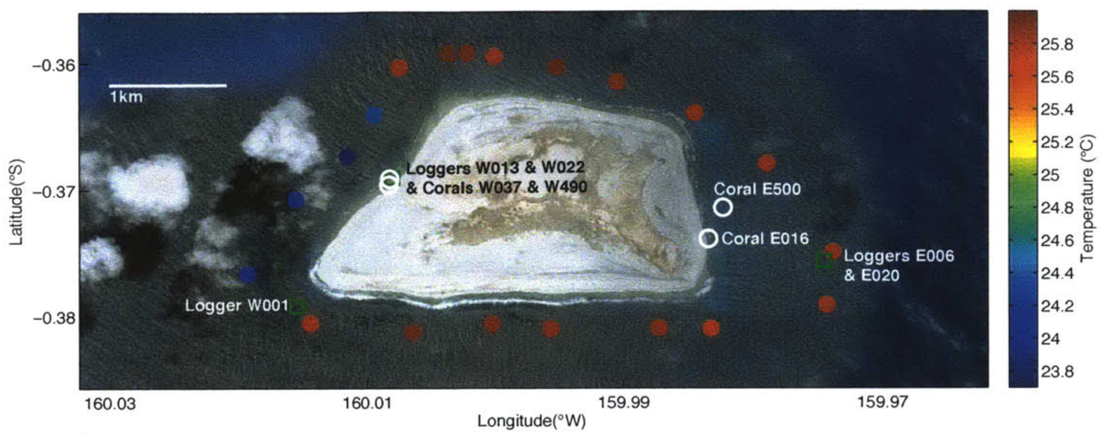

Figure 2-1: Jarvis Island showing locations of temperature loggers (green squares) and coral colonies sampled for this study (white circles). The filled circles represent the water temperature at 10 m from conductivity-temperature-depth (CTD) casts conducted in March 2000 [Gove et al., 2006]. Colder west side temperatures result from topographic upwelling of the Equatorial Undercurrent. The scale bar indicates the 1 km distance.

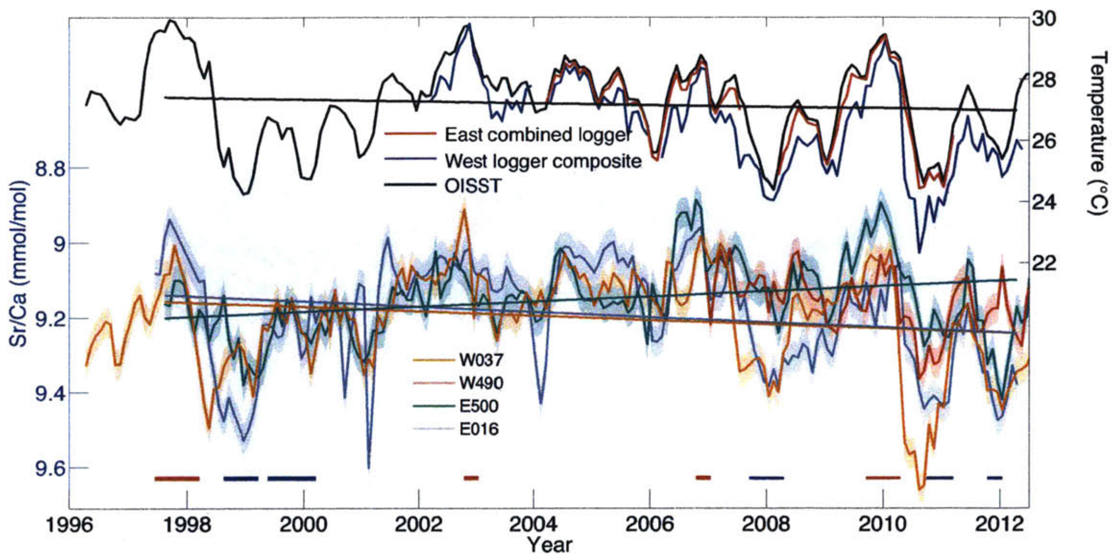

Figure 2-2: (top) Average monthly OISST-gridded temperatures [Reynolds et al., 2002] from the 1° × 1° box centered on Jarvis Island (black) compared with the average monthly west side logger composite (blue) and average monthly east side combined logger (red). (bottom) Sr/Ca records (mmol/mol) from all four corals with 1σ analytical error (0.04 mmol/mol) shaded. The thick red horizontal lines indicate the El Niño periods as defined by Oceanic Niño Index (ONI: 3 month running mean of ERSST v3b SST anomalies in the Niño 3.4 region 5°N–5°S, 120–170°W [Smith et al., 2008]) $\geq$1.0, and the heavy blue horizontal lines indicate the La Niña periods as defined by ONI $\leq$ -1.0. The solid lines denote the 1997–2012 trends in OISST (black) and coral Sr/Ca records (colors). Slopes and errors are provided in Table 2-2.

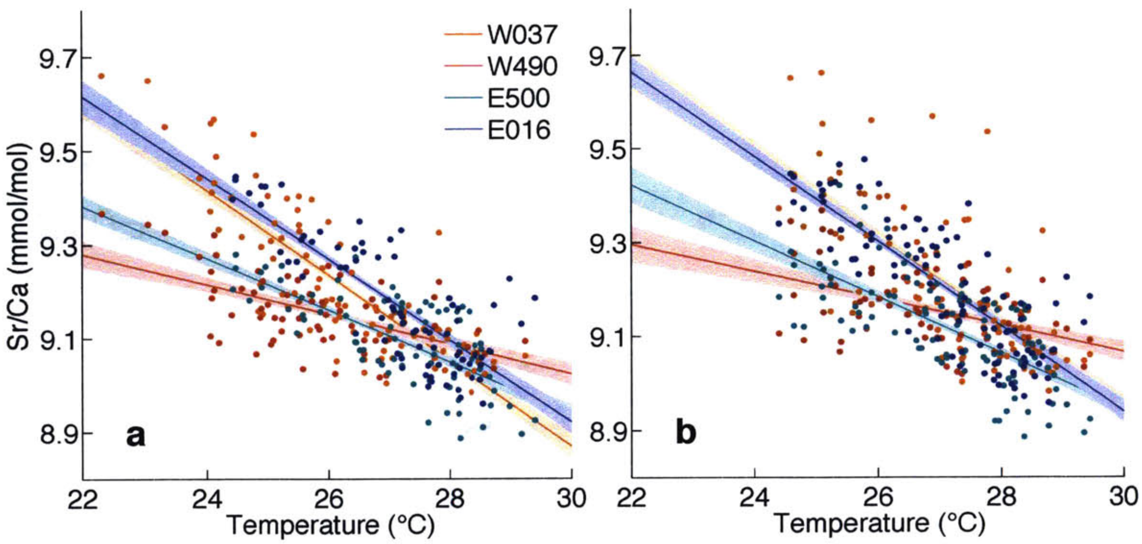

Figure 2-3: (a) Regression of coral Sr/Ca from each of the four cores onto *in situ* logger data (west side composite for west side corals and east side combined logger for east side corals). The shaded error bars represent the regression errors. Slopes are statistically different except W037 versus E016 ($p > 0.99$) and W490 versus E500 ($p < 0.10$; Table 2-1). Population means are all statistically different except for W037 versus E016. Slopes and errors are provided in Table 2-1. (b) Regression of coral Sr/Ca onto OISST for each of the four cores for the period of 2006–2012. The shading represents the regression errors. Slopes are statistically different except W037 and E016, which are within error ($p > 0.99$; Table 2-1).

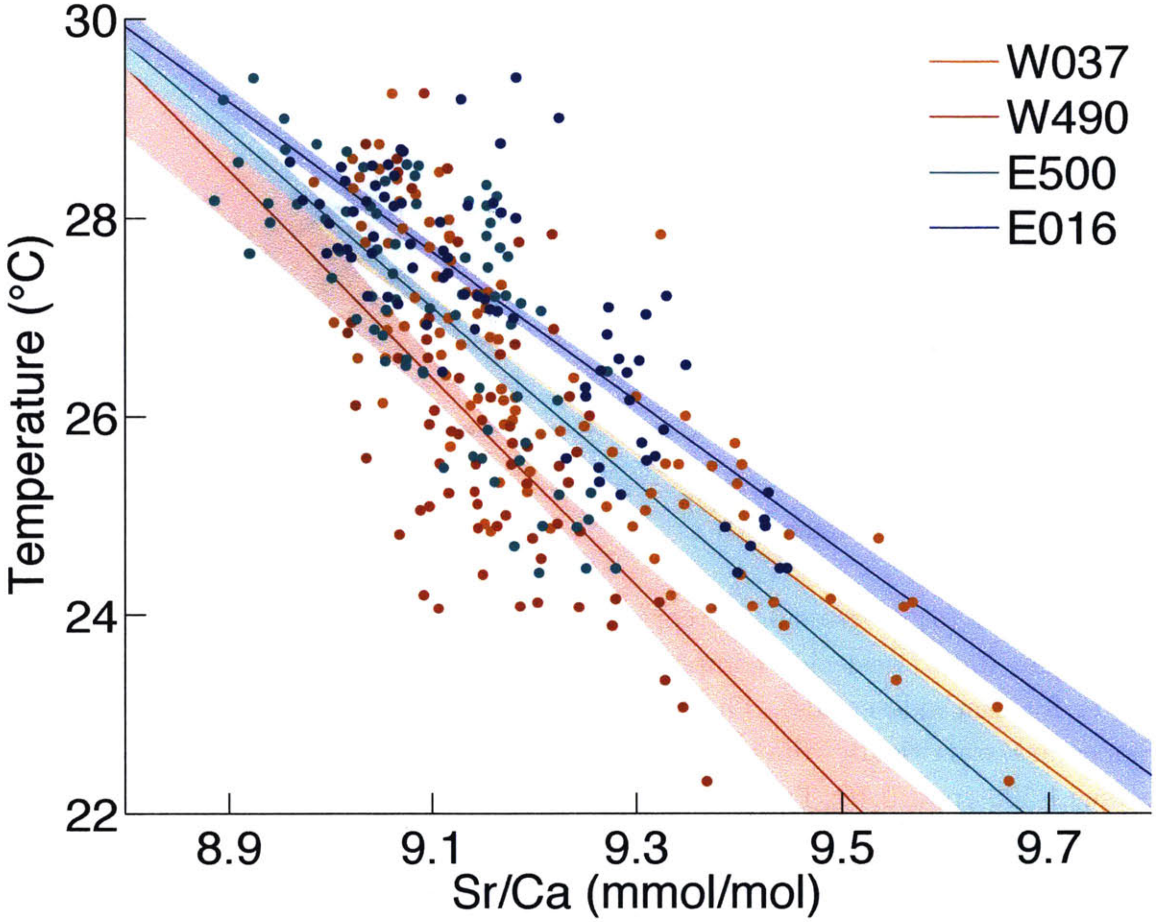

Figure 2-4: Regression of *in situ* logger data onto coral Sr/Ca from each of the four cores. Although only the regressions of W037 and E500 are within error, the slopes for all four corals are within error (Table 2-1). Standard errors of inverse prediction range from 0.744 ± 0.001°C (1σ, n = 78) for E016 to 1.21 ± 0.01°C (1σ, n = 65) for W490.

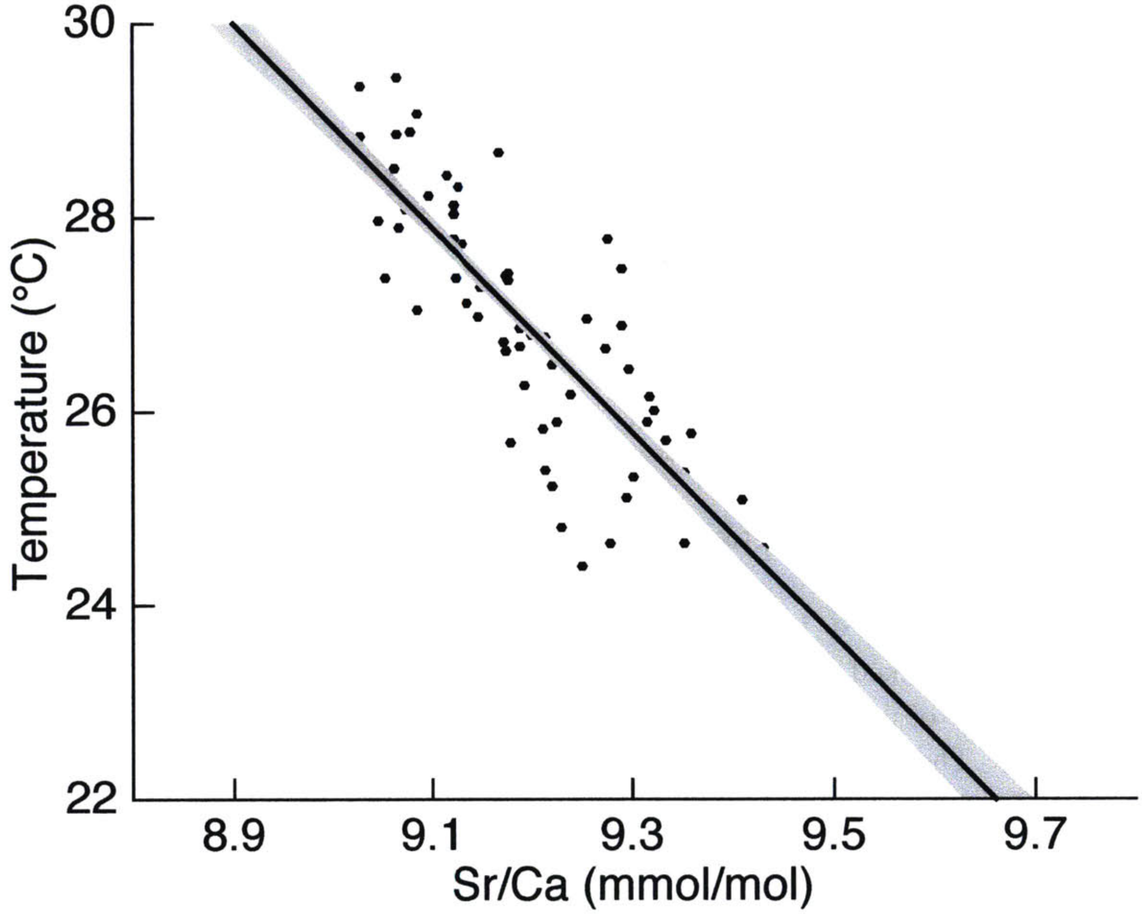

Figure 2-5: Regression of stacked Sr/Ca (black circles) onto OISST (black, with shading indicating the error on regression). Standard error of inverse prediction is 0.779 ± 0.006°C (1σ, n = 65).

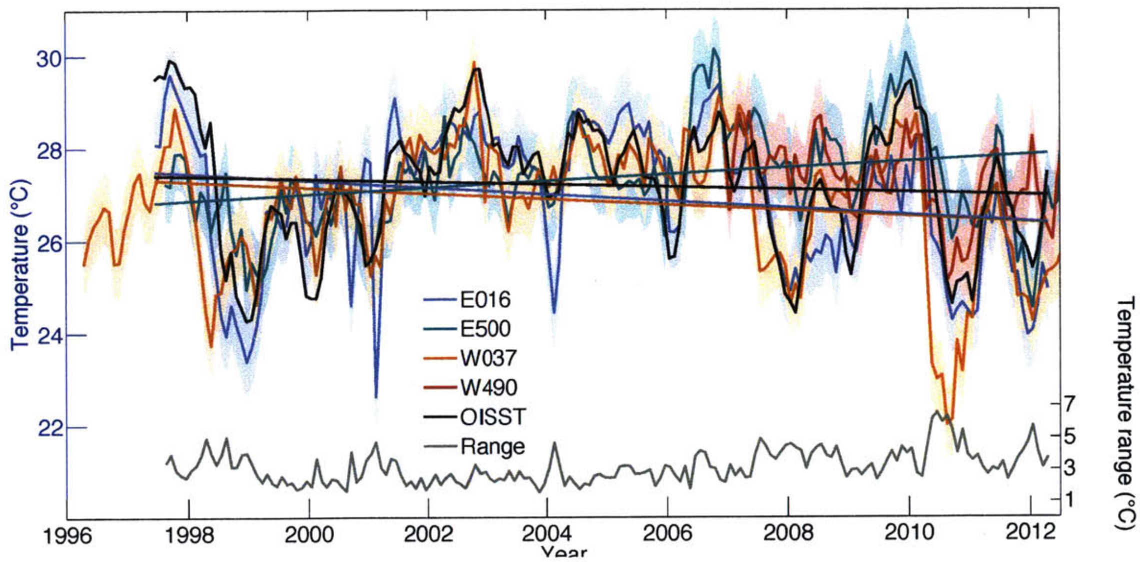

Figure 2-6: Derived temperatures from all four corals generated using the regression of stacked Sr/Ca on OISSTs (Figure 2-5). The shading indicates the standard error of prediction for the stack regression, 0.779 ± 0.006°C (1σ, n = 65; Table 2-1). The gray solid line below tracks the maximum difference between temperatures derived from each of the corals at a given time point. This difference averages 3.8°C over the period covered by all four corals. The solid lines denote the 1997–2012 trends in OISST (black) and coral Sr/Ca records (colors). Although OISST suggests no trend and two corals suggest cooling trend (E016 and W037), these trend slopes are within error of each other and are not significant. Conversely, the trend in E500 is significant ($p < 0.02$) and indicates that the east side of Jarvis Island warmed over this time period.

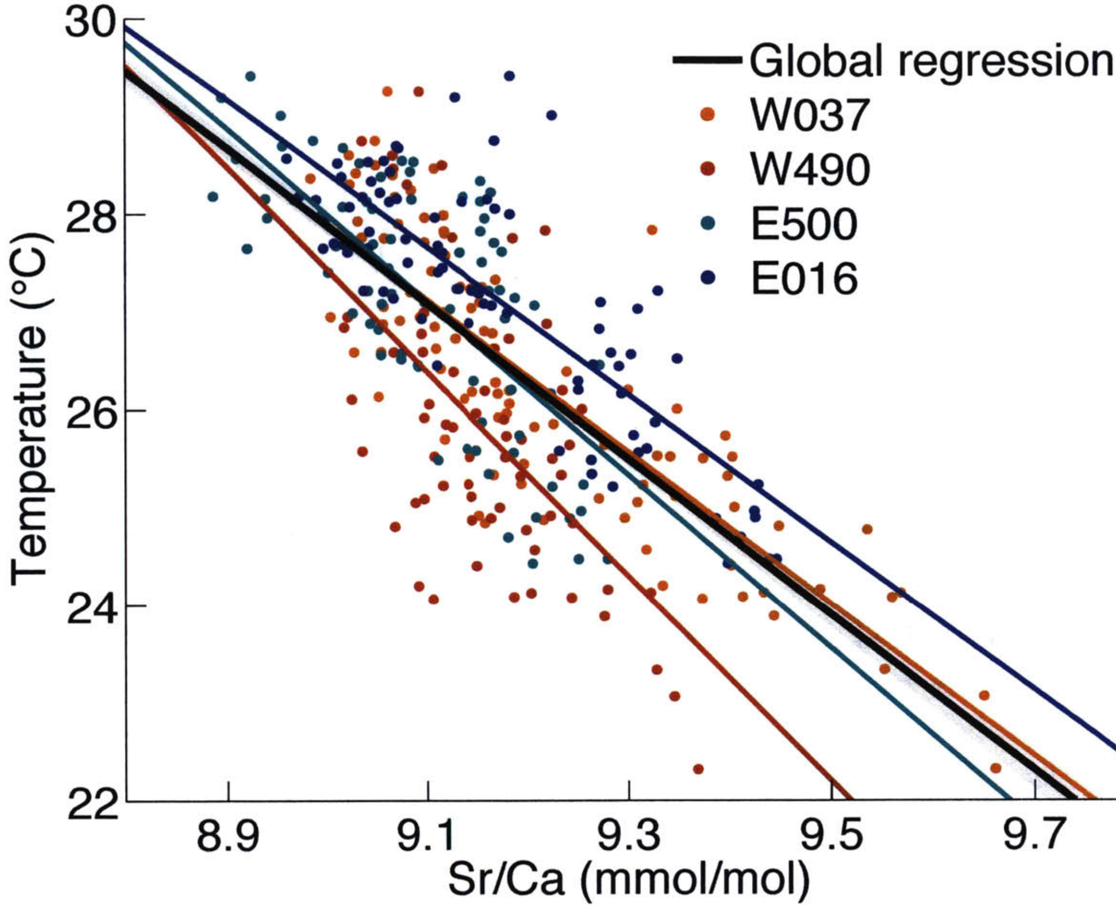

Figure 2-7: Global regression of Sr/Ca onto logger temperatures (black, with shading indicating standard error of prediction, 1.023 ± 0.003°C, 1σ, n = 359). Sr/Ca values and coral-specific regressions for W037, W490, E016, and E500 are plotted in orange, red, blue, and green, respectively.

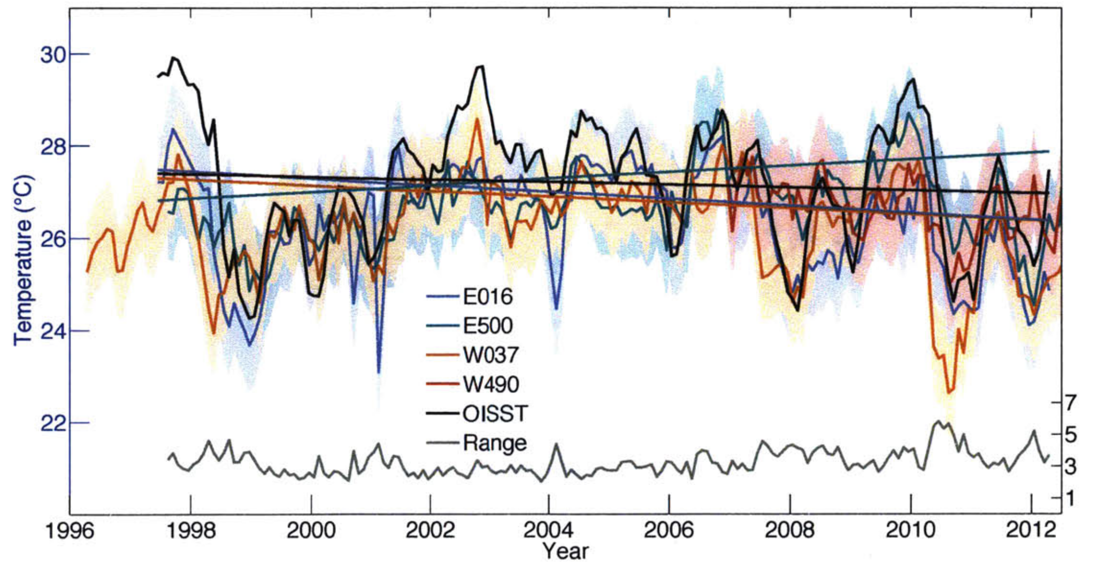

Figure 2-8: Derived temperatures from all four corals generated using the global regression on logger temperature (Figure 2-7). The shading indicates the standard error of prediction for the global regression, 1.023 ± 0.003°C (1σ, n = 359; Table 2-1). The difference between maximum and minimum derived temperatures from all corals at a given time point is plotted in gray and averages 3.8°C over the period covered by all four corals. The solid lines denote the 1997–2012 trends in OISST (black) and coral Sr/Ca records (colors). All trend slopes are within error of each other except for E500, which suggests significant ($p < 0.02$) warming.

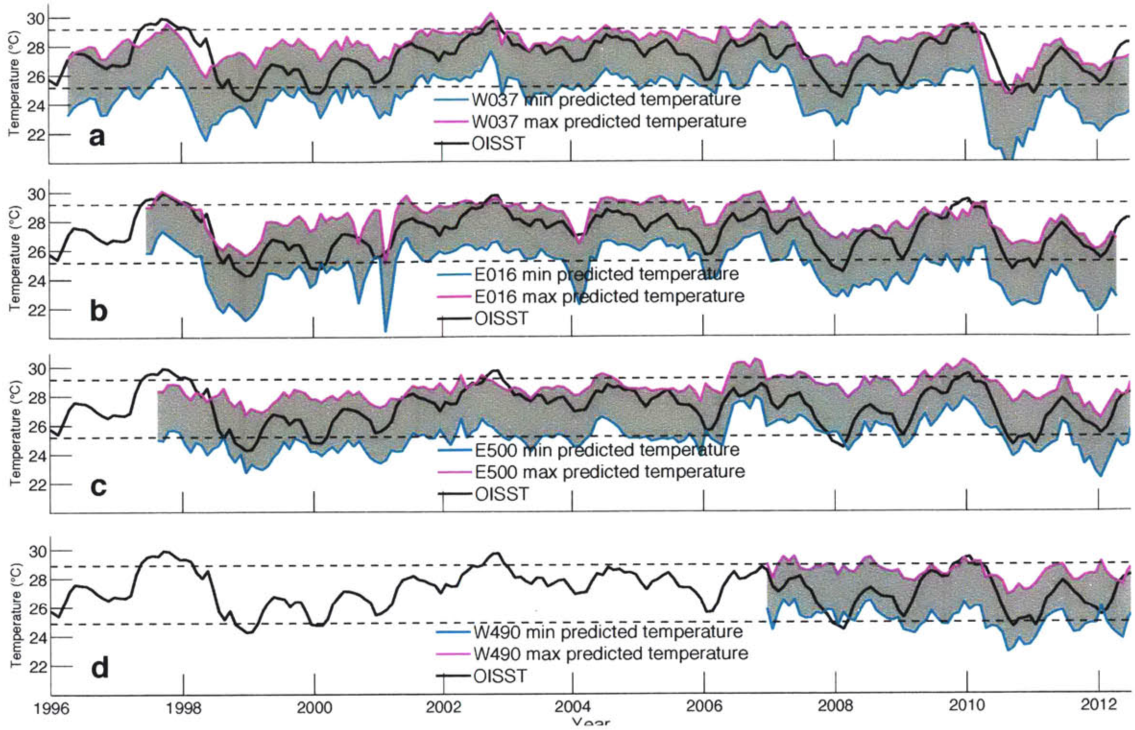

Figure 2-9: (a) Derived temperatures from W037 generated by applying all four regressions on logger temperatures (Figure 2-4) to its Sr/Ca record. The magenta line marks the maximum estimate plus one standard error of prediction, and the blue line marks the minimum estimate minus one standard error of prediction. The gray shading represents the range of possible estimates within ± 1 standard error of prediction. OISST is indicated by the black line, with dashed horizontal lines indicating ± 2°C from the mean for the period covered by the three long records: W037, E016, and E500. (b–d) Same as in Figure 2-9a but for E016, E500, and W490, respectively. The average difference between maximum and minimum derived temperatures over the range of Sr/Ca values measured is 3.7°C.

Table 2-1: Regressions of Sr/Ca on temperature and temperature on Sr/Ca

Coral	Depth (m)	Mean Sr/Ca 2006-2012 (mmol/mol)	Regression of Sr/Ca on *in situ* logger					Regression of Sr/Ca on OISST				
			Slope (mmol/mol /°C)	b (mol/m mol)	R, $p<0.05$	n	Error of prediction (°C)	Slope (mmol/mol /°C)	b (mol/m mol)	R, $p<0.05$	n	Error of prediction (°C)
W037	13m	9.26±0.02	−0.09±0.01	11.6±0.3	-0.84	95		−0.09±0.02	11.7±0.5	-0.72	98	
W490	8m	9.16±0.01	−0.03±0.01	10.0±0.3	-0.58	65		−0.03±0.01	9.9±0.4	-0.47	65	
E500	5m	9.13±0.01	−0.06±0.01	10.6±0.4	-0.7	78		−0.06±0.01	10.7±0.3	-0.69	98	
E016	5m	9.26±0.01	−0.09±0.01	11.6±0.4	-0.81	78		−0.09±0.01	11.7±0.4	-0.81	98	

Coral	Depth (m)	Mean Sr/Ca 2006-2012 (mmol/mol)	Regression of *in situ* logger on Sr/Ca					Regression of OISST on Sr/Ca				
			Slope (°C/mol/ mmol)	b (°C)	R, $p<0.05$	n	Error of prediction (°C)	Slope (°C/mol/ mmol)	b (°C)	R, $p<0.05$	n	Error of prediction (°C)
W037	13m	9.26±0.02	−8±1	98±9	-0.84	95	0.798±0.006[a]	−6±1	78±13	-0.72	98	0.967±0.009[a]
W490	8m	9.16±0.01	−10±1	122±34	-0.58	65	1.21±0.01[a]	−8±4	98±33	-0.47	65	1.19±0.01[a]
E500	5m	9.13±0.01	−9±2	98±19	-0.7	78	0.904±0.006[a]	−9±2	98±33	-0.69	98	0.874±0.009[a]
E016	5m	9.26±0.01	−8±1	96±11	-0.81	78	0.744±0.004[a]	−9±2	112±15	-0.81	98	0.773±0.006[a]
Stack regression								−11±2	124±17	-0.82	65	±1.9[b]
Global regression			−7.9±0.9	99±8	-0.72	359	±1.9[b]					

[a] Standard error of prediction ± 1σ

[b] Range of predicted temperatures

Table 2-2. Trend slopes over period common to three long corals (1997-2012)

Timeseries	Slope	Trend[a]	95% confidence interval
W037 Sr/Ca	0.006 mmol/mol/yr [b]	**cooling**	0.001 to 0.011 mmol/mol/yr
E016 Sr/Ca	0.007 mmol/mol/yr [b]	**cooling**	0.002 to 0.012 mmol/mol/yr
E500 Sr/Ca	-0.007 mmol/mol/yr [c]	**warming**	-0.010 to -0.003 mmol/mol/yr
OISST	-0.029 °C/yr	No trend	-0.076 to 0.018 °C/yr

[a] Trends significant at 95% confidence level in bold

[b] Statistically indistinguishable from each other

[c] Statistically different from other two coral trends

Table 2-3. Trend slopes over period common to west logger composite and OISST (2002-2012)

Timeseries	Slope	Trend[a]	95% confidence interval
W037 Sr/Ca	0.028 mmol/mol/yr [b]	**cooling**	0.021 to 0.036 mmol/mol/yr
E016 Sr/Ca	0.030 mmol/mol/yr [b]	**cooling**	0.024 to 0.037 mmol/mol/yr
E500 Sr/Ca	0.005 mmol/mol/yr [c]	no trend	-0.001 to 0.011 mmol/mol/yr
West logger	-0.300 °C/yr [d]	**cooling**	-0.373 to -0.227 °C/yr
OISST	-0.196 °C/yr [d]	**cooling**	-0.263 to -0.130 °C/yr

[a] Trends significant at 95% confidence level in bold

[b] Statistically indistinguishable from each other

[c] Statistically different from other two coral trends

[d] Statistically indistinguishable from other temperature trend

Table 2-4. Trend slopes over period common to west logger composite, combined east logger, and OISST (2004-2012)

Timeseries	Slope	Trend[a]	95% confidence interval
W037 Sr/Ca	0.039 mmol/mol/yr [b]	**cooling**	0.025 to 0.053 mmol/mol/yr
E016 Sr/Ca	0.041 mmol/mol/yr [b]	**cooling**	0.029 to 0.052 mmol/mol/yr
E500 Sr/Ca	0.001 mmol/mol/yr [c]	no trend	-0.009 to 0.011 mmol/mol/yr
West logger	-0.379 °C/yr [d]	**cooling**	-0.524 to -0.233 °C/yr
East logger	-0.223 °C/yr [d]	**cooling**	-0.345 to -0.101 °C/yr
OISST	-0.204 °C/yr [d]	**cooling**	-0.334 to -0.074

[a] Trends significant at 95% confidence level in bold

[b] Statistically indistinguishable from each other

[c] Statistically different from other two coral trends

[d] Statistically indistinguishable from other temperature trends

Chapter 3

20th century warming of the tropical Atlantic captured by Sr-U paleothermometry[2]

3.1 Abstract

The skeletons of tropical, long-lived corals are valuable archives of ocean conditions with potential to extend the short instrumental record into the past. However, accessing that information has been compromised by uncertainties associated with the application of single element-ratio coral thermometers, including Sr/Ca. A new approach, Sr-U, combines Sr/Ca and U/Ca to constrain the influence of Rayleigh fractionation on the temperature dependence of Sr/Ca [*DeCarlo et al.*, 2016]. Here, we build on the initial Pacific *Porites* Sr-U calibration to include multiple Atlantic and Pacific coral genera spanning a temperature range of 23.2-30.1 °C, and show that Sr-U is strongly correlated with average temperature over which coral growth occurs (R=-0.96, P<0.01, n=19). We constructed a multi-species, spatial Sr-U-SST calibration ($T_{SrU} = -11 \pm 1(SrU - 9) + (28.0 \pm 0.1)$; standard error of prediction = 0.6 °C (1σ, n=19), validated on a *Pocillopora* coral not included in the calibration, and applied it to a Puerto Rico *Orbicella faveolata* to derive a sea surface temperature (SST) record from 1900 to 2010 AD. Comparison of Sr-U derived SST with the instrumental record of SST indicates that Sr-U captures actual SST (within 0.32 °C), multi-decadal variability and the 20th century warming trend (0.06 °C per decade), patterns that were replicated in a second coral from a neighboring island. Conversely, Sr/Ca records from the same two coral cores were inconsistent with each other and did not capture the absolute SST, variability or trends. Our results suggest that Sr-U paleothermometery is promising for

---

[2] Submitted to *Paleoceanography* as: Alice E. Alpert, Anne L. Cohen, Delia W. Oppo, Glenn A. Gaetani, Edwin A. Hernandez-Delgado, Thomas M. DeCarlo, Amos Winter, and Meagan E. Gonneea, Warming of the tropical Atlantic captured by Sr-U paleothermometry.

downcore reconstructions of mean ocean temperatures, multi-decadal variability and centennial trends.

3.2 Introduction

The instrumental record of SST extends back to ~1856 but is considered less reliable with increasingly sparse coverage prior to the 1950s [*Deser et al.*, 2010]. 65 years of reliable data is too short to enable robust assessment of shifts in mean temperature associated with anthropogenic activity [*Latif et al.*, 2006; *Enfield and Cid-Serrano*, 2010; *Solomon et al.*, 2011; *Otto et al.*, 2013; *Trenberth and Fasullo*, 2013] or to characterize multi-decadal variability and trends [*Johns et al.*, 2011; *Kilbourne et al.*, 2014]. The annually-banded skeletons of massive, long-lived corals are a potentially valuable archive of ocean temperature conditions that can be used to extend the instrumental record across space and back in time. Sr/Ca [*Smith et al.*, 1979; *Beck et al.*, 1992] is currently the most widely used coral proxy thermometer [e.g., *Carilli et al.*, 2014; *DeLong et al.*, 2014; *Wu et al.*, 2014; *Thompson et al.*, 2015; *Toth et al.*, 2015]. However, many studies show that Sr/Ca-derived temperatures do not consistently capture mean SST (e.g., *Goodkin et al.* [2005]; *Saenger et al.* [2008]; *Alpert et al.* [2016]), SST trends (e.g., *Smith et al.* [2006]; *Scott et al.* [2010]; *Grove et al.* [2013]; *Carilli et al.* [2014]; *Alpert et al.* [2016]) or multi-decadal variability (e.g., *Nurhati et al.* [2011]) evident in the post-1950 instrumental record. Indeed, reconstructing absolute SST, variability, and trends from Sr/Ca is complicated by "vital effects," processes that distort the temperature dependence of Sr/Ca [*de Villiers et al.*, 1994; *Cohen et al.*, 2002].

Multiple lines of evidence point to effects of Rayleigh fractionation, associated with the precipitation of coral aragonite in a semi-isolated calcifying space, as the source of Sr/Ca "vital effects" [*Cohen et al.*, 2006; *Gaetani and Cohen*, 2006; *Gagnon et al.*, 2007]. When the $CaCO_3$ saturation state of the coral's calcifying fluid is high (low), more (less) aragonite precipitates and its Sr/Ca ratio decreases (increases), and these changes can occur independently of temperature. For example, in laboratory culture, coral Sr/Ca increased with decreasing seawater pH at constant temperature, because the precipitation efficiency of the coral decreases with seawater acidification [*Cohen et al.*, 2009].

A novel paleothermometer, Sr-U, builds on the concept of Rayleigh-based Multielement Thermometry proposed in *Cohen and Gaetani* [2010] and *Gaetani et al.*, [2011], combining element ratios to account for the influence of Rayleigh fractionation on coral Sr/Ca. *DeCarlo et al.* [2015] showed that the U/Ca ratio of aragonite precipitated abiogenically from seawater is dependent on seawater carbonate ion concentration [CO_3^{2-}] and that coral U/Ca tracks the [CO_3^{2-}] of the calcifying fluid. Subsequently, *DeCarlo et al.* [2016] proposed combining coral Sr/Ca and U/Ca to counter the "vital effect" on Sr/Ca. Using a suite of Pacific *Porites* corals collected live from seven coral reef sites, *DeCarlo et al.* [2016] showed that *Porites* Sr-U was strongly correlated with SST over a temperature range from 23.2-30.1 °C.

Here we examine the relationship between Sr-U of four additional coral genera used in paleo-oceanographic SST reconstructions, derive a universal multi-species, multi-ocean Sr-U to SST calibration, and apply the new thermometer down core to construct SST timeseries. We compared the Sr-U-derived SST with Sr/Ca-derived SST timeseries using the same Sr/Ca data.

3.3 Material and Methods:

3.3.1 Corals:

3.3.1.1 Extended Sr-U-SST Spatial Calibration:

We generated Sr/Ca and U/Ca from eight corals representing four Scleractinian genera and seven reef sites (Table 3-1, Figures B-1, B-2, B-3, B-4). All colonies were sampled live (Figure 3-3-3-1, Table 3-1). The Bermuda corals were stained *in situ* with sodium alizarin sulphonate dye in June 2000, on September 18, 2000, and on January 24, 2001 prior to collection on June 1, 2001 (Figure B-5) [*Cohen et al.*, 2004].

All cores and branches were slabbed along the axis of maximum growth using a water-cooled IsoMet 1000 Precision saw, and scanned using the Siemens Volume Zoom Spiral Computerized Tomography (CT) Scanner at the Woods Hole Oceanographic Institution [*Saenger et al.*, 2009; *Vásquez-Bedoya et al.*, 2012] (Figure B-6). Faster growing corals were sub-sampled for solution ICPMS analysis following the procedure described in *Alpert et al.* [2016]. First, the coral slabs were ultra-sonicated in deionized water to remove coral dust. Using annual bands visible in the CT scans to guide sampling resolution, 50-80 µg coral powder was milled at 0.6-1.0 mm intervals (depending on growth rate) using a Minicraft MB170 drill fitted with an 0.3 mm diameter diamond bit.

Two *Pocillopora damicornis* colonies were collected in the Gulf of Chiriqui, Pacific Panama in November 2011, one from the Canales Norte and another from Pacora Island 3.5 km away. Two lateral branches from each of the colonies were sub-sampled along the axis of maximum growth (Figure B7) using a Minicraft MB170 drill fitted with a 0.3 mm diameter diamond bit. No annual bands were visible in CT scans of the branches so we assumed a linear extension rate of ~1.5 cm per year [*Guzmán and Cortés*, 1993] to guide our sampling resolution of 1 mm. As the Sr/Ca and U/Ca values from the two branches of PAN-PD-014 match very closely (Figure B1), we combined data from the two branches into a single dataset. We likewise combined data from the two branches of PAN-PD-017 into a single dataset.

Slow-growing corals, Bermuda *Diploria labyrinthiformis* (BER-DL-003) and *Orbicella franksii* (BER-OF-001) and Yucatan *Siderastrea sideraea* (Jardin C, [*Gonneea*, 2014]) were analyzed using laser ablation-ICPMS. Sections of Bermuda BER-OF-001 and BER-DL-003 were epoxy-mounted in a 25.4 mm diameter aluminum ring, and a thin section of Jardin C was epoxy-mounted on a glass slide. All samples were polished down to 0.3 µm-alumina suspension [*Cohen et al.*, 2004].

3.3.1.2 Temporal reconstruction:

The spatial calibration derived here was used to reconstruct a continuous, inter-annually resolved SST timeseries spanning most of the 20th century. We compared the Sr-U-derived SST record with instrumental SST to assess the ability of Sr-U to capture SST means, inter-annual variability and the 20th century warming trend. Two cores from colonies of *O. faveolata* were analyzed for the timeseries reconstruction. One colony was cored live on Mona Island, Puerto Rico in 2012 in 7 m water depth. The other coral was cored live at Pinacles Reef in 1991 in 7 m water depth. Both cores were CT scanned, slabbed, sonicated and sub-sampled as described above. Sr/Ca and U/Ca values were collected using solution ICPMS.

3.3.2. Inductively-Coupled Plasma Mass Spectrometry:

3.3.2.1. Solution analyses:

Solution analyses followed the procedure described in *Alpert et al.* [2016]. Counts of ^{88}Sr, ^{238}U, and ^{48}Ca were measured on a single-collector Element 2 inductively coupled plasma mass spectrometer (ICPMS) at the Woods Hole Oceanographic Institution. Coral powders from CUR-DL-882, STX-MA-001, PR-MA-003, PAN-PD-014, PAN-PD-017, PR-OF-001, and PR-OF-002 were dissolved in 5% trace metal grade nitric acid. Sr/Ca values were determined by calibration to a curve of standards derived from coral skeleton (JCp-1) [*Okai et al.*, 2002; *Hathorne et al.*, 2013], fish otoliths (FEBS-1, NIES) [*Yoshinaga et al.*, 2000; *Sturgeon*, 2005], and limestone (NBS-1) [*Fernandez et al.*, 2011], and U/Ca values were standardized to JCp-1. Repeated measurements of an in-house secondary coral standard indicate an external precision of ±0.035 mmol/mol (1σ, n=173, 0.4% relative) for Sr/Ca and 0.02 µmol/mol for U/Ca (1σ, n=173, 0.019% relative) and the ICPMS was stable throughout our study. We have previously measured the Sr/Ca and U/Ca values of three aliquots of JCp-1 powder as 8.870 ± 0.028 mmol/mol and 1.23 ± 0.01 µmol/mol [*Alpert et al.*, 2016] which is within uncertainty of the mean, and within the range of precision, reported from JCp-1 analyses conducted in 21 different laboratories [*Hathorne et al.*, 2013].

3.3.2.2. Laser ablation analyses:

Sr/Ca and U/Ca of slow-growing corals (≤5 mm/yr) BER-OF-001, BER-DL-003 and Jardin C were measured using the UP-193 nm New Wave Research laser ablation system mounted to the Element 2 ICPMS at WHOI. We targeted the base of the crystal bundles (fasciculi), generating a sampling track that ran parallel to the centers of calcification, while avoiding the centers themselves

[*Cohen and Thorrold*, 2007]. For BER-DL-003, we used a laser beam 100 µm in diameter at 6Hz with 4 sec dwell time for pre-ablation, 9 Hz and 65 sec dwell time for the ablation. Sampling spots were spaced 250 µm apart. An external USGS carbonate standard MACS-3 was analyzed every 22 samples and used to construct a standard curve forced through the origin. The standard deviation of intensities measured in MACS-3 was 0.9% for Sr/Ca and 4.7% for U/Ca (1σ, n=5). BER-OF-001 spots were 75 µm in diameter centered 150 µm apart, with a 100 µm diameter preablation spot. A die-pressed pellet of JCp-1 coral powder and standard MACS-3 were analyzed every eight samples. Each standard was measured three times and the average value of the three measurements was used to construct a standard curve forced through the origin. The standard deviation of averaged JCp-1 measurements was 1.1% for Sr/Ca and 2.2% for U/Ca (1σ, n=6). The standard deviation of averaged MACS-3 measurements was 1.0% for Sr/Ca and 14.2% for U/Ca (1σ, n=6). For analysis of the Yucatan coral Jardin C, the laser was operated at 10 Hz with a 100 µm spot size centered 200 µm apart. Sr/Ca values were determined using a calibration curve of standards including JCp-1, FEBS-1, and NIES, run every 8 samples. U/Ca values were standardized to JCp-1. We used published values from *Jochum et al.* [2012] for MACS-3 and from *Hathorne et al.* [2013] for JCp-1. Sr/Ca and U/Ca data are provided in Supplementary figures S1, S2, S3, and S4.

3.3.3. Age Models:

With the exception of the *Pocillopora* corals, annual density bands visible in 3-D CT scans were used to construct a first order chronology with an estimated error of ±1 year (Figure B6). The CT-based age models were fine-tuned using the seasonal correlation between Sr/Ca and temperature (e.g., *Guilderson et al.*

[2004]). The maximum "adjustment" of any point was 8 months. The age model for BER-DL-003 was based upon growth rates estimated in *Cohen et al.* [2004]. The slab prepared from BER-OF-001 for laser ablation analyses could not be CT scanned and therefore age control was based upon the assumption that cyclic Sr/Ca variability was related to annual temperature cycles.

3.3.4. Temperature data for the calibration:

In situ logged temperatures are available for Jarvis Island, Palmyra, Palau, Pacora Island and the Red Sea sites [*Pineda et al.*, 2009; *Cantin et al.*, 2010; *Barkley et al.*, 2015; *Alpert et al.*, 2016]. At other sites, logger data were available but discontinuous or not covering the same time period as the coral records. For these sites, we first verified that monthly averaged logger temperatures were consistent with contemporaneous monthly optimal interpolation SSTs (OISST v.3b, *Reynolds et al.* [2002]), which were then used instead.

SST at John Smith's Bay, Bermuda, was recorded daily between 1996 and 2001 by *in situ* Onset Stowaway XTI temperature data loggers at 13 m depth. As this record does not cover the entire period corresponding to the coral analyses and is discontinuous, we compared monthly averaged logger data to OISST values for a $1^\circ x1^\circ$ grid box centered on Bermuda Island. On average the OISST values are 0.17 $^\circ C$ warmer than those of the logger. The correlation coefficient between the two records is 0.92, a student t-test indicates that their means are statistically indistinguishable, and an f-test indicates that their variances are statistically indistinguishable. Therefore we used OISST for the local grid box to estimate temperature at the John Smith's Bay site during the time period over which the coral skeleton was analyzed (1994 to 2000).

SST near Willemstad, Curacao, 14 km east of the coral collection site was recorded daily between March 1999 and September 2000 by an *in situ* Onset HOBO TidbiT v2 temperature logger deployed at 5 m depth. On average the OISST values are 0.02 °C cooler than those of the logger. The correlation coefficient between monthly averaged logger temperature and OISST for this location is 0.99, a student t-test and an f-test indicate that their means and variances respectively, are statistically indistinguishable. Therefore we used OISST for the local gridbox to estimate temperature at the Curacao coral collection site during the time period over which the skeleton was analyzed (2012-2013).

Bihourly water temperature was measured at Buck Island National Monument, St Croix, 8 km away from the coral STX-OA-001 collection site between January 1992 and January 2007 by a Ryan TempMentor 1.0 at a depth of 10 m [*Saenger et al.*, 2008]. As these temperatures were statistically indistinguishable from OISST from the gridbox containing St Croix [*Saenger et al.*, 2008], we used OISST to estimate temperature at the St Croix collection site during the time period over which the skeleton was analyzed (1995-2000).

OISST from Yucatan is in good agreement with average monthly SST recorded at a site within the Puerto Morelos lagoon [*Rodríguez-Martínez et al.*, 2010; *Gonneea*, 2014] and we used OISST to estimate temperature at the collection site.

SST at Mona Island, Puerto Rico was recorded daily between 2009 and 2014 by three *in situ* Onset Stowaway XTI temperature data loggers within 500 m of the PR-OF-001 core location at 12 and 13 m depth. We compared monthly averaged logger data to OISST values for the 1°x1° grid box containing Mona Island. The average difference between temperature from each of the three loggers and OISST is 0.10 °C or less. The correlation coefficients between loggers and OISST are larger than 0.98, student t-tests indicate that their means are statistically indistinguishable, and f-tests indicate that their variances are statistically indistinguishable. Therefore we used OISST for the local grid box to estimate temperature at the Mona Island coral collection site.

SST at Pacora Island, Panama was recorded hourly from May 2001 to March 2002 by an Onset TidbiT temperature data logger deployed at 7 m depth. Its average water temperature is 0.4 °C lower than OISST from the local grid box, so we use logger temperature as the most accurate estimate of water temperature at the coral location. As the logger record is missing the month of April we use OISST from the local grid box for that month in our calculation of average SST at this site.

Logger data are not available for the Canales Norte Panama site so we used monthly OISST temperature as a best estimate for water temperature. Temperature data available for La Parguera, Puerto Rico are based upon bucket measurements made at the dock and are warmer than temperatures at the reef location where the coral colony grew. Instead, OISST temperatures are used for La Parguera and Mona Island, located in the same OISST 1°x1° grid box.

3.3.5. Estimating the temperature range over which coral growth occurs:

Alizarin Red S stainlines emplaced in the Bermuda corals were used to constrain seasonality of skeletal growth and estimate the average temperature over which growth occurs. With the exception of Bermuda, all corals used in this study are from low latitude sites (≤22°) that experience low amplitude seasonal temperature (<6 $^\circ$C) cycles. These sites are characterized by a combination of low amplitude light cycles and a high amount of annual incoming solar energy. Thus we proceeded under the assumption that these corals accrete skeleton throughout the year and we used the mean annual recorded temperature as the mean annual growth temperature. However, at 32 $^\circ$N, Bermuda experiences large seasonality in temperature and light, and independent evidence suggests that coral calcification rates on Bermuda vary by more than a factor of three between summer maxima and winter minima [*Cohen et al.*, 2004; *Venti et al.*, 2014].

Both Bermuda corals analyzed in this study were stained three times (06/02/2000, 09/24/2000, and 01/24/2001) over the course of one year and harvested one year after the first staining (06/01/2001), such that the surface marks a fourth time point [*Cohen et al.*, 2004]. However, the *O. franksii* coral (BER-OF-001) captured only two of three stainlines; the mid-January stainline (01/24/2001) was missing completely, indicating lack of growth during the coolest period of the year. To accurately estimate the temperature over which BER-OF-001 skeletal growth occurred, we measured the distances between stains along the thecal growth axis, using a Nikon SMZ1500 microscope (See Figure B5 and *Cohen et al.* [2004] Figure 3-4). We then weighted the OISST monthly temperature according to the proportions indicated by the stain lines using a code in MATLAB™ designed to minimize the month-to-month difference in growth rate. We estimate that the average growth temperature of BER-OF-001 was 25.12 $^\circ$C, 1.97 $^\circ$C warmer than the average annual temperature at this site (Figure B8).

3.3.6 Temperature reanalysis product

To assess the fidelity of the long SST timeseries constructed from the Sr-U thermometer, we compared the two long Sr-U-derived SST records from Puerto Rico with the National Oceanic and Atmospheric Administration's (NOAA's) Extended Reconstructed Sea Surface Temperature (ERSST v.3b) product [*Smith et al.*, 2008]. ERSST uses global spatial correlation scales identified in satellite data available since 1981. These are combined with spatially and temporally discontinuous observations prior to the satellite era to generate a globally complete gridded dataset extending from 1854 to present. Although the corals were collected on reefs 100 km apart, both collection locations fall within the same grid box so we compare both coral Sr-U-derived SST records to the same ERSST timeseries. We used the same timeseries to assess the Sr/Ca records from the two corals.

3.3.7 Calculation of Sr-U

"Sr-U" is a geochemical quantity determined by the relationship of Sr/Ca and U/Ca values in coral skeleton, as defined by *DeCarlo et al.* [2016]. Combining multiple element/Ca values accounts for the effects of Rayleigh fractionation and the resulting Sr-U value reflects water temperature. We calculated Sr-U according to the expression in *DeCarlo et al.* [2016]:

$$SrU = f(U/Ca)\,;\; U/Ca = 1.1\,\mu mol/mol \qquad \text{(Eq.3-1)}$$

where $f(U/Ca)$ is the slope and intercept resulting from ordinary least squares regression of Sr/Ca on U/Ca for a given time period examined on a given coral colony, evaluated at U/Ca of 1.1 µmol/mol (Figure 3-2A, Table 3-1). Since a distribution of Sr/Ca and U/Ca values is needed to determine their relationship $f(U/Ca)$, Sr/Ca and U/Ca data spanning several years are required to generate a single Sr-U value, thus there is an upper limit to the temporal resolution of SST reconstructions using Sr-U. The possible temporal resolution is typically better where SST variability, and hence geochemical variability, is seasonal rather than inter-annual since a greater range in Sr/C and U/Ca is captured over a shorter time span.

We applied the spatial Sr-U and Sr/Ca calibrations (Eq.3-2 and 3-3) to generate inter-annually-resolved multi-decade long SST records from two *O. faveolata* corals collected on Mona Island (PR-OA-001 spanning 1897-2011) and Pinacles Reef (PR-OA-002, spanning 1951-1991), Puerto Rico. Neither coral was used to construct the calibrations. First we calculated an Sr-U value for a 3-year period, or "bin," at the top of PR-OA-001 spanning the period 2008-2011 and centered at 2009.5. Then we calculated another Sr-U value for the 3-year period beginning 1.5 years before the beginning of the top bin, now spanning 2006.5-2009.5 and centered at 2008. We continued to shift the beginning of each bin back in time by 1.5 years to create a timeseries of Sr-U values with nominal resolution of 1.5 years (Figure 3-3A). We repeated this for coral PR-OA-002. We also generated Sr/Ca timeseries, averaging Sr/Ca values for each core over the same bins used to calculate Sr-U values.

3.3.7 Statistics

Throughout this paper we use the ordinary least squares method for regression and the ANOVA function in MATLAB to compare trend slopes. We use a 95% confidence level (α=0.05) for statistical significance and uncertainty is reported as $\pm 1\sigma$.

3.4 Results

3.4.1 Spatial Calibration:

In Figure 3-2A, Sr-U for each coral analyzed for the spatial calibration is plotted against the average annual growth temperature for each coral. The original *Porites* data [*DeCarlo et al.*, 2016] are included. The correlation between Sr-U of multiple coral species and temperature is highly significant over the temperature range 23.2 to 30.1 °C (R=-0.96, P<0.01, n=19, Figure 3-2A, Table 3-1).

We derived an expression relating Sr-U to mean annual growth temperature, using ordinary least squares to regress temperature on Sr-U:

$$T_{SrU} = -11 \pm 1(SrU - 9) + (28.0 \pm 0.1) \qquad \text{(Eq.3-2)}$$

where *Sr-U* the value resulting from Eq.3-1 and T_{SrU} is the resulting derived temperature. The standard error of prediction of this regression is 0.6 °C (1σ, n=19). This expression derived using corals from five genera distributed in both the Pacific and Atlantic oceans is statistically indistinguishable from that of *DeCarlo et al.* [2016] derived using only Pacific *Porites* corals.

The average Sr/Ca ratio of each coral, over the same time period, is shown in Figure 3-2B, also against average annual growth temperature. We also derived an expression relating mean Sr/Ca to mean annual growth temperature using ordinary least squares:

$$T_{Sr/ca} = -8 \pm 2(\overline{SrCa}) + 102 \pm 17 \qquad \text{(Eq.3-3)}$$

where $\overline{Sr/Ca}$ is mean Sr/Ca in mmol/mol and $T_{Sr/Ca}$ is the resulting derived temperature (R=-0.76, P<0.01, n=19). The mean standard error of prediction of this regression is 1.4 °C (1σ, n=19).

3.4.2 Verification

We withheld a second *P. damicornis* colony (PAN-PD-017) from the extended spatial calibration and used it to validate the calibration. Estimated mean temperature from this second colony is 0.7 °C cooler than *in situ* temperature logger data (Figure 3-4), just outside the 1σ of the standard error of prediction for the Sr-U thermometer.

3.4.3 Timeseries

Application of the spatial Sr-U to SST calibration to two *O. faveolata* corals that were excluded from the calibration captured absolute SST, multi-decadal variability and the 20th century warming trend. The mean difference between PR-OF-001 Sr-U derived SST and ERSST over the full time period of the record is 0.31 °C and Sr-U derived SST accurately captures the 20th century warming trend of 0.06 °C/decade, which is statistically indistinguishable from that in the ERSST reanalysis product [*Smith et al.*, 2008] over the same time period (Table 3-2). The Sr-U derived SST from PR-OF-001 also captures the timing of interannual variability evident in the instrumental record ($R=0.62$, $p<0.01$, $n=62$) but overestimates the amplitude, by 0.3 °C on average (Figure 3-3A). *In situ* logger temperature records from the coral sampling site on Mona Island, albeit of short duration, are consistent with satellite SST. Therefore, we assume the satellite SST accurately represents in situ SST and it is the coral that overestimates the actual SST variability on inter-annual timescales. 98% of individual Sr-U values from PR-OF-001 versus instrumental temperature fall within the 95% confidence interval of the calibration line (Figure 3-5A). Although these data predict the same mean temperature as the calibration, the timeseries data form a trend with a shallower slope, such that warm temperatures have slightly lower Sr-U values and cold temperatures have slightly higher Sr-U values. Using the calibration line therefore overestimates both warming and cooling. (Figure 3-3A). We hypothesize that because the Sr-U to SST calibration is derived from time series of Sr/Ca and U/Ca as long as 12 years accurate reconstruction of variability on $\leq$ 3-year timescales is not yet possible with the calibration derived here.

To test our hypothesis, we binned the Sr-U data from PR-OF-001 into 10-year bins staggered by 5 years (Figure 3-5B), with nominal resolution of 5 years. On this multidecadal timescale, the derived temperatures accurately capture the amplitude of variability in ERSST. Variability in derived and instrumental temperatures remains highly correlated but the mean difference in amplitude is reduced to 0.2 $^\circ$C (for 10-year bins, $R=0.79$, $p<0.01$, $n=17$, Figure 3-5B and 5C).

Sr-U derived SST from PR-OF-001 and PR-OF-002 is in good agreement for the overlapping time period (1951-1991), differing on average by 0.4 $^\circ$C (Figure 3-3A). The two timeseries are also significantly correlated ($R=0.71$, $p<0.01$, $n=24$, Figure 3-6).

Conversely, Sr/Ca does not correlate with OISST for either coral on seasonal, annual, 3-year, or 5-year time-scales and we were therefore unable to construct an Sr/Ca-SST calibration at either site. Thus, we took the same approach with Sr/Ca as we did with Sr-U, applying the spatial Sr/Ca-SST calibration (Eq.3-3) to the downcore Sr/Ca record from the same *O. faveolata* colonies (Figure 3-3B). We compared the Sr/Ca-derived SST records from each coral with the ERSST reanalysis product. Contemporaneous Sr/Ca values from the two colonies are not correlated ($R=-0.20$, $P=0.35$, $n=24$, Figure 3-6) and differ on average by 0.10 mmol/mol, an equivalent of 0.8 $^\circ$C. The mean Sr/Ca derived temperature from PR-OF-001 is 1.9 $^\circ$C cooler than ERSST and the mean Sr/Ca derived temperature from PR-OF-002 is 2.1 $^\circ$C cooler than ERSST. The PR-OF-001 Sr/Ca record fails to capture the 20th century warming trend but instead shows a cooling trend (not statistically significant, Table 3-2). The absence of a warming trend and underestimated temperatures hold when bin size is increased to 5 years (Figure 3-5C).

Typically, temporal, not spatial calibrations are applied to reconstruct SST from Sr/Ca. As noted, the absence of a strong correlation between Sr/Ca and ERSST precluded deriving local calibrations at these sites, consistent with previous work from a nearby coral core [*Kilbourne et al.*, 2008; 2010]. Many temporal Sr/Ca-SST calibrations exist for Caribbean *Orbicella spp.* including one derived from stained colonies using *in situ* logged temperatures [*Swart et al.*, 2002], and which was previously used to reconstruct SST near Puerto Rico [*Kilbourne et al.*, 2008; 2010]. We applied this and other calibration equations from the Caribbean [*Saenger et al.*, 2008] to the Sr/Ca timeseries from PR-OF-001 (Figure 7). Regardless of calibration, none of the SST reconstructions derived using only Sr/Ca accurately estimate mean SST or capture the 20th century warming trend (Table 3-2); in fact derived temperatures using the other calibrations underestimate mean SST even more than using the spatial calibration.

3.5 Discussion and outlook

Extending the short instrumental record of SST across space and back in time is a high priority for paleoceanographic studies. The skeletons of annually banded, long-lived corals are ideal archives of oceanographic variability, capable of recording information at sub-seasonal resolution, continuously for many centuries, and fossil corals can be accurately dated with U-series. Single element ratio thermometers, including Sr/Ca, have been applied to corals with mixed success, largely due to the distortion of the temperature-dependence of element/Ca by "vital effects." In response to the recognition that "vital effects" limit the interpretation of paleoclimate records, new thermometers based on fundamental understanding of element partitioning and coral biomineralization processes, have been proposed, including Li/Mg [*Montagna et al.*, 2014], RBME [*Cohen and Gaetani*, 2010; *Gaetani et al.*, 2011] and Sr-U [*DeCarlo et al.*, 2016].

This study focused on expanding and applying the Sr-U thermometer across space and coral genera, and through time. We expanded the initial *Porites*-only Sr-U to SST calibration to include multiple Pacific and Atlantic coral genera that are commonly used in paleo-climate reconstructions, and used the multi-genera spatial calibration to test the ability of Sr-U to capture mean SST, multi-decadal variability and century-long trends in two corals from the tropical Atlantic.

Our results show that Sr-U of multiple coral genera (*Porites, Siderastrea, Diploria, Orbicella, Pocillopora*), calculated from seasonally-resolved Sr/Ca and U/Ca data generated for each coral over several consecutive years, correlates with the mean SST of the same interval, over a temperature range spanning 23.2-30.1 °C ($R=-0.96$, $P<0.01$, $n=19$, $1\sigma=0.6$ °C, Figure 3-2A, Table 3-1). In Bermuda corals that exhibit strongly seasonal growth or no growth for part of the year, Sr-U correlates with the estimated temperature over which growth occurs. There is a strong possibility that the difference we observed between mean annual temperature and mean growth temperature will have to be considered when conducting Sr-U thermometry using corals from other high latitude reef sites.

Application of the multi-genera spatial calibration to Sr-U timeseries from two *O. faveolata* corals from Puerto Rico that were not included in the calibration (Figure 3-3A) accurately capture mean SST over the full length of each record to within 0.5 $^\circ$C, as well as the 20th century warming trend and timing of inter-annual variability. Further development of Sr-U thermometry will focus on increasing the temporal resolution over which SST can be derived, currently estimated to be 5 years. Nevertheless, despite this current limitation, our results show that Sr-U thermometry accurately captures much of the information needed for interpretation of climate variability and change: absolute SST, decadal variability and long-term trends. Further, Sr-U derived SST is a marked improvement over Sr/Ca-derived SSTs, which at our sites failed to capture the 20th century warming trend and were 1.9-2.1 $^\circ$C colder than observed.

3.6 Acknowledgments:

We are grateful to Kathryn Pietro (WHOI) and Gretchen Swarr (WHOI) for lab assistance; the entire crew of Seadragon and to Emily Penn and Ron Ritter of Pangaea Exploration; to Pat Lohmann (WHOI), Kathryn Pietro (WHOI), Ann Tarrant (WHOI), and Richard Camilli (WHOI) for assistance collecting corals; to Roy Armstrong (UPR) for providing the Mayaguez Bay coral; to Jose Pineda (WHOI) for providing temperature logger data; and to Mark Vermeij of Carmabi, Curacao for providing temperature logger data and permitting assistance.

This study was supported by an NSF Graduate Research Fellowship to A.A., NSF-OCE-1338320 to G.A.G and A.L.C., NSF-OCE-1031971 to A.L.C., NSF-OCE-0926986 to A.L.C and D.W.O., and WHOI Access to the Sea #27500056. The authors declare no competing financial interest. The coral geochemical data used in this paper is included in a supplementary dataset

available online and will be archived at http://www.ncdc.noaa.gov/data-access/paleoclimatology-data/datasets.

3.7 References:

Alpert, A. E., A. L. Cohen, D. W. Oppo, T. M. DeCarlo, J. M. Gove, and C. W. Young (2016), Comparison of equatorial Pacific sea surface temperature variability and trends with Sr/Ca records from multiple corals, *Paleoceanography 31*(2). doi: 10.1002/2015PA002897

Barkley, H. C., A. L. Cohen, Y. Golbuu, V. R. Starczak, T. M. DeCarlo, and K. E. Shamberger (2015), Changes in coral reef communities across a natural gradient in seawater pH, *Science advances*, *1*(5), e1500328

Beck, J. W., R. L. Edwards, E. Ito, F. W. Taylor, J. Recy, F. Rougerie, P. Joannot, and C. Henin (1992), Sea-surface temperature from coral skeletal strontium/calcium ratios, *Science*, *257*(5070), 644-647

Cantin, N. E., A. L. Cohen, K. B. Karnauskas, A. M. Tarrant, and D. C. McCorkle (2010), Ocean warming slows coral growth in the central Red Sea, *Science*, *329*(5989), 322-325

Carilli, J. E., H. V. McGregor, J. J. Gaudry, S. D. Donner, M. K. Gagan, S. Stevenson, H. Wong, and D. Fink (2014), Equatorial Pacific coral geochemical records show recent weakening of the Walker Circulation, *Paleoceanography*, *29*(11), 1031-1045. doi:10.1002/2014PA002683.

Cohen, A., and G. Gaetani (2010), Ion partitioning and the geochemistry of coral skeletons: solving the mystery of the vital effect, *EMU Notes in Mineralogy*, *11*, 377-397.

Cohen, A., and S. R. Thorrold (2007), Recovery of temperature records from slow-growing corals by fine scale sampling of skeletons, *Geophysical Research Letters*, *34*(17). doi:10.1029/2007GL030967.

Cohen, A., K. E. Owens, G. D. Layne, and N. Shimizu (2002), The effect of algal symbionts on the accuracy of Sr/Ca paleotemperatures from coral, *Science*, *296*(5566), 331-333

Cohen, A., G. A. Gaetani, T. Lundälv, B. H. Corliss, and R. Y. George (2006), Compositional variability in a cold-water scleractinian, Lophelia pertusa: New insights into "vital effects", *Geochemistry, Geophysics, Geosystems*, *7*(12). doi:10.1029/2006GC001354.

Cohen, A., D. C. McCorkle, S. de Putron, G. A. Gaetani, and K. A. Rose (2009), Morphological and compositional changes in the skeletons of new coral recruits reared in acidified seawater: Insights into the biomineralization response to ocean acidification, *Geochemistry, Geophysics, Geosystems*, *10*(7). doi:10.1002/ggge.20095.

Cohen, A. L., S. R. Smith, M. S. McCartney, and J. van Etten (2004), How brain corals record climate: an integration of skeletal structure, growth and chemistry of Diploria labyrinthiformis from Bermuda, *Marine Ecology Progress Series*, *271*, 147-158

de Villiers, S., G. T. Shen, and B. K. Nelson (1994), The SrCa-temperature relationship in coralline aragonite: Influence of variability in (SrCa) seawater and skeletal growth parameters, *Geochimica et Cosmochimica Acta*, *58*(1), 197-208

DeCarlo, T. M., G. A. Gaetani, M. Holcomb, and A. L. Cohen (2015), Experimental determination of factors controlling U/Ca of aragonite precipitated from seawater: Implications for interpreting coral skeleton, *Geochimica et Cosmochimica Acta*, *162*, 151-165

DeCarlo, T. M., G. A. Gaetani, A. L. Cohen, G. L. Foster, A. E. Alpert, and J. Stewart (2016), Coral Sr-U Thermometry, *Paleoceanography.*

DeLong, K. L., J. A. Flannery, R. Z. Poore, T. M. Quinn, C. R. Maupin, K. Lin, and C. C. Shen (2014), A reconstruction of sea surface temperature variability in the southeastern Gulf of Mexico from 1734–2008 CE using cross-dated Sr/Ca records from the coral Siderastrea siderea, *Paleoceanography*, *29*(5). doi:10.1002/2013PA002524.

Deser, C., M. A. Alexander, S.-P. Xie, and A. S. Phillips (2010), Sea surface temperature variability: Patterns and mechanisms, *Annual Review of Marine Science*, *2*, 115-143.

Enfield, D. B., and L. Cid-Serrano (2010), Secular and multidecadal warmings in the North Atlantic and their relationships with major hurricane activity, *International Journal of Climatology*, *30*(2), 174-184

Fernandez, D. P., A. C. Gagnon, and J. F. Adkins (2011), An Isotope Dilution ICP-MS Method for the Determination of Mg/Ca and Sr/Ca Ratios in Calcium Carbonate, *Geostandards and Geoanalytical Research*, *35*(1), 23-37

Gaetani, G. A., and A. L. Cohen (2006), Element partitioning during precipitation of aragonite from seawater: a framework for understanding paleoproxies, *Geochimica et Cosmochimica Acta*, *70*(18), 4617-4634

Gaetani, G. A., A. L. Cohen, Z. Wang, and J. Crusius (2011), Rayleigh-based, multi-element coral thermometry: A biomineralization approach to developing climate proxies, *Geochimica et Cosmochimica Acta*, *75*(7), 1920-1932

Gagnon, A. C., J. F. Adkins, D. P. Fernandez, and L. F. Robinson (2007), Sr/Ca and Mg/Ca vital effects correlated with skeletal architecture in a scleractinian deep-sea coral and the role of Rayleigh fractionation, *Earth and Planetary Science Letters*, *261*(1), 280-295

Gonneea, M. E. (2014), Temporal variability in chemical cycling of the subterranean estuary and associated chemical loading to the coastal ocean, Massachusetts Institute of Technology and Woods Hole Oceanographic Institution.

Goodkin, N. F., K. A. Hughen, A. L. Cohen, and S. R. Smith (2005), Record of Little Ice Age sea surface temperatures at Bermuda using a growth-dependent calibration of coral Sr/Ca, *Paleoceanography*, *20*(4). doi:10.1029/2005PA001140.

Grove, C. A., S. Kasper, J. Zinke, M. Pfeiffer, D. Garbe-Schönberg, and G. J. A. Brummer (2013), Confounding effects of coral growth and high SST variability on skeletal Sr/Ca: implications for coral paleothermometry, *Geochemistry, Geophysics, Geosystems*, *14*(4), 1277-1293. doi:10.1002/ggge.20095.

Guilderson, T., D. Schrag, and M. Cane (2004), Surface water mixing in the Solomon Sea as documented by a high-resolution coral 14C record, *Journal of Climate*, *17*(5), 1147-1156

Guzmán, H., and J. Cortés (1993), Comparison between Caribbean and eastern Pacific coral reefs, *Revista de biología tropical*, *41*(3A), 535-557

Hathorne, E. C., A. Gagnon, T. Felis, J. Adkins, R. Asami, W. Boer, N. Caillon, D. Case, K. M. Cobb, and E. Douville (2013), Inter-laboratory study for coral Sr/Ca and other element/Ca ratio measurements, *Geochemistry, Geophysics, Geosystems*. doi:10.1002/ggge.20230.

Jochum, K. P., D. Scholz, B. Stoll, U. Weis, S. A. Wilson, Q. Yang, A. Schwalb, N. Börner, D. E. Jacob, and M. O. Andreae (2012), Accurate trace element analysis of speleothems and biogenic calcium carbonates by LA-ICP-MS, *Chemical Geology*, *318*, 31-44

Johns, W. E., M. O. Baringer, L. Beal, S. Cunningham, T. Kanzow, H. L. Bryden, J. Hirschi, J. Marotzke, C. Meinen, and B. Shaw (2011), Continuous, array-based estimates of Atlantic Ocean heat transport at 26.5 N, *Journal of Climate*, *24*(10), 2429-2449

Kilbourne, K., T. Quinn, R. Webb, T. Guilderson, J. Nyberg, and A. Winter (2008), Paleoclimate proxy perspective on Caribbean climate since the year 1751: Evidence of cooler temperatures and multidecadal variability, *Paleoceanography*, *23*(3). doi:10.1029/2008PA001598.

Kilbourne, K., T. Quinn, R. Webb, T. Guilderson, J. Nyberg, and A. Winter (2010), Coral windows onto seasonal climate variability in the northern Caribbean since 1479, *Geochemistry, Geophysics, Geosystems*, *11*(10). doi:10.1029/2010GC003171.

Kilbourne, K. H., M. A. Alexander, and J. A. Nye (2014), A low latitude paleoclimate perspective on Atlantic multidecadal variability, *Journal of Marine Systems*, *133*, 4-13

Latif, M., M. Collins, H. Pohlmann, and N. Keenlyside (2006), A review of predictability studies of Atlantic sector climate on decadal time scales, *Journal of Climate*, *19*(23), 5971-5987

Montagna, P., M. McCulloch, E. Douville, M. L. Correa, J. Trotter, R. Rodolfo-Metalpa, D. Dissard, C. Ferrier-Pages, N. Frank, and A. Freiwald (2014), Li/Mg systematics in scleractinian corals: Calibration of the thermometer, *Geochimica et Cosmochimica Acta*, *132*, 288-310

Nurhati, I. S., K. M. Cobb, and E. Di Lorenzo (2011), Decadal-scale SST and salinity variations in the central tropical Pacific: Signatures of natural and anthropogenic climate change, *Journal of Climate*, *24*(13), 3294-3308

Okai, T., A. Suzuki, H. Kawahata, S. Terashima, and N. Imai (2002), Preparation of a New Geological Survey of Japan Geochemical Reference Material: Coral JCp-1, *Geostandards newsletter*, *26*(1), 95-99

Otto, A., F. E. Otto, O. Boucher, J. Church, G. Hegerl, P. M. Forster, N. P. Gillett, J. Gregory, G. C. Johnson, and R. Knutti (2013), Energy budget constraints on climate response, *Nature Geoscience*, *6*(6), 415-416

Pineda, J., N. B. Reyns, and V. R. Starczak (2009), Complexity and simplification in understanding recruitment in benthic populations, *Population ecology*, *51*(1), 17-32

Reynolds, R. W., N. A. Rayner, T. M. Smith, D. C. Stokes, and W. Wang (2002), An improved in situ and satellite SST analysis for climate, *Journal of Climate*, *15*(13), 1609-1625

Rodríguez-Martínez, R. E., F. Ruíz-Rentería, B. v. Tussenbroek, G. Barba-Santos, E. Escalante-Mancera, G. Jordán-Garza, and E. Jordán-Dahlgren (2010), Environmental state and tendencies of the Puerto Morelos CARICOMP site, Mexico, *Revista de biología tropical*, *58*, 23-43

Saenger, C., A. L. Cohen, D. W. Oppo, and D. Hubbard (2008), Interpreting sea surface temperature from strontium/calcium ratios in Montastrea corals: Link with growth rate and implications for proxy reconstructions, *Paleoceanography*, *23*(3). doi:10.1029/2007PA001572.

Saenger, C., A. L. Cohen, D. W. Oppo, R. B. Halley, and J. E. Carilli (2009), Surface-temperature trends and variability in the low-latitude North Atlantic since 1552, *Nature Geoscience*, *2*(7), 492-495

Scott, R. B., C. L. Holland, and T. M. Quinn (2010), Multidecadal trends in instrumental SST and coral proxy Sr/Ca records, *Journal of Climate*, *23*(5), 1017-1033

Smith, J. M., T. M. Quinn, K. P. Helmle, and R. B. Halley (2006), Reproducibility of geochemical and climatic signals in the Atlantic coral Montastraea faveolata, *Paleoceanography*, *21*(1). doi: 10.1029/2005PA001187

Smith, S., R. Buddemeier, R. Redalje, and J. Houck (1979), Strontium-calcium thermometry in coral skeletons, *Science*, *204*(4391), 404-407

Smith, T. M., R. W. Reynolds, T. C. Peterson, and J. Lawrimore (2008), Improvements to NOAA's historical merged land-ocean surface temperature analysis (1880-2006), *Journal of Climate*, *21*(10), 2283-2296

Solomon, A., L. Goddard, A. Kumar, J. Carton, C. Deser, I. Fukumori, A. M. Greene, G. Hegerl, B. Kirtman, and Y. Kushnir (2011), Distinguishing the roles of natural and anthropogenically forced decadal climate variability: implications for prediction, *Bulletin of the American Meteorological Society*, *92*(2), 141

Sturgeon, R. E., S. N. Willie, L. Yang, R. Greenberg, R. O. Spatz, Z. Chen, C. Scriver, V. Clancy, J. W. Lam, and S. Thorrold (2005), Certification of a fish otolith reference ma- terial in support of quality assurance for trace element analysis, *J. Anal. At. Spectrom*, *20*(10), 1067–1071

Swart, P., H. Elderfield, and M. Greaves (2002), A high-resolution calibration of Sr/Ca thermometry using the Caribbean coral Montastraea annularis, *Geochemistry, Geophysics, Geosystems*, *3*(11), 1-11. doi:10.1029/2002GC000306.

Thompson, D. M., J. E. Cole, G. T. Shen, A. W. Tudhope, and G. A. Meehl (2015), Early twentieth-century warming linked to tropical Pacific wind strength, *Nature Geoscience*, *8*(2), 117-121

Toth, L. T., R. B. Aronson, K. M. Cobb, H. Cheng, R. L. Edwards, P. R. Grothe, and H. R. Sayani (2015), Climatic and biotic thresholds of coral-reef shutdown, *Nature Climate Change*, *5*, 369-374

Trenberth, K. E., and J. T. Fasullo (2013), An apparent hiatus in global warming?, *Earth's Future*, *1*(1), 19-32

Vásquez-Bedoya, L. F., A. L. Cohen, D. W. Oppo, and P. Blanchon (2012), Corals record persistent multidecadal SST variability in the Atlantic Warm Pool since 1775 AD, *Paleoceanography*, *27*(3). doi: 10.1029/2012PA002313

Venti, A., A. Andersson, and C. Langdon (2014), Multiple driving factors explain spatial and temporal variability in coral calcification rates on the Bermuda platform, *Coral Reefs*, *33*(4), 979-997

Wu, H. C., M. Moreau, B. K. Linsley, D. P. Schrag, and T. Corrège (2014), Investigation of sea surface temperature changes from replicated coral Sr/Ca variations in the eastern equatorial Pacific (Clipperton Atoll) since 1874, *Palaeogeography, Palaeoclimatology, Palaeoecology*, *412*, 208-222

Yoshinaga, J., A. Nakama, M. Morita, and J. S. Edmonds (2000), Fish otolith reference material for quality assurance of chemical analyses, *Marine Chemistry*, *69*(1), 91-97

3.8 Figures and tables

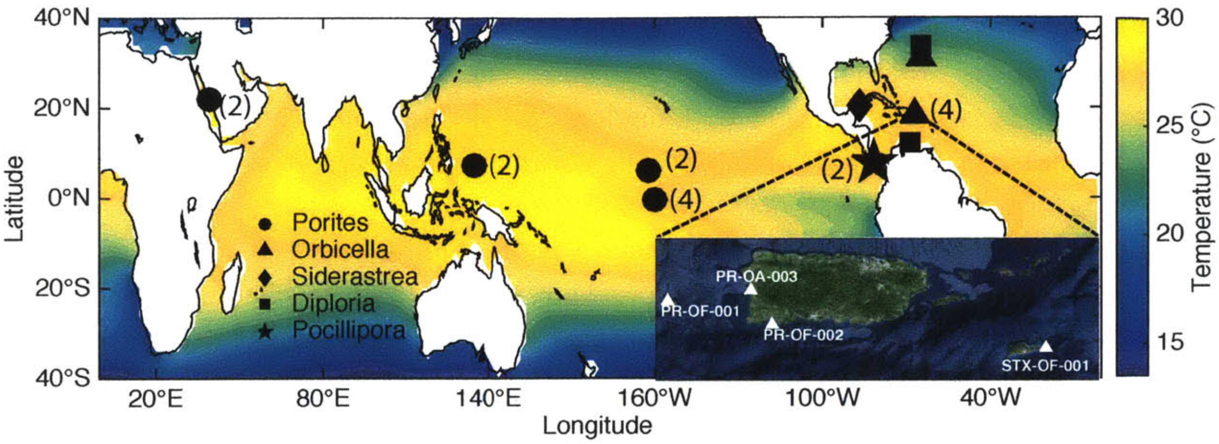

Figure 3-1. Map of 1981-2015 mean OISST [*Reynolds et al.*, 2002] showing locations of corals used in this study. Circles represent *Porites* sp., triangles represent *Orbicella* sp., squares represent *Diploria labyrinthiformis*, the diamond represents a *Siderastrea siderea*, and the star represents two *Pocillopora damicornis* colonies. *Porites* sp. were previously published in *DeCarlo et al.*, [*2016*], all others are new to this study.

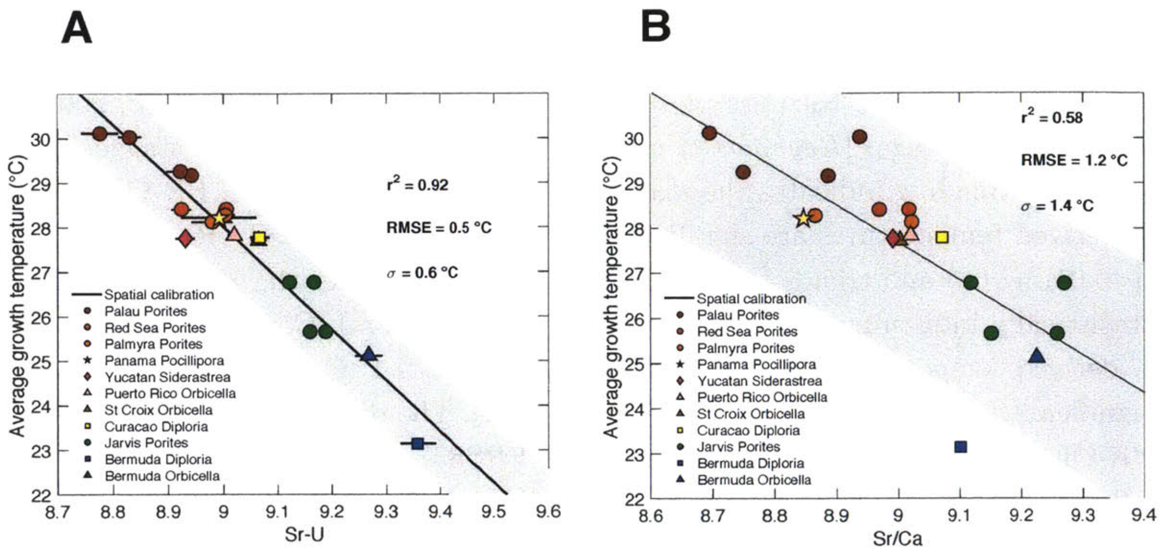

Figure 3-2. A) Regression of coral Sr-U onto average temperature. Temperatures for Bermuda corals are adjusted to reflect temperature over which growth occurs. Horizontal error bars represent the error on each Sr-U (1σ) value, i.e., the uncertainty of Sr/Ca at U/Ca=1.1 μmol/mol for a given coral. Shading indicates the 95% confidence interval for the regression. 1σ propagated uncertainty of prediction for reconstructed temperatures is 0.7 ° C, 1σ standard error of prediction is 0.6 ° C.
B) Regression of mean Sr/Ca onto average temperature. Temperatures for Bermuda corals are adjusted to reflect temperature over which growth occurs. Horizontal error bars represent the standard error of the mean Sr/Ca (1σ) for each coral based upon an analytical error of 0.035 mmol/mol. Shading indicates the 95% confidence interval for the regression. 1σ standard error of prediction is 1.4 ° C.

Figure 3-3. A) Temperatures derived using the spatial Sr-U calibration shown in Figure 3-2A: timeseries from *O. faveolata* PR-OF-001 (red) and PR-OF-002 (purple) from Puerto Rico are plotted with ERSST (black) [*Smith et al.,* 2008] and OISST (orange) [*Reynolds et al.*, 2002]. Data are in 3-year bins staggered by 1.5 years. Shading indicates the standard error of prediction (1σ). PR-OF-001 Sr-U derived temperatures are significantly correlated with ERSST ($R=0.62$, $p<0.01$, $n=62$) and trends for PR-OF-001 and ERSST over the 20th century are statistically indistinguishable (shown in respective colors). Contemporaneous Sr-U derived temperatures from the two cores average 0.4 °C apart and are significantly correlated ($R=0.71$, $p<0.01$, $n=24$). The difference in mean between PR-OF-001 Sr-U derived temperatures and ERSST over the 20th century is <0.3 °C. When the spatial Sr-U regression is applied to PR-OF-002, the difference between PR-OF-002 mean derived temperatures and ERSST is 0.3 °C. B) Temperatures derived from the same two *O. faveolata* corals using the spatial Sr/Ca calibration (Figure 3-2B): PR-OF-001 (green) and PR-OF-002 (brown). Shading indicates the analytical standard error of the mean (1σ). There is no trend in PR-OF-001 derived temperatures over the 20th century. Seasonal, annual, 3-year mean, and 5-year mean Sr/Ca does not correlate with OISST for either core. The mean difference between PR-OF-001 Sr/Ca derived temperatures and ERSST over the 20th century is 1.9 °C. When the spatial Sr/Ca regression is applied to PR-OF-002, the mean difference between PR-OF-002 derived temperatures and ERSST is 2.1 °C.

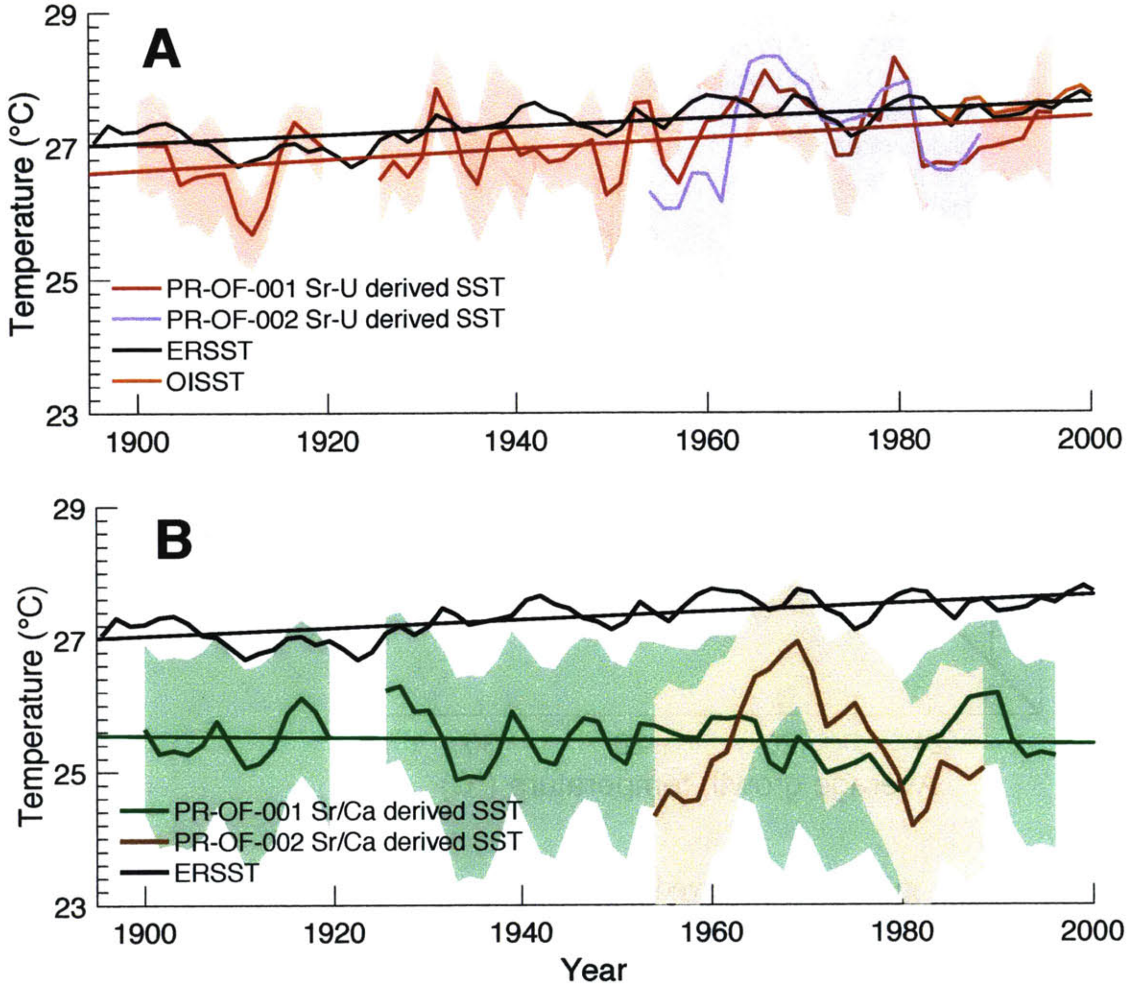
A
B
Temperature (°C)
Year
29
27
25
23
1900
1920
1940
1960
1980
2000
PR-OF-001 Sr-U derived SST
PR-OF-002 Sr-U derived SST
ERSST
OISST
PR-OF-001 Sr/Ca derived SST
PR-OF-002 Sr/Ca derived SST
ERSST

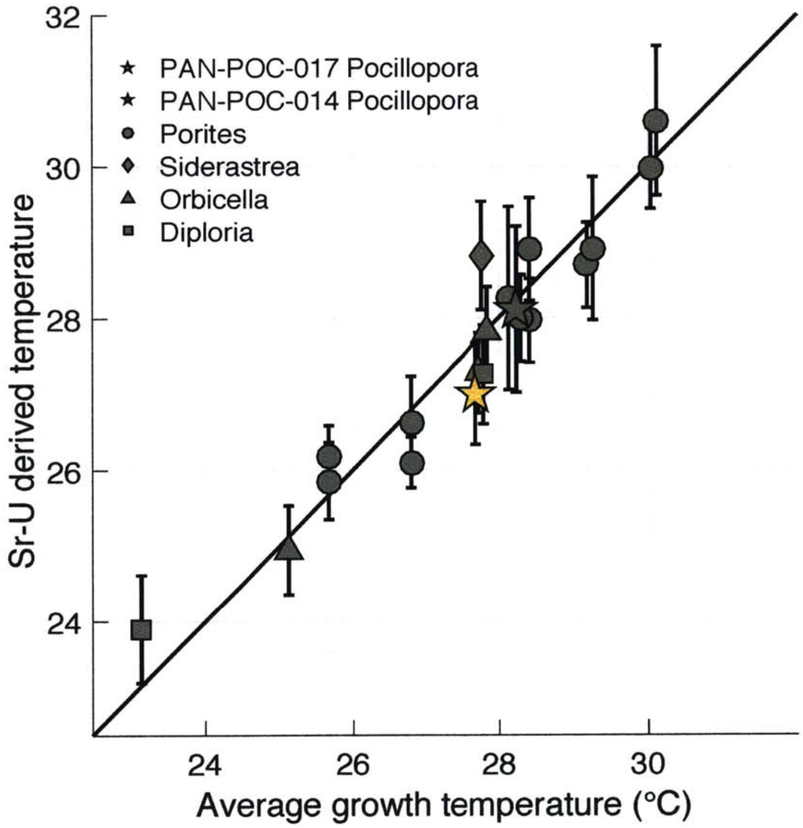

Figure 3-4. In gray, Sr-U derived temperatures for all corals in extended spatial calibration plotted against average growth temperature. In orange, Panama *P. damicornis* PAN-PD-017 used for calibration verification. PAN-PD-017 estimated temperature is 0.7 °C cooler than *in situ* logger measured temperature, within 1σ of the standard error of prediction for the Sr-U thermometer.

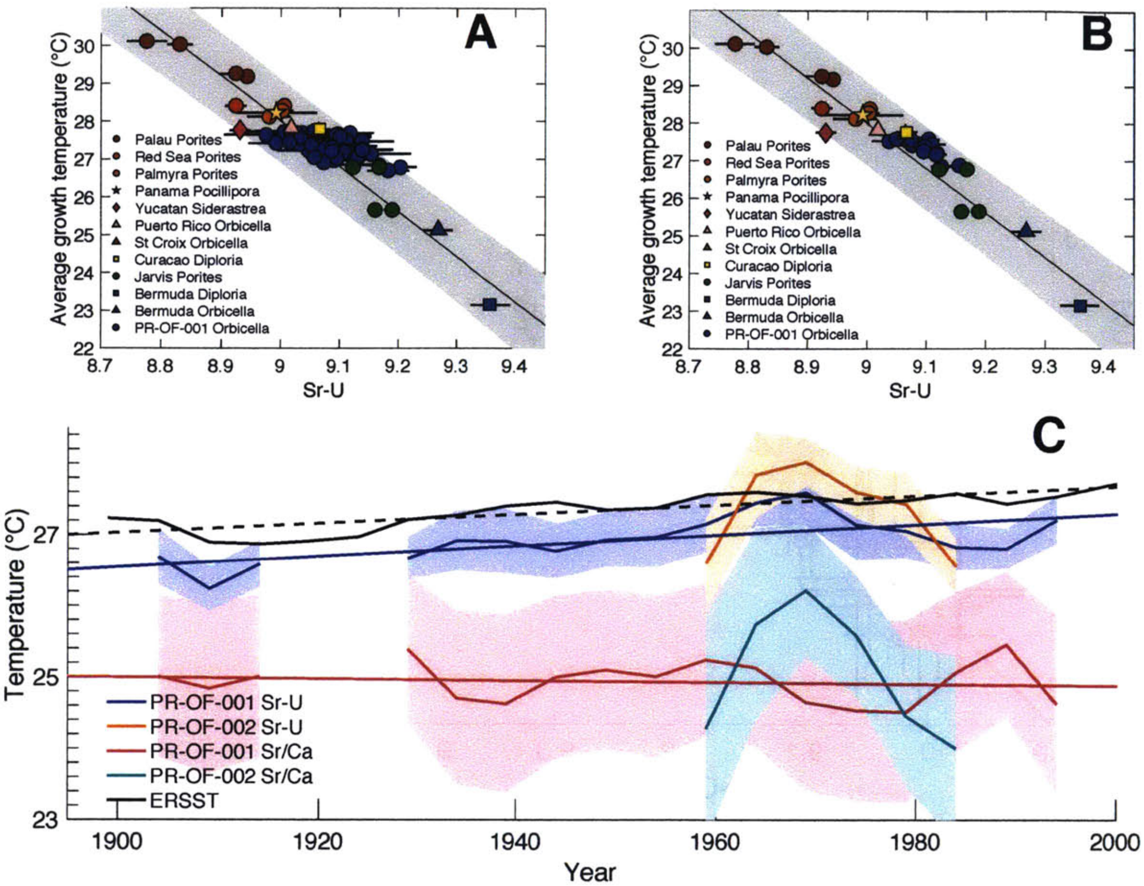

Figure 3-5. A) In blue, Sr-U values from Puerto Rico *O. faveolata* PR-OF-001 in 3-year bins plotted against 20th century ERSST [*Smith et al.,* 2008] (R=-0.62, p<0.01, n=62), along with spatial regression of modern Sr-U values on mean growth temperature shown in Figure 3-2A. Shading indicates the 95% confidence interval for the regression. 1σ propagated uncertainty of prediction for PR-OF-001 derived temperatures is 0.6° C. B) Same as A) but Sr-U values from PR-OF-001 are in 10-year bins (R=0.79, p<0.01, n=17). 1σ propagated uncertainty of prediction for PR-OF-001 derived temperatures is 0.3° C. C) Temperatures derived using the spatial calibration applied to 10-yr binned Sr-U values: timeseries from *O. faveolata* PR-OF-001 (blue) and PR-OF-002 (orange) are plotted with ERSST (black) [*Smith et al.,* 2008]. Shading indicates the standard error of prediction (1σ). Temperatures derived using the Sr/Ca spatial regression are shown in pink for PR-OF-001 and green for PR-OF-002. The difference between mean Sr-U derived temperatures and mean ERSST is 0.3° C for both PR-OF-001 and PR-OF-002. The slope of the in Sr-U derived SSTs from PR-OF-001 over the 20th century is positive and indistinguishable from ERSST. There is no significant trend in Sr/Ca derived SST.

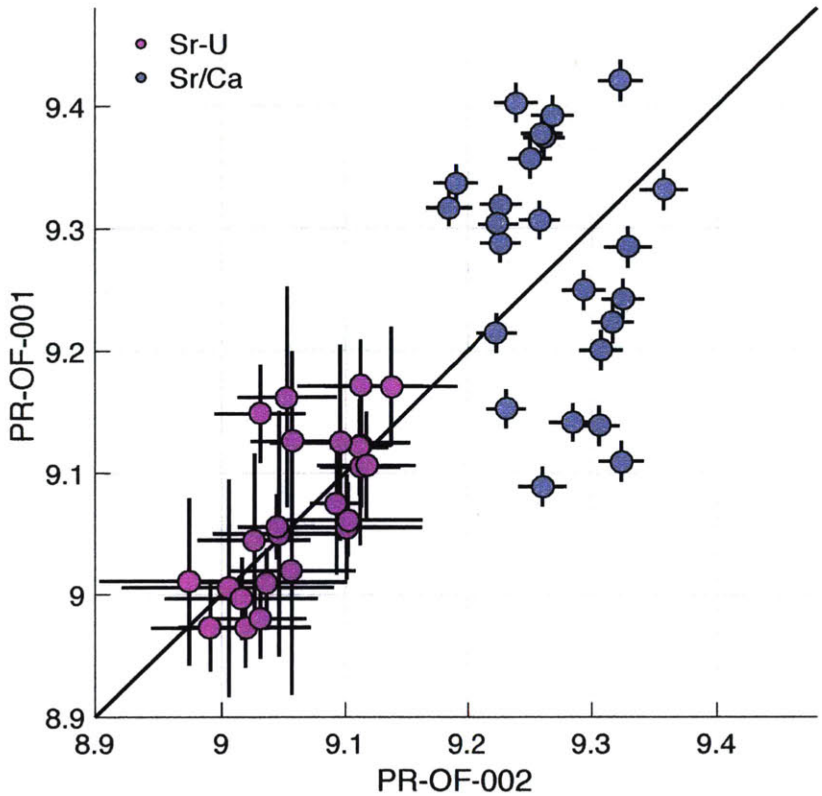

Figure 3-6. In pink, Sr-U values from *O. faveolata* PR-OF-001 are plotted with contemporaneous Sr-U values from *O. faveolata* PR-OF-002, both from Puerto Rico (R=0.71, p<0.01, n=24). Contemporaneous mean Sr/Ca values from the same two corals are plotted in blue and are not significantly correlated (R=-0.20, p=0.35, n=24).

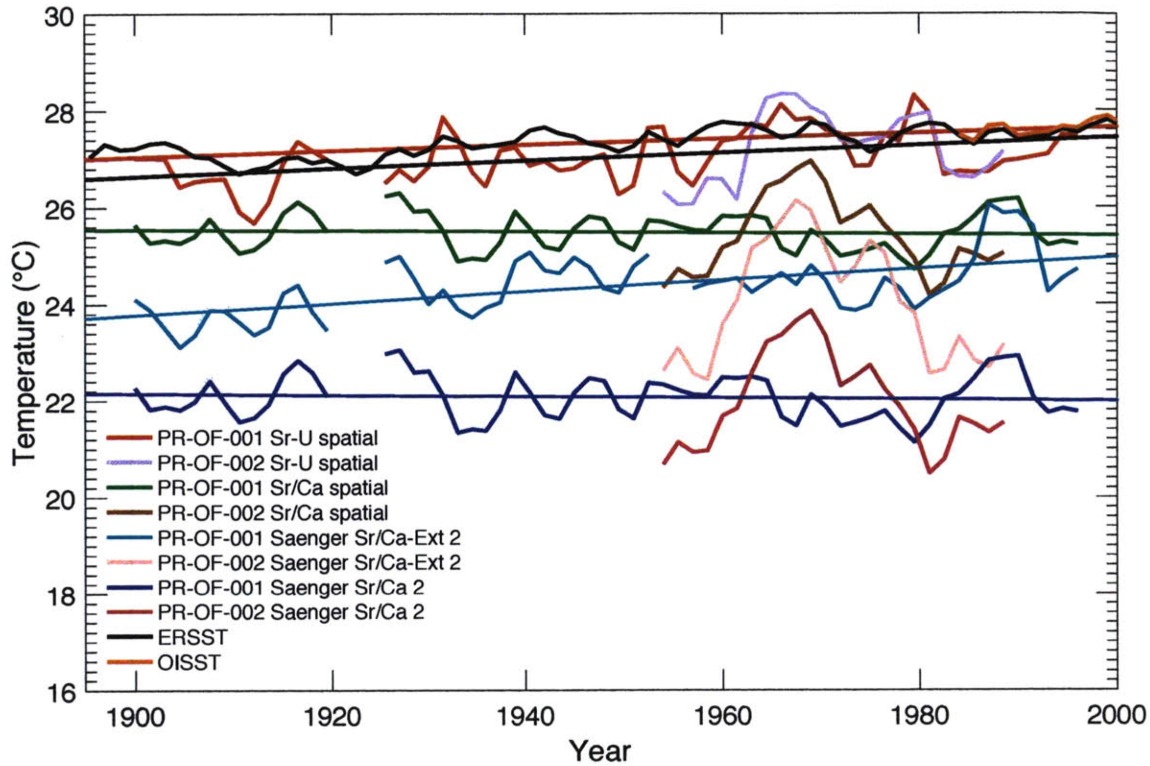

Figure 3-7: ERSST (black) [*Smith et al.*, 2008] and OISST (orange) [*Reynolds et al.*, 2002] compated to Sr-U (red and grey) and Sr/Ca (cyan and green) temperature estimates from *O. faveolata* PR-OF-001 and PR-OF-002 from Puerto Rico derived using the spatial Sr-U and Sr/Ca calibrations (Figures 3-2A and 3-2B, respectively). Also shown are temperatures derived using published Sr/Ca calibrations with and without incorporating mean annual extension rate [*Saenger et al.*, 2008]. Data are in 3-year bins, 1900-1996 trends are marked, and 1σ uncertainties on estimated temperatures are indicated by the vertical bars at right. Only Sr-U derived SSTs accurately estimate mean temperatures and replicate the instrumental warming trend. Sr/Ca derived temperatures using other published calibrations [*Swart et al.*, 2002; *Kibourne et al.*, 2008] underestimate mean SST more than the *Saenger et al.* [2008] calibrations. **Table 3-1:** Coral collection and geochemical information

Table 3-1: Coral collection and geochemical information

Coral	Species	Location	Depth (m)	Extension rate (cm/yr)	Mean temperature (°C) (yrs in record)	r^2 Sr/Ca to U/Ca	Sr-U	Mean Sr/Ca (mmol /mol)
From [DeCarlo et al., in review]								
Jarvis West W490	*Porites* sp.	0.3696°S 160.0083°W	7	1.3	27.67 (2007-2012)	0.81	9.19	9.15
Jarvis West W497	*Porites* sp.	0.3689°S 160.0081°W	16	1.9	27.67 (2007-2012)	0.64	9.16	9.25
Jarvis East 16	*Porites* sp.	0.3739°S 159.9834°W	5	1.3	26.79 (2007-2012)	0.86	9.17	9.29
Jarvis East E500	*Porites* sp.	0.3715°S 159.9823°W	5	1.5	26.79 (2007-2012)	0.49	9.12	9.12
Palmyra 2	*Porites* sp.	5.8664°N 162.1095°W	13	1.3	28.13 (2006-2010)	0.07	8.98	9.02
Palmyra 3	*Porites* sp.	5.8664°N 162.1095°W	13	1.2	28.29 (1998-2010)	0.44	8.99	8.89
Red Sea 1	*Porites* sp.	22.0314°N 38.8778°E	1	0.9	28.41 (1998-2009)	0.23	9.00	9.02
Red Sea 44	*Porites* sp.	22.0314°N 38.8778°E	5	0.9	28.41 (2005-2009)	0.46	8.92	8.97
Palau 23 (Airai)	*Porites* sp.	7.3321°N 134.5602°E	4	1.6	29.18 (1997-1999)	0.36	8.94	8.89
Palau 221 (Uchelbeluu)[a]	*Porites* sp.	7.267°N 134.521°E	5	0.7	29.26 (2008-2009)	0.79	8.92	8.66
Palau 229 (Uchelbeluu)[a]	*Porites* sp.	7.267°N 134.521°E	5	0.8	29.26 (2008-2009)	0.79	8.92	8.82
Palau 180 (Nikko Bay)	*Porites* sp.	7.3248°N 134.4684°E	6	0.9	30.04 (1997-1999)	0.29	8.83	8.94
Palau 168 (Nikko Bay)[a]	*Porites* sp.	7.3248°N 134.4684°E	3	0.6	30.12 (2008-2009)	0.30	8.78	8.66
Palau 169 (Nikko Bay)[a]	*Porites* sp.	7.3248°N 134.4684°E	6	0.9	30.12 (2008-2009)	0.30	8.78	8.72
This study: calibration								
BER-DL-003 (Bermuda)	*Diploria labyrinthformis*	32.32°N 64.71°W	13	0.5	23.15[b] (1995-1998)	0.60	9.10	9.35
BER-OF-001 (Bermuda)	*Orbicella franksi*	32.32°N 64.71°W	13	0.2	25.12[b,e] (1994-2000)	0.62	9.22	9.27
STX-OA-001 (St Croix)	*Orbicella annularis*	17.74°N 64.58°W	0.5	1.1	27.73[b] (1995-2000)	0.60	9.00	9.06
Jardin C (Yucatan)	*Siderastrea sidera*	20.8321°N 86.8789°W	3	0.3	27.76[c] (1997-2009)	0.32	8.99	8.93
CUR-DL-882 (Curacao)	*Diploria labyrinthformis*	12.2021°N 69.0829°W	4	0.7	27.79[b] (2012-2013)	0.04	9.07	9.07
PR-OA-003 (Mayguez Bay, PR)	*Orbicella annularis*	18.2°N 67.2°W	<10	0.8	27.84[c] (2000-2005)	0.77	9.02	9.02
PAN-PD-014 (Canales Norte, Panama)	*Pocillopora damicornis*	9.73°N 81.58°W	~3	.7 (L) 0.9 (R)	28.23[c] (2007-2010)	0.11	8.85	8.99
This study: verification								
PAN-PD-017 (Pacora, Panama)	*Pocillopora damicornis*	9.76°N 81.57°W	~3	0.3 (L&R)	27.68[d] (2008-2010)	0.28	8.94	9.09
This study: timeseries								
PR-OF-001 (Mona Island,PR)	*Orbicella faveolata*	18.1153°N 67.9374°W	7		1897-2011			
PR-OF-002 (Pinacles, PR)	*Orbicella faveolata*	17.93°N 67.01°W	7		1951-1991			

[a] PAL-P-168 and PAL-P-169 (Nikko Bay), and PAL-P-221 and PAL-P-229 (Uchelbeluu) were grouped together to calculate Sr-U

[b] OISST temperature [*Smith et al.*, 2008], logger verified

[c] OISST temperature

[d] logger temperature

Table 3-2: Temperature trends 1900-1996 (3-year bins)

Record	Trend[a] (°C/decade) (95% confidence interval)	Mean difference from ERSST (°C)	Uncertainty, 2σ (°C)
ERSST [*Smith et al.*, 2008]	**0.06 (0.04, 0.08)**		0.1
PR-OF-001 Sr-U derived	**0.06 (0.03, 0.1)**	0.3	1.2
PR-OF-001 Sr/Ca derived	-0.01 (-0.04, 0.02)	1.5	2.0
PR-OF-001 Saenger Sr/Ca derived	-0.02 (-0.05, 0.03)	5.3	
PR-OF-001 Saenger Sr/Ca-ext derived	**0.10 (0.07, 0.16)**	3.0	1.4

[a]ERSST and trends within error of ERSST in bold, others are not within error of any of these

Chapter 4

Modest Little Ice Age cooling of the Western Tropical Atlantic

4.1 Abstract

Proxy evidence indicates that the high latitude Northern Hemisphere was up to 1-2 °C cooler during the Little Ice Age (LIA; 1450-1850) than the mid-20th century. Conversely, records from the western tropical Atlantic (WTA) are inconsistent, ranging from 0 to -4 °C. The colder end of these estimates is inconsistent with model predictions of higher sensitivity to external forcing at high latitudes than the tropics. Here we apply a novel coral thermometer, Sr-U, to estimate sea surface temperatures (SSTs) in the WTA (Puerto Rico) during the early LIA. From 1465-1560, SSTs were 1.1 °C cooler than the mid-20th century mean reconstructed SST but within error of early 20th century SST prior to anthropogenic warming of the WTA. However, our data suggest that the early LIA was not chronically cold. Rather, strong multidecadal variability is apparent as are short intervals of warmth comparable to late the 20th century.

4.2 Introduction

Paleoclimate records spanning the past millennium suggest relatively warm temperatures from 950 to 1250CE during the so-called the Medieval Climate Anomaly (MCA), compared to the later period known as the Little Ice Age (LIA; 1450 to 1850CE) [*Masson-Delmotte et al.*, 2013]. There is emerging consensus that frequent and strong volcanic activity was an important forcing of the MCA-LIA transition, and that solar variability also played a role [*Crowley*, 2000; *Jones and Mann*, 2004; *Masson-Delmotte et al.*, 2013; *Schleussner and Feulner*, 2013;

McGregor et al., 2015; *Tierney et al.*, 2015]. A role for the Atlantic Meridional Overturning Circulation (AMOC) in amplifying the external forcing via feedback mechanisms, has been suggested [*Broecker*, 2000; *Swingedouw et al.*, 2011; *Park and Latif*, 2012], and both proxy and modeling studies implicate a weakened AMOC in sustaining LIA cooling [*Broecker*, 2000; *Lund et al.*, 2006; *Wanamaker et al.*, 2012; *Knudsen et al.*, 2014]. Evidence of a southward shift of the Intertropical Convergence Zone (ITCZ; e.g., *Schneider et al.* [2014] and references therein) during the LIA indicates reduced transport of heat between hemispheres, as expected during an AMOC reduction. Multidecadal variability within the LIA has also been attributed to volcanic and solar forcing [*Gray et al.*, 2004; *Mann et al.*, 2009; *Otterå et al.,* 2010; *Knudsen et al.*, 2011], as well as internal variability [*Delworth and Mann*, 2000; *Jungclaus et al.*, 2005; *Knight et al.*, 2005].

Tree ring and ice core records constrain cooling of Northern high latitude surface air temperatures (SATs) during the LIA to 1-2 $^\circ$C relative to the mid-20th century [*Overpeck et al.*, 1997; *Fischer et al.*, 1998; *Marcott et al.*, 2013]. Based on global climate models [*Holland and Bitz*, 2003] and 20th century observations [*Johannessen et al.*, 2004] low latitude temperatures are expected to be less sensitive, i.e., less cooling in the LIA [*Landrum et al.*, 2013]. The high resolution and low-latitude location of coral-based geochemical records makes them uniquely suited to address uncertainties in LIA SST and climate processes. However a study of Sr/Ca and δ^{18}O coral proxy records found no skill in their reconstructions of western tropical Atlantic SST trends [*Tierney et al.*, 2015]. Further, Sr/Ca-based SSTs for the WTA LIA are inconsistent, and range from no cooling to as much as 4 $^\circ$C cooler than today [*Haase-Schramm et al.*, 2003; *Saenger et al.*, 2008; 2009b; *Kilbourne et al.*, 2010; *DeLong et al.*, 2014]. The colder end of these estimates is comparable to or larger than estimates for the Last Glacial Maximum (LGM) cooling [*Waelbroeck et al.*, 2009].

We used a novel coral paleothermometer, Sr-U [*DeCarlo et al.*, 2016; *Alpert et al.*, in review] to reconstruct SST during the earliest part of the LIA at Pinacles Reef, southwestern Puerto Rico. Pinacles Reef is geographically well-placed to capture larger scale Caribbean temperature variability (Figure 4-1). 5 year low-pass filtered NOAA Extended Reconstructed SST (ERSST v3b) [*Smith et al.*, 2008] from the gridbox centered on Pinacles Reef is significantly correlated with SST in the entire Caribbean Sea (Figure 4-1), showing that our study site correlates broadly across the WTA. SST at the site is positively correlated ($R=0.59$, $P<0.001$) with the Atlantic Multidecadal Oscillation (AMO) a prominent mode of SST variability that characterizes low frequency North Atlantic variability in the instrumental era [*Schlesinger and Ramankutty*, 1994; *Enfield et al.*, 2001].

The Sr-U thermometer uses U/Ca to account for "vital effects" on coral Sr/Ca that are linked to fluctuations in the carbonate ion concentration [CO_3^{2-}] of the coral's calcifying fluid. Aragonite U/Ca is related to calcifying fluid [CO_3^{2-}] [*DeCarlo et al.*, 2016] and when used in combination with Sr/Ca, effectively corrects for the "vital effect" and significantly increases both the accuracy and precision of the derived SSTs [*DeCarlo et al.*, 2016; *Alpert et al.*, in review]. Our Sr-U derived SST record, albeit discontinuous due to diagenesis, provides new insight into both the magnitude of centennial scale LIA cooling in the WTA and the amplitude of multidecadal variability.

4.3 Material and Methods

An *Orbicella faveolata* colony called E1P was collected in 1994 at 7 m depth at Pinacles reef, Puerto Rico (Figure 4-1) [*Watanabe et al.*, 2002, *Winter and Sammarco* 2010]. U/Th dates indicate that the E1P coral colony died in ~1670 [*Kilbourne et al.*, 2010] (all dates reported are Common Era, CE). Mg/Ca and $\delta^{18}O$ data from E1P are reported in *Watanabe et al.* [2002] and short sections of Sr/Ca data in *Kilbourne et al.* [2010].

E1P was previously X-rayed and slabbed (see *Kilbourne et al.* [2008], Figure 1). All slabs were separately ultrasonicated in deionized water to remove coral dust. 50-80 μg coral powder was milled at 1 mm intervals using a Minicraft MB170 drill with a diamond bit. E1P Sr/Ca is identical to previous values reported by *Kilbourne et al.* [2010] in 3 of 4 windows (Figure C-1). As described in *Kilbourne et al.* [2010], several sections of diagenesis and borings are visible in E1P to the naked eye and in X-ray images as abnormally dense areas of skeleton. These sections were avoided and SEM imaging did not reveal any diagenesis in the sampled sections (Figure C-2).

Counts of ^{88}Sr and ^{48}Ca were collected on two single-collector Element2 inductively coupled plasma mass spectrometers at WHOI. Sr/Ca ratios were determined by calibration to published standards derived from coral skeleton (JCp-1) [*Okai et al.*, 2002; *Hathorne et al.*, 2013], fish otoliths (FEBS-1, NIES) [*Yoshinaga et al.*, 2000; *Sturgeon*, 2005], and limestone (NBS-1) [*Fernandez et al.*, 2011]. The JCp-1 standard has a Sr/Ca ratio (8.838 ± 0.042 mmol/mol) similar to coral samples (8.8 – 9.7 mmol/mol), whereas Sr/Ca ratios of FEBS-1, NIES, and NBS-19 are all less than 3 mmol/mol. Repeated measurements of an in-house secondary coral standard indicate an external precision of ± 0.04 mmol/mol (1σ, n=274, 0.4% relative) for Sr/Ca and 0.02 μmol/mol for U/Ca (1σ, n=274, 0.019% relative) and the instrument was stable throughout the study.

Uncertainty estimates take this analytical precision into account through calculation of the standard error of prediction. We measured the Sr/Ca ratio of JCp-1 by calibration to an independent set of standards as 8.870 ± 0.028 mmol/mol [*Alpert et al.*, 2016], which is within uncertainty of the mean, and within the range of precision, reported from JCp-1 analyses conducted in 21 different laboratories [*Hathorne et al.*, 2013].

U-Th dating of the bottom of core E1P performed by *Kilbourne et al.* [2010] indicates an age of 1462 ± 5 years. The age model is based upon counting annual bands from this date and agrees with that of *Kilbourne et al.* [2010]. Age control for a discontinuous section is based upon counting annual bands from a U/Th date of 1446 ± 4 years.

Sr-U was calculated according to the expression in *DeCarlo et al.* [2016]:

$$Sr\text{-}U = f(U/Ca);\ U/Ca = 1.1\ \mu mol/mol \qquad \text{(Eq.4-1)}$$

where f(U/Ca) is the slope and intercept resulting from ordinary least squares regression of Sr/Ca on U/Ca for a given coral colony or time period, evaluated at U/Ca of 1.1 µmol/mol. We calculated Sr-U values both for 3-year bins offset by 1.5 years, and for 10-year bins offset by 5 years. *Alpert et al.* [in review] found that reconstructing SST based on Sr-U values at 3-year resolution overestimated point-to-point variability while 10-year resolution did not. We reconstructed SST at 10-year resolution using the Sr-U to SST spatial calibration described in *Alpert et al.* [in review]:

$$T_D = -11 \pm 1(SrU - 9) + 28.0 \pm 0.1$$

(Eq.4-2)

where *Sr-U* is the value resulting from Eq.4-1 and T_D is the resulting derived temperature. The standard error of prediction for reconstructed temperatures is 0.6 °C (1σ, n=19) [*Alpert et al.*, in review].

To derive Sr/Ca-SSTs, we used a regression equation from *Kilbourne et al.* [2008] based upon a calibration between SSTs and Sr/Ca in the top (modern section) of the core. We applied this to mean Sr/Ca for the same bins used for Sr-U values, in E1P as well as PR-OF-001, PR-OF-002, and the 20^{th} century data from the core containing E1P published in *Kilbourne et al.* [2008]. Uncertainty is reported as $\pm 1\sigma$ unless indicated otherwise.

4.4 Results

The Sr-U record from E1P spans 1445-1674, disrupted by gaps where diagenesis, identified in X-ray, precluded subsampling and analysis of skeleton. At Pinacles, each absolute SST value is estimated from 10 years of Sr-U data [*Alpert et al.*, in review]. Figure 4-2 presents our raw Sr-U record derived from 3-year bins of Sr/Ca and U/Ca data (top) offset by 1.5 years and our Sr-U derived SST record, reconstructed from 10-year bins of data offset by 5 years (bottom). Data from E1P are compared with Sr-U and Sr-U derived SSTs from modern Puerto Rico corals from Mona island and Pinacles Reef, and the instrumental record of SST (Figure 4-2, black line).

The mean SST derived from the modern Pinacles coral is within 0.2 °C of ERSST [*Smith et al.*, 2008] (Figure 4-2, bottom curve). Over the longest continuous section of E1P, spanning 1465-1560, reconstructed temperatures yield a mean cooling of 1.1 ± 0.6 °C relative to the 1958-1988 mean Sr-U derived SST from the modern Pinacles Reef coral [*Alpert et al.*, in review]. We estimated SSTs at Pinacles based upon mean Sr-U reconstructed SSTs at Mona Island, Puerto Rico over 1899-1919 and the 0.13 °C warmer mean of Sr-U reconstructed SSTs at Pinacles than Mona over the two records' overlapping time period. We estimate that Pinacles SSTs were 0.7 °C cooler in the early 20th century than over the 1958-1988 period. This results in a 0.4 °C difference between the 1465-1560 mean SST and early 20th century SST. With an error of 0.6 °C for both 20th century and LIA reconstructed SSTs, the two periods are within error of each other. All but one of the reconstructed SSTs over the discontinuous record spanning 1446 to 1638 are within error of the estimated early 20th century SST.

Multidecadal SST variability is evident in the record. Within the longest continuous section of the record, a single multidecadal cycle spans the 70-year period 1488 to 1558, with amplitude comparable to 20th century AMO variability as recorded by the Sr-U from the modern coral from Pinacles (Figure 4-2, top). We also observe a progressive cooling in the 1450s following the eruption of Kuwae [*Gao et al.*, 2008] followed by a sharp SST rise.

The Sr/Ca-derived SSTs from this coral suggest a much larger mean cooling, of 3.9 °C, during the LIA relative to the top of core (Figure 4-3) [*Kilbourne et al.*, 2008; 2010]. Multidecadal variability in the Sr/Ca record is in phase with that in the Sr-U record but the amplitude of variability is 4 °C, larger than variability in Sr-U derived SST or ERSST in the 20th century.

4.5 Discussion

4.5.1. Little Ice Age cooling

With continental configuration and orbital forcing virtually identical to that of today, the LIA presents an excellent opportunity to examine both the sensitivity of the tropics to external forcing and the characteristics and drivers of multidecadal SST variability in the WTA. The mean 1.1 °C cooling from 1465-1560 at Pinacles, relative to 1958-1988, is comparable to or smaller than the 1-2

°C LIA cooling of northern high latitude SAT documented by proxy [*Overpeck et al.*, 1997; *Fischer et al.*, 1998; *Mann et al.*, 2009; *Marcott et al.*, 2013] and historical records [*Manley*, 1974]. The Sr-U derived record at Pinacles does not support Sr/Ca based evidence [*Kilbourne et al.*, 2010] of greater cooling in the tropical Atlantic than at high northern latitudes. Moreover, there is no significant difference between Pinacles reconstructed SSTs from the continuous LIA section 1465-1560 and those estimated for the early 20th century, prior to anthropogenic greenhouse gas forcing [*Bindoff et al.*, 2013].

Our results also provide insight into the reason for the wide range (0 to 4 °C) of WTA Sr/Ca-derived SST estimates for the LIA [*Haase-Schramm et al.*, 2003; *Saenger et al.*, 2008; *Saenger et al.*, 2009b; *Kilbourne et al.*, 2010; *DeLong et al.*, 2014]. Sr/Ca-derived 20th century SSTs from the two modern Puerto Rico corals are very different from each other, both in mean and trend. Depending on which of two modern Puerto Rico corals [*Alpert et al.,* in review] are used as a modern day reference point, Sr/Ca may indicate almost no cooling during the LIA or up to 3.9 °C cooling (Figure 4-3). Conversely, cooling inferred from Sr-U is the same regardless of which modern coral is used for comparison. Since Sr-U derived SST from both the Puerto Rico sites is consistent with ERSST (Figure 4-3), disagreements in Sr/Ca between individuals are likely due to offsets in Sr/Ca associated with vital effects [*De villiers et al.*, 1995; *Cohen et al.*, 2002; *Goodkin et al.*, 2005; *Linsley et al.*, 2006; *Cahyarini et al.*, 2009; *Pfeiffer et al.*, 2009; *Alpert et al.*, 2016]. Pinacles Sr-U derived SST agrees better with estimates derived from Sr/Ca regressions incorporating annual extension rate than Sr/Ca alone [*Saenger et al.*, 2008; *Kilbourne et al.*, 2010], indicating that in some corals, the "vital effects" that drive Sr/Ca distortions are also reflected in changes in growth rate. However, this is not always the case (e.g., *Smith et al.*, [2006]).

The magnitude of cooling at Pinacles is comparable to maximum cooling estimated from foraminiferal Mg/Ca from the Cariaco Basin (Figure 4-4) [*Black et al.*, 2007]. The coolest period of the Cariaco record occurs after the continuous section of the Pinacles record, underscoring both the importance of additional continuous records and the possibility that the coldest period of the LIA may not have been contemporaneous at all sites. The Pinacles record is largely within error of a tree ring-based compilation of northern hemisphere SAT [*PAGES 2k Consortium*, 2013], which along with the Cariaco record suggests modest LIA cooling relative to the late 20th century and minimal LIA cooling relative to the early 20th century (Figure 4-4). The degree of cooling at Pinacles agrees with polar amplification of temperature change observed in coupled climate model runs of the past [*Landrum et al.*, 2013] and future [*Pithan and Mauritsen*, 2014], as well as with 20th century observations [*Johannessen et al.*, 2004].

4.5.2. Multidecadal variability

A 30-year record of Sr-U derived SST from a modern Pinacles coral [*Alpert et al.*, in review] accurately captures mean SST but reveals a larger amplitude of multidecadal variability than concurrent ERSST (Figure 4-2, bottom curve). The higher amplitude may reflect reef-scale (local) departures from ERSST but cannot be conclusively attributed without *in situ* temperature data.

The single cycle of multidecadal variability from 1488 to 1558 is comparable in amplitude to 20th century multidecadal variability at Pinacles as recorded by the corals (Figure 4-2). However, the cold period of this cycle (1493-1553) is significantly cooler (1.2-1.4 $^{\circ}$C) than the 1958-1988 Pinacles temperatures (Figure 4-2, bottom curve). LIA multidecadal variability at Pinacles does not correspond to SST reconstructed from foraminiferal Mg/Ca in the Cariaco Basin (Figure 4-4) [*Black et al.*, 2007]. However the Cariaco record is based upon radiocarbon dates with uncertainties of ± 50 years [*Black*, 1998] and disagreement could reflect age model differences.

The 3-year resolution Sr-U record reveals a notable downturn in temperature (Figure 4-2, top curve) in the 1450s, corresponding, within timescale error, to the timing of one of the largest volcanic eruptions of the past millennium, Kuwae, in 1452 [*Gao et al.*, 2008]. The SST record cannot resolve this progressive cooling, but the single SST point in the 1450s is the coldest in the record, and the only LIA SST significantly different from early 20^{th} century estimated Pinacles SST. The abrupt cooling visible in the Sr-U record could reflect an initial response to the eruption on a 1-3 year timescale due to radiative backscatter by sulfate aerosol particles [*Stenchikov et al.*, 1998; *Robock*, 2000]. A tree-ring based northern hemisphere SAT record reveals a reduction in temperatures concurrent with that of the coral proxy record (Figure 4-4). Note that considering the possible overestimate of 20^{th} century variability by a modern Pinacles coral we are cautious in interpreting absolute SST on timescales of less than 30 years.

4.6. Conclusions and future outlook

Pinacles LIA SST (1465-1560) was on mean 1.1 °C cooler than the 1958-1988 mean Sr-U derived SST and ERSST at the same location, and within error of early 20^{th} century estimated SSTs. In light of evidence that suggests that the tropics should be less sensitive than the high latitudes to external forcing, our results seem more reasonable than the 3.9 °C cooling derived from Sr/Ca of the same samples. The amplitude of multidecadal variability was comparable to the

20th century, and short intervals of warmth comparable to the late 20th century were present. Longer, continuous well-dated records are needed to further investigate low latitude SST response to volcanic and solar forcings.

4.7 Acknowledgments

We are grateful to Kathryn Pietro (WHOI) and Gretchen Swarr (WHOI) for lab assistance; and to Caroline Ummenhofer and Sloan Coats for insightful discussions. This study was supported by an Ocean Exploration Institute graduate student award to A.E.A. and NSF-OCE-1338320 to G.A.G and A.L.C.

4.8 References

Alpert, A. E., A. L. Cohen, D. W. Oppo, T. M. DeCarlo, J. M. Gove, and C. W. Young (2016), Comparison of equatorial Pacific sea surface temperature variability and trends with Sr/Ca records from multiple corals, *Paleoceanography.* doi: 10.1002/2015PA002897

Alpert, A. E., A. L. Cohen, D. W. Oppo, G. A. Gaetani, E. A. Hernandez-Delgado, T. M. DeCarlo, A. Winter, and M. E. Gonneea (in review), 20th century warming of the tropical Atlantic captured by Sr-U paleothermometry *Paleoceanography*

Bindoff, N. L., P. A. Stott, M. AchutaRao, M. R. Allen, N. Gillett, D. Gutzler, K. Hansingo, G. Hegerl, Y. Hu, and S. Jain (2013), Detection and attribution of climate change: from global to regional, *In: Climate Change 2013: The Physical Science* Basis. Contribution of Working Group I to the Fifth Assessment Report of the Intergovernmental Panel on Climate Change, Cambridge University Press, Cambridge, United Kingdom and New York, NY, USA, pp. 867–952, doi:10.1017/CBO9781107415324.022

Black, D. E., M. A. Abahazi, R. C. Thunell, A. Kaplan, E. J. Tappa, and L. C. Peterson (2007), An 8-century tropical Atlantic SST record from the Cariaco Basin: Baseline variability, twentieth-century warming, and Atlantic hurricane frequency, *Paleoceanography*, *22*(4)

Black, D. E. (1998), Decadal-to century scale climate variability in the tropical north Atlantic as recorded in sediments from the anoxic Cariaco Basin, Venezuela

Broecker, W. S. (2000), Was a change in thermohaline circulation responsible for the Little Ice Age?, *Proceedings of the National Academy of Sciences*, *97*(4), 1339-1342

Cahyarini, S. Y., M. Pfeiffer, and W.-C. Dullo (2009), Improving SST reconstructions from coral Sr/Ca records: multiple corals from Tahiti (French Polynesia), *International Journal of Earth Sciences*, *98*(1), 31-40

Crowley, T. J. (2000), Causes of climate change over the past 1000 years, *Science*, *289*(5477), 270-277

Cohen, A., K. E. Owens, G. D. Layne, and N. Shimizu (2002), The effect of algal symbionts on the accuracy of Sr/Ca paleotemperatures from coral, *Science*, *296*(5566), 331-333

Crowley, T. J. (2000), Causes of climate change over the past 1000 years, *Science*, *289*(5477), 270-277

Dahl, K. A., A. J. Broccoli, and R. J. Stouffer (2005), Assessing the role of North Atlantic freshwater forcing in millennial scale climate variability: A tropical Atlantic perspective, *Climate Dynamics*, *24*(4), 325-346

de Villiers, S., G. T. Shen, and B. K. Nelson (1994), The SrCa-temperature relationship in coralline aragonite: Influence of variability in (SrCa) seawater and skeletal growth parameters, *Geochimica et Cosmochimica Acta*, *58*(1), 197-208.

DeCarlo, T. M., G. A. Gaetani, A. L. Cohen, G. L. Foster, A. E. Alpert, and J. Stewart (2016), Coral Sr-U Thermometry, *Paleoceanography*

DeLong, K. L., J. A. Flannery, R. Z. Poore, T. M. Quinn, C. R. Maupin, K. Lin, and C. C. Shen (2014), A reconstruction of sea surface temperature variability in the southeastern Gulf of Mexico from 1734–2008 CE using cross-dated Sr/Ca records from the coral Siderastrea siderea, *Paleoceanography*, *29*(5). doi:10.1002/2013PA002524.

Delworth, T. L., and M. E. Mann (2000), Observed and simulated multidecadal variability in the Northern Hemisphere, *Climate Dynamics*, *16*(9), 661-676

Enfield, D. B., A. M. Mestas-Nuñez, and P. J. Trimble (2001), The Atlantic multidecadal oscillation and its relation to rainfall and river flows in the continental US, *Geophysical Research Letters*, *28*(10), 2077-2080

Fernandez, D. P., A. C. Gagnon, and J. F. Adkins (2011), An Isotope Dilution ICPelation to rainfall and river flows in the continental US, variability: A trop, *Geostandards and Geoanalytical Research*, *35*(1), 23-37

Fischer, H., M. Werner, D. Wagenbach, M. Schwager, T. Thorsteinnson, F. Wilhelms, J. Kipfstuhl, and S. Sommer (1998), Little ice age clearly recorded in northern Greenland ice cores, *Geophys. Res. Lett.*, *25*(10), 1749-1752

Gao, C., A. Robock, and C. Ammann (2008), Volcanic forcing of climate over the past 1500 years: An improved ice core-based index for climate models, *Journal of Geophysical Research: Atmospheres*, *113*(D23)

Goodkin, N. F., K. A. Hughen, A. L. Cohen, and S. R. Smith (2005), Record of Little Ice Age sea surface temperatures at Bermuda using a growth-dependent calibration of coral Sr/Ca, *Paleoceanography*, *20*(4). doi:10.1029/2005PA001140.

Gray, S. T., L. J. Graumlich, J. L. Betancourt, and G. T. Pederson (2004), A tree-ring based reconstruction of the Atlantic Multidecadal Oscillation since 1567 AD, *Geophysical Research Letters*, *31*(12)

Haase-Schramm, A., F. Böhm, A. Eisenhauer, W. C. Dullo, M. M. Joachimski, B. Hansen, and J. Reitner (2003), Sr/Ca ratios and oxygen isotopes from sclerosponges: Temperature history of the Caribbean mixed layer and thermocline during the Little Ice Age, *Paleoceanography*, *18*(3). doi:10.1029/2002PA000830.

Hathorne, E. C., A. Gagnon, T. Felis, J. Adkins, R. Asami, W. Boer, N. Caillon, D. Case, K. M. Cobb, and E. Douville (2013), Inter-laboratory study for coral Sr/Ca and other element/Ca ratio measurements, *Geochemistry, Geophysics, Geosystems*. doi:10.1002/ggge.20230.

Hegerl, G., F. Zwiers, P. Braconnot, N. Gillet, Y. Luo, J. Marengo, N. Nicholls, J. Penner, and P. Stott (2007), Understanding and attributing climate change

Haug, G. H., K. A. Hughen, D. M. Sigman, L. C. Peterson, and U. Röhl (2001), Southward migration of the intertropical convergence zone through the Holocene, *Science*, *293*(5533), 1304-1308

Hodell, D. A., M. Brenner, J. H. Curtis, R. Medina-Gonzalez, E. I.-C. Can, A. Albornaz-Pat, and T. P. Guilderson (2005), Climate change on the Yucatan Peninsula during the little ice age, *Quaternary Research*, *63*(2), 109-121

Holland, M. M., and C. M. Bitz (2003), Polar amplification of climate change in coupled models, *Climate Dynamics*, *21*(3-4), 221-232

Johannessen, O. M., L. Bengtsson, M. W. Miles, S. I. Kuzmina, V. A. Semenov, G. V. Alekseev, A. P. Nagurnyi, V. F. Zakharov, L. P. Bobylev, and L. H. Pettersson (2004), Arctic climate change: Observed and modelled temperature and sea-ice variability, *Tellus A*, *56*(4), 328-341

Jones, P. D., and M. E. Mann (2004), Climate over past millennia, *Reviews of Geophysics*, *42*(2)

Jungclaus, J. H., H. Haak, M. Latif, and U. Mikolajewicz (2005), Arctic-North Atlantic interactions and multidecadal variability of the meridional overturning circulation, *Journal of climate*, *18*(19), 4013-4031

Kang, S. M., D. M. Frierson, and I. M. Held (2009), The tropical response to extratropical thermal forcing in an idealized GCM: The importance of radiative feedbacks and convective parameterization, *Journal of the atmospheric sciences*, *66*(9), 2812-2827

Kang, S. M., I. M. Held, D. M. Frierson, and M. Zhao (2008), The response of the ITCZ to extratropical thermal forcing: Idealized slab-ocean experiments with a GCM, *Journal of Climate*, *21*(14), 3521-3532

Kilbourne, K., T. Quinn, R. Webb, T. Guilderson, J. Nyberg, and A. Winter (2008), Paleoclimate proxy perspective on Caribbean climate since the year 1751: Evidence of cooler temperatures and multidecadal variability, *Paleoceanography*, *23*(3). doi:10.1029/2008PA001598.

Kilbourne, K., T. Quinn, R. Webb, T. Guilderson, J. Nyberg, and A. Winter (2010), Coral windows onto seasonal climate variability in the northern Caribbean since 1479, *Geochemistry, Geophysics, Geosystems*, *11*(10). doi:10.1029/2010GC003171.

Knight, J. R., R. J. Allan, C. K. Folland, M. Vellinga, and M. E. Mann (2005), A signature of persistent natural thermohaline circulation cycles in observed climate, *Geophysical Research Letters*, *32*(20)

Knudsen, M. F., M.-S. Seidenkrantz, B. H. Jacobsen, and A. Kuijpers (2011), Tracking the Atlantic Multidecadal Oscillation through the last 8,000 years, *Nature Communications*, *2*, 178

Knudsen, M. F., B. H. Jacobsen, M.-S. Seidenkrantz, and J. Olsen (2014), Evidence for external forcing of the Atlantic Multidecadal Oscillation since termination of the Little Ice Age, *Nature communications*, *5*

Landrum, L., B. L. Otto-Bliesner, E. R. Wahl, A. Conley, P. J. Lawrence, N. Rosenbloom, and H. Teng (2013), Last millennium climate and its variability in CCSM4, *Journal of Climate*, *26*(4), 1085-1111

Linsley, B. K., A. Kaplan, Y. Gouriou, J. Salinger, P. B. Demenocal, G. M. Wellington, and S. S. Howe (2006), Tracking the extent of the South Pacific Convergence Zone since the early 1600s, *Geochemistry, Geophysics, Geosystems*, *7*(5). doi:10.1029/2005GC001115.

Lund, D. C., J. Lynch-Stieglitz, and W. B. Curry (2006), Gulf Stream density structure and transport during the past millennium, *Nature*, *444*(7119), 601-604

Manley, G. (1974), Central England temperatures: monthly means 1659 to 1973, *Quarterly Journal of the Royal Meteorological Society*, *100*(425), 389-405

Mann, M. E., Z. Zhang, S. Rutherford, R. S. Bradley, M. K. Hughes, D. Shindell, C. Ammann, G. Faluvegi, and F. Ni (2009), Global signatures and dynamical origins of the Little Ice Age and Medieval Climate Anomaly, *Science*, *326*(5957), 1256-126

Marcott, S. A., J. D. Shakun, P. U. Clark, and A. C. Mix (2013), A reconstruction of regional and global temperature for the past 11,300 years, *science*, *339*(6124), 1198-1201

Masson-Delmotte, V., M. Schulz, A. Abe-Ouchi, J. Beer, A. Ganopolski, J. González Rouco, E. Jansen, K. Lambeck, J. Luterbacher, and T. Naish (2013), Information from paleoclimate archives, *Climate change*, 383-464

McGregor, H. V., M. N. Evans, H. Goosse, G. Leduc, B. Martrat, J. A. Addison, P. G. Mortyn, D. W. Oppo, M.-S. Seidenkrantz, and M.-A. Sicre (2015), Robust global ocean cooling trend for the pre-industrial Common Era, *Nature Geoscience*

Okai, T., A. Suzuki, H. Kawahata, S. Terashima, and N. Imai (2002), Preparation of a New Geological Survey of Japan Geochemical Reference Material: Coral JCp-1, *Geostandards newsletter*, *26*(1), 95-99

Otterå, O. H., M. Bentsen, H. Drange, and L. Suo (2010), External forcing as a metronome for Atlantic multidecadal variability, *Nature Geoscience*, *3*(10), 688-694

Overpeck, J., K. Hughen, D. Hardy, R. Bradley, R. Case, M. Douglas, B. Finney, K. Gajewski, G. Jacoby, and A. Jennings (1997), Arctic environmental change of the last four centuries, *Science*, *278*(5341), 1251-1256

Past Global Changes 2k Consortium (2013), Continental-Scale Temperature Variability during the Past Two Millennia, *Nature Geoscience*, *6*(5)

Park, W., and M. Latif (2012), Atlantic meridional overturning circulation response to idealized external forcing, *Climate dynamics*, *39*(7-8), 1709-1726

Pfeiffer, M., W.-C. Dullo, J. Zinke, and D. Garbe-Schönberg (2009), Three monthly coral Sr/Ca records from the Chagos Archipelago covering the period of 1950–1995 AD: reproducibility and implications for quantitative reconstructions of sea surface temperature variations, *International Journal of Earth Sciences*, *98*(1), 53-66

Pithan, Felix, and Thorsten Mauritsen. "Arctic amplification dominated by temperature feedbacks in contemporary climate models." *Nature Geoscience* 7.3 (2014): 181-184.

Robock, A. (2000), Volcanic eruptions and climate, *Reviews of Geophysics*, *38*(2), 191-219

Saenger, C., A. L. Cohen, D. W. Oppo, and D. Hubbard (2008), Interpreting sea surface temperature from strontium/calcium ratios in Montastrea corals: Link with growth rate and implications for proxy reconstructions, *Paleoceanography*, *23*(3). doi:10.1029/2007PA001572.

Saenger, C., P. Chang, L. Ji, D. W. Oppo, and A. L. Cohen (2009a), Tropical Atlantic climate response to low –latitude and extratropical sea-surface temperature: A Little Ice Age perspective, *Geophysical Research Letters*, *36*(11)

Saenger, C., A. L. Cohen, D. W. Oppo, R. B. Halley, and J. E. Carilli (2009b), Surface-temperature trends and variability in the low-latitude North Atlantic since 1552, *Nature Geoscience*, *2*(7), 492-495

Schlesinger, M. E., and N. Ramankutty (1994), An oscillation in the global climate system of period 65-70 years, *Nature*, *367*(6465), 723-726

Schleussner, C., and G. Feulner (2013), A volcanically triggered regime shift in the subpolar North Atlantic Ocean as a possible origin of the Little Ice Age, *Clim. Past*, *9*(3), 1321-1330

Schneider, T., T. Bischoff, and G. H. Haug (2014), Migrations and dynamics of the intertropical convergence zone, *Nature*, *513*(7516), 45-53

Shindell, D. T., G. A. Schmidt, M. E. Mann, D. Rind, and A. Waple (2001), Solar forcing of regional climate change during the Maunder Minimum, *Science*, *294*(5549), 2149-2152

Smith, J. M., T. M. Quinn, K. P. Helmle, and R. B. Halley (2006), Reproducibility of geochemical and climatic signals in the Atlantic coral Montastraea faveolata, *Paleoceanography*, *21*(1)

Smith, T. M., R. W. Reynolds, T. C. Peterson, and J. Lawrimore (2008), Improvements to NOAA's historical merged land-ocean surface temperature analysis (1880-2006), *Journal of Climate*, *21*(10), 2283-2296

Stenchikov, G. L., I. Kirchner, A. Robock, H. F. Graf, J. C. Antuna, R. Grainger, A. Lambert, and L. Thomason (1998), Radiative forcing from the 1991 Mount Pinatubo volcanic eruption, *Journal of Geophysical Research: Atmospheres*, *103*(D12), 13837-13857

Stendel, M., I. A. Mogensen, and J. H. Christensen (2006), Influence of various forcings on global climate in historical times using a coupled atmosphere–ocean general circulation model, *Climate Dynamics*, *26*(1), 1-15

Sturgeon, R. E., S. N. Willie, L. Yang, R. Greenberg, R. O. Spatz, Z. Chen, C. Scriver, V. Clancy, J. W. Lam, and S. Thorrold (2005), Certification of a fish otolith reference ma- terial in support of quality assurance for trace element analysis, *J. Anal. At. Spectrom*, *20*(10), 1067–1071

Swingedouw, D., L. Terray, C. Cassou, A. Voldoire, D. Salas-Mélia, and J. Servonnat (2011), Natural forcing of climate during the last millennium: fingerprint of solar variability, *Climate Dynamics*, *36*(7-8), 1349-1364

Tierney, J. E., N. J. Abram, K. J. Anchukaitis, M. N. Evans, C. Giry, K. H. Kilbourne, C. P. Saenger, H. C. Wu, and J. Zinke (2015), Tropical sea surface temperatures for the past four centuries reconstructed from coral archives, *Paleoceanography*, *30*(3), 226-252

Vellinga, M., and R. A. Wood (2002), Global climatic impacts of a collapse of the Atlantic thermohaline circulation, *Climatic Change*, *54*(3), 251-267

Vuille, M., S. Burns, B. Taylor, F. Cruz, B. Bird, M. Abbott, L. Kanner, H. Cheng, and V. Novello (2012), A review of the South American monsoon history as recorded in stable isotopic proxies over the past two millennia, *Climate of the Past*, *8*(4), 1309-1321

Waelbroeck, C., A. Paul, M. Kucera, A. Rosell-Melé, M. Weinelt, R. Schneider, A. Mix, A. Abelmann, L. Armand, and E. Bard (2009), Constraints on the magnitude and patterns of ocean cooling at the Last Glacial Maximum, *Nature Geoscience*, *2*(2), 127-132

Wanamaker, A. D., P. G. Butler, J. D. Scourse, J. Heinemeier, J. Eiríksson, K. L. Knudsen, and C. A. Richardson (2012), Surface changes in the North Atlantic meridional overturning circulation during the last millennium, *Nature Communications*, *3*, 899

Watanabe, T., A. Winter, T. Oba, R. Anzai, and H. Ishioroshi (2002), Evaluation of the fidelity of isotope records as an environmental proxy in the coral Montastraea, *Coral Reefs*, *21*(2), 169-17

Winter, A. and P.W. Sammarco (2010), Lunar banding in the scleractinian coral Montastraea faveolata: fine-scale structure and influence of temperature, Journal of Geophysical Research, *115*, doi:10.1029/2009JG001264.

Yoshinaga, J., A. Nakama, M. Morita, and J. S. Edmonds (2000), Fish otolith reference material for quality assurance of chemical analyses, *Marine Chemistry*, *69*(1), 91-97

Zhang, R., and T. L. Delworth (2006), Impact of Atlantic multidecadal oscillations on India/Sahel rainfall and Atlantic hurricanes, *Geophysical Research Letters*, *33*(17)

Zorita, E., H. Von Storch, F. J. Gonzalez-Rouco, U. Cubasch, J. Luterbacher, S. Legutke, I. Fischer-Bruns, and U. Schlese (2004), Climate evolution in the last five centuries simulated by an atmosphere-ocean model: global temperatures, the North Atlantic Oscillation and the Late Maunder Minimum, *Meteorologische Zeitschrift*, *13*(4), 271-289

4.9 Figures

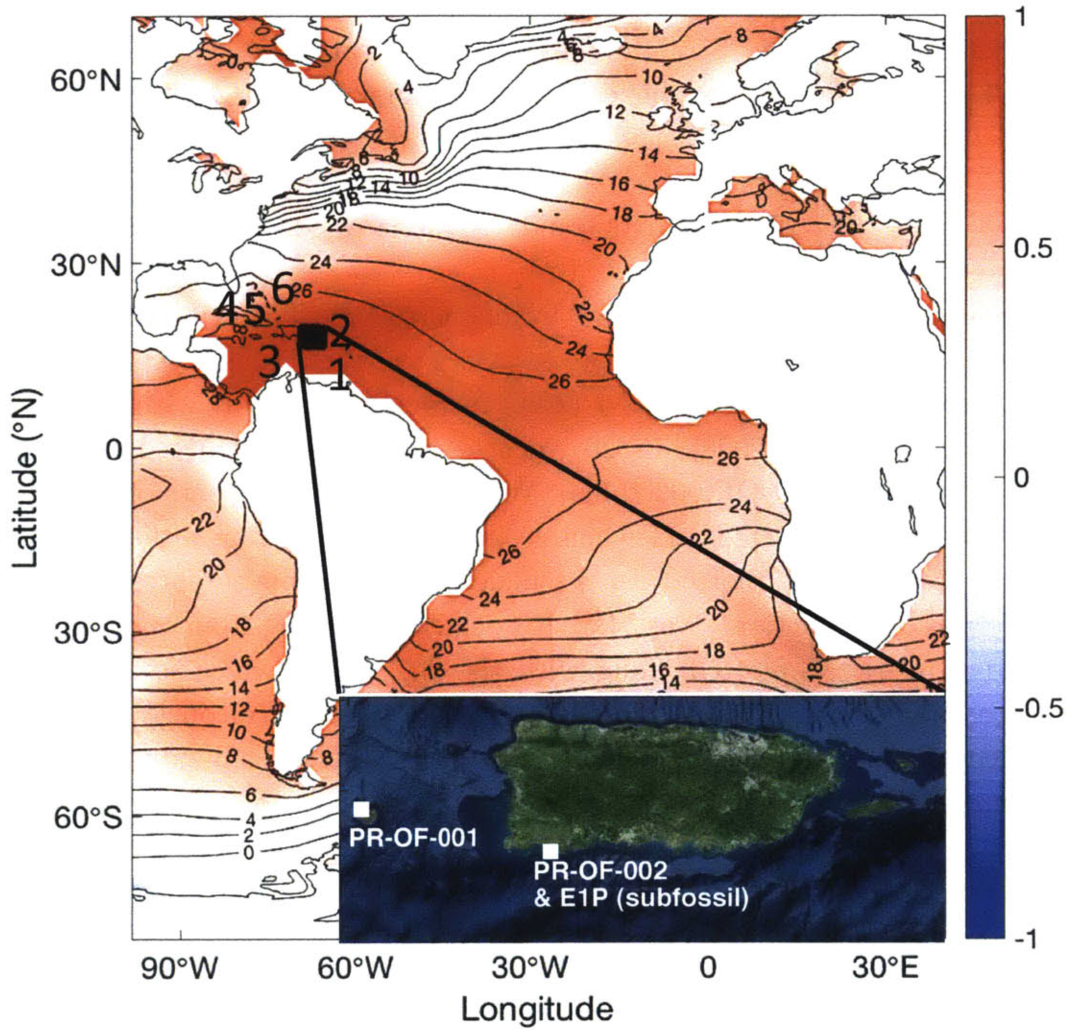

Figure 4-1: Map showing locations of modern *Orbicella faveolata* subfossil E1P [*Watanabe et al.*, 2001; *Kilbourne et al.*, 2008; 2010] and modern cores PR-OF-001 and PR-OF-002 [*Alpert et al.*, in review]. Colored shading corresponds to the correlation coefficient with 5 year low-pass filtered ERSST [*Smith et al.*, 2008] from the gridbox containing the coral locations and black contours indicate mean ERSST, 1854-2010. Locations of other studies mentioned in this paper are marked by numbers: 1) *Black et al.*, [2007]; 2) *Saenger et al.*, [2008]; 3) *Haase-Schraam et al.*, [2003]; 4) *DeLong et al.*, [2014]; 5) *Lund et al.*, [2006]; 6) *Saenger et al.*, [2009].

Figure 4-2: Top curves: Sr-U values at 3-year resolution from Puerto Rico Pinacles subfossil coral E1P (pink) and in 20th century, Pinacles modern coral PR-OF-002 (dashed pink) *Alpert et al.*, in review], and Puerto Rico Mona modern coral PR-OF-001 (purple) [*Alpert et al.*, in review]. Shading represents ± 1σ propagated uncertainty. Straight purple line indicates 20th century trend in PR-OF-001 Sr-U. Gray shaded boxes indicate Sporer and Maunder Minima in TSI [*Hegerl et al.,* 2007], red dashed lines mark large volcanic eruptions [*Gao et al.,* 2008]. The horizontal black dashed line represents estimated Pinacles SST in 1900 based upon the 20th century trend in Mona modern coral PR-OF-001 reconstructed SSTs.

Bottom curves: Sr-U reconstructed SST from Puerto Rico Pinacles subfossil coral E1P at 10-year resolution (blue) expressed as anomalies from 1958-1988 mean reconstructed SST at Pinacles [*Alpert et al.,* in review], which is within 0.25 °C of ERSST [*Smith et al.*, 2008]. In 20th century, Sr-U reconstructed SST from Pinacles modern coral PR-OF-002 (blue). When fewer than 10 years of Sr-U data exist no SST is reconstructed and when a single bin exists from a discontinuous section, the estimate is plotted as a single point. Shading represents ± 1σ standard error of prediction (0.6 °C). Reconstructed SSTs from modern coral PR-OF-001 (green) are plotted along with the 20th trend, which is statistically identical to that of ERSST over the same period. Pinacles reconstructed SSTs from the continuous LIA section 1465-1560 are not statistically different from those estimated in 1900.

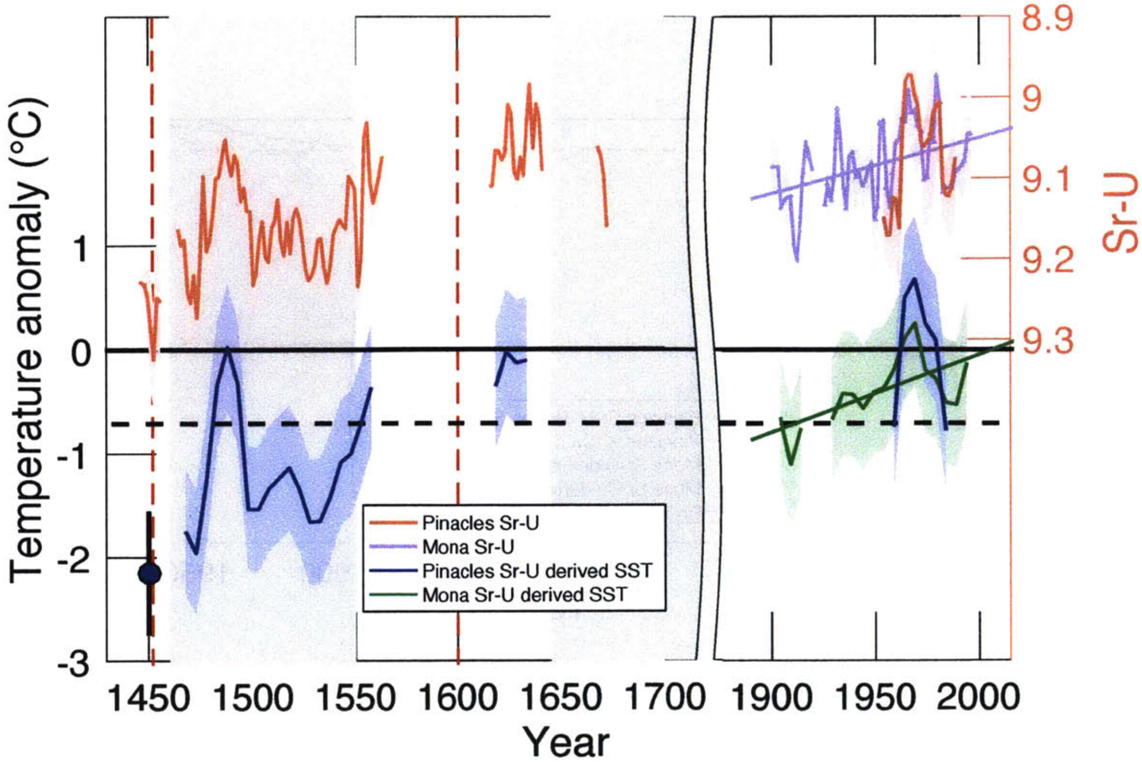

Temperature anomaly (°C)
1
0
-1
-2
-3
1450
1500
1550
1600
1650
1700
1900
1950
2000
Year
8.9
9
9.1
9.2
9.3
Sr-U
Pinacles Sr-U
Mona Sr-U
Pinacles Sr-U derived SST
Mona Sr-U derived SST

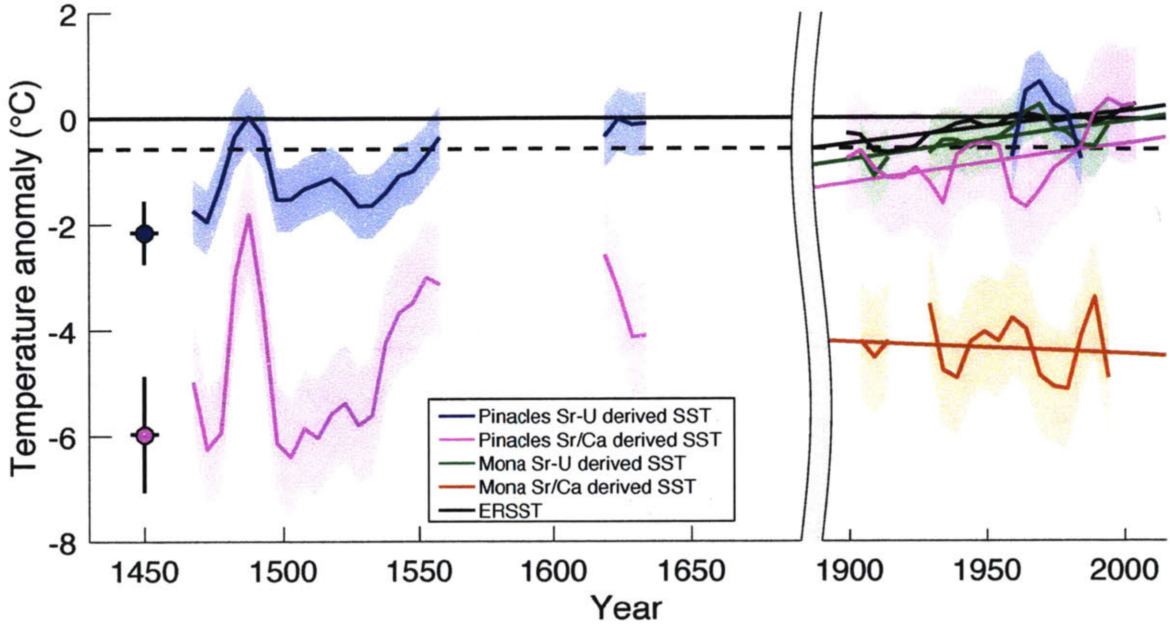

Figure 4-3: Sr-U reconstructed SST from Puerto Rico Pinacles subfossil coral E1P at 10-year resolution (blue) expressed as anomalies from the 1958-1988 mean [*Alpert et al.*, in review]. In 20th century, Sr-U reconstructed SST from Pinacles modern coral PR-OF-002 (green) and Puerto Rico Mona modern coral PR-OF-001 (blue). When fewer than 10 years of Sr-U data exist no SST is reconstructed and when a single bin exists from a discontinuous section, the estimate is plotted as a single point. Shading represents ± 1σ standard error of prediction (0.6 $^\circ$C). The horizontal black dashed line represents estimated Pinacles SST in 1900 based upon the 20th century trend in Mona modern coral PR-OF-001 reconstructed SSTs. Sr/Ca reconstructed SST from Puerto Rico Pinacles subfossil coral E1P (pink) and Mona modern coral PR-OF-002 (orange) expressed as anomalies. Sr/Ca reconstructed SST from the top of E1P core reported in *Kilbourne et al.,* [2008, 2010] plotted in pink. Shading represents ± 1σ uncertainty reported in *Kilbourne et al.,* [2010] (1.1 $^\circ$C). Sr/Ca reconstructed SST is estimated using the local Pinacles calibration *Kilbourne et al.*, [2008] from the top of the core of which E1P is a part. ERSST [*Smith et al.*, 2008] is plotted in black. 20th century trends are plotted in respective colors. Sr-U reconstructed SST trend from Mona modern coral PR-OF-002 is identical to that of ERSST, that of Sr/Ca reconstructed SST from Mona modern coral PR-OF-002 and the top of E1P are different.

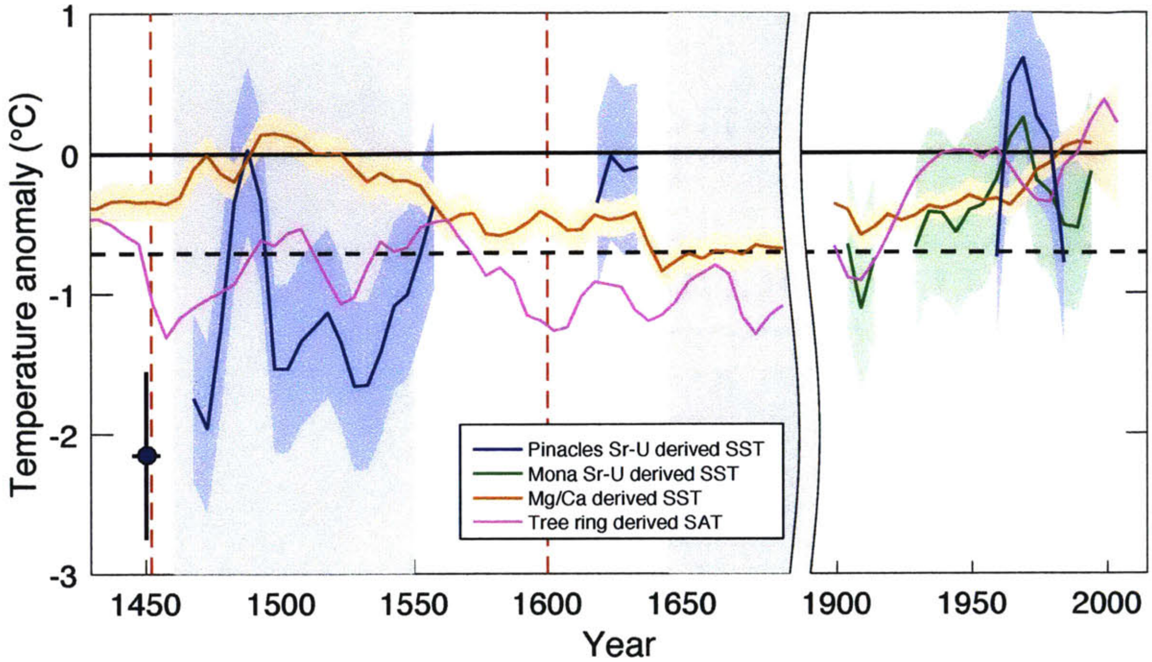

Figure 4-4: Sr-U reconstructed SST from Puerto Rico Pinacles subfossil coral E1P at 10-year resolution (blue) expressed as anomalies from the 1958-1988 mean [*Alpert et al.*, in review]. In 20th century, Sr-U reconstructed SST from Pinacles modern coral PR-OF-002 (green) and Puerto Rico Mona modern coral PR-OF-001 (blue). When fewer than 10 years of Sr-U data exist no SST is reconstructed and when a single bin exists from a discontinuous section, the estimate is plotted as a single point. Shading represents ± 1σ standard error of prediction (0.6 °C). The horizontal black dashed line represents estimated Pinacles SST in 1900 based upon the 20th century trend in Mona modern coral PR-OF-001 reconstructed SSTs. SST reconstructed from foramineferal Mg/Ca from the Cariaco basin is plotted in orange [*Black et al.*, 2007] and a northern hemisphere SAT record reconstructed from tree rings [*PAGES 2k Consortium*, 2013] is plotted in pink. Gray shaded boxes indicate Sporer and Maunder Minima in TSI [*Hegerl et al.*, 2007], red dashed lines mark large volcanic eruptions [*Gao et al.*, 2008].

Chapter 5

Conclusions

5.1 Thesis conclusions

I have refined and applied geochemical methods in coral paleoceanography to reconstruct sea surface temperatures (SSTs) during several periods of the Little Ice Age (LIA; 1450-1850). The LIA was a period of widespread cooling and provides an excellent interval to examine climate sensitivity to reasonably well-known external radiative forcings and characterize multidecadal variability. Questions remain regarding the amplitude of tropical SST cooling during the LIA and few records resolve multidecadal LIA SST variability.

To accomplish my goal of reconstructing past SSTs I thoroughly investigated coral geochemical paleothermometers. I assessed the ability of a common coral SST proxy, Sr/Ca, to capture SST mean, trends, and interannual variability. I found intercolony inconsistencies that could only be attributed to "vital effects" associated with biologically mediated calcification process. I quantified the resulting uncertainty of temperatures reconstructed using the Sr/Ca paleothermometer as $\pm$ 2 $^\circ$C, too large to reliably reconstruct SST trends or interannual variability. The Sr/Ca results demonstrate a clear need to account for "vital effects." To address this source of uncertainty in Sr/Ca I temporally and spatially expanded and refined a new coral paleothermometer, Sr-U, that uses information from Sr/Ca and U/Ca to extract a temperature signal separate from variability associated with the calcification process. I showed that a single

Sr-U to SST relationship captures spatial SST variability in a wide range of coral genera, with an uncertainty of ± 0.6 °C. Applied to timeseries, Sr-U accurately captures mean SST, trend, and variability at a site in the western tropical Atlantic (WTA) and is replicable within error between two corals. Sr-U-derived SSTs consistently provide more accurate SST estimates than Sr/Ca-derived SSTs in the same cores, and also have smaller uncertainty. Unlike Sr/Ca, Sr-U does not require a local or genus-specific modern calibration and can be applied to reconstruct SST from subfossil corals with no modern section. Having a universal calibration greatly advances options for acquiring reliable paleotemperature estimates from coral geochemisty.

I used Sr-U to reconstruct LIA SSTs in the WTA with unprecedented accuracy. Some previous Sr/Ca-derived estimates of WTA SST during the LIA suggest a larger degree of sensitivity to external forcing in the tropics than the high latitudes. Larger LIA cooling in the tropics is inconsistent with polar amplification of temperature change suggested by both observations of 20th century warming and simulations by global climate models (GCMs). Over the longest continuous section of the record, 1465 to 1560, I find a mean cooling of 1.1 °C relative to the mid-20th century. The results reconcile paleoclimatic reconstructions with model and observational estimates of meridional gradients in temperature change. Reconstructed SSTs are consistent with, although not diagnostic of, weakened Atlantic Meridional Overturning Circulation (AMOC) as a mechanism for large scale cooling driven by external radiative forcings. The record reveals multidecadal variability comparable to the 20th century and several periods of temperatures as warm as the mid-20th century. The timing of multidecadal variability may indicate sensitivity to volcanic eruptions but also points to internally driven variability.

5.2 Remaining uncertainty and future directions

Additional, complete LIA records are required for replication of multidecadal variability and higher confidence in the WTA SST response to volcanic and solar forcing. A key period for further investigation is the 19th century, the beginning of which was marked by several large volcanic eruptions, and which some records indicate was the coolest part of the last millennium [*McGregor et al.*, 2015].

Comparison of the WTA reconstruction and additional proxy records to externally forced and unforced GCM simulations for the last millennium could help understand SST response to radiative forcing. First, relatively accurate models or families of models must be identified. WTA SST in forced last millennium runs of the nine models included in the most recent Paleoclimate Intercomparison Model Project (PMIP3) varies widely (Figure 5-1). While models that better capture the 20th century warming trend, MIROC and FGOALS, indicate a greater degree of LIA cooling and sensitivity to external forcing, further investigation is required to determine whether the 20th century warming reflects realistic climate processes in these models. Eventually models could be used to evaluate the relative importance of various external forcings, mechanisms for amplification, and internal variability, as well as estimate future warming.

Sr-U could be applied to reconstruct SST in the equatorial Pacific and better constrain recent trends and sensitivity of this key region. Sr-U derived SST could reconcile disagreements among various reanalysis products based on instrumental data. Identifying recent trends would help determine whether there is a disagreement between observations and 20th century simulations on shifts in the Pacific zonal SST gradient. Additional Sr-U derived SST records will hopefully improve paleoclimate reanalyses [*Hakim et al.*, 2016].

More work remains to better understand the mechanisms and proper application of Sr-U. Future investigation could advance on two fronts: more geochemical modeling, and generating more Sr-U timeseries to understand whether there is a difference between its spatial versus temporal variability.

Both of these approaches may be employed to better understand the impact of seasonal growth bias on Sr-U values. Seasonal growth bias could explain why estimated temperatures from corals collected from several subtropical sites are too warm (Appendix D). Seasonal growth bias is difficult to quantify and its impact on the relationship between Sr/Ca and U/Ca is yet unclear. Seasonal growth rate could be better quantified by counting monthly skeletal dissepiments, to determine if the proportion of growth during warmer periods explains the difference between estimated and real temperatures. In addition, quantifying seasonal growth bias at tropical sites could explain the small degree of uncertainty on Sr-U derived SSTs in the spatial calibration. Another avenue to tackle this problem could be to modify the calcification model described by *DeCarlo et al* [2016] to examine the effects of seasonally-varying calcification rates on aragonite Sr-U values.

Geochemical modeling could also address the observation that the relationship between SST and Sr-U appears to be slightly shallower for temporally varying SST (Figure 3-5a). The slightly different relationship could reflect differences in the response of calcification rate and Rayleigh fractionation to changes in SST on annual and interannual timescales than to differences in mean SST described by the spatial calibration. The calcification model could also be used to explore whether shifts in the relationships between calcifying fluid

$[CO_3^{2-}]$, calcification rate, and Rayleigh fractionation explain the observed shallowing of the SST to Sr-U slope.

Replication of Sr-U in modern timeseries from additional corals could determine whether the shallower SST to Sr-U relationship is pervasive, and whether a single calibration can be applied to reconstruct temporal SST variability from multiple coral genera.

5.3 Figure

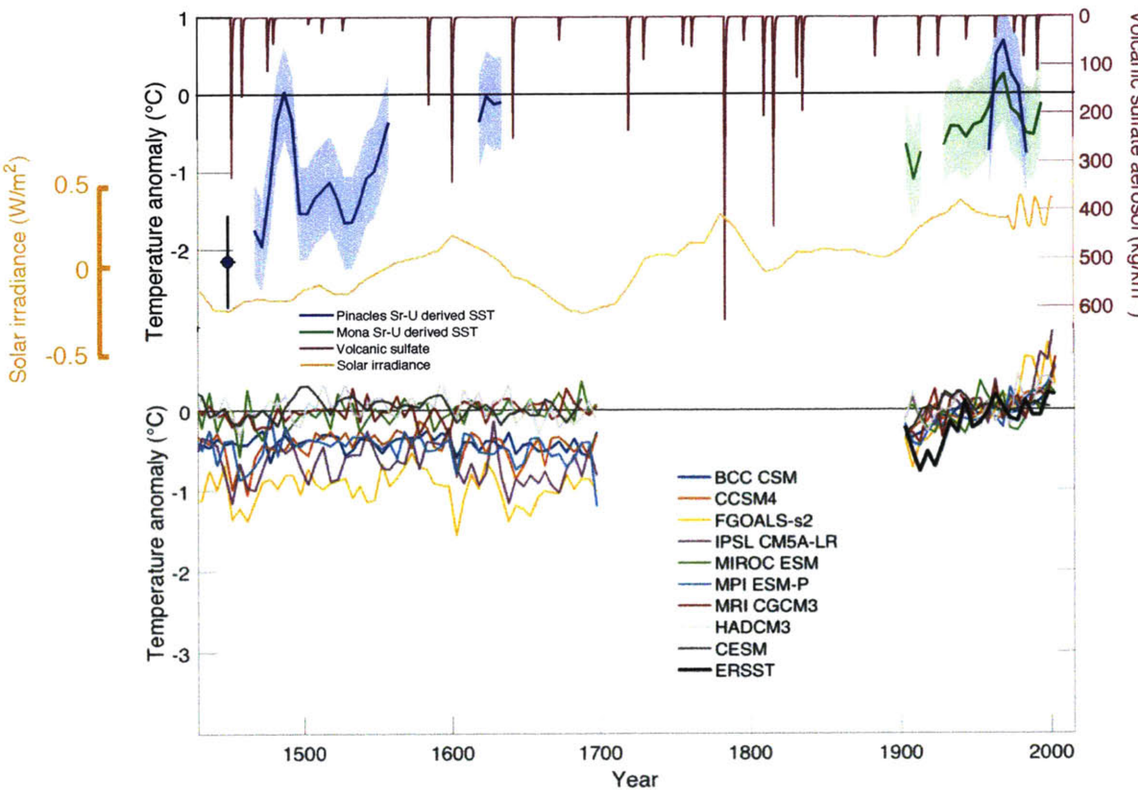

Figure 5-1: Top: WTA Sr-U derived SST anomalies relative to 1958-1988 (blue, green) plotted with solar irradiance forcing [*Hegerl et al.*, 2007] (gold), and volcanic aerosol loading [*Gao et al.*, 2008] (maroon). Bottom: SST anomalies relative to 1958-1988 in nine PMIP3 models and ERSST reanalysis [*Smith et al.*, 2008].

5.4 References

DeCarlo, T. M., G. A. Gaetani, A. L. Cohen, G. L. Foster, A. E. Alpert, and J. Stewart (2016), Coral Sr-U Thermometry, *Paleoceanography*

Gao, C., A. Robock, and C. Ammann (2008), Volcanic forcing of climate over the past 1500 years: An improved ice core-based index for climate models, *Journal of Geophysical Research: Atmospheres*, *113*(D23)

Hakim, G. J., J. Emile-Geay, E. J. Steig, D. Noone, D. M. Anderson, R. Tardif, N. Steiger, and W. A. Perkins (2016), The Last Millennium Climate

Reanalysis Project: Framework and First Results, *Journal of Geophysical Research: Atmospheres*

Hegerl, G., F. Zwiers, P. Braconnot, N. Gillet, Y. Luo, J. Marengo, N. Nicholls, J. Penner, and P. Stott (2007), Understanding and attributing climate change

Smith, J. M., T. M. Quinn, K. P. Helmle, and R. B. Halley (2006), Reproducibility of geochemical and climatic signals in the Atlantic coral Montastraea faveolata, *Paleoceanography*, *21*(1)

McGregor, H. V., M. N. Evans, H. Goosse, G. Leduc, B. Martrat, J. A. Addison, P. G. Mortyn, D. W. Oppo, M.-S. Seidenkrantz, and M.-A. Sicre (2015), Robust global ocean cooling trend for the pre-industrial Common Era, *Nature Geoscience*

Appendix A

Supplementary information, figures, and data for Chapter 2

A1. W037-W497 splice

Two cores, W037 and W497, from the same colony were spliced to produce a longer record (Figure A-2). The overlapping period includes seven samples from W497 and 12 samples from W037. The average difference in Sr/Ca between nearest neighbors is 0.03±0.02 mmol/mol (1σ, n=7). Given the small number of overlapping data points for core W497, and the observation that the difference between cores is less than the standard deviation of the consistency standards we did not impose any correction for a potential offset. The spliced record includes all W037 data points, and only includes W497 data points after the end of the W037 record.

A2. E016 sampling

Core E016 displays complex corallite structure and is not optimal for geochemical sampling. Previous studies in Porites corals have found higher Sr/Ca values in "valleys" than in adjacent "bumps" [Alibert and McCulloch, 1997; Cohen and Hart, 1997; Alibert and Kinsley, 2008] and the optimal sampling path is along central axis of the corallite bundle with corallites extending parallel to the sampling surface [DeLong et al., 2013]. We have addressed a potential issue in the sampling track of core E016 by sampling along the "bump" adjacent to a "valley" (dashed red line in Figure A-2e). Sr/Ca values are higher in the "valley" than the "bump" (Figure A-3) and we use those from the "bump." The sampling track is at a slight angle to the corallites in the bottom year of the record (Figure

A2e), although it is not in a "valley." This section does not display anomalously high Sr/Ca values.

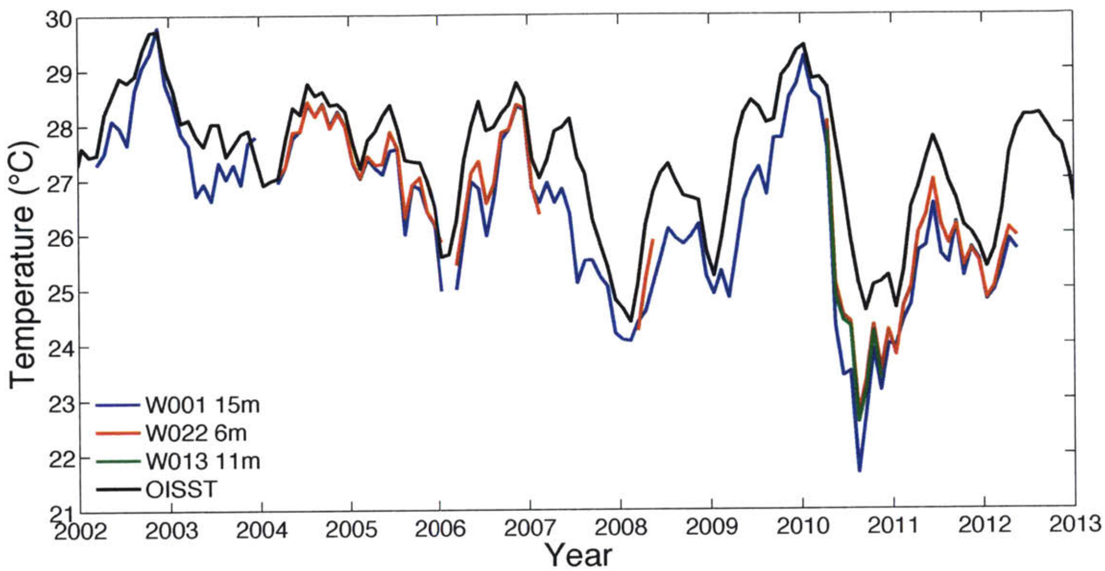

Figure A1. West side logger composite temperature timeseries: W001 (15 m; blue), W022 (6 m; red), and W013 (11 m; green). For reference OISST [*Reynolds et al.*, 2002] is plotted in black. One standard deviation of concurrent logger measurements is 0.07 ° C. Logger locations are marked in Figure. 2-1.

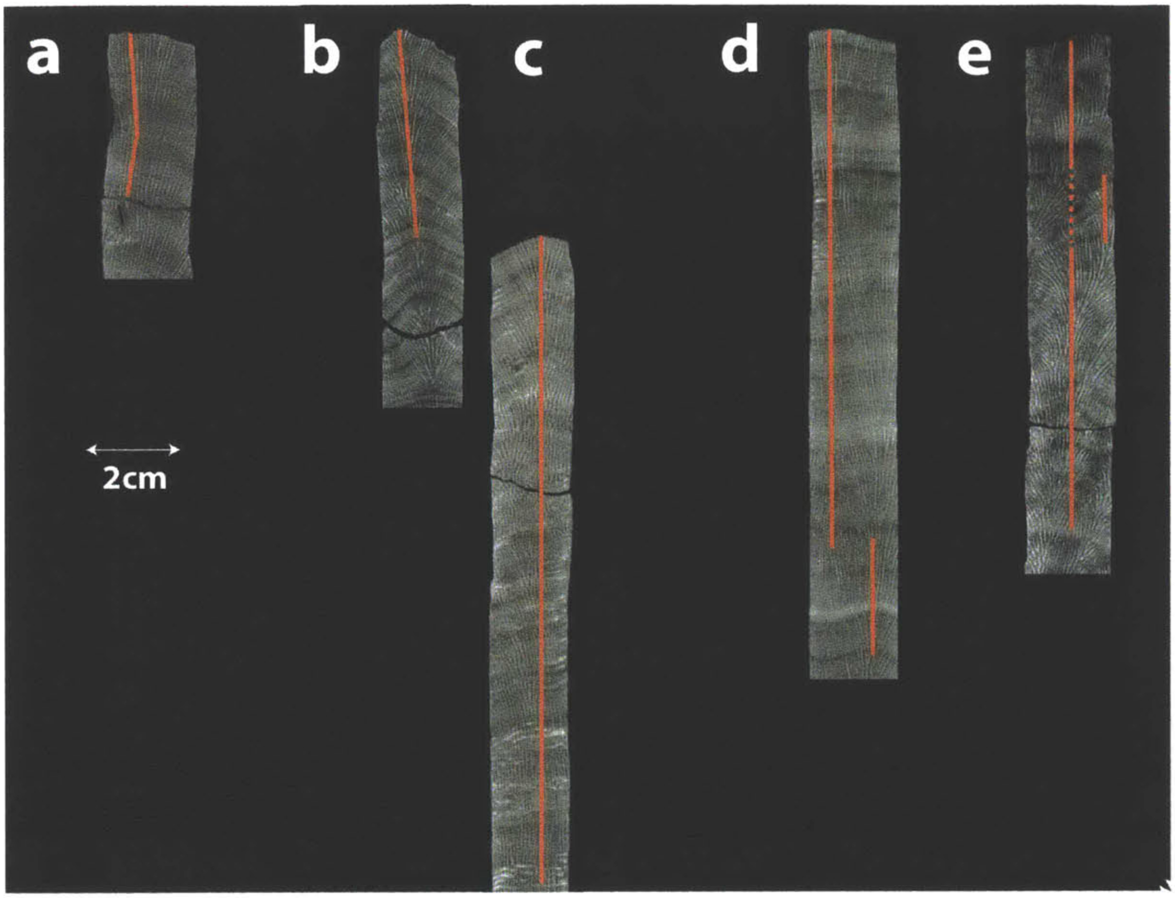

Figure A2. Computerized Tomography (CT) scans of cores a) W497, b) W037, c) W490, d) E500, and e) E016. Annual density couplets visible as light and dark bands, with the low-density band formed in summer marked for each year. Red lines mark sampling axes, scale bar indicates distance in centimeters. W490 and W037 were cored from the same coral and records were spliced together (Figure A3), with the top of W037 corresponding to 2010.3. White regions in W037 indicate high density, but no evidence of infilling is visible by manipulating the 3-dimensional CT scan or in Scanning Electron Microscope (SEM) imaging. The dotted section of the E016 sampling axis indicates a "valley" in the coral surface. The adjacent "bump" was sampled and values were spliced into the record (Figure A-3). The high Sr/Ca values in the spliced W037 record during the 2007-08 La Nina (Figure 2-2) do not correspond to a "valley".

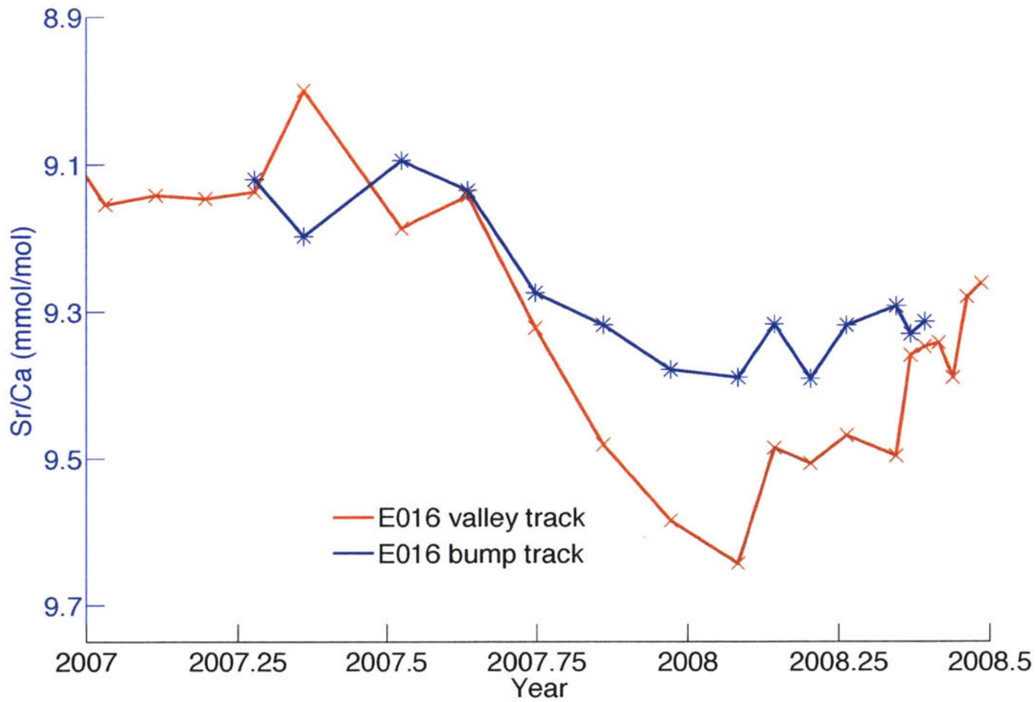

Figure A3. Sr/Ca of "valley" (dashed red line in Figure A-2e) and "bump" (adjacent solid red line in Figure A-2e) tracks in core E016. The "valley" track shows evidence of anomalously high Sr/Ca values [*Alibert and McCulloch, 1997*]. Where both values exist the "bump" value is used.

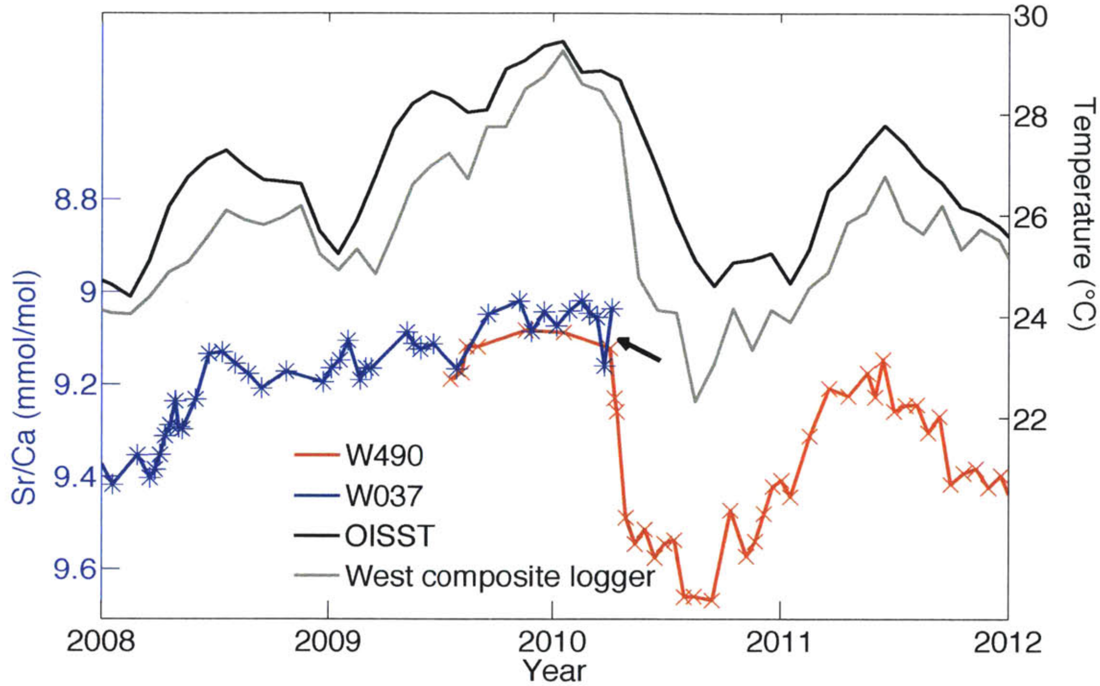

Figure A4. Sr/Ca of W037 and W497, cored from the same coral, plotted with OISST (black; *Reynolds et al.* [2002]) and west logger composite temperature (gray). Black arrow indicates location of splice. Average offset is 0.03±0.02 mmol/mol (1σ, n=7).

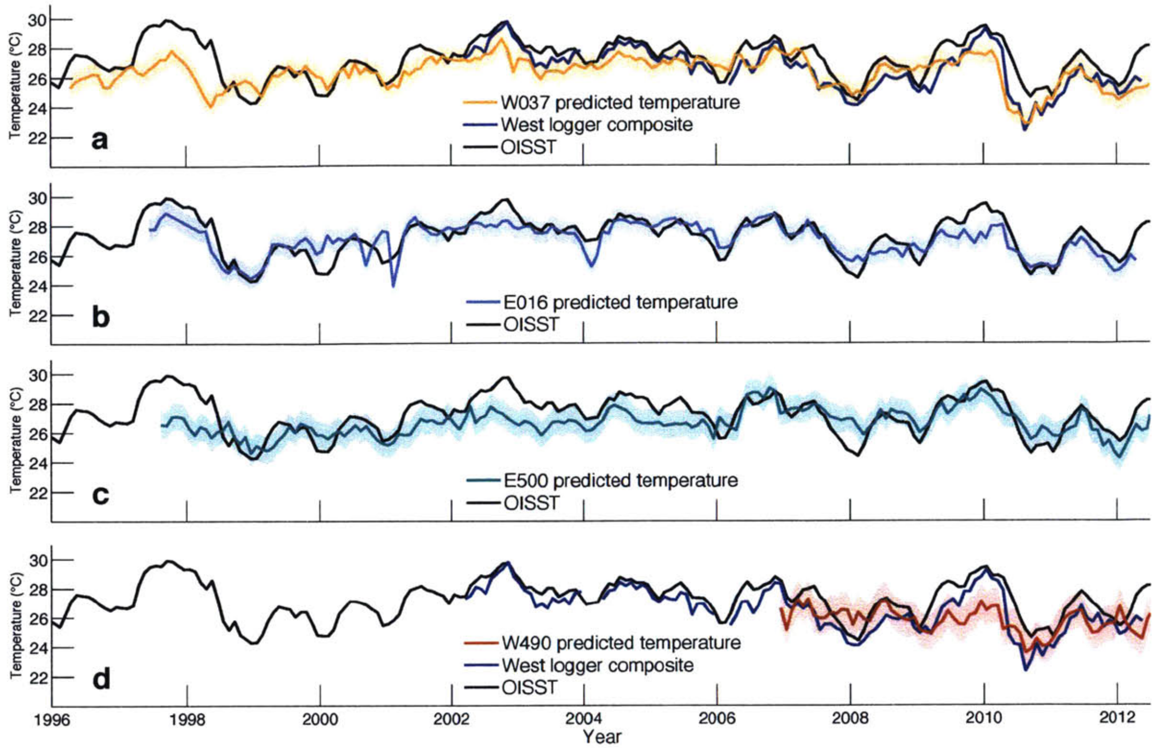

Figure A5. A) Temperatures estimated based on Sr/Ca from core W037, applying the regression of west logger composite temperature onto Sr/Ca from W037, plotted with west logger composite temperature (blue) and OISST (black; *Reynolds et al.* [2002]). Shaded errors indicate one standard error of prediction. B-D) Same as in A but for E016, E500, and W490, respectively. Each record is generated by applying the temperature-Sr/Ca regression specific to that coral (Table 2-1).

References

Alibert, C., and M. T. McCulloch (1997), Strontium/calcium ratios in modern Porites corals from the Great Barrier Reef as a proxy for sea surface temperature: Calibration of the thermometer and monitoring of ENSO, *Paleoceanography*, 12(3), 345-363, doi:10.1029/97PA00318.

Alibert, C., and L. Kinsley (2008), A 170-year Sr/Ca and Ba/Ca coral record from the western Pacific warm pool: 1. What can we learn from an unusual coral record?, *Journal of Geophysical Research: Oceans (1978–2012)*, *113*(C4), doi: 10.1029/2006JC003979.

Cohen, A. L., and S. R. Hart (1997), The effect of colony topography on climate signals in coral skeleton, *Geochimica et Cosmochimica Acta*, *61*(18), 3905-3912.

Hathorne, E. C., A. Gagnon, T. Felis, J. Adkins, R. Asami, W. Boer, N. Caillon, D. Case, K. M. Cobb, and E. Douville (2013), Inter-laboratory study for coral Sr/Ca and other element/Ca ratio measurements, *Geochemistry, Geophysics, Geosystems*, *14*(9), 3730-3750, doi:10.1002/ggge.20230.

Reynolds, R. W., N. A. Rayner, T. M. Smith, D. C. Stokes, and W. Wang (2002), An improved in situ and satellite SST analysis for climate, *Journal of Climate*, *15*(13), 1609-1625.

A.3 Sr/Ca data for all corals, loggers, and satellite SST used in this paper

Year	E016 Sr/Ca (mmol/mol)	East combined logger (°C)
2012.29	9.38	NaN
2012.21	9.33	NaN
2012.12	9.42	NaN
2012.04	9.47	NaN
2011.96	9.48	NaN
2011.87	9.42	NaN
2011.79	9.35	NaN
2011.71	9.35	NaN
2011.62	9.29	NaN
2011.54	9.21	NaN
2011.46	9.18	NaN
2011.37	9.25	NaN
2011.29	9.21	NaN
2011.21	9.29	26.16
2011.12	9.43	25.23
2011.04	9.44	24.47
2010.96	9.43	24.90
2010.87	9.41	24.69
2010.79	9.42	24.96
2010.71	9.45	24.47
2010.62	9.40	24.43
2010.54	9.32	25.60
2010.46	9.29	26.44
2010.37	9.27	27.09
2010.29	9.06	28.54
2010.21	9.07	28.67
2010.12	9.07	28.69
2010.04	9.18	29.41
2009.96	9.13	29.19
2009.87	9.22	29.00
2009.79	9.17	28.75
2009.71	9.11	27.96

Year	E500 Sr/Ca (mmol/mol)	East combined logger (°C)
2012.54	9.01	NaN
2012.46	9.20	NaN
2012.37	9.22	NaN
2012.29	9.17	NaN
2012.21	9.25	NaN
2012.12	9.34	NaN
2012.04	9.42	NaN
2011.96	9.37	NaN
2011.87	9.29	NaN
2011.79	9.33	NaN
2011.71	9.21	NaN
2011.62	9.21	NaN
2011.54	9.07	NaN
2011.46	9.05	NaN
2011.37	9.18	NaN
2011.29	9.20	NaN
2011.21	9.22	26.16
2011.12	9.26	25.23
2011.04	9.25	24.47
2010.96	9.21	24.90
2010.87	9.18	24.69
2010.79	9.25	24.96
2010.71	9.28	24.47
2010.62	9.21	24.43
2010.54	9.14	25.60
2010.46	9.09	26.44
2010.37	9.10	27.09
2010.29	9.07	28.54
2010.21	9.02	28.67
2010.12	8.96	28.69
2010.04	8.92	29.41
2009.96	8.89	29.19

2009.62	9.18	27.99
2009.54	9.17	28.05
2009.46	9.16	28.14
2009.37	9.11	27.40
2009.29	9.16	27.08
2009.21	9.25	26.29
2009.12	9.31	25.73
2009.04	9.28	25.21
2008.96	9.23	25.58
2008.87	9.27	26.46
2008.79	9.35	26.51
2008.71	9.28	26.58
2008.62	9.27	26.82
2008.54	9.31	27.02
2008.46	9.30	26.56
2008.37	9.33	25.87
2008.29	9.31	25.56
2008.21	9.39	24.89
2008.12	9.34	NaN
2008.04	9.39	NaN
2007.96	9.37	NaN
2007.87	9.33	NaN
2007.79	9.29	NaN
2007.71	9.23	NaN
2007.62	9.15	NaN
2007.54	9.18	26.99
2007.46	9.11	27.67
2007.37	9.02	27.69
2007.29	9.12	27.44
2007.21	9.14	27.21
2007.12	9.14	26.88
2007.04	9.15	27.18
2006.96	9.06	28.43
2006.87	8.96	28.56
2006.79	8.97	28.18
2006.71	8.99	28.14
2006.62	9.00	27.65
2006.54	9.04	27.65

2009.87	8.95	29.00
2009.79	8.99	28.75
2009.71	8.94	27.96
2009.62	8.99	27.99
2009.54	9.05	28.05
2009.46	9.08	28.14
2009.37	9.00	27.40
2009.29	9.05	27.08
2009.21	9.15	26.29
2009.12	9.19	25.73
2009.04	9.23	25.21
2008.96	9.15	25.58
2008.87	9.09	26.46
2008.79	9.07	26.51
2008.71	9.07	26.58
2008.62	9.05	26.82
2008.54	9.12	27.02
2008.46	9.05	26.56
2008.37	9.16	25.87
2008.29	9.19	25.56
2008.21	9.24	24.89
2008.12	9.18	NaN
2008.04	9.12	NaN
2007.96	9.12	NaN
2007.87	9.13	NaN
2007.79	9.12	NaN
2007.71	9.11	NaN
2007.62	9.06	NaN
2007.54	9.03	26.99
2007.46	9.01	27.67
2007.37	9.05	27.69
2007.29	9.06	27.44
2007.21	9.04	27.21
2007.12	9.04	26.88
2007.04	9.06	27.18
2006.96	9.08	28.43
2006.87	8.91	28.56
2006.79	8.89	28.18

2006.46	9.07	28.15
2006.37	9.08	27.74
2006.29	9.17	27.06
2006.21	9.25	26.20
2006.12	9.26	25.34
2006.04	9.26	25.48
2005.96	9.11	26.45
2005.87	9.09	26.92
2005.79	9.13	27.23
2005.71	9.04	27.21
2005.62	9.07	27.14
2005.54	9.04	27.82
2005.46	9.05	28.21
2005.37	9.00	27.95
2005.29	9.01	27.70
2005.21	9.02	27.61
2005.12	9.06	27.21
2005.04	9.08	27.50
2004.96	9.06	28.12
2004.87	9.04	28.33
2004.79	9.04	28.17
2004.71	9.04	28.53
2004.62	9.01	28.37
2004.54	9.01	28.52
2004.46	9.02	28.07
2004.37	9.14	28.12
2004.29	9.12	27.60
2004.21	9.33	27.21
2004.12	9.43	NaN
2004.04	9.32	NaN
2003.96	9.21	NaN
2003.87	9.13	NaN
2003.79	9.13	NaN
2003.71	9.12	NaN
2003.62	9.10	NaN
2003.54	9.06	NaN
2003.46	9.12	NaN
2003.37	9.13	NaN

2006.71	8.97	28.14
2006.62	8.92	27.65
2006.54	8.92	27.65
2006.46	8.94	28.15
2006.37	9.06	27.74
2006.29	9.21	27.06
2006.21	9.18	26.20
2006.12	9.16	25.34
2006.04	9.11	25.48
2005.96	9.27	26.45
2005.87	9.18	26.92
2005.79	9.13	27.23
2005.71	9.17	27.21
2005.62	9.19	27.14
2005.54	9.15	27.82
2005.46	9.16	28.21
2005.37	9.16	27.95
2005.29	9.17	27.70
2005.21	9.18	27.61
2005.12	9.15	27.21
2005.04	9.16	27.50
2004.96	9.15	28.12
2004.87	9.15	28.33
2004.79	9.14	28.17
2004.71	9.09	28.53
2004.62	9.05	28.37
2004.54	9.03	28.52
2004.46	9.02	28.07
2004.37	9.04	28.12
2004.29	9.13	27.60
2004.21	9.16	27.21
2004.12	9.20	NaN
2004.04	9.21	NaN
2003.96	9.17	NaN
2003.87	9.14	NaN
2003.79	9.13	NaN
2003.71	9.15	NaN
2003.62	9.14	NaN

2003.29	9.13	NaN
2003.21	9.07	NaN
2003.12	9.07	NaN
2003.04	9.09	NaN
2002.96	9.08	NaN
2002.87	9.02	NaN
2002.79	9.02	NaN
2002.71	9.07	NaN
2002.62	9.06	NaN
2002.54	9.07	NaN
2002.46	9.04	NaN
2002.37	9.03	NaN
2002.29	9.05	NaN
2002.21	9.07	NaN
2002.12	9.09	NaN
2002.04	9.09	NaN
2001.96	9.08	NaN
2001.87	9.11	NaN
2001.79	9.14	NaN
2001.71	9.14	NaN
2001.62	9.10	NaN
2001.54	9.06	NaN
2001.46	8.99	NaN
2001.37	9.03	NaN
2001.29	9.13	NaN
2001.21	9.39	NaN
2001.12	9.60	NaN
2001.04	9.12	NaN
2000.96	9.11	NaN
2000.87	9.18	NaN
2000.79	9.27	NaN
2000.71	9.41	NaN
2000.62	9.21	NaN
2000.54	9.13	NaN
2000.46	9.17	NaN
2000.37	9.19	NaN
2000.29	9.17	NaN
2000.21	9.21	NaN
2003.54	9.14	NaN
2003.46	9.19	NaN
2003.37	9.24	NaN
2003.29	9.19	NaN
2003.21	9.15	NaN
2003.12	9.14	NaN
2003.04	9.17	NaN
2002.96	9.15	NaN
2002.87	9.12	NaN
2002.79	9.08	NaN
2002.71	9.07	NaN
2002.62	9.03	NaN
2002.54	9.10	NaN
2002.46	9.11	NaN
2002.37	9.15	NaN
2002.29	9.02	NaN
2002.21	9.12	NaN
2002.12	9.20	NaN
2002.04	9.15	NaN
2001.96	9.10	NaN
2001.87	9.15	NaN
2001.79	9.15	NaN
2001.71	9.13	NaN
2001.62	9.14	NaN
2001.54	9.12	NaN
2001.46	9.18	NaN
2001.37	9.24	NaN
2001.29	9.24	NaN
2001.21	9.23	NaN
2001.12	9.30	NaN
2001.04	9.32	NaN
2000.96	9.31	NaN
2000.87	9.28	NaN
2000.79	9.23	NaN
2000.71	9.17	NaN
2000.62	9.21	NaN
2000.54	9.17	NaN
2000.46	9.21	NaN

2000.12	9.14	NaN
2000.04	9.28	NaN
1999.96	9.31	NaN
1999.87	9.22	NaN
1999.79	9.17	NaN
1999.71	9.19	NaN
1999.62	9.25	NaN
1999.54	9.25	NaN
1999.46	9.23	NaN
1999.37	9.22	NaN
1999.29	9.22	NaN
1999.21	9.38	NaN
1999.12	9.45	NaN
1999.04	9.50	NaN
1998.96	9.53	NaN
1998.87	9.49	NaN
1998.79	9.45	NaN
1998.71	9.41	NaN
1998.62	9.48	NaN
1998.54	9.44	NaN
1998.46	9.35	NaN
1998.37	9.28	NaN
1998.29	9.10	NaN
1998.21	9.10	NaN
1998.12	9.08	NaN
1998.04	9.05	NaN
1997.96	9.02	NaN
1997.87	8.99	NaN
1997.79	8.97	NaN
1997.71	8.94	NaN
1997.62	8.98	NaN
1997.54	9.08	NaN
1997.46	9.08	NaN

2000.37	9.25	NaN
2000.29	9.21	NaN
2000.21	9.24	NaN
2000.12	9.27	NaN
2000.04	9.24	NaN
1999.96	9.24	NaN
1999.87	9.19	NaN
1999.79	9.17	NaN
1999.71	9.15	NaN
1999.62	9.22	NaN
1999.54	9.17	NaN
1999.46	9.24	NaN
1999.37	9.28	NaN
1999.29	9.34	NaN
1999.21	9.36	NaN
1999.12	9.35	NaN
1999.04	9.32	NaN
1998.96	9.38	NaN
1998.87	9.25	NaN
1998.79	9.31	NaN
1998.71	9.26	NaN
1998.62	9.14	NaN
1998.54	9.20	NaN
1998.46	9.22	NaN
1998.37	9.26	NaN
1998.29	9.20	NaN
1998.21	9.18	NaN
1998.12	9.24	NaN
1998.04	9.19	NaN
1997.96	9.11	NaN
1997.87	9.10	NaN
1997.79	9.10	NaN
1997.71	9.17	NaN

Year	W037 Sr/Ca (mmol/mol)	West composite logger (° C)
2012.71	9.31	NaN
2012.62	9.45	NaN
2012.54	9.30	NaN
2012.46	9.33	NaN
2012.37	9.34	25.70
2012.29	9.35	26.00
2012.21	9.37	25.50
2012.12	9.40	25.00
2012.04	9.45	24.81
2011.96	9.40	25.52
2011.87	9.40	25.73
2011.79	9.40	25.32
2011.71	9.30	26.20
2011.62	9.28	25.64
2011.54	9.25	25.90
2011.46	9.17	26.78
2011.37	9.18	26.06
2011.29	9.23	25.85
2011.21	9.22	24.87
2011.12	9.32	24.57
2011.04	9.44	23.89
2010.96	9.43	24.13
2010.87	9.55	23.34
2010.79	9.49	24.16
2010.71	9.65	23.06
2010.62	9.66	22.32
2010.54	9.56	24.08
2010.46	9.57	24.12
2010.37	9.54	24.77
2010.29	9.32	27.83
2010.21	9.11	28.46
2010.12	9.02	28.60
2010.04	9.06	29.25
2009.96	9.05	28.74
2009.87	9.05	28.49

Year	W490 Sr/Ca (mmol/mol)	West composite logger (° C)
2012.71	9.09	NaN
2012.62	9.06	NaN
2012.54	9.09	NaN
2012.46	9.15	NaN
2012.37	9.28	25.70
2012.29	9.25	26.00
2012.21	9.22	25.50
2012.12	9.17	25.00
2012.04	9.07	24.81
2011.96	9.18	25.52
2011.87	9.18	25.73
2011.79	9.19	25.32
2011.71	9.23	26.20
2011.62	9.24	25.64
2011.54	9.18	25.90
2011.46	9.09	26.78
2011.37	9.10	26.06
2011.29	9.12	25.85
2011.21	9.15	24.87
2011.12	9.21	24.57
2011.04	9.28	23.89
2010.96	9.32	24.13
2010.87	9.33	23.34
2010.79	9.28	24.16
2010.71	9.35	23.06
2010.62	9.37	22.32
2010.54	9.24	24.08
2010.46	9.20	24.12
2010.37	9.20	24.77
2010.29	9.22	27.83
2010.21	9.07	28.46
2010.12	9.07	28.60
2010.04	9.09	29.25
2009.96	9.03	28.74
2009.87	9.11	28.49

2009.79	9.03	27.76
2009.71	9.06	27.75
2009.62	9.13	26.72
2009.54	9.15	27.23
2009.46	9.12	26.99
2009.37	9.11	26.62
2009.29	9.12	25.70
2009.21	9.16	24.84
2009.12	9.17	25.33
2009.04	9.15	24.92
2008.96	9.19	25.24
2008.87	9.18	26.19
2008.79	9.18	25.96
2008.71	9.21	25.82
2008.62	9.17	25.92
2008.54	9.14	26.11
2008.46	9.15	25.58
2008.37	9.27	25.09
2008.29	9.30	24.89
2008.21	9.40	24.40
2008.12	9.37	24.06
2008.04	9.41	24.08
2007.96	9.33	24.20
2007.87	9.31	25.05
2007.79	9.31	25.23
2007.71	9.33	25.52
2007.62	9.34	25.52
2007.54	9.35	25.11
2007.46	9.24	26.38
2007.37	9.11	26.84
2007.29	9.03	26.59
2007.21	9.00	26.95
2007.12	9.05	26.59
2007.04	9.06	26.87
2006.96	9.02	28.30
2006.87	8.98	28.36
2006.79	9.03	27.92
2006.71	9.12	27.80

2009.79	9.13	27.76
2009.71	9.19	27.75
2009.62	9.18	26.72
2009.54	9.14	27.23
2009.46	9.10	26.99
2009.37	9.17	26.62
2009.29	9.19	25.70
2009.21	9.25	24.84
2009.12	9.23	25.33
2009.04	9.22	24.92
2008.96	9.14	25.24
2008.87	9.16	26.19
2008.79	9.15	25.96
2008.71	9.13	25.82
2008.62	9.10	25.92
2008.54	9.02	26.11
2008.46	9.03	25.58
2008.37	9.10	25.09
2008.29	9.16	24.89
2008.21	9.15	24.40
2008.12	9.11	24.06
2008.04	9.19	24.08
2007.96	9.09	24.20
2007.87	9.09	25.05
2007.79	9.12	25.23
2007.71	9.11	25.52
2007.62	9.14	25.52
2007.54	9.15	25.11
2007.46	9.13	26.38
2007.37	9.02	26.84
2007.29	9.07	26.59
2007.21	9.02	26.95
2007.12	9.10	26.59
2007.04	9.22	26.87
2006.96	9.08	28.30
2006.87	NaN	28.36
2006.79	NaN	27.92
2006.71	NaN	27.80

2006.62	9.16		26.80
2006.54	9.17		26.28
2006.46	9.15		27.09
2006.37	9.06		27.05
2006.29	9.05		26.14
2006.21	9.20		25.44
2006.12	9.17	NaN	
2006.04	9.15	NaN	
2005.96	9.15		26.18
2005.87	9.11		26.42
2005.79	9.09		26.94
2005.71	9.07		26.91
2005.62	9.17		26.16
2005.54	9.12		27.57
2005.46	9.10		27.71
2005.37	9.08		27.20
2005.29	9.13		27.25
2005.21	9.10		27.41
2005.12	9.15		27.03
2005.04	9.17		27.32
2004.96	9.12		27.98
2004.87	9.08		28.24
2004.79	9.10		27.96
2004.71	9.07		28.39
2004.62	9.07		28.17
2004.54	9.03		28.41
2004.46	9.07		27.89
2004.37	9.12		27.82
2004.29	9.16		27.24
2004.21	9.18	NaN	
2004.12	9.13	NaN	
2004.04	9.17	NaN	
2003.96	9.16		27.79
2003.87	9.13		27.68
2003.79	9.18		26.92
2003.71	9.21		27.29
2003.62	9.19		27.02
2003.54	9.19		27.32

2006.62	NaN		26.80
2006.54	NaN		26.28
2006.46	NaN		27.09
2006.37	NaN		27.05
2006.29	NaN		26.14
2006.21	NaN		25.44
2006.12	NaN	NaN	
2006.04	NaN	NaN	
2005.96	NaN		26.18
2005.87	NaN		26.42
2005.79	NaN		26.94
2005.71	NaN		26.91
2005.62	NaN		26.16
2005.54	NaN		27.57
2005.46	NaN		27.71
2005.37	NaN		27.20
2005.29	NaN		27.25
2005.21	NaN		27.41
2005.12	NaN		27.03
2005.04	NaN		27.32
2004.96	NaN		27.98
2004.87	NaN		28.24
2004.79	NaN		27.96
2004.71	NaN		28.39
2004.62	NaN		28.17
2004.54	NaN		28.41
2004.46	NaN		27.89
2004.37	NaN		27.82
2004.29	NaN		27.24
2004.21	NaN	NaN	
2004.12	NaN	NaN	
2004.04	NaN	NaN	
2003.96	NaN		27.79
2003.87	NaN		27.68
2003.79	NaN		26.92
2003.71	NaN		27.29
2003.62	NaN		27.02
2003.54	NaN		27.32

2003.46	9.19	26.63
2003.37	9.26	26.94
2003.29	9.20	26.72
2003.21	9.10	27.63
2003.12	9.09	27.85
2003.04	9.08	28.38
2002.96	9.20	28.76
2002.87	9.00	29.78
2002.79	8.91	29.32
2002.71	8.97	29.06
2002.62	9.05	28.64
2002.54	9.04	27.65
2002.46	9.09	27.96
2002.37	9.08	28.09
2002.29	9.11	27.50
2002.21	9.09	27.29
2002.12	9.10	NaN
2002.04	9.09	NaN
2001.96	9.09	NaN
2001.87	9.06	NaN
2001.79	9.12	NaN
2001.71	9.07	NaN
2001.62	9.09	NaN
2001.54	9.17	NaN
2001.46	9.18	NaN
2001.37	9.23	NaN
2001.29	9.20	NaN
2001.21	9.33	NaN
2001.12	9.31	NaN
2001.04	9.35	NaN
2000.96	9.28	NaN
2000.87	9.20	NaN
2000.79	9.20	NaN
2000.71	9.17	NaN
2000.62	9.22	NaN
2000.54	9.13	NaN
2000.46	9.25	NaN
2000.37	9.16	NaN

2003.46	NaN	26.63
2003.37	NaN	26.94
2003.29	NaN	26.72
2003.21	NaN	27.63
2003.12	NaN	27.85
2003.04	NaN	28.38
2002.96	NaN	28.76
2002.87	NaN	29.78
2002.79	NaN	29.32
2002.71	NaN	29.06
2002.62	NaN	28.64
2002.54	NaN	27.65
2002.46	NaN	27.96
2002.37	NaN	28.09
2002.29	NaN	27.50
2002.21	NaN	27.29

2000.29	9.21	NaN
2000.21	9.28	NaN
2000.12	9.35	NaN
2000.04	9.25	NaN
1999.96	9.24	NaN
1999.87	9.20	NaN
1999.79	9.15	NaN
1999.71	9.21	NaN
1999.62	9.20	NaN
1999.54	9.15	NaN
1999.46	9.20	NaN
1999.37	9.23	NaN
1999.29	9.22	NaN
1999.21	9.32	NaN
1999.12	9.41	NaN
1999.04	9.34	NaN
1998.96	9.29	NaN
1998.87	9.27	NaN
1998.79	9.30	NaN
1998.71	9.30	NaN
1998.62	9.33	NaN
1998.54	9.39	NaN
1998.46	9.39	NaN
1998.37	9.50	NaN
1998.29	9.43	NaN
1998.21	9.33	NaN
1998.12	9.24	NaN
1998.04	9.15	NaN
1997.96	9.10	NaN
1997.87	9.06	NaN
1997.79	9.01	NaN
1997.71	9.08	NaN
1997.62	9.09	NaN
1997.54	9.13	NaN
1997.46	9.17	NaN
1997.37	9.22	NaN
1997.29	9.20	NaN
1997.21	9.14	NaN

1997.12	9.16	NaN
1997.04	9.21	NaN
1996.96	9.26	NaN
1996.87	9.32	NaN
1996.79	9.33	NaN
1996.71	9.22	NaN
1996.62	9.21	NaN
1996.54	9.23	NaN
1996.46	9.25	NaN
1996.37	9.28	NaN
1996.29	9.33	NaN

Year	OISST ($^\circ$C) [Reynolds et al., 2002]
2013.12	26.09
2013.04	26.11
2012.96	27.06
2012.87	27.61
2012.79	27.75
2012.71	27.98
2012.62	28.19
2012.54	28.16
2012.46	28.16
2012.37	27.92
2012.29	27.47
2012.21	26.43
2012.12	25.71
2012.04	25.39
2011.96	25.79
2011.87	26.02
2011.79	26.16
2011.71	26.64
2011.62	26.96
2011.54	27.42
2011.46	27.77

2011.37	27.35
2011.29	26.85
2011.21	26.48
2011.12	25.32
2011.04	24.65
2010.96	25.24
2010.87	25.12
2010.79	25.06
2010.71	24.60
2010.62	25.10
2010.54	25.90
2010.46	26.89
2010.37	27.78
2010.29	28.67
2010.21	28.86
2010.12	28.83
2010.04	29.44
2009.96	29.35
2009.87	29.06
2009.79	28.89
2009.71	28.09
2009.62	28.04
2009.54	28.32
2009.46	28.44
2009.37	28.21
2009.29	27.72
2009.21	26.78
2009.12	25.90
2009.04	25.24
2008.96	25.69
2008.87	26.62
2008.79	26.67
2008.71	26.71
2008.62	26.97
2008.54	27.29
2008.46	27.12
2008.37	26.77
2008.29	26.19

2008.21	25.12
2008.12	24.41
2008.04	24.65
2007.96	24.81
2007.87	25.41
2007.79	25.81
2007.71	26.28
2007.62	27.11
2007.54	27.41
2007.46	28.12
2007.37	27.96
2007.29	27.89
2007.21	27.37
2007.12	27.04
2007.04	27.39
2006.96	28.50
2006.87	28.77
2006.79	28.37
2006.71	28.22
2006.62	27.96
2006.54	27.90
2006.46	28.43
2006.37	27.98
2006.29	27.36
2006.21	26.27
2006.12	25.64
2006.04	25.59
2005.96	26.50
2005.87	26.97
2005.79	27.32
2005.71	27.33
2005.62	27.36
2005.54	27.94
2005.46	28.37
2005.37	28.17
2005.29	27.88
2005.21	27.73
2005.12	27.21

2005.04	27.66
2004.96	28.25
2004.87	28.39
2004.79	28.36
2004.71	28.61
2004.62	28.54
2004.54	28.76
2004.46	28.20
2004.37	28.32
2004.29	27.73
2004.21	27.04
2004.12	26.99
2004.04	26.91
2003.96	27.39
2003.87	27.91
2003.79	27.85
2003.71	27.64
2003.62	27.44
2003.54	28.03
2003.46	28.03
2003.37	27.62
2003.29	27.80
2003.21	28.10
2003.12	28.05
2003.04	28.65
2002.96	29.03
2002.87	29.72
2002.79	29.70
2002.71	29.38
2002.62	28.91
2002.54	28.79
2002.46	28.87
2002.37	28.54
2002.29	28.21
2002.21	27.47
2002.12	27.44
2002.04	27.59
2001.96	26.97

2001.87	27.51
2001.79	27.64
2001.71	27.82
2001.62	27.91
2001.54	28.17
2001.46	28.03
2001.37	27.89
2001.29	27.35
2001.21	26.22
2001.12	25.83
2001.04	25.57
2000.96	25.46
2000.87	26.34
2000.79	26.59
2000.71	26.87
2000.62	27.02
2000.54	27.11
2000.46	27.12
2000.37	26.70
2000.29	26.26
2000.21	25.20
2000.12	24.75
2000.04	24.76
1999.96	24.81
1999.87	25.66
1999.79	26.40
1999.71	26.40
1999.62	26.05
1999.54	26.58
1999.46	26.66
1999.37	26.76
1999.29	26.37
1999.21	25.77
1999.12	24.85
1999.04	24.31
1998.96	24.27
1998.87	24.54
1998.79	24.81

1998.71	25.75
1998.62	25.16
1998.54	25.75
1998.46	27.27
1998.37	28.57
1998.29	28.03
1998.21	28.43
1998.12	29.19
1998.04	29.35
1997.96	29.32
1997.87	29.57
1997.79	29.86
1997.71	29.92
1997.62	29.54
1997.54	29.59
1997.46	29.50
1997.37	29.13
1997.29	28.28
1997.21	26.85
1997.12	26.67
1997.04	26.70
1996.96	26.76
1996.87	26.52
1996.79	26.70
1996.71	26.96
1996.62	27.29
1996.54	27.50
1996.46	27.53
1996.37	27.60
1996.29	27.14
1996.21	26.23
1996.12	25.40
1996.04	25.65
1995.96	25.87
1995.87	26.08
1995.79	25.71
1995.71	26.45
1995.62	26.81

1995.54	27.44
1995.46	28.04
1995.37	28.27
1995.29	27.97
1995.21	27.76
1995.12	28.00
1995.04	28.66
1994.96	29.08
1994.87	29.09
1994.79	28.62
1994.71	28.28
1994.62	28.71
1994.54	28.47
1994.46	28.22
1994.37	27.96
1994.29	27.74
1994.21	26.81
1994.12	26.46
1994.04	26.49
1993.96	27.10

Appendix B

Supplementary figures and data for Chapter 3

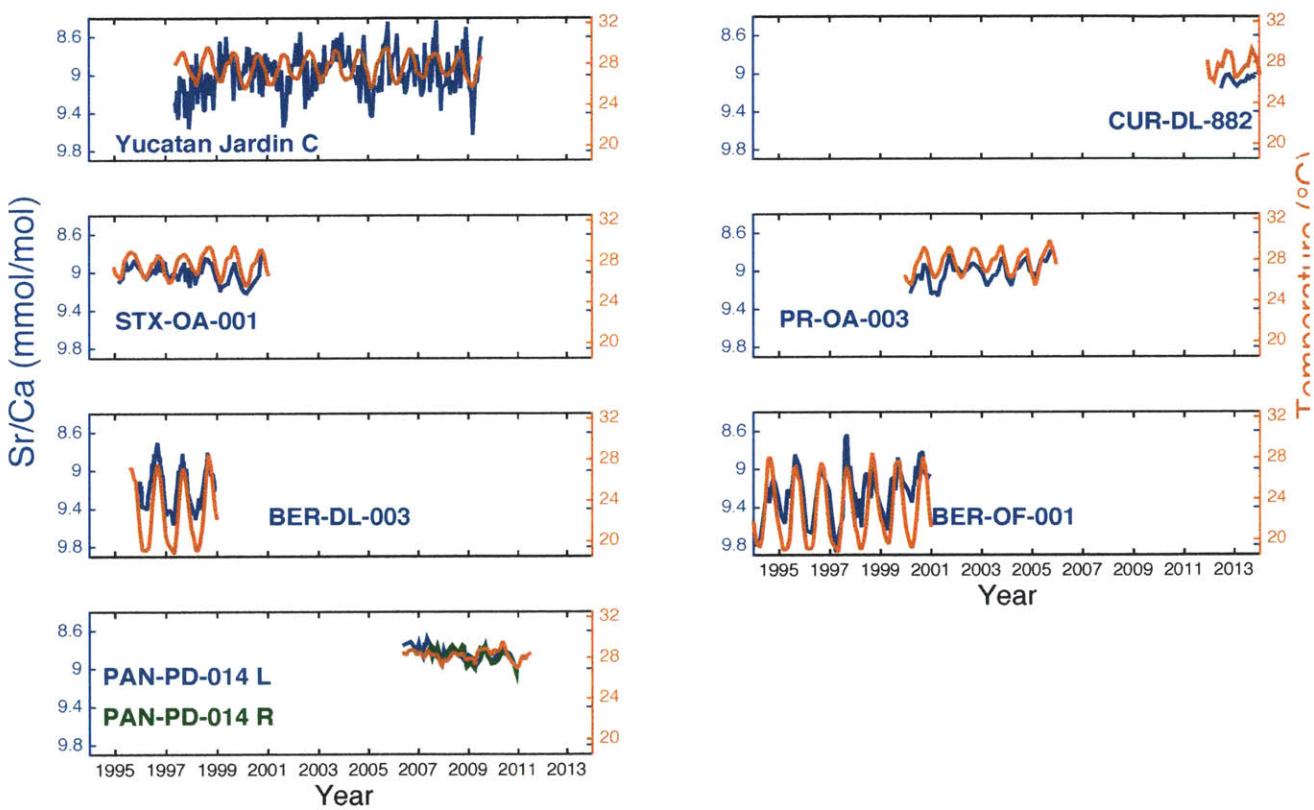

Figure B-1: Sr/Ca and monthly SST for corals new to the spatial calibration. SST is from OISST in the 1°x1° grid box corresponding to each collection location. The Panama Pocillipora has two branches, left, "L," and right, "R." In the calibration we combine these into one dataset. Please see *DeCarlo et al.* [2016] for Sr/Ca values for the additional 14 corals included in the spatial calibration.

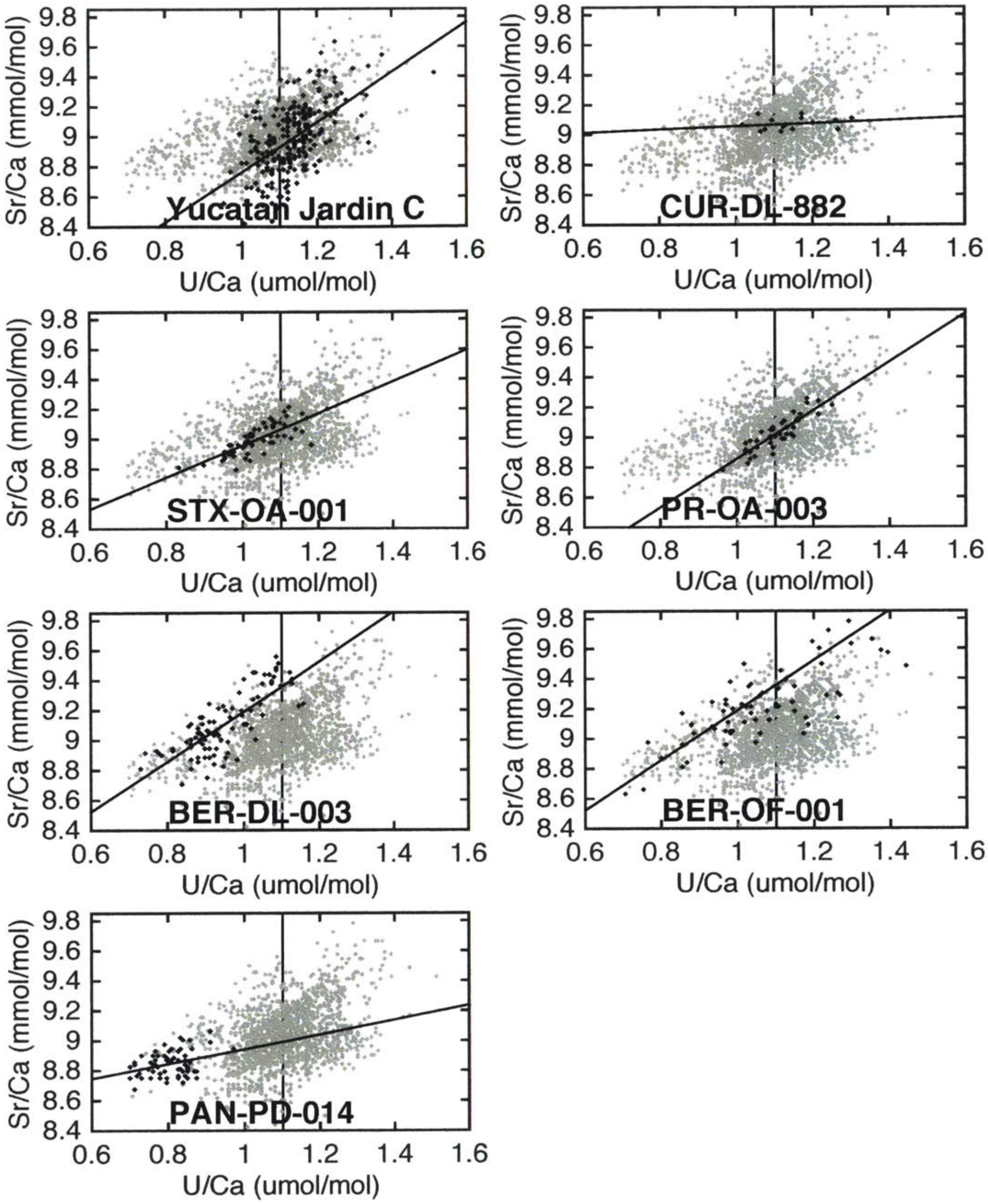

Figure B-2: Sr/Ca vs U/Ca scatterplots for corals new to the spatial calibration. In each subplot data for all 19 corals are plotted in gray, data from the coral in each subplot are plotted in black. In each subplot the regression of Sr/Ca on U/Ca for the individual coral is indicated by a sloping solid black line. A vertical solid black line denotes U/Ca=1.1 umol/mol. Sr-U is defined as the Sr/Ca value corresponding to the intersection between these two lines.

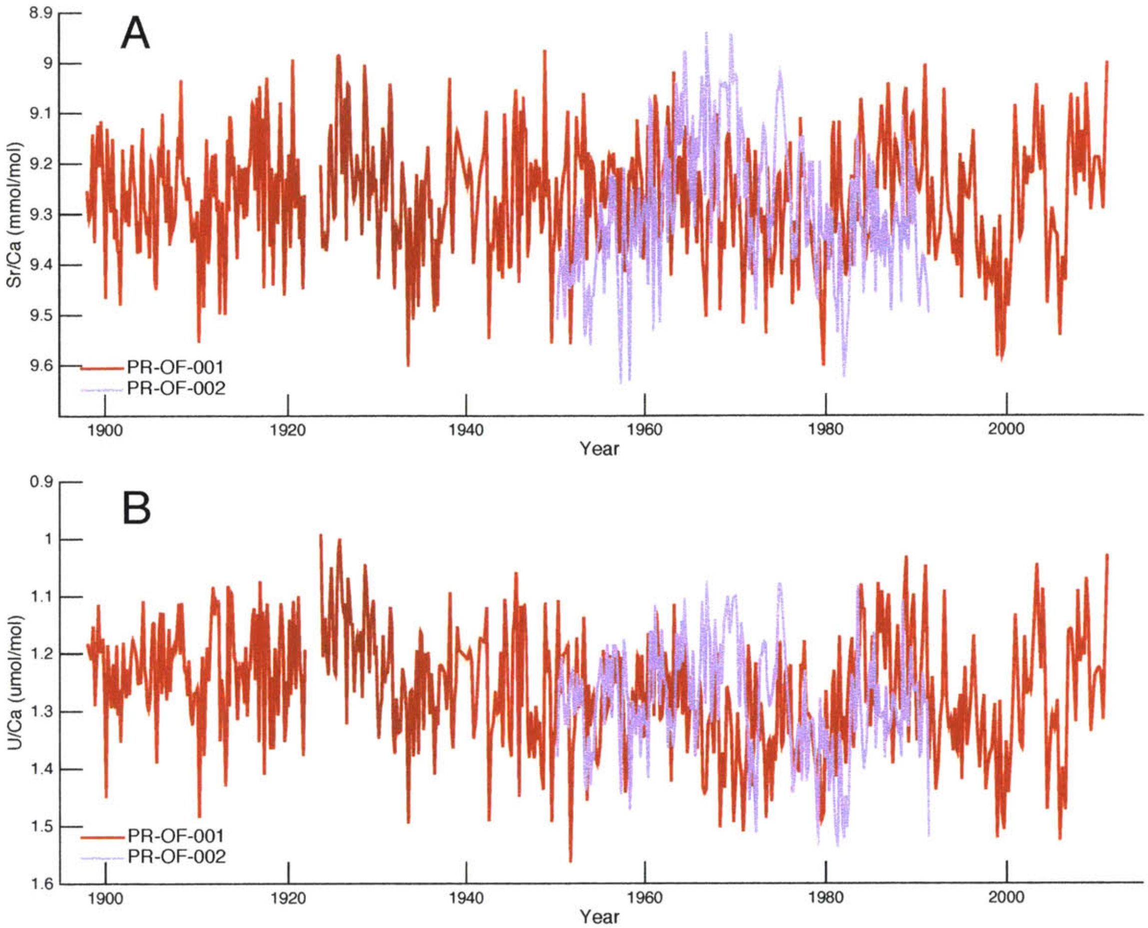

Figure B-3: A) Sr/Ca from PR-OF-001 and PR-OF-002. Shaded error bars indicate analytical uncertainty of 0.035 mmol/mol. B) U/Ca from PR-OF-001 and PR-MF-002. Shaded error bars indicate analytical uncertainty of 0.02 umol/mol.

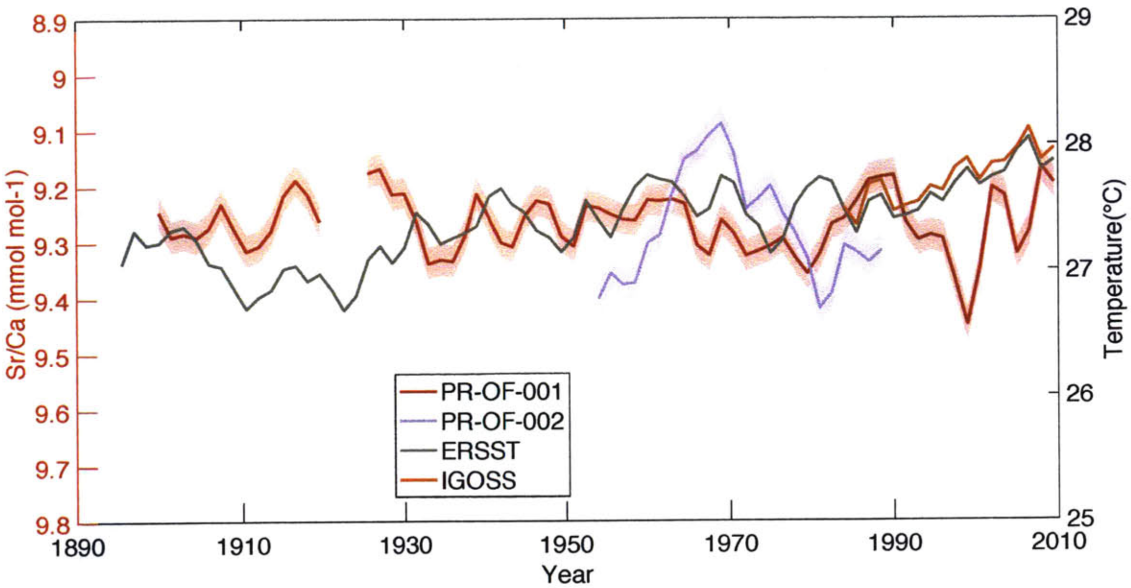

Figure B-4: Sr/Ca timeseries from *O. faveolata* PR-MF-001 and PR-OF-002 from Puerto Rico with ERSST [*Smith et al.*, 2008] and OISST [*Reynolds et al.*, 2002]. Data are in 3-year bins and shading indicates the analytical standard error of the mean (1σ). Annual mean Sr/Ca does not correlate with OISST for either core and 3-year binned Sr/Ca does not correlate to ERSST in either core. Contemporaneous Sr/Ca values from the two cores average 0.10 mmol/mol apart. There is no significant trend in Sr/Ca from either core.

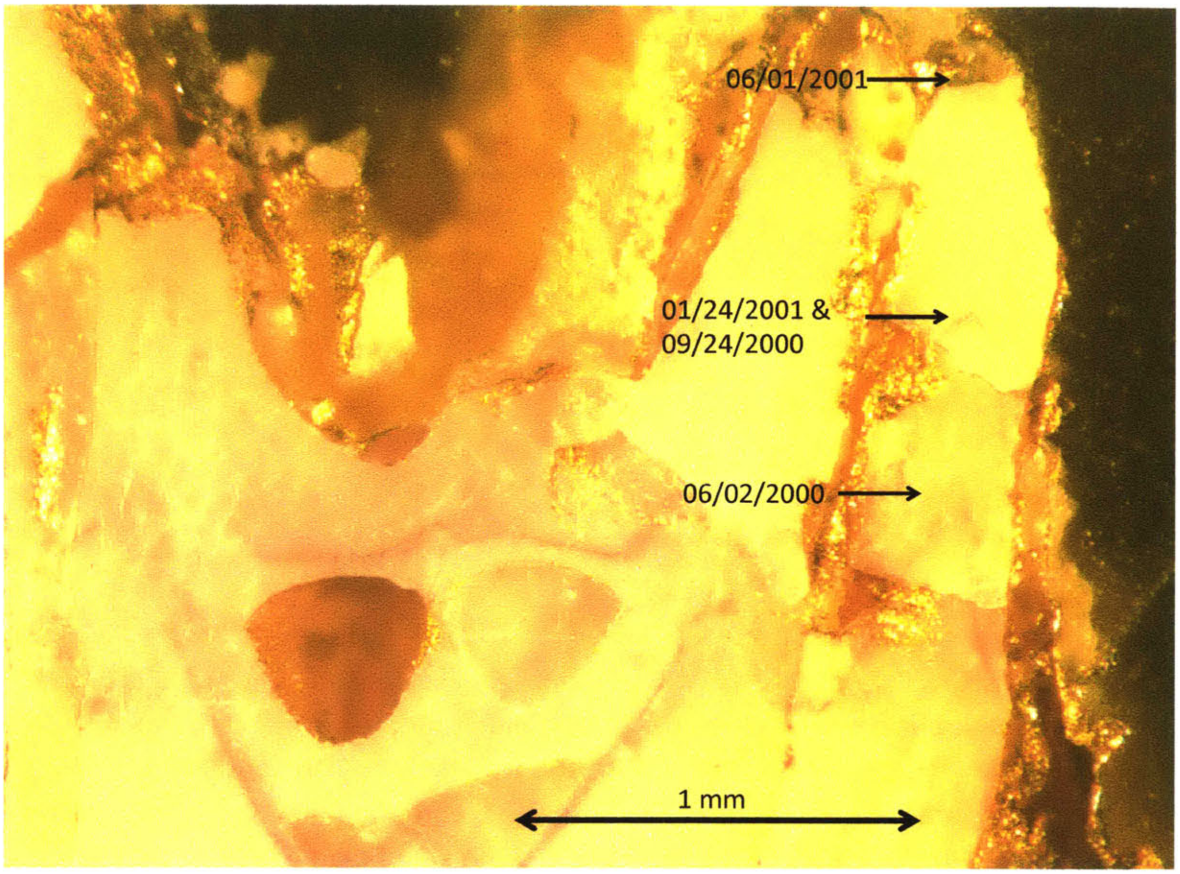

Figure B-5: Stain lines on *O. franksi* from Bermuda photographed through a Nikon SMZ1500 microscope at 6x magnification. The coral was stained with Alizarin red dye on June 2, 2000, September 24, 2000, and January 24, 2001, and was collected on June 1, 2001. Only two stain lines are visible, indicating that the coral was not calcifying during the coldest staining period in January 2001. Please see *Cohen et al.* [2004] for a detailed description of staining methods.

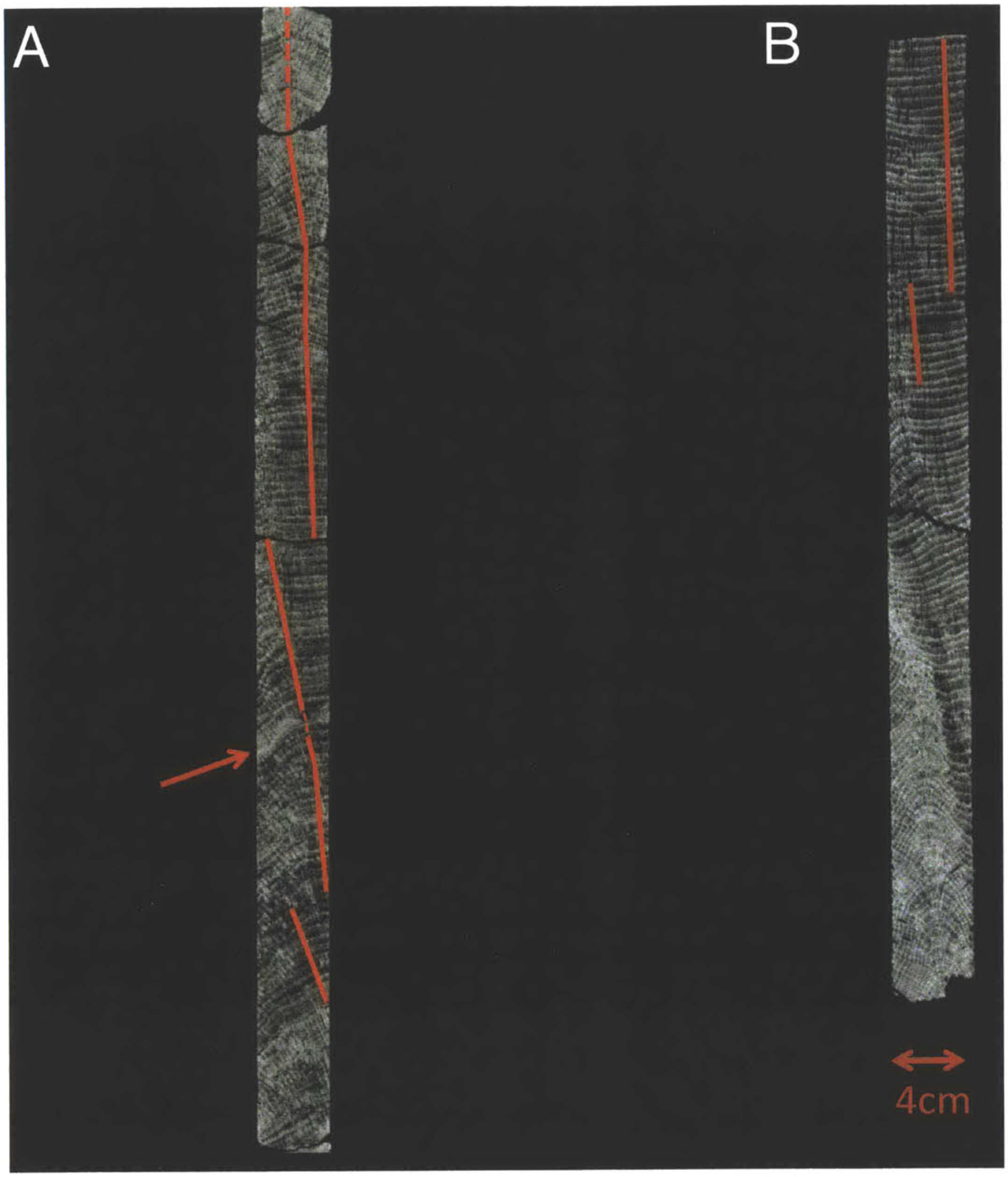

Figure B-6: CT scans for the long cores PR-OF-001 (A) and and PR-OF-002 (B). Scanning was carried out according to methods described in *DeCarlo et al.*, [*2016*]. Annual density couplets are visible as light and dark bands. Drill tracks are marked in red. Lighter grays corresponding to increased skeletal density due to stress following the well-documented 1998 bleaching event in Puerto Rico [*Goreau et al.*, 2000; *Winter et al.*, 1998] are visible at the top of PR-OF-001. This section is denoted by a dashed drill track line and was omitted from the Sr/Ca and SrU records. The red arrow and dashed drill track section further down the core mark a high density stress band in 1923. Partial mortality and secondary crystal growth (Figure B9) are visible, and this section was omitted from the Sr/Ca and SrU records.

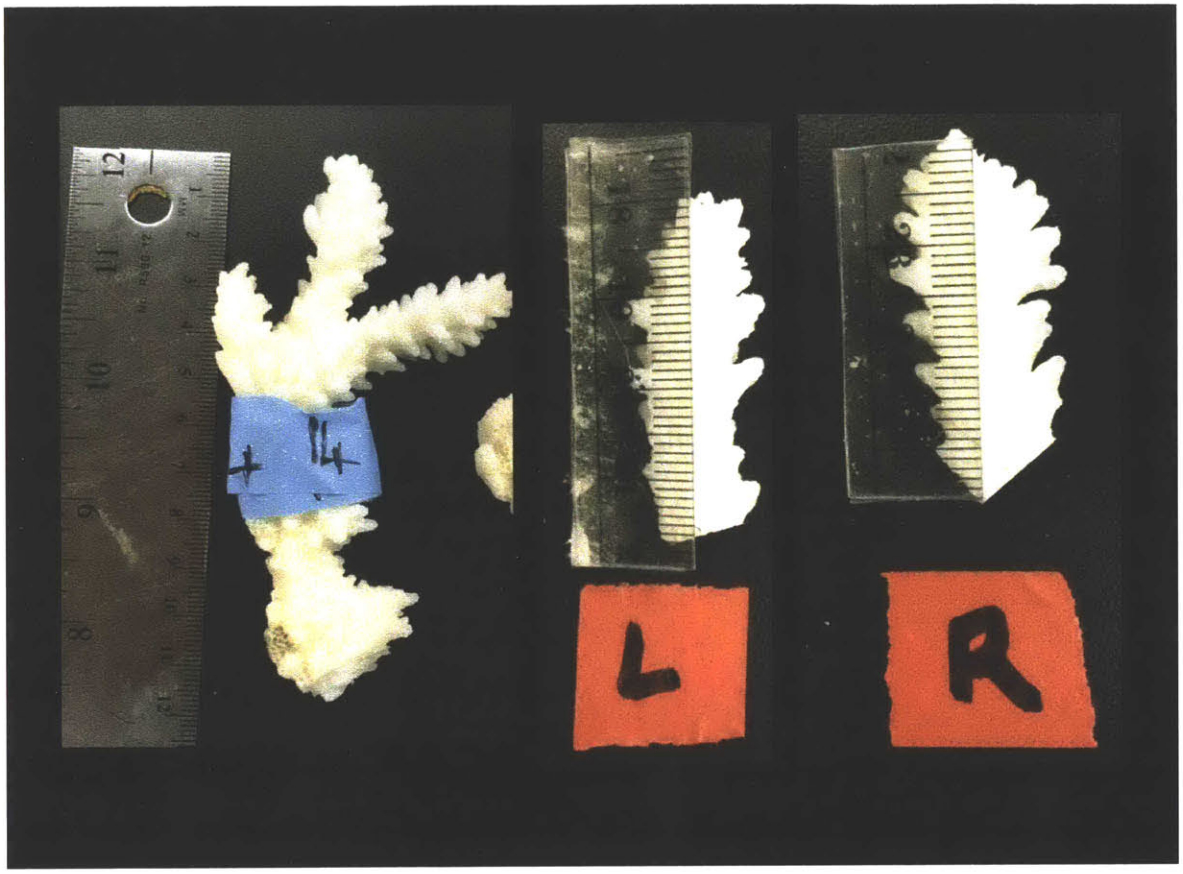

Figure B-7: PAN-PD-014 left (L) and right (R) branches.

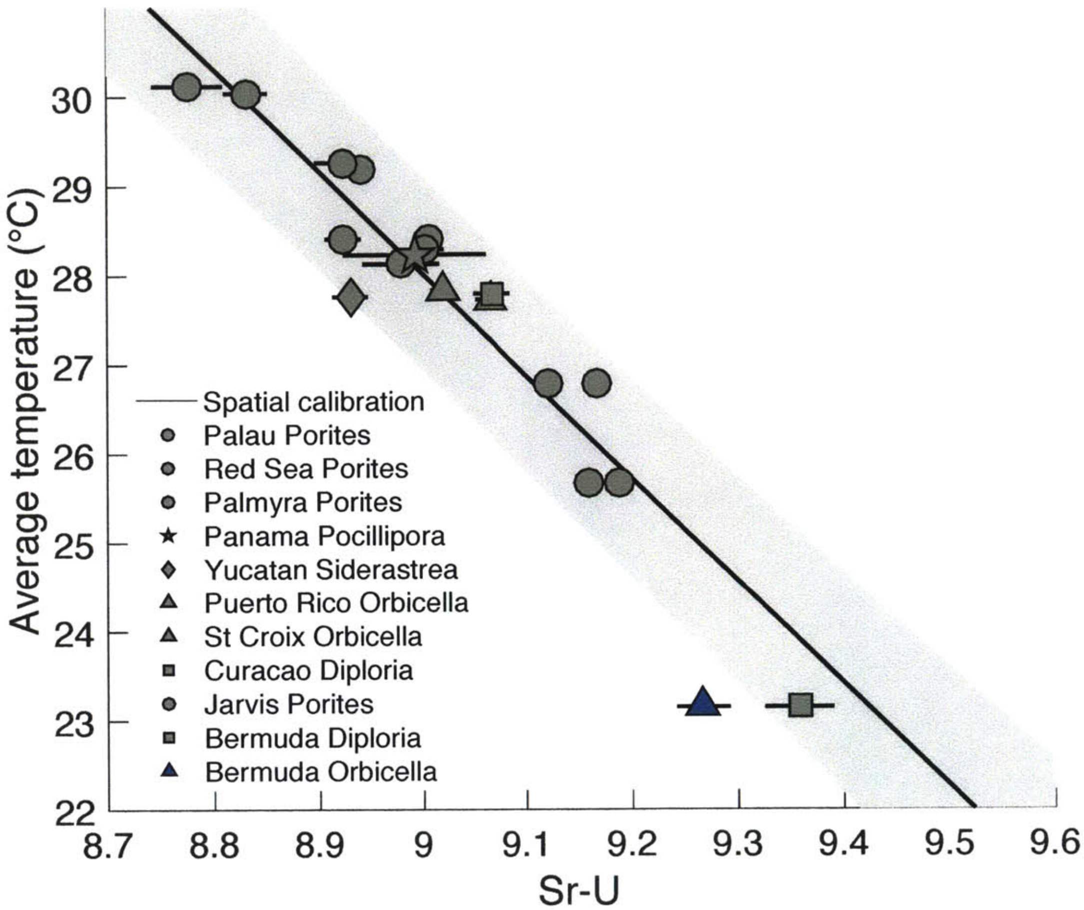

Figure B-8: Sr-U derived temperatures for all corals in calibration plotted against average annual temperature. Bermuda Orbicella franksii is plotted in blue and measured annual temperature is not adjusted for variable seasonal extension rate. Estimated temperature for Bermuda *Orbicella franksii* is 1.8 °C cooler than annual average temperature. The extended spatial calibration regression line is plotted with 95% confidence interval. Note that this regression was derived using average growth temperature of Bermuda *Orbicella franksii* adjusted for variable seasonal extension rates.

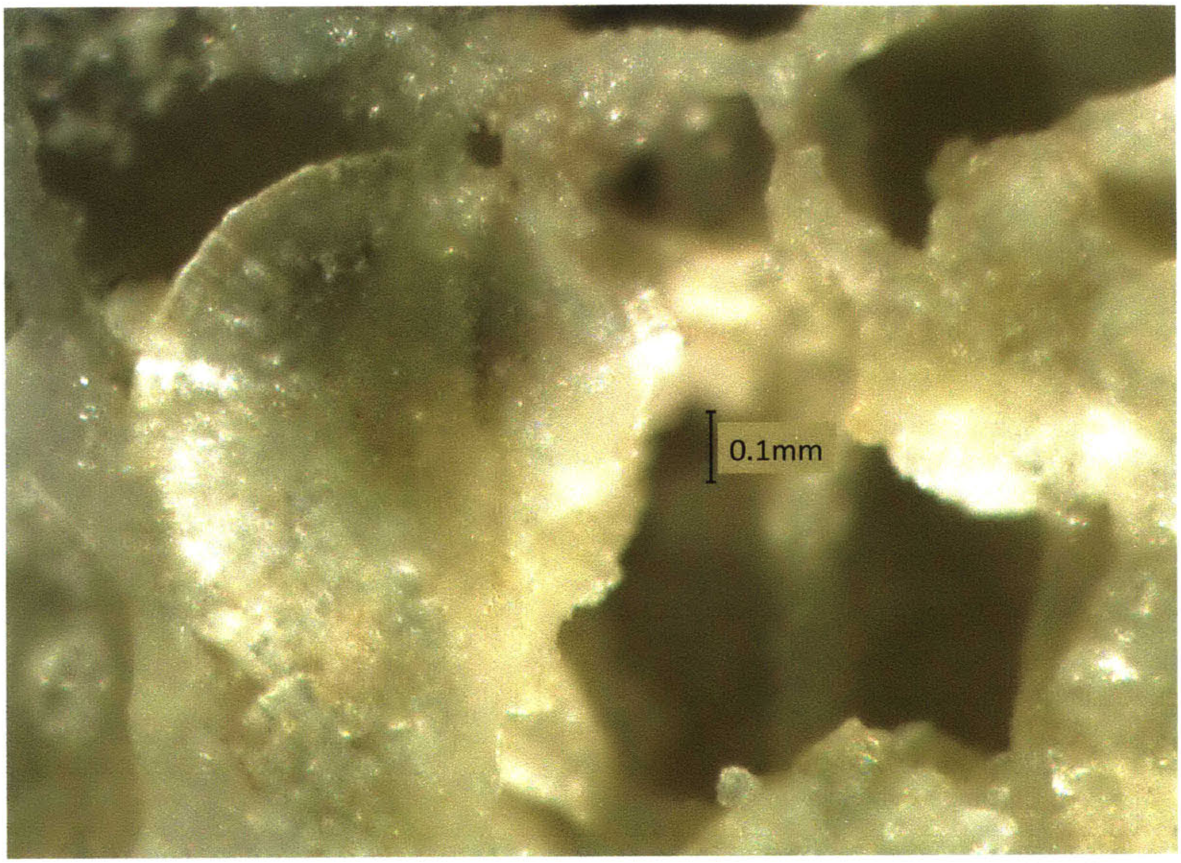

Figure B-9: Spherical secondary crystal growth within a 1923 stress band in and PR-OF-001 photographed through a Nikon SMZ1500 microscope. We omit this section from the Sr/Ca and SrU records.

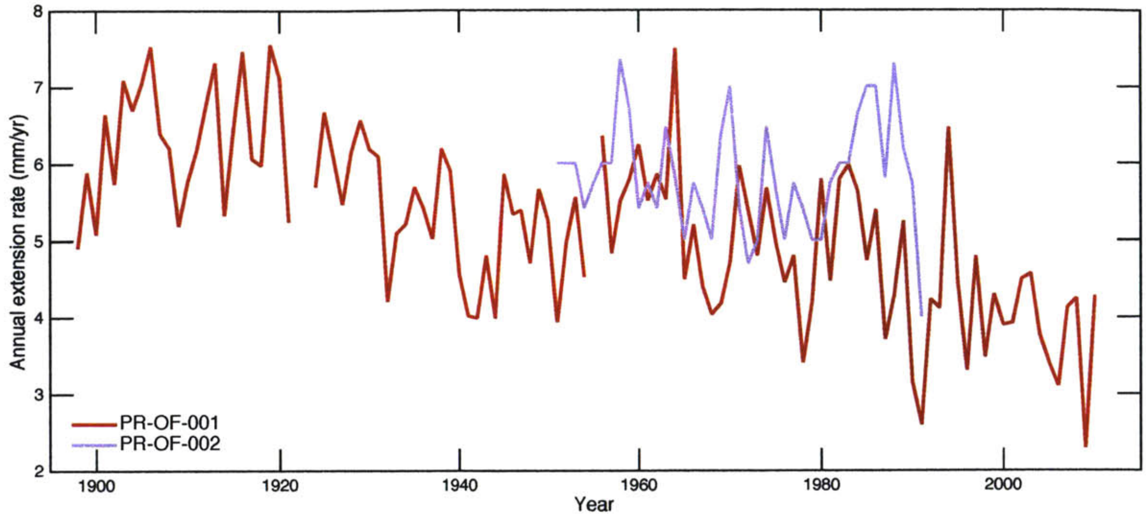

Figure B-10: Annual extension rate from and PR-OF-001 and PR-OF-002. The -0.02 mm/yr decreasing trend in and PR-OF-001 is significant ($P<0.05$).

References

Cohen, A. L., S. R. Smith, M. S. McCartney, and J. van Etten (2004), How brain corals record climate: an integration of skeletal structure, growth and chemistry of Diploria labyrinthiformis from Bermuda, *Marine Ecology Progress Series*, *271*, 147-158.

DeCarlo, T. M., G. A. Gaetani, A. L. Cohen, G. L. Foster, A. E. Alpert, and J. Stewart (2016), Coral Sr-U Thermometry, *Paleoceanography*.

Goreau, T., T. McClanahan, R. Hayes, and A. Strong (2000), Conservation of coral reefs after the 1998 global bleaching event, *Conservation Biology*, *14*(1), 5-15.

Reynolds, R. W., N. A. Rayner, T. M. Smith, D. C. Stokes, and W. Wang (2002), An improved in situ and satellite SST analysis for climate, *Journal of Climate*, *15*(13), 1609-1625.

Smith, T. M., R. W. Reynolds, T. C. Peterson, and J. Lawrimore (2008), Improvements to NOAA's historical merged land-ocean surface temperature analysis (1880-2006), *Journal of Climate*, *21*(10), 2283-2296.

Winter, A., R. Appeldoorn, A. Bruckner, E. Williams Jr, and C. Goenaga (1998), Sea surface temperatures and coral reef bleaching off La Parguera, Puerto Rico (northeastern Caribbean Sea), *Coral reefs*, *17*(4), 377-382.

B.1 Sr/Ca and U/Ca data for all corals in calibration

Sr/Ca uncertainty: 0.035 mmol/mol	U/Ca uncertainty: 0.02 μmol/mol,

BER-DL-003

Year	Sr/Ca (mmol/mol)	U/Ca (μmol/mol)
1998.93	9.20	1.00
1998.91	9.20	0.95
1998.88	9.11	0.89
1998.86	9.08	0.88
1998.83	9.04	0.92
1998.81	9.03	0.89
1998.79	9.02	0.87
1998.76	9.05	0.89
1998.74	8.99	0.88
1998.72	9.00	0.88
1998.69	8.95	0.86
1998.67	8.89	0.88
1998.64	8.89	0.91
1998.62	8.80	0.86
1998.61	8.87	0.86
1998.60	8.89	0.90
1998.59	8.94	0.93
1998.53	9.00	0.86
1998.46	9.16	0.89
1998.31	9.40	1.00
1998.28	9.28	1.04
1998.25	9.38	1.05
1998.21	9.42	1.08
1998.18	9.45	1.12
1998.15	9.51	1.09
1998.13	9.43	1.06
1998.10	9.46	1.02
1997.85	9.23	0.95
1997.82	9.13	0.91
1997.80	8.97	0.86
1997.77	9.05	0.91
1997.75	9.05	0.89
1997.72	9.05	0.88
1997.69	8.90	0.78
1997.67	8.92	0.74
1997.64	8.81	0.73

1997.63	8.92	0.77
1997.61	8.92	0.78
1997.60	9.04	0.93
1997.58	8.92	0.81
1997.57	8.94	0.81
1997.55	9.01	0.94
1997.51	9.09	0.86
1997.49	8.99	0.85
1997.44	9.16	0.89
1997.39	9.28	1.02
1997.33	9.48	1.08
1997.28	9.56	1.08
1997.22	9.44	1.07
1997.12	9.40	1.07
1997.01	9.46	1.09
1996.98	9.45	1.03
1996.95	9.31	0.99
1996.91	9.24	0.91
1996.88	9.08	0.97
1996.87	9.06	0.91
1996.85	9.04	0.94
1996.84	9.05	0.91
1996.82	9.01	0.90
1996.81	8.97	0.89
1996.79	8.95	0.90
1996.78	8.95	0.91
1996.76	8.85	0.88
1996.76	8.86	0.88
1996.75	8.90	0.92
1996.75	8.88	0.95
1996.74	8.90	0.93
1996.67	8.70	0.84
1996.63	8.75	0.90
1996.59	8.84	0.92
1996.55	8.87	0.98
1996.54	9.01	1.03
1996.53	8.82	0.94
1996.49	8.99	0.96
1996.45	8.91	0.96
1996.42	9.07	1.02
1996.40	9.10	1.00
1996.37	9.11	1.01
1996.35	9.17	1.05
1996.32	9.22	1.14
1996.30	9.25	1.16
1996.27	9.38	1.13

1996.25	9.40	1.13
1996.13	9.37	1.10
1996.05	9.38	1.07
1996.03	9.15	0.96
1996.02	9.18	1.00
1996.00	9.22	0.93
1995.99	9.11	0.86
1995.97	9.12	0.92
1995.95	9.21	0.97
1995.94	9.24	1.04
1995.92	9.21	1.02

BER-OF-003

Year	Sr/Ca (mmol/mol)	U/Ca (μmol/mol)
2000.94	9.05	0.98
2000.84	9.10	0.88
2000.75	9.03	1.17
2000.65	8.82	0.86
2000.53	8.84	0.86
2000.42	9.11	0.98
2000.39	8.97	0.97
2000.35	9.07	0.94
2000.32	9.18	0.96
2000.29	9.17	1.03
2000.26	9.29	1.06
2000.23	9.35	1.03
2000.05	9.21	0.98
1999.86	9.13	1.05
1999.68	8.88	0.80
1999.59	9.22	1.04
1999.50	9.09	0.93
1999.41	9.10	1.02
1999.32	9.38	0.98
1999.23	9.64	1.19
1999.09	9.46	1.11
1998.96	9.36	1.04
1998.82	9.21	1.02
1998.68	8.96	0.85
1998.61	9.30	1.26
1998.53	9.19	1.08
1998.46	9.04	0.99
1998.38	9.06	0.97
1998.31	9.24	0.97
1998.23	9.60	1.22
1998.17	9.31	1.06

1998.11	9.39	1.12
1998.05	9.51	1.01
1997.99	9.26	0.97
1997.92	9.24	0.93
1997.86	9.17	0.85
1997.80	8.97	0.77
1997.74	9.04	0.89
1997.68	8.63	0.70
1997.59	8.67	0.75
1997.50	9.49	1.22
1997.41	9.59	1.38
1997.32	9.73	1.24
1997.23	9.87	1.38
1996.97	9.23	1.01
1996.70	9.04	0.98
1996.59	9.03	1.06
1996.44	9.34	1.11
1996.28	9.67	1.35
1996.07	9.64	1.30
1995.94	9.23	1.10
1995.81	8.97	1.05
1995.61	8.84	0.96
1995.52	9.14	1.26
1995.42	9.29	1.27
1995.33	9.21	1.10
1995.23	9.57	1.39
1995.09	9.49	1.44
1994.96	9.28	1.23
1994.82	9.13	1.08
1994.77	9.10	1.18
1994.72	9.15	1.18
1994.67	9.25	1.14
1994.62	9.35	1.15
1994.57	9.19	1.15
1994.52	9.21	1.10
1994.23	9.79	1.29

STX-OA-001

Year	Sr/Ca (mmol/mol)	U/Ca (µmol/mol)
2000.84	8.81	0.83
2000.75	8.79	0.98
2000.66	9.02	1.07
2000.17	9.21	1.12
2000.07	9.20	1.22
1999.98	9.16	1.16

1999.79	9.01	1.02
1999.69	8.91	0.97
1999.61	8.96	0.96
1999.51	9.04	1.02
1999.43	9.11	1.08
1999.37	9.12	1.08
1999.27	9.14	1.07
1999.19	9.15	1.11
1999.13	9.18	1.11
1999.05	9.10	1.09
1998.97	9.07	1.04
1998.89	8.99	1.01
1998.80	8.91	0.97
1998.72	8.89	0.95
1998.64	8.86	0.94
1998.56	8.85	1.02
1998.48	8.90	1.06
1998.40	8.99	1.05
1998.32	8.98	1.07
1998.24	9.04	1.03
1998.16	9.11	1.06
1998.11	9.02	1.02
1998.05	9.03	1.09
1998.00	8.96	1.01
1997.94	9.14	1.17
1997.89	9.09	1.11
1997.83	8.96	0.97
1997.78	9.07	1.08
1997.72	8.91	1.01
1997.60	8.96	1.18
1997.49	9.07	1.14
1997.37	9.02	1.11
1997.26	9.02	1.02
1997.14	9.07	1.06
1997.05	9.02	1.07
1996.96	8.90	0.97
1996.87	8.88	0.98
1996.78	8.97	1.01
1996.69	8.82	0.90
1996.60	9.00	1.13
1996.51	8.98	1.08
1996.24	9.06	1.03
1996.12	9.02	1.01
1996.00	8.97	1.02
1995.87	8.92	0.95
1995.75	8.88	0.95

1995.63	8.94	1.00
1995.52	8.97	0.99
1995.42	8.87	1.00
1995.31	9.06	1.16
1995.20	9.09	1.08

CUR-DL-882

Year	Sr/Ca (mmol/mol)	U/Ca (µmol/mol)
2013.78	9.04	1.08
2013.70	9.03	1.15
2013.62	9.06	1.12
2013.54	9.03	1.27
2013.45	9.08	1.20
2013.37	9.09	1.09
2013.29	9.09	1.26
2013.21	9.11	1.31
2013.12	9.14	1.17
2013.01	9.10	1.17
2012.90	9.06	1.13
2012.79	9.01	1.12
2012.70	9.02	1.06
2012.60	9.06	1.02
2012.51	9.14	1.06

Jardin C (Yucatan)

Year	Sr/Ca (mmol/mol)	U/Ca (µmol/mol)
2009.55	1.07	8.60
2009.49	1.12	8.66
2009.43	1.15	8.87
2009.37	1.18	9.08
2009.31	1.16	9.00
2009.25	1.20	9.31
2009.19	1.24	9.63
2009.13	1.13	9.19
2009.06	1.24	9.14
2008.92	1.21	8.50
2008.85	1.13	8.98
2008.80	1.12	8.63
2008.75	1.13	8.85
2008.70	1.08	9.14
2008.65	1.07	8.97
2008.61	1.06	9.08
2008.56	1.08	8.69

2008.51	1.11	9.18
2008.46	1.16	9.18
2008.37	1.17	9.06
2008.29	1.13	9.20
2008.21	1.20	8.76
2008.13	1.15	9.09
2007.96	1.01	9.14
2007.92	1.10	9.38
2007.88	1.04	8.93
2007.85	1.10	8.85
2007.81	1.03	9.13
2007.78	1.08	8.94
2007.74	1.00	8.43
2007.70	1.10	8.53
2007.67	1.08	8.90
2007.63	1.10	8.60
2007.60	1.14	8.70
2007.56	1.14	9.08
2007.52	1.17	8.87
2007.49	1.09	9.18
2007.45	1.14	8.96
2007.42	1.07	9.01
2007.38	1.12	8.85
2007.35	1.07	8.88
2007.31	1.03	8.97
2007.27	1.03	8.66
2007.24	1.05	9.12
2007.20	1.03	9.17
2007.14	1.05	9.23
2007.07	0.99	9.01
2007.01	1.06	8.89
2006.94	1.10	8.78
2006.87	1.12	9.12
2006.81	1.06	8.77
2006.75	1.07	8.79
2006.68	1.14	8.95
2006.61	1.14	8.98
2006.55	1.18	9.14
2006.48	1.17	9.20
2006.42	1.15	8.97
2006.35	1.17	9.08
2006.29	1.15	9.05
2006.23	1.02	9.01
2006.16	0.95	8.56
2006.10	0.97	8.76
2006.04	1.07	8.78

2005.98	1.00	8.82
2005.91	1.02	8.98
2005.85	1.11	9.11
2005.79	1.08	8.44
2005.73	1.06	8.61
2005.66	1.07	8.68
2005.60	1.07	8.68
2005.54	1.03	9.17
2005.48	1.12	9.01
2005.42	1.18	9.18
2005.35	1.16	9.12
2005.29	1.32	9.15
2005.23	1.14	9.12
2005.17	1.22	9.44
2005.10	1.51	9.43
2005.04	1.28	9.25
2004.99	1.31	9.00
2004.93	1.32	9.29
2004.88	1.17	8.89
2004.83	1.01	8.58
2004.77	1.20	8.85
2004.72	1.17	9.14
2004.67	1.27	9.29
2004.61	1.16	8.89
2004.56	1.25	9.10
2004.50	1.21	9.03
2004.45	1.18	9.02
2004.39	1.20	9.02
2004.34	1.16	8.93
2004.29	1.05	8.90
2004.23	1.03	8.69
2004.18	1.06	8.84
2004.13	1.05	8.85
2004.06	1.03	8.91
2004.00	1.09	8.90
2003.94	1.08	8.55
2003.87	1.08	8.66
2003.81	1.13	8.86
2003.75	1.10	8.60
2003.69	1.09	8.85
2003.62	1.06	8.63
2003.56	1.13	8.83
2003.50	1.13	8.89
2003.44	1.13	8.92
2003.38	1.18	8.92
2003.31	1.15	8.98

2003.25	1.12	8.68
2003.19	1.15	9.08
2003.13	1.16	8.97
2003.06	1.10	8.87
2003.00	1.12	8.93
2002.93	1.17	9.15
2002.87	1.14	9.15
2002.80	1.11	8.83
2002.74	1.22	9.22
2002.67	1.19	9.15
2002.61	1.22	9.26
2002.55	1.09	8.85
2002.48	1.12	9.36
2002.42	1.11	8.84
2002.35	1.16	8.96
2002.29	1.06	8.55
2002.20	1.02	8.91
2002.12	1.01	8.67
2002.04	1.08	8.90
2001.95	1.08	8.89
2001.87	1.14	9.20
2001.79	1.17	9.00
2001.71	1.30	9.46
2001.62	1.37	9.55
2001.54	1.19	8.94
2001.46	1.16	9.15
2001.37	1.22	9.15
2001.29	1.09	8.84
2001.21	1.11	9.01
2001.13	1.11	8.86
2001.04	1.05	8.97
2001.00	1.05	8.81
2000.97	1.13	9.10
2000.93	1.08	8.77
2000.89	1.07	8.83
2000.85	1.12	8.94
2000.81	1.14	9.23
2000.77	1.15	9.15
2000.74	1.11	8.86
2000.70	1.15	9.19
2000.66	1.14	8.96
2000.62	1.14	8.96
2000.59	1.08	8.76
2000.55	1.14	8.93
2000.51	1.11	8.78
2000.47	1.15	9.03

2000.43	1.14	8.79
2000.39	1.26	9.18
2000.36	1.17	8.81
2000.32	1.15	8.91
2000.28	1.12	8.71
2000.24	1.13	8.79
2000.21	1.11	8.70
2000.16	1.13	8.97
2000.11	1.14	8.88
2000.06	1.17	9.00
2000.01	1.34	8.97
1999.96	1.11	9.05
1999.91	1.12	9.15
1999.86	1.07	8.96
1999.81	1.01	8.82
1999.76	1.16	9.01
1999.71	1.09	8.97
1999.67	1.33	9.27
1999.62	1.16	8.78
1999.57	1.19	8.81
1999.52	1.16	8.81
1999.47	1.17	8.79
1999.42	1.14	8.86
1999.37	1.12	8.59
1999.32	1.22	8.96
1999.27	1.08	8.78
1999.22	1.08	8.98
1999.17	1.09	8.96
1999.13	1.05	8.64
1999.08	1.18	9.04
1999.04	1.15	8.91
1999.00	1.21	9.06
1998.96	1.16	9.00
1998.92	1.12	9.11
1998.87	1.25	9.36
1998.83	1.18	9.16
1998.79	1.12	9.09
1998.75	1.09	8.99
1998.71	1.17	9.21
1998.67	1.19	9.01
1998.63	1.18	8.98
1998.58	1.24	8.98
1998.54	1.19	9.36
1998.50	1.15	9.38
1998.46	1.17	9.19
1998.42	1.10	9.09

1998.38	1.07	8.90
1998.34	1.12	9.04
1998.29	1.14	9.09
1998.25	1.20	9.30
1998.21	1.12	8.76
1998.17	1.16	9.19
1998.13	1.12	9.06
1998.09	1.15	9.03
1998.05	1.14	9.36
1998.02	1.12	8.89
1997.98	1.10	9.24
1997.95	1.20	9.45
1997.91	1.21	9.56
1997.88	1.20	9.16
1997.84	1.24	9.27
1997.80	1.16	9.27
1997.77	1.18	9.45
1997.73	1.17	9.13
1997.69	1.15	9.04
1997.66	1.18	9.16
1997.62	1.20	9.16
1997.59	1.25	9.16
1997.55	1.16	9.00
1997.51	1.20	9.41
1997.48	1.34	9.46
1997.44	1.18	9.16
1997.41	1.25	9.39
1997.37	1.26	9.28

PR-OA-003

Year	Sr/Ca (mmol/mol)	U/Ca (µmol/mol)
2005.76	8.78	0.96
2005.56	8.91	1.02
2005.36	8.87	1.04
2005.16	9.07	1.15
2005.07	9.03	1.14
2004.98	9.02	1.13
2004.88	8.99	1.09
2004.79	8.86	1.03
2004.64	8.90	1.03
2004.49	8.96	1.02
2004.33	8.99	1.13
2004.18	9.15	1.17
2004.08	9.11	1.15
2003.99	9.06	1.13

2003.89	8.89	1.10
2003.79	8.86	1.04
2003.67	8.98	1.05
2003.55	9.05	1.09
2003.44	9.05	1.09
2003.32	9.11	1.12
2003.20	9.16	1.22
2003.01	9.02	1.11
2002.83	8.96	1.02
2002.64	8.92	1.02
2002.49	8.98	1.03
2002.33	9.01	1.10
2002.18	9.01	1.15
2002.04	8.96	1.09
2001.89	9.00	1.09
2001.75	8.82	1.03
2001.63	8.93	1.05
2001.51	9.07	1.09
2001.39	9.11	1.16
2001.27	9.26	1.19
2001.15	9.22	1.25
2001.00	9.24	1.21
2000.86	8.99	1.12
2000.71	8.92	1.09
2000.62	9.10	1.12
2000.53	9.04	1.07
2000.44	9.05	1.09
2000.35	9.12	1.16
2000.26	9.17	1.15
2000.17	9.24	1.18

PAN-PD-014

Year	Sr/Ca (mmol/mol)	U/Ca (μmol/mol)	Branch
2010.95	9.00	0.86	R
2010.93	9.07	0.91	R
2010.73	8.90	0.73	R
2010.54	8.85	0.71	R
2010.34	8.83	0.70	R
2010.20	8.90	0.76	R
2010.07	8.94	0.83	R
2009.93	8.95	0.81	R
2009.85	8.89	0.81	R
2009.76	8.87	0.80	R
2009.68	8.76	0.75	R
2009.60	8.78	0.72	R

2009.51	8.86	0.82	R
2009.47	8.84	0.77	R
2009.43	8.80	0.79	R
2009.35	8.84	0.76	R
2009.26	9.00	0.84	R
2009.09	8.94	0.86	R
2008.93	8.98	0.91	R
2008.87	8.90	0.84	R
2008.82	8.76	0.84	R
2008.76	8.75	0.85	R
2008.68	8.79	0.87	R
2008.60	8.85	0.86	R
2008.48	8.79	0.87	R
2008.35	8.75	0.83	R
2008.14	8.83	0.85	R
2007.92	8.93	0.80	R
2007.76	8.77	0.72	R
2007.69	8.85	0.71	R
2007.62	8.81	0.74	R
2007.56	8.88	0.76	R
2007.49	8.77	0.78	R
2007.42	8.80	0.87	R
2010.93	9.02	0.83	L
2010.64	8.84	0.84	L
2010.35	8.79	0.76	L
2010.14	8.86	0.76	L
2009.93	8.93	0.77	L
2009.85	8.90	0.77	L
2009.76	8.84	0.76	L
2009.68	8.75	0.79	L
2009.47	8.91	0.79	L
2009.26	8.98	0.79	L
2009.14	8.88	0.79	L
2009.01	8.86	0.80	L
2008.93	8.94	0.83	L
2008.70	8.87	0.83	L
2008.58	8.82	0.77	L
2008.35	8.80	0.85	L
2008.23	8.81	0.83	L
2008.10	8.88	0.84	L
2008.01	8.80	0.84	L
2007.93	8.95	0.97	L
2007.59	8.77	0.82	L
2007.47	8.75	0.78	L
2007.34	8.68	0.71	L
2007.29	8.75	0.70	L

2007.23	8.75	0.73	L
2007.18	8.87	0.81	L
2007.10	8.82	0.85	L
2007.01	8.73	0.84	L
2006.93	8.81	0.83	L
2006.68	8.71	0.79	L
2006.43	8.75	0.87	L

B.2 Sr/Ca and U/Ca data for all corals to which calibration was applied

PR-OF-001

Year	Sr/Ca (mmol/mol)	U/Ca (μmol/mol)
1997.44	9.36	1.27
1997.23	9.31	1.31
1996.95	9.43	1.40
1996.62	9.36	1.31
1996.28	9.13	1.17
1996.01	9.20	1.27
1995.79	9.27	1.32
1995.56	9.26	1.36
1995.33	9.24	1.22
1995.12	9.20	1.30
1994.97	9.47	1.42
1994.82	9.18	1.27
1994.67	9.31	1.29
1994.52	9.40	1.37
1994.37	9.38	1.36
1994.22	9.35	1.30
1994.03	9.38	1.37
1993.78	9.31	1.31
1993.54	9.29	1.33
1993.30	9.23	1.28
1993.06	9.05	1.09
1992.82	9.25	1.28
1992.59	9.34	1.31
1992.36	9.35	1.39
1992.11	9.39	1.44
1991.73	9.23	1.24
1991.34	9.38	1.39
1990.98	9.00	1.05
1990.65	9.21	1.18
1990.32	9.26	1.30
1990.06	9.24	1.35
1989.87	9.20	1.24
1989.68	9.10	1.10

1989.49	9.11	1.13
1989.30	9.20	1.20
1989.10	9.36	1.36
1988.87	9.05	1.03
1988.64	9.08	1.10
1988.41	9.25	1.26
1988.17	9.23	1.30
1987.90	9.18	1.15
1987.62	9.15	1.25
1987.34	9.34	1.39
1987.09	9.15	1.23
1986.91	9.04	1.10
1986.72	9.15	1.13
1986.54	9.25	1.23
1986.35	9.15	1.17
1986.17	9.08	1.09
1985.96	9.15	1.17
1985.75	9.19	1.08
1985.53	9.35	1.29
1985.32	9.33	1.29
1985.11	9.23	1.17
1984.94	9.35	1.33
1984.76	9.34	1.29
1984.58	9.34	1.27
1984.40	9.39	1.29
1984.22	9.17	1.12
1984.05	9.11	1.12
1983.88	9.07	1.08
1983.72	9.16	1.17
1983.55	9.32	1.26
1983.38	9.15	1.19
1983.22	9.24	1.24
1983.05	9.40	1.37
1982.87	9.22	1.17
1982.70	9.25	1.20
1982.53	9.30	1.24
1982.36	9.40	1.29
1982.18	9.42	1.39
1981.96	9.33	1.31
1981.73	9.28	1.35
1981.50	9.11	1.17
1981.27	9.29	1.34
1981.06	9.34	1.42
1980.89	9.12	1.23
1980.72	9.15	1.26
1980.55	9.37	1.37

1980.37	9.39	1.36
1980.20	9.39	1.37
1979.98	9.32	1.27
1979.74	9.60	1.48
1979.49	9.51	1.49
1979.25	9.35	1.36
1978.95	9.46	1.42
1978.28	9.32	1.31
1978.03	9.31	1.31
1977.82	9.34	1.31
1977.61	9.20	1.18
1977.40	9.23	1.24
1977.19	9.11	1.22
1976.97	9.45	1.41
1976.74	9.35	1.36
1976.51	9.31	1.37
1976.29	9.48	1.44
1976.07	9.16	1.22
1975.86	9.28	1.34
1975.66	9.18	1.23
1975.46	9.28	1.24
1975.25	9.32	1.35
1975.06	9.42	1.37
1974.89	9.22	1.18
1974.72	9.23	1.19
1974.55	9.27	1.33
1974.37	9.37	1.39
1974.20	9.40	1.34
1974.00	9.45	1.46
1973.80	9.36	1.35
1973.59	9.21	1.36
1973.38	9.54	1.49
1973.17	9.30	1.37
1972.98	9.34	1.33
1972.80	9.29	1.29
1972.61	9.31	1.35
1972.43	9.30	1.33
1972.24	9.17	1.22
1971.90	9.42	1.43
1971.74	9.27	1.30
1971.58	9.19	1.22
1971.41	9.15	1.19
1971.25	9.32	1.36
1971.07	9.40	1.41
1970.86	9.52	1.51
1970.65	9.35	1.41

1970.44	9.27	1.39
1970.23	9.27	1.30
1970.01	9.22	1.42
1969.77	9.37	1.49
1969.53	9.24	1.33
1969.29	9.14	1.28
1969.05	9.15	1.26
1968.80	9.37	1.43
1968.55	9.32	1.37
1968.30	9.49	1.50
1968.06	9.10	1.21
1967.83	9.17	1.20
1967.60	9.28	1.37
1967.38	9.27	1.30
1966.96	9.29	1.33
1966.77	9.51	1.44
1966.58	9.44	1.44
1966.40	9.39	1.43
1966.21	9.26	1.28
1965.98	9.22	1.24
1965.75	9.36	1.37
1965.51	9.27	1.32
1965.27	9.14	1.23
1965.08	9.17	1.26
1964.68	9.38	1.37
1964.55	9.30	1.30
1964.42	9.13	1.16
1964.28	9.21	1.28
1964.15	9.33	1.31
1963.97	9.19	1.18
1963.79	9.19	1.23
1963.60	9.26	1.29
1963.42	9.24	1.29
1963.24	9.02	1.11
1963.07	9.32	1.28
1962.90	9.42	1.42
1962.73	9.14	1.24
1962.56	9.09	1.25
1962.39	9.18	1.23
1962.22	9.19	1.20
1962.04	9.21	1.26
1961.86	9.33	1.31
1961.68	9.35	1.32
1961.50	9.17	1.22
1961.31	9.09	1.13
1961.13	9.06	1.12

1960.98	9.32	1.31
1960.82	9.22	1.18
1960.66	9.26	1.21
1960.50	9.29	1.28
1960.34	9.12	1.17
1960.18	9.34	1.34
1960.01	9.28	1.27
1959.84	9.39	1.35
1959.67	9.23	1.20
1959.49	9.21	1.28
1959.32	9.18	1.21
1959.15	9.11	1.20
1958.97	9.33	1.33
1958.79	9.25	1.28
1958.61	9.19	1.27
1958.44	9.23	1.40
1958.26	9.22	1.32
1958.06	9.36	1.38
1957.84	9.42	1.44
1957.62	9.27	1.29
1957.39	9.21	1.21
1957.17	9.38	1.34
1957.01	9.21	1.20
1956.85	9.28	1.25
1956.70	9.28	1.21
1956.54	9.18	1.23
1956.38	9.21	1.27
1956.23	9.19	1.29
1956.07	9.18	1.20
1955.90	9.25	1.29
1955.56	9.29	1.32
1955.39	9.19	1.20
1955.22	9.28	1.30
1955.22	9.24	1.28
1955.02	9.37	1.36
1954.79	9.38	1.40
1954.57	9.29	1.38
1954.35	9.21	1.27
1954.13	9.19	1.29
1953.95	9.31	1.33
1953.78	9.18	1.25
1953.60	9.39	1.46
1953.42	9.16	1.26
1953.24	9.06	1.14
1953.05	9.21	1.26
1952.86	9.19	1.28

1952.66	9.18	1.29
1952.46	9.11	1.17
1952.27	9.28	1.33
1952.04	9.38	1.36
1951.77	9.56	1.56
1951.50	9.10	1.19
1951.23	9.20	1.20
1951.02	9.23	1.20
1950.82	9.26	1.22
1950.63	9.37	1.27
1950.44	9.31	1.11
1950.25	9.23	1.23
1950.06	9.35	1.35
1949.89	9.38	1.34
1949.72	9.56	1.49
1949.55	9.32	1.25
1949.37	9.23	1.20
1949.20	9.27	1.23
1949.00	8.97	1.11
1948.79	9.31	1.44
1948.58	9.34	1.41
1948.36	9.21	1.32
1948.15	9.25	1.35
1947.96	9.19	1.29
1947.78	9.28	1.38
1947.59	9.22	1.36
1947.41	9.20	1.30
1947.22	9.35	1.38
1947.04	9.39	1.34
1946.85	9.13	1.17
1946.66	9.13	1.12
1946.47	9.07	1.12
1946.28	9.30	1.29
1946.10	9.10	1.12
1945.93	9.44	1.45
1945.77	9.27	1.22
1945.60	9.05	1.06
1945.43	9.10	1.14
1945.27	9.22	1.17
1945.07	9.40	1.38
1944.82	9.41	1.35
1944.56	9.26	1.19
1944.30	9.10	1.10
1944.07	9.43	1.36
1943.86	9.28	1.20
1943.66	9.41	1.30

1943.46	9.31	1.31
1943.25	9.26	1.27
1943.03	9.37	1.32
1942.78	9.36	1.34
1942.53	9.55	1.49
1942.28	9.10	1.12
1942.02	9.18	1.18
1941.52	9.23	1.17
1941.03	9.34	1.32
1940.81	9.40	1.35
1940.59	9.23	1.21
1940.37	9.20	1.19
1940.15	9.25	1.21
1939.13	9.15	1.19
1938.97	9.14	1.15
1938.81	9.17	1.25
1938.65	9.23	1.28
1938.49	9.38	1.37
1938.33	9.29	1.33
1938.17	9.03	1.09
1937.97	9.16	1.24
1937.77	9.28	1.30
1937.57	9.29	1.23
1937.17	9.36	1.22
1936.98	9.29	1.22
1936.80	9.48	1.33
1936.61	9.35	1.29
1936.43	9.49	1.41
1936.24	9.43	1.29
1936.06	9.27	1.23
1935.89	9.31	1.31
1935.71	9.17	1.20
1935.54	9.21	1.23
1935.36	9.24	1.20
1935.19	9.40	1.33
1935.00	9.23	1.17
1934.80	9.28	1.16
1934.61	9.48	1.37
1934.42	9.22	1.19
1934.23	9.37	1.28
1934.03	9.51	1.38
1933.84	9.37	1.26
1933.65	9.29	1.27
1933.46	9.60	1.50
1933.27	9.33	1.31
1933.05	9.25	1.26

1932.81	9.20	1.23
1932.56	9.37	1.34
1932.32	9.34	1.34
1932.10	9.32	1.28
1931.94	9.45	1.37
1931.77	9.36	1.34
1931.61	9.08	1.15
1931.45	9.04	1.12
1931.28	9.18	1.20
1931.12	9.23	1.23
1930.96	9.29	1.23
1930.80	9.15	1.25
1930.63	9.13	1.17
1930.47	9.28	1.28
1930.31	9.34	1.30
1930.15	9.43	1.35
1930.00	9.30	1.29
1929.85	9.23	1.19
1929.70	9.26	1.20
1929.54	9.16	1.11
1929.39	9.26	1.13
1929.24	9.21	1.15
1929.09	9.31	1.23
1928.92	9.14	1.14
1928.76	9.05	1.08
1928.60	9.00	1.04
1928.44	9.23	1.17
1928.28	9.34	1.28
1928.11	9.22	1.16
1927.93	9.23	1.20
1927.74	9.18	1.17
1927.56	9.26	1.19
1927.37	9.27	1.27
1927.19	9.21	1.15
1927.02	9.17	1.15
1926.85	9.05	1.10
1926.68	9.04	1.07
1926.52	9.35	1.32
1926.35	9.07	1.11
1926.18	9.18	1.13
1926.03	9.22	1.11
1925.88	9.02	1.05
1925.73	8.99	1.00
1925.58	8.99	1.02
1925.43	9.09	1.09
1925.28	9.30	1.24

1925.13		9.31		1.23
1924.96		9.24		1.14
1924.79		9.12		1.05
1924.62		9.15		1.11
1924.44		9.33		1.24
1924.27		9.37		1.20
1924.08		9.34		1.14
1923.85	NaN		NaN	
1923.62	NaN		NaN	
1921.83	NaN		NaN	
1921.64	NaN		NaN	
1921.45	NaN		NaN	
1921.26	NaN		NaN	
1921.09	NaN		NaN	
1920.81		9.29		1.26
1920.67		9.23		1.17
1920.53		8.99		1.11
1920.39		9.27		1.21
1920.25		9.37		1.27
1920.11		9.18		1.14
1919.98		9.30		1.29
1919.85		9.23		1.25
1919.72		9.38		1.33
1919.59		9.46		1.35
1919.46		9.26		1.20
1919.33		9.20		1.14
1919.20		9.08		1.11
1919.05		9.19		1.18
1918.88		9.32		1.31
1918.72		9.22		1.24
1918.55		9.25		1.19
1918.38		9.44		1.37
1918.22		9.21		1.24
1918.05		9.36		1.37
1917.88		9.12		1.20
1917.71		9.03		1.11
1917.54		9.13		1.16
1917.37		9.45		1.41
1917.20		9.11		1.13
1917.06		9.23		1.20
1916.92		9.05		1.07
1916.79		9.33		1.35
1916.66		9.07		1.13
1916.52		9.23		1.23
1916.39		9.25		1.25
1916.26		9.09		1.12

1916.12	9.08	1.14
1915.97	9.17	1.18
1915.82	9.20	1.23
1915.67	9.21	1.23
1915.51	9.30	1.31
1915.36	9.21	1.19
1915.21	9.31	1.29
1915.03	9.21	1.22
1914.84	9.28.	1.24
1914.65	9.20	1.22
1914.46	9.39	1.32
1914.27	9.27	1.22
1914.10	9.19	1.21
1913.96	9.22	1.15
1913.83	9.12	1.10
1913.69	9.11	1.09
1913.56	9.29	1.29
1913.42	9.15	1.08
1913.29	9.38	1.36
1913.15	9.50	1.43
1913.00	9.36	1.31
1912.86	9.28	1.27
1912.71	9.31	1.24
1912.56	9.50	1.35
1912.41	9.27	1.11
1912.27	9.29	1.12
1912.12	9.18	1.11
1911.96	9.27	1.13
1911.80	9.18	1.08
1911.63	9.21	1.12
1911.47	9.35	1.18
1911.31	9.40	1.25
1911.15	9.15	1.19
1910.98	9.27	1.24
1910.81	9.49	1.38
1910.63	9.27	1.21
1910.46	9.37	1.29
1910.29	9.56	1.49
1910.11	9.30	1.26
1909.92	9.35	1.27
1909.73	9.32	1.27
1909.53	9.36	1.32
1909.34	9.28	1.30
1909.15	9.23	1.21
1908.99	9.27	1.27
1908.83	9.25	1.23

1908.67	9.24	1.23
1908.50	9.22	1.17
1908.34	9.03	1.11
1908.18	9.19	1.20
1908.02	9.15	1.11
1907.86	9.21	1.15
1907.71	9.31	1.20
1907.55	9.32	1.18
1907.39	9.33	1.21
1907.23	9.25	1.19
1907.08	9.36	1.27
1906.95	9.17	1.16
1906.69	9.32	1.28
1906.56	9.25	1.23
1906.43	9.24	1.23
1906.29	9.10	1.13
1906.16	9.23	1.27
1906.02	9.18	1.13
1905.88	9.17	1.16
1905.74	9.32	1.26
1905.60	9.45	1.39
1905.46	9.43	1.28
1905.32	9.24	1.15
1905.18	9.20	1.15
1905.03	9.19	1.21
1904.88	9.39	1.28
1904.73	9.30	1.30
1904.58	9.34	1.29
1904.43	9.30	1.24
1904.28	9.29	1.23
1904.14	9.13	1.11
1904.00	9.18	1.17
1903.85	9.38	1.25
1903.71	9.31	1.22
1903.57	9.38	1.25
1903.43	9.32	1.21
1903.29	9.25	1.20
1903.15	9.23	1.19
1902.97	9.16	1.18
1902.80	9.22	1.21
1902.62	9.32	1.27
1902.45	9.25	1.23
1902.27	9.32	1.28
1902.11	9.26	1.25
1901.96	9.17	1.18
1901.81	9.34	1.27

1901.66	9.48	1.35
1901.52	9.38	1.26
1901.37	9.37	1.31
1901.22	9.29	1.18
1901.05	9.35	1.30
1900.85	9.15	1.22
1900.65	9.30	1.29
1900.45	9.25	1.25
1900.25	9.13	1.18
1900.07	9.47	1.45
1899.90	9.27	1.27
1899.73	9.20	1.17
1899.57	9.12	1.20
1899.40	9.21	1.20
1899.23	9.12	1.11
1899.05	9.19	1.21
1898.84	9.36	1.29
1898.64	9.14	1.15

PR-OF-001

Year	Sr-U (3yr bins)	Sr-U uncertainty (1σ)	Reconstructed SST ($^\circ$C, 3yr bins) 1σ uncertainty : 0.6 $^\circ$C	ERSST ($^\circ$C)
1997.5	9.07	0.05	27.2	27.69
1996	9.05	0.08	27.5	27.54
1994.5	9.05	0.05	27.5	27.60
1993	9.08	0.04	27.1	27.46
1991.5	9.09	0.04	27.0	27.43
1990	9.09	0.02	27.0	27.40
1988.5	9.09	0.02	26.9	27.59
1987	9.11	0.03	26.7	27.54
1985.5	9.11	0.02	26.7	27.29
1984	9.11	0.02	26.7	27.47
1982.5	9.12	0.04	26.7	27.69
1981	9.01	0.08	27.9	27.73
1979.5	8.97	0.07	28.3	27.65
1978	9.06	0.05	27.4	27.51
1976.5	9.05	0.05	27.5	27.23
1975	9.10	0.06	26.9	27.13
1973.5	9.10	0.06	26.8	27.35
1972	9.04	0.03	27.5	27.44
1970.5	9.04	0.07	27.6	27.69
1969	9.02	0.06	27.8	27.74

1967.5	9.02	0.05	27.8	27.48
1966	8.99	0.05	28.1	27.42
1964.5	9.03	0.04	27.7	27.58
1963	9.03	0.05	27.7	27.69
1961.5	9.05	0.04	27.4	27.72
1960	9.06	0.03	27.4	27.75
1958.5	9.10	0.06	26.9	27.65
1957	9.14	0.05	26.4	27.47
1955.5	9.11	0.05	26.7	27.25
1954	9.03	0.04	27.7	27.39
1952.5	9.03	0.03	27.6	27.55
1951	9.14	0.05	26.4	27.25
1949.5	9.15	0.07	26.3	27.14
1948	9.08	0.05	27.1	27.26
1946.5	9.09	0.03	27.0	27.31
1945	9.11	0.03	26.8	27.46
1943.5	9.11	0.03	26.8	27.52
1942	9.09	0.02	27.0	27.65
1940.5	9.10	0.05	26.9	27.58
1939	9.07	0.04	27.2	27.35
1937.5	9.07	0.07	27.2	27.30
1936	9.14	0.05	26.4	27.26
1934.5	9.11	0.04	26.7	27.21
1933	9.05	0.04	27.4	27.37
1931.5	9.01	0.03	27.9	27.46
1930	9.10	0.03	26.8	27.18
1928.5	9.13	0.02	26.5	27.06
1927	9.11	0.02	26.8	27.20
1925.5	9.13	0.02	26.5	27.09
1924	NaN	NaN	NaN	NaN
1922.5	NaN	NaN	NaN	NaN
1921	NaN	NaN	NaN	NaN
1919.5	9.09	0.03	27.0	26.97
1918	9.07	0.02	27.2	26.92
1916.5	9.06	0.01	27.4	27.04
1915	9.10	0.02	26.9	27.01
1913.5	9.17	0.03	26.1	26.85
1912	9.20	0.03	25.7	26.79
1910.5	9.18	0.04	25.9	26.70
1909	9.12	0.03	26.6	26.86
1907.5	9.12	0.04	26.6	27.03
1906	9.13	0.03	26.5	27.06
1904.5	9.14	0.03	26.4	27.24
1903	9.09	0.03	27.0	27.35
1901.5	9.09	0.04	27.0	27.32
1900	9.09	0.04	27.0	27.22

PR-OF-001

Year	Sr-U (10yr bins)	Sr-U uncertainty (1σ)	Reconstructed SST ($^\circ$ C, 10yr bins) 1σ uncertainty : 0.6 $^\circ$ C	ERSST ($^\circ$ C)
1994	9.07	0.02	27.2	27.54
1989	9.11	0.02	26.8	27.44
1984	9.10	0.02	26.8	27.58
1979	9.08	0.02	27.1	27.48
1974	9.08	0.03	27.1	27.44
1969	9.04	0.03	27.6	27.54
1964	9.05	0.02	27.4	27.60
1959	9.08	0.02	27.2	27.56
1954	9.09	0.03	27.0	27.38
1949	9.09	0.02	26.9	27.35
1944	9.11	0.02	26.8	27.46
1939	9.10	0.03	26.9	27.40
1934	9.10	0.02	26.9	27.28
1929	9.12	0.01	26.7	27.21
1924	NaN	NaN	NaN	NaN
1919	NaN	NaN	NaN	NaN
1914	9.12	0.02	26.6	26.97
1909	9.16	0.02	26.2	26.91
1904	9.12	0.02	26.7	26.87

PR-OF-002

Year	Sr/Ca (mmol/mol)	U/Ca (μmol/mol)
1989.92	9.33	1.27
1989.72	9.21	1.26
1989.52	9.32	1.25
1989.35	9.16	1.19
1989.23	9.18	1.23
1989.10	9.37	1.33
1988.98	9.37	1.32
1988.85	9.31	1.30
1988.73	9.35	1.26
1988.60	9.35	1.32
1988.48	9.11	1.11
1988.32	9.48	1.38
1988.12	9.33	1.32
1987.92	9.31	1.34

1987.72	9.28	1.30
1987.52	9.32	1.28
1987.35	9.37	1.27
1987.20	9.49	1.31
1987.06	9.40	1.33
1986.92	9.34	1.33
1986.77	9.37	1.34
1986.63	9.29	1.26
1986.49	9.41	1.38
1986.35	9.30	1.30
1986.06	9.39	1.31
1985.92	9.37	1.31
1985.77	9.27	1.25
1985.63	9.25	1.30
1985.49	9.46	1.37
1985.35	9.22	1.16
1985.20	9.19	1.21
1985.06	9.38	1.26
1984.92	9.25	1.22
1984.77	9.18	1.24
1984.63	9.27	1.29
1984.49	9.30	1.36
1984.33	9.38	1.38
1984.17	9.46	1.40
1984.00	9.30	1.35
1983.83	9.33	1.30
1983.67	9.24	1.25
1983.50	9.14	1.08
1983.33	9.26	1.33
1983.17	9.41	1.34
1983.00	9.23	1.25
1982.83	9.23	1.24
1982.67	9.40	1.35
1982.50	9.50	1.46
1982.33	9.53	1.50
1982.17	9.58	1.45
1982.00	9.62	1.52
1981.83	9.52	1.50
1981.67	9.35	1.38
1981.50	9.32	1.34
1981.32	9.54	1.54
1981.12	9.48	1.51
1980.92	9.46	1.47
1980.72	9.32	1.34
1980.52	9.29	1.40
1980.32	9.41	1.44

1980.12	9.28	1.33
1979.92	9.35	1.38
1979.72	9.34	1.31
1979.52	9.34	1.37
1979.32	9.19	1.28
1979.12	9.47	1.53
1978.92	9.46	1.46
1978.72	9.37	1.36
1978.52	9.19	1.31
1978.33	9.26	1.32
1978.17	9.19	1.32
1978.00	9.36	1.40
1977.83	9.37	1.42
1977.67	9.26	1.23
1977.50	9.14	1.29
1977.32	9.18	1.42
1977.12	9.15	1.33
1976.92	9.22	1.32
1976.72	9.39	1.36
1976.52	9.34	1.42
1976.32	9.39	1.44
1976.12	9.27	1.36
1975.06	9.03	1.10
1974.92	9.02	1.08
1974.77	9.05	1.08
1974.63	9.06	1.14
1974.49	9.12	1.25
1974.32	9.21	1.23
1974.12	9.32	1.26
1973.92	9.30	1.28
1973.72	9.39	1.29
1973.52	9.24	1.26
1973.32	9.14	1.18
1973.12	9.12	1.18
1972.92	9.21	1.20
1972.72	9.20	1.21
1972.52	9.32	1.34
1972.29	9.49	1.51
1972.04	9.38	1.41
1971.79	9.31	1.35
1971.54	9.41	1.46
1971.35	9.20	1.33
1971.20	9.22	1.31
1971.06	9.27	1.28
1970.92	9.14	1.20
1970.77	9.13	1.17

1970.63	9.09	1.15
1970.49	9.18	1.29
1970.35	9.28	1.28
1970.20	9.03	1.15
1970.06	9.02	1.10
1969.77	9.04	1.10
1969.63	8.95	1.11
1969.49	8.94	1.15
1969.32	9.14	1.17
1969.12	9.05	1.10
1968.92	9.04	1.13
1968.72	9.05	1.15
1968.52	9.04	1.25
1968.32	9.03	1.18
1968.12	9.31	1.32
1967.92	9.19	1.22
1967.72	9.07	1.14
1967.52	9.14	1.26
1967.33	9.36	1.32
1967.17	9.05	1.16
1967.00	9.02	1.15
1966.83	8.94	1.07
1966.67	9.26	1.29
1966.50	9.11	1.20
1966.32	9.02	1.11
1966.12	9.12	1.21
1965.92	9.19	1.27
1965.72	9.15	1.34
1965.52	9.32	1.38
1965.32	9.10	1.19
1965.12	9.28	1.30
1964.92	9.20	1.28
1964.72	9.11	1.20
1964.52	8.98	1.17
1964.35	8.98	1.10
1964.20	9.15	1.22
1964.06	9.06	1.14
1963.92	9.16	1.22
1963.77	9.16	1.23
1963.63	9.08	1.17
1963.49	9.04	1.17
1963.32	9.29	1.32
1963.12	9.34	1.36
1962.92	9.29	1.32
1962.72	9.19	1.30
1962.52	9.36	1.37

1962.33	9.13	1.25
1962.17	9.22	1.25
1962.00	9.24	1.23
1961.83	9.31	1.16
1961.67	9.52	1.29
1961.50	9.35	1.21
1961.32	9.35	1.23
1961.12	9.25	1.12
1960.92	9.53	1.29
1960.72	9.09	1.16
1960.52	9.07	1.16
1960.33	9.44	1.42
1960.17	9.30	1.32
1960.00	9.27	1.32
1959.83	9.29	1.29
1959.67	9.33	1.32
1959.50	9.39	1.38
1959.35	9.25	1.29
1959.23	9.28	1.31
1959.10	9.32	1.31
1958.98	9.37	1.34
1958.85	9.36	1.32
1958.73	9.32	1.29
1958.60	9.25	1.28
1958.48	9.34	1.40
1958.33	9.63	1.47
1958.17	9.42	1.28
1958.00	9.39	1.27
1957.83	9.32	1.20
1957.67	9.21	1.18
1957.50	9.41	1.31
1957.33	9.64	1.45
1957.17	9.53	1.36
1957.00	9.42	1.25
1956.83	9.36	1.19
1956.67	9.23	1.19
1956.50	9.22	1.19
1956.33	9.32	1.31
1956.17	9.22	1.21
1956.00	9.39	1.28
1955.83	9.32	1.18
1955.67	9.33	1.24
1955.50	9.46	1.32
1955.32	9.31	1.25
1955.12	9.28	1.21
1954.92	9.34	1.25

1954.72	9.37	1.26
1954.52	9.42	1.30
1954.33	9.46	1.38
1954.17	9.46	1.38
1954.00	9.56	1.43
1953.83	9.44	1.35
1953.67	9.45	1.35
1953.50	9.52	1.44
1953.33	9.54	1.42
1953.17	9.28	1.30
1953.00	9.27	1.25
1952.83	9.39	1.28
1952.67	9.44	1.29
1952.50	9.29	1.24

PR-OF-002

Year	Sr-U (3yr bins)	Sr-U uncertainty (1σ)	Reconstructed SST ($^\circ$C, 3yr bins) 1σ uncertainty : 0.6°C	ERSST ($^\circ$C)
1988.5	9.07	0.06	27.2	27.59
1987	9.10	0.06	26.8	27.54
1985.5	9.12	0.05	26.6	27.29
1984	9.12	0.04	26.6	27.47
1982.5	9.11	0.04	26.8	27.69
1981	9.01	0.09	28.0	27.73
1979.5	9.01	0.07	27.9	27.65
1978	9.02	0.10	27.8	27.51
1976.5	9.05	0.10	27.4	27.23
1975	9.06	0.04	27.4	27.13
1973.5	9.06	0.03	27.3	27.35
1972	9.06	0.03	27.4	27.44
1970.5	9.01	0.03	27.9	27.69
1969	9.00	0.03	28.1	27.74
1967.5	8.97	0.03	28.3	27.48
1966	8.97	0.04	28.3	27.42
1964.5	8.98	0.03	28.2	27.58
1963	9.04	0.07	27.5	27.69
1961.5	9.16	0.09	26.2	27.72
1960	9.13	0.07	26.6	27.75
1958.5	9.12	0.08	26.6	27.65
1957	9.17	0.05	26.1	27.47
1955.5	9.17	0.04	26.0	27.25
1954	9.15	0.04	26.3	27.39

PR-OF-002

Year	Sr-U (10yr bins)	Sr-U uncertainty (1σ)	Reconstructed SST ($^\circ$C, 10yr bins) 1σ uncertainty : 0.6 $^\circ$C	ERSST ($^\circ$C)
1984	9.13	0.03	26.6	27.58
1979	9.05	0.03	27.4	27.48
1974	9.04	0.02	27.6	27.44
1969	9.00	0.02	28.0	27.54
1964	9.02	0.03	27.8	27.60
1959	9.12	0.04	26.6	27.56

PAN-PD-017

Depth (mm)	Sr/Ca (mmol/mol)	U/Ca (μmol/mol)	Branch
0	9.14	1.08	A
1	9.03	1.05	A
2	9.10	1.08	A
3	9.07	1.06	A
4	9.04	1.02	A
5	9.02	0.99	A
6	8.97	0.94	A
7	8.98	0.87	A
8	8.93	0.84	A
9	8.90	0.84	A
10	9.03	0.89	A
11	8.97	0.87	A
12	8.95	0.75	A
13	9.01	0.76	A
14	8.94	0.88	A
15	8.93	0.79	A
16	8.90	0.77	A
17	8.84	0.84	A
18	8.90	0.80	A
19	8.94	0.82	A
20	9.01	0.95	A
21	8.88	0.88	A
22	8.89	0.84	A
23	8.92	0.90	A
24	8.99	0.80	A

25	8.96	0.86	A
26	8.99	0.85	A
27	8.96	0.81	A
28	8.92	0.92	A
29	8.97	0.87	A
30	8.79	0.82	A
31	8.94	0.85	A
32	8.85	0.87	A
33	9.10	0.92	A
34	9.01	0.83	A
35	9.08	0.78	A
36	9.09	0.96	A
37	9.14	1.11	A
38	9.00	0.90	A
39	9.18	1.12	A
40	8.89	0.93	A
41	8.96	0.86	A
42	8.97	0.89	A
43	8.94	0.92	A
44	8.96	0.81	A
45	8.94	0.86	A
46	8.83	0.78	A
47	8.83	0.80	A
48	8.75	0.77	A
49	8.68	0.74	A
50	8.83	0.78	A
51	8.92	0.81	A
52	8.97	0.80	A
53	8.98	0.78	A
54	9.13	0.87	A
55	8.95	0.90	A
56	8.89	0.83	A
57	8.90	0.85	A
58	8.90	0.71	A
59	8.88	0.84	A
60	8.78	0.93	A
61	8.94	0.87	A
62	8.83	0.91	A
63	8.98	0.88	A
64	8.90	0.87	A
65	8.81	0.94	A
66	8.94	0.79	A
67	8.92	0.76	A
68	8.93	0.83	A
69	9.00	0.97	A
1	9.00	0.91	B

2	9.00	0.94	B
3	9.00	0.88	B
4	9.10	0.93	B
5	9.01	0.93	B
6	8.94	0.91	B
7	8.93	0.87	B
8	8.98	0.87	B
9	8.95	0.87	B
10	8.87	0.81	B
11	8.94	0.86	B
12	8.85	0.78	B
13	8.93	0.85	B
14	9.05	0.97	B
15	8.93	0.91	B
16	8.89	0.85	B
17	8.88	0.86	B
18	8.87	0.83	B
19	8.88	0.83	B
20	8.94	0.80	B
21	8.93	0.84	B
22	8.84	0.85	B
23	8.86	0.80	B
24	8.94	0.84	B
25	8.92	0.77	B
26	8.86	0.82	B
27	8.91	0.83	B
28	8.99	0.88	B
29	8.88	0.86	B
30	8.94	0.93	B
31	8.94	0.86	B
32	8.84	0.82	B
33	8.85	0.86	B
34	8.85	0.84	B
35	8.97	0.87	B
36	9.07	0.90	B
37	8.97	0.87	B
38	8.85	0.84	B
39	8.89	0.82	B
40	9.04	0.82	B
41	9.06	0.81	B
42	8.91	0.77	B
43	9.00	0.86	B
44	8.89	0.89	B
45	8.97	0.92	B
46	9.00	0.86	B
47	8.98	0.91	B

48	9.00	0.88	B
49	9.07	0.87	B
51	8.85	0.76	B
52	8.80	0.87	B
53	8.91	0.88	B
54	8.76	0.85	B
55	8.79	0.90	B
56	8.89	0.87	B
57	8.93	0.84	B
58	8.80	0.86	B
59	8.84	0.83	B
60	8.89	0.78	B
61	8.89	0.85	B
62	8.95	0.81	B
63	9.05	0.83	B
64	8.97	0.88	B
65	9.00	0.85	B
67	8.98	0.84	B
68	8.94	0.94	B
69	9.02	1.02	B
70	8.93	0.90	B

Appendix C

Supplementary figures, and data for Chapter 4

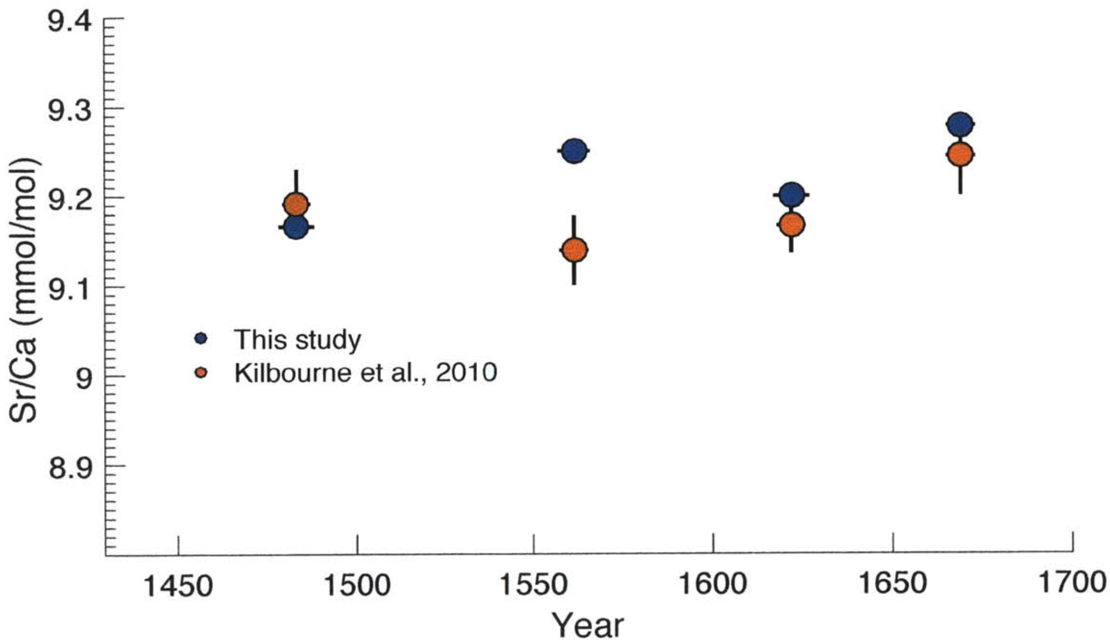

Figure C-1: Sr/Ca values from 8 to 9-year windows published in *Kilbourne et al.* [2010] (red) and separately analyzed in this study (blue). Vertical error bars represent one standard deviation of the mean based upon analytical uncertainty and horizontal bars represent the time period over which Sr/Ca was averaged.

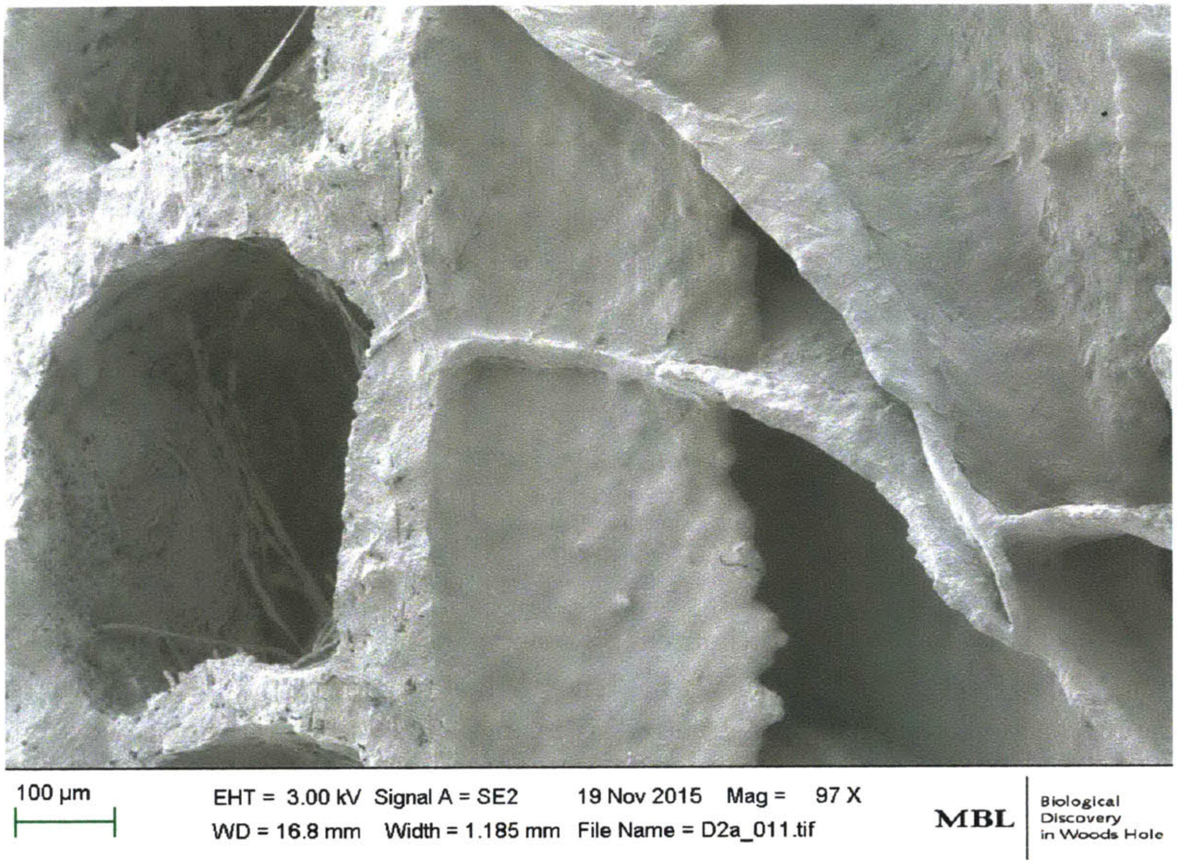

Figure C-2: Scanning Electron Microscope image of representative section of coral E1P from the 1450s showing well preserved thecal wall and septa without evidence of secondary aragonite or calcite crystals.

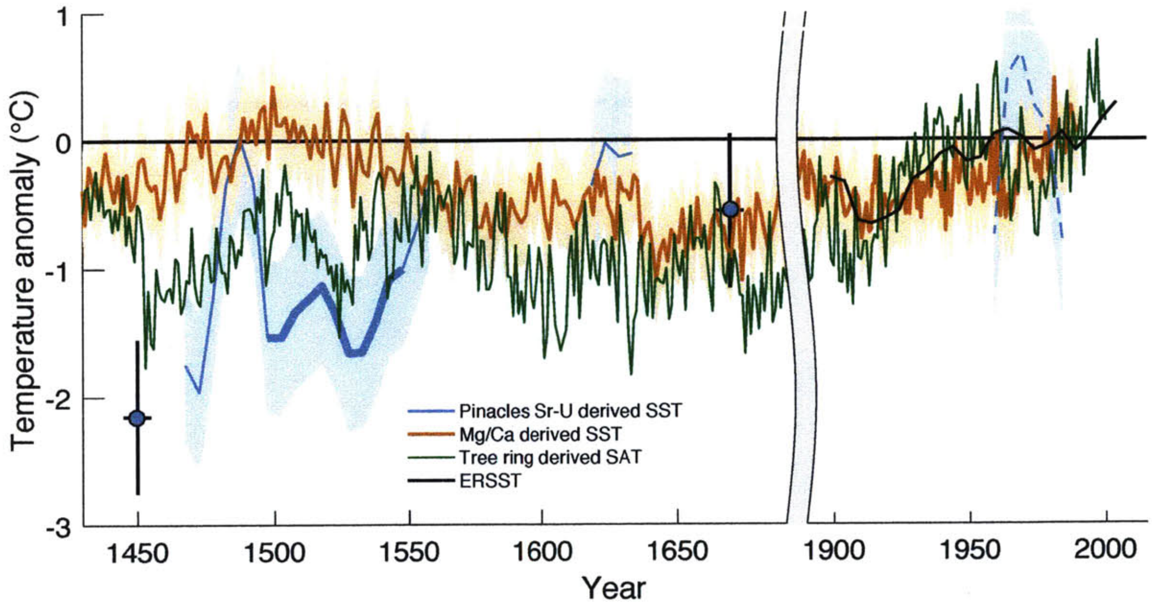

Figure C-3: Timeseries of SrU-estimated SST anomalies from 1958-1988 from E1P (LIA) and PR-OF-001 (20th century) in blue. When a single bin exists from a discontinuous section, the estimate is plotted as a single point. SST reconstructed from foramineferal Mg/Ca from the Cariaco basin is plotted in orange [*Black et al.*, 2007] and a northern hemisphere SAT record reconstructed from tree rings [*PAGES 2k Consortium*, 2013] is plotted in green. Shading on all timeseries indicates a standard deviation of uncertainty. ERSST [*Smith et al.*, 2008] is plotted in the 20th century. The Kuwae eruption of 1452 [*Gao et al.*, 2008] is indicated by a dashed red line.

References:

Black, D. E., M. A. Abahazi, R. C. Thunell, A. Kaplan, E. J. Tappa, and L. C. Peterson (2007), An 8-century tropical Atlantic SST record from the Cariaco Basin: Baseline variability, twentieth-century warming, and Atlantic hurricane frequency, *Paleoceanography*, *22*(4)

Gao, C., A. Robock, and C. Ammann (2008), Volcanic forcing of climate over the past 1500 years: An improved ice core-based index for climate models, *Journal of Geophysical Research: Atmospheres*, *113*(D23)

Kilbourne, K., T. Quinn, R. Webb, T. Guilderson, J. Nyberg, and A. Winter (2010), Coral windows onto seasonal climate variability in the northern Caribbean since 1479, *Geochemistry, Geophysics, Geosystems*, *11*(10). doi:10.1029/2010GC003171.

Past Global Changes 2k Consortium (2013), Continental-Scale Temperature Variability during the Past Two Millennia, *Nature Geoscience*, *6*(5)

Smith, T. M., R. W. Reynolds, T. C. Peterson, and J. Lawrimore (2008), Improvements to NOAA's historical merged land-ocean surface temperature analysis (1880-2006), *Journal of Climate*, *21*(10), 2283-2296

C.1 Subfossil data

Year	Sr/Ca (mmol/mol, uncertainty 0.04)	U/Ca (µmol/mol, uncertainty 0.02)
1673.43	9.28	1.23
1673.28	9.43	1.32
1673.13	9.31	1.20
1672.98	9.24	1.16
1672.83	9.44	1.31
1672.67	9.46	1.23
1672.52	9.41	1.22
1672.37	9.36	1.25
1672.07	9.15	1.21
1671.95	9.45	1.32
1671.86	9.27	1.23
1671.76	9.25	1.30
1671.66	9.39	1.32
1671.57	9.30	1.32
1671.47	9.28	1.25
1671.36	9.29	1.25
1671.25	9.17	1.19
1671.14	9.20	1.21
1671.02	9.22	1.28
1670.90	9.37	1.35
1670.78	9.27	1.29
1670.28	9.17	1.15
1670.16	9.14	1.14
1669.91	9.33	1.26
1669.78	9.18	1.20
1669.66	9.23	1.23
1669.53	9.25	1.20
1669.40	9.28	1.24
1669.27	9.34	1.31
1669.14	9.30	1.26
1669.02	9.30	1.28
1668.90	9.33	1.29

1668.78	9.26	1.23
1668.66	9.36	1.28
1668.55	9.42	1.29
1668.43	9.29	1.28
1668.31	9.19	1.18
1668.20	9.26	1.22
1668.08	9.23	1.22
1667.96	9.19	1.22
1667.84	9.19	1.24
1667.72	9.30	1.27
1667.59	9.19	1.24
1667.47	9.17	1.17
1667.35	9.28	1.26
1667.23	9.16	1.19
1667.11	9.36	1.32
1666.98	9.25	1.24
1666.86	9.29	1.29
1666.75	9.23	1.27
1666.63	9.24	1.23
1666.51	9.28	1.31
1666.39	9.28	1.26
1666.27	9.20	1.22
1666.15	9.29	1.27
1666.03	9.27	1.27
1665.93	9.12	1.19
1665.83	9.31	1.31
1665.73	9.36	1.31
1665.63	9.36	1.31
1665.53	9.24	1.33
1665.43	9.21	1.28
1643.42	9.10	1.08
1643.24	9.02	1.12
1643.07	8.95	1.08
1642.89	9.15	1.13
1642.71	9.16	1.18
1642.51	9.11	1.16
1642.31	9.25	1.18
1641.97	9.19	1.13
1641.84	9.22	1.15
1641.71	9.44	1.31
1641.59	9.05	1.21
1641.46	9.22	1.17
1641.33	9.19	1.15
1641.21	9.17	1.14
1641.08	9.38	1.27
1640.96	9.14	1.15

1640.85	9.09	1.22
1640.74	9.36	1.24
1640.63	9.25	1.23
1640.52	9.03	1.06
1640.38	9.17	1.13
1640.25	9.17	1.18
1640.14	9.26	1.23
1640.03	9.26	1.23
1639.92	9.31	1.25
1639.81	9.10	1.15
1639.70	9.36	1.30
1639.59	9.29	1.22
1639.48	9.13	1.18
1639.37	9.11	1.15
1639.26	9.14	1.15
1639.15	9.17	1.13
1639.04	9.13	1.15
1638.94	9.07	1.20
1638.85	9.36	1.26
1638.76	8.98	1.14
1638.67	9.12	1.15
1638.58	8.89	1.17
1638.49	9.10	1.15
1638.40	9.09	1.19
1638.31	9.13	1.19
1638.22	9.10	1.18
1638.03	9.15	1.21
1637.93	9.15	1.20
1637.83	9.18	1.21
1637.72	9.16	1.22
1637.61	9.31	1.28
1637.51	9.23	1.21
1637.40	9.35	1.26
1637.29	9.17	1.23
1637.19	9.24	1.25
1637.08	9.33	1.32
1636.97	9.22	1.27
1636.84	9.18	1.20
1636.71	9.25	1.29
1636.59	9.24	1.29
1636.46	9.27	1.33
1636.33	9.36	1.30
1636.21	9.25	1.29
1636.08	9.41	1.40
1635.96	9.25	1.25
1635.86	9.31	1.30

1635.76	9.23	1.26
1635.66	9.29	1.28
1635.56	9.26	1.26
1635.46	9.25	1.25
1635.36	9.30	1.28
1635.26	9.25	1.29
1635.16	9.24	1.29
1635.06	9.17	1.20
1634.97	9.12	1.19
1634.88	9.25	1.24
1634.79	9.25	1.27
1634.71	9.32	1.30
1634.62	9.33	1.29
1634.53	8.99	1.27
1634.45	9.48	1.42
1634.36	9.08	1.19
1634.27	9.16	1.22
1634.18	9.41	1.39
1634.10	9.30	1.27
1634.01	9.29	1.31
1633.92	9.16	1.30
1633.81	9.49	1.37
1633.71	9.43	1.33
1633.52	9.25	1.31
1633.42	9.53	1.47
1633.33	9.53	1.41
1633.24	9.25	1.24
1633.05	9.42	1.35
1632.95	9.32	1.28
1632.85	9.31	1.27
1632.75	9.32	1.28
1632.65	9.20	1.19
1632.56	9.24	1.18
1632.46	8.90	1.38
1632.36	9.10	1.22
1632.26	9.46	1.39
1632.16	9.24	1.24
1632.06	9.33	1.34
1631.97	9.22	1.23
1631.89	9.17	1.19
1631.81	9.30	1.22
1631.73	9.00	1.26
1631.65	9.26	1.23
1631.57	9.16	1.17
1631.49	9.31	1.27
1631.41	9.45	1.33

1631.33	9.05	1.19
1631.25	9.19	1.15
1631.17	9.27	1.26
1631.09	9.23	1.24
1631.01	9.29	1.24
1630.92	9.27	1.28
1630.82	9.31	1.26
1630.72	9.35	1.28
1630.63	9.24	1.19
1630.53	9.38	1.34
1630.43	9.30	1.27
1630.34	9.18	1.15
1629.48	9.26	1.17
1629.34	9.53	1.37
1629.21	9.23	1.16
1629.07	9.41	1.32
1628.93	9.25	1.18
1628.79	9.18	1.15
1628.66	9.21	1.22
1628.52	9.16	1.16
1628.38	9.19	1.16
1628.24	9.26	1.24
1628.10	9.20	1.16
1627.97	9.16	1.24
1627.86	9.40	1.34
1627.74	9.35	1.27
1627.62	9.35	1.30
1627.51	9.46	1.33
1627.39	9.27	1.22
1627.28	9.34	1.32
1627.16	9.28	1.22
1627.04	9.27	1.23
1626.92	9.29	1.24
1626.81	9.15	1.24
1626.71	9.14	1.14
1626.60	9.34	1.31
1626.50	9.29	1.29
1626.40	9.35	1.28
1626.29	9.47	1.35
1626.19	9.41	1.28
1626.09	9.33	1.25
1625.99	9.37	1.28
1625.89	9.37	1.27
1625.79	9.42	1.29
1625.70	9.30	1.20
1625.60	9.20	1.17

1625.50	9.17	1.16
1625.40	9.22	1.21
1625.28	9.19	1.22
1625.16	9.10	1.19
1625.06	9.06	1.18
1624.97	9.03	1.20
1624.88	9.07	1.16
1624.79	9.14	1.13
1624.70	8.90	1.09
1624.61	9.13	1.17
1624.52	9.24	1.32
1624.43	9.20	1.27
1624.34	9.20	1.26
1624.25	9.30	1.34
1624.16	9.12	1.19
1624.07	9.33	1.32
1623.98	9.16	1.24
1623.88	9.04	1.19
1623.78	9.49	1.42
1623.68	9.19	1.29
1623.59	9.38	1.33
1623.49	9.31	1.26
1623.39	9.47	1.37
1623.29	9.38	1.36
1623.20	9.24	1.24
1623.10	9.37	1.31
1623.00	9.28	1.24
1622.91	9.29	1.25
1622.82	9.15	1.18
1622.73	9.24	1.24
1622.64	9.31	1.29
1622.55	9.25	1.22
1622.45	9.19	1.17
1622.36	9.15	1.12
1622.27	9.13	1.14
1622.18	9.13	1.15
1622.09	9.37	1.28
1622.00	9.16	1.17
1621.89	9.17	1.15
1621.78	9.12	1.12
1621.67	9.30	1.23
1621.56	9.10	1.13
1621.44	9.34	1.31
1621.33	9.34	1.28
1621.22	9.14	1.17
1621.11	9.14	1.15

1621.00	9.19	1.19
1620.90	9.07	1.08
1620.79	9.05	1.09
1620.69	9.38	1.33
1620.59	9.29	1.25
1620.49	8.98	1.05
1620.38	9.29	1.29
1620.28	9.16	1.17
1620.18	9.15	1.15
1620.08	9.24	1.18
1619.97	9.18	1.15
1619.86	9.21	1.16
1620.03	9.25	1.20
1619.92	9.07	1.08
1619.81	9.15	1.15
1619.70	9.12	1.09
1619.59	9.08	1.08
1619.49	9.12	1.16
1619.38	9.15	1.19
1619.27	9.16	1.19
1619.16	9.08	1.14
1619.05	8.97	1.10
1618.95	9.07	1.15
1618.85	9.05	1.13
1618.75	9.09	1.20
1618.65	9.09	1.12
1618.56	9.00	1.06
1618.46	9.03	1.11
1618.36	9.17	1.20
1618.26	9.11	1.12
1618.16	9.13	1.16
1618.06	9.21	1.20
1617.96	9.12	1.16
1617.85	9.18	1.17
1617.74	9.22	1.25
1617.63	9.15	1.15
1617.52	9.28	1.23
1617.41	9.26	1.23
1617.30	9.17	1.18
1617.19	9.11	1.14
1617.08	9.10	1.17
1616.97	9.12	1.14
1616.86	9.17	1.17
1616.76	9.19	1.17
1616.65	9.24	1.16
1616.54	9.17	1.10

1616.43	9.17	1.11
1616.32	9.16	1.18
1616.22	9.25	1.23
1616.11	9.22	1.20
1616.00	9.13	1.15
1615.93	9.19	1.12
1615.93	9.26	1.18
1615.85	9.12	1.06
1615.72	9.08	1.07
1615.65	9.13	1.18
1615.57	9.09	1.12
1615.49	9.22	1.21
1615.41	9.17	1.13
1615.33	9.13	1.16
1615.22	9.14	1.17
1615.11	9.15	1.17
1615.04	9.25	1.21
1614.96	9.34	1.29
1614.88	9.18	1.21
1614.80	9.19	1.17
1614.72	9.32	1.25
1614.64	9.21	1.16
1614.56	9.37	1.25
1614.48	9.14	1.13
1614.40	9.24	1.21
1614.32	9.26	1.21
1614.23	9.14	1.15
1614.14	9.08	1.15
1614.05	9.22	1.18
1613.96	9.28	1.19
1613.87	9.14	1.12
1613.78	9.23	1.15
1613.69	9.15	1.10
1613.60	9.14	1.08
1613.52	9.08	1.06
1613.43	9.15	1.10
1613.34	9.19	1.15
1613.25	9.23	1.14
1613.16	9.17	1.11
1613.10	9.19	1.08
1565.80	9.26	1.08
1565.60	8.68	0.94
1565.40	9.03	0.99
1565.20	8.94	1.09

1565.00	9.28	1.26
1564.80	9.37	1.31
1564.60	9.46	1.43
1564.40	9.31	1.36
1564.20	9.58	1.40
1564.00	9.49	1.35
1563.92	9.58	1.39
1563.83	9.38	1.26
1563.75	9.17	1.14
1563.67	9.30	1.24
1563.58	9.05	1.06
1563.50	8.81	0.98
1563.42	9.11	1.08
1563.33	9.36	1.30
1563.25	9.45	1.37
1563.17	9.37	1.30
1563.08	9.26	1.24
1563.00	9.50	1.34
1562.86	9.27	1.20
1562.71	9.19	1.12
1562.57	9.13	1.14
1562.43	9.05	1.10
1562.29	9.07	1.15
1562.14	8.98	1.23
1562.00	9.13	1.15
1561.91	9.19	1.14
1561.82	9.15	1.23
1561.73	9.08	1.11
1561.64	9.04	1.09
1561.55	9.18	1.10
1561.45	9.22	1.13
1561.36	8.99	1.06
1561.27	9.24	1.15
1561.18	9.13	1.21
1561.09	9.25	1.25
1561.00	9.30	1.15
1560.88	9.46	1.21
1560.75	9.21	1.14
1560.63	9.40	1.26
1560.50	9.36	1.21
1560.38	9.45	1.22
1560.25	9.29	1.18
1560.13	9.36	1.18
1560.00	8.79	0.97
1559.91	9.22	1.23
1559.82	9.17	1.14

1559.73	9.14	1.11
1559.64	9.22	1.23
1559.55	9.18	1.19
1559.45	9.09	1.16
1559.36	9.21	1.26
1559.27	9.18	1.18
1559.18	9.14	1.11
1559.09	9.05	1.07
1559.00	9.14	1.10
1558.86	9.40	1.20
1558.71	9.24	1.15
1558.57	9.25	1.12
1558.43	9.27	1.06
1558.29	9.50	1.22
1558.14	9.14	1.09
1558.00	9.56	1.48
1557.88	8.78	1.05
1557.75	9.36	1.27
1557.63	9.39	1.26
1557.50	9.36	1.23
1557.38	9.38	1.18
1557.25	9.22	1.20
1557.13	9.53	1.31
1557.00	9.51	1.35
1556.88	9.50	1.37
1556.75	9.37	1.38
1556.63	9.45	1.31
1556.50	8.78	1.20
1556.38	9.25	1.24
1556.25	9.21	1.22
1556.13	9.31	1.28
1556.00	9.09	1.08
1555.90	9.02	1.09
1555.80	9.08	1.12
1555.70	9.16	1.08
1555.60	9.08	1.13
1555.50	9.25	1.15
1555.40	9.23	1.10
1555.30	9.25	1.21
1555.20	9.20	1.09
1555.10	8.81	1.08
1555.00	9.23	1.21
1554.92	8.59	1.06
1554.83	9.09	1.09
1554.75	9.05	1.24
1554.67	9.14	1.30

1554.58	9.50	1.36
1554.50	9.51	1.29
1554.42	9.33	1.28
1554.33	9.23	1.22
1554.25	9.15	1.17
1554.17	9.34	1.29
1554.08	9.26	1.22
1554.00	9.35	1.32
1553.91	9.29	1.27
1553.82	9.23	1.17
1553.73	9.21	1.19
1553.64	9.37	1.26
1553.55	9.27	1.14
1553.45	9.17	1.24
1553.36	8.97	1.07
1553.27	9.27	1.33
1553.18	9.21	1.08
1553.09	9.07	1.12
1553.00	9.10	1.11
1552.88	9.15	1.20
1552.75	9.40	1.34
1552.63	9.00	1.08
1552.50	9.24	1.23
1552.38	9.09	1.17
1552.25	9.14	1.07
1552.13	9.21	1.10
1552.00	9.36	1.16
1551.89	9.22	1.16
1551.78	9.34	1.20
1551.67	9.41	1.09
1551.56	9.35	1.06
1551.44	9.47	1.19
1551.33	9.38	1.17
1551.22	9.09	1.07
1551.11	9.43	1.14
1551.00	9.42	1.18
1550.80	9.20	1.13
1550.60	9.34	1.13
1550.40	9.34	1.16
1550.20	9.23	1.15
1550.00	9.15	1.16
1549.90	9.36	1.22
1549.80	9.27	1.17
1549.70	9.36	1.19
1549.60	9.20	1.15
1549.50	9.10	1.12

1549.40	9.34	1.11
1549.30	9.41	1.21
1549.20	8.99	1.05
1549.10	8.99	1.08
1549.00	8.93	1.10
1548.90	9.02	1.02
1548.80	8.97	1.05
1548.70	9.11	1.09
1548.60	9.13	1.11
1548.50	9.04	1.11
1548.40	9.08	1.07
1548.30	9.02	1.06
1548.20	9.04	1.08
1548.10	9.18	1.11
1548.00	9.09	1.10
1547.89	9.12	1.06
1547.78	9.00	1.03
1547.67	9.04	1.10
1547.56	9.12	1.15
1547.44	9.11	1.13
1547.33	9.11	1.11
1547.22	9.08	1.05
1547.11	9.06	1.14
1547.00	9.22	1.20
1546.90	9.36	1.18
1546.80	9.00	1.07
1546.70	9.21	1.13
1546.60	9.21	1.18
1546.50	9.48	1.23
1546.40	9.44	1.27
1546.30	9.24	1.17
1546.20	9.37	1.17
1546.10	9.20	1.15
1546.00	9.51	1.32
1545.89	9.41	1.29
1545.78	9.31	1.22
1545.67	9.05	1.21
1545.56	9.31	1.25
1545.44	9.30	1.23
1545.33	9.23	1.23
1545.22	9.10	1.15
1545.11	9.17	1.18
1545.00	9.45	1.31
1544.89	9.44	1.26

1544.78	9.32	1.20
1544.67	9.28	1.15
1544.56	9.43	1.26
1544.44	9.35	1.22
1544.33	9.44	1.20
1544.22	9.29	1.12
1544.11	9.21	1.09
1544.00	9.19	1.16
1543.89	9.08	1.02
1543.78	9.23	1.15
1543.67	9.14	1.09
1543.56	9.21	1.13
1543.44	9.35	1.20
1543.33	9.40	1.22
1543.22	9.34	1.23
1543.11	9.40	1.33
1543.00	9.19	1.19
1542.90	9.14	1.14
1542.80	9.14	1.10
1542.70	9.25	1.14
1542.60	9.15	1.13
1542.50	9.13	1.16
1542.40	9.16	1.15
1542.30	9.11	1.07
1542.20	9.14	1.08
1542.10	9.09	1.10
1542.00	9.16	1.14
1541.89	9.12	1.12
1541.78	9.15	1.17
1541.67	9.11	1.11
1541.56	9.41	1.19
1541.44	9.24	1.16
1541.33	9.15	1.08
1541.22	9.15	1.09
1541.11	9.25	1.15
1541.00	9.31	1.22
1540.90	9.44	1.23
1540.80	9.35	1.26
1540.70	9.36	1.21
1540.60	9.29	1.17
1540.50	9.22	1.05
1540.40	9.24	1.14
1540.30	9.07	1.07
1540.20	9.23	1.17
1540.10	9.27	1.20
1540.00	9.18	1.11

1539.88	9.07	1.07
1539.75	9.15	1.05
1539.63	9.34	1.21
1539.50	9.13	1.11
1539.38	9.27	1.22
1539.25	9.25	1.13
1539.13	9.09	1.13
1539.00	9.25	1.14
1538.90	9.21	1.14
1538.80	9.29	1.16
1538.70	9.17	1.20
1538.60	9.31	1.29
1538.50	9.11	1.16
1538.40	9.17	1.13
1538.30	9.30	1.18
1538.20	9.06	1.09
1538.10	9.08	1.09
1538.00	9.26	1.15
1537.91	9.32	1.11
1537.82	9.24	1.09
1537.73	9.25	1.12
1537.64	9.31	1.12
1537.55	9.24	1.12
1537.45	9.59	1.29
1537.36	9.39	1.12
1537.27	9.32	1.11
1537.18	9.38	1.18
1537.09	9.24	1.10
1537.00	9.34	1.17
1536.90	9.45	1.25
1536.80	9.40	1.17
1536.70	9.22	1.08
1536.60	9.46	1.28
1536.50	9.26	1.17
1536.40	9.52	1.27
1536.30	9.49	1.27
1536.20	9.36	1.24
1536.10	9.30	1.23
1536.00	9.37	1.17
1535.89	9.14	1.17
1535.78	9.27	1.18
1535.67	9.30	1.15
1535.56	9.23	1.16
1535.44	9.22	1.10
1535.33	9.34	1.15
1535.22	9.22	1.09

1535.11	9.34	1.18
1535.00	9.16	1.08
1534.90	9.27	1.10
1534.80	9.40	1.21
1534.70	9.40	1.19
1534.60	9.28	1.14
1534.50	9.21	1.16
1534.40	9.28	1.17
1534.30	9.20	1.11
1534.20	9.26	1.12
1534.10	9.28	1.19
1534.00	9.31	1.23
1533.90	9.31	1.15
1533.80	9.47	1.28
1533.70	9.32	1.20
1533.60	9.39	1.27
1533.50	9.33	1.18
1533.40	9.37	1.16
1533.30	9.21	1.11
1533.20	9.10	1.05
1533.10	9.44	1.31
1533.00	9.28	1.18
1532.90	9.17	1.10
1532.80	9.08	1.13
1532.70	9.20	1.15
1532.60	9.19	1.13
1532.50	9.33	1.19
1532.40	9.40	1.23
1532.30	8.91	1.10
1532.20	9.50	1.23
1532.10	9.60	1.40
1532.00	9.43	1.25
1531.91	9.50	1.22
1531.82	9.17	1.10
1531.73	9.28	1.12
1531.64	9.33	1.15
1531.55	9.40	1.17
1531.45	9.32	1.18
1531.36	9.43	1.23
1531.27	9.10	1.10
1531.18	9.25	1.04
1531.09	9.50	1.22
1531.00	9.32	1.15
1530.86	9.46	1.20
1530.71	9.38	1.17
1530.57	9.27	1.10

1530.43	9.59	1.27
1530.29	9.47	1.32
1530.14	9.56	1.26
1530.00	8.77	0.95
1529.89	9.00	1.06
1529.78	9.38	1.19
1529.67	9.32	1.13
1529.56	9.16	1.04
1529.44	9.27	1.11
1529.33	9.47	1.21
1529.22	9.54	1.28
1529.11	9.49	1.25
1529.00	9.38	1.20
1528.88	9.65	1.32
1528.75	9.30	1.17
1528.63	9.50	1.28
1528.50	9.29	1.13
1528.38	9.24	1.09
1528.25	9.21	1.10
1528.13	9.15	1.08
1528.00	9.33	1.19
1527.92	9.40	1.21
1527.85	9.42	1.29
1527.77	9.27	1.11
1527.69	9.48	1.26
1527.62	9.41	1.25
1527.54	9.44	1.26
1527.46	9.30	1.16
1527.38	9.40	1.25
1527.31	9.31	1.20
1527.23	9.46	1.26
1527.15	9.65	1.43
1527.08	9.45	1.30
1527.00	9.44	1.29
1526.90	9.25	1.20
1526.80	9.24	1.18
1526.70	9.57	1.36
1526.60	9.33	1.15
1526.50	9.37	1.17
1526.40	9.30	1.12
1526.30	9.38	1.11
1526.20	9.12	1.01
1526.10	9.09	1.07
1526.00	9.32	1.18
1525.90	9.32	1.17
1525.80	9.23	1.14

1525.70	9.43	1.28
1525.60	9.30	1.14
1525.50	9.36	1.18
1525.40	9.44	1.23
1525.30	9.46	1.27
1525.20	9.32	1.13
1525.10	9.30	1.15
1525.00	9.25	1.13
1524.91	9.42	1.20
1524.82	9.26	1.12
1524.73	9.14	1.08
1524.64	9.12	1.08
1524.55	9.30	1.15
1524.45	9.29	1.20
1524.36	9.14	1.10
1524.27	9.33	1.19
1524.18	9.30	1.18
1524.09	9.24	1.18
1524.00	9.27	1.23
1523.80	9.20	1.13
1523.60	9.24	1.15
1523.40	9.25	1.16
1523.20	9.27	1.25
1523.00	9.25	1.18
1522.89	9.28	1.21
1522.78	9.49	1.22
1522.67	9.59	1.32
1522.56	9.43	1.27
1522.44	9.43	1.19
1522.33	9.48	1.28
1522.22	9.42	1.21
1522.11	9.54	1.27
1522.00	9.28	1.15
1521.90	9.38	1.16
1521.80	9.32	1.16
1521.70	9.27	1.13
1521.60	9.29	1.14
1521.50	9.53	1.27
1521.40	9.39	1.11
1521.30	9.26	1.12
1521.20	8.78	0.95
1521.10	9.03	1.11
1521.00	8.87	1.03
1520.89	8.80	0.99
1520.78	8.89	1.04
1520.67	8.91	1.06

1520.56	9.40	1.19
1520.44	9.36	1.12
1520.33	9.23	1.14
1520.22	9.30	1.20
1520.11	9.34	1.25
1520.00	9.46	1.33
1519.89	9.38	1.24
1519.78	9.33	1.15
1519.67	9.46	1.25
1519.56	9.35	1.18
1519.44	9.33	1.14
1519.33	9.22	1.12
1519.22	9.27	1.13
1519.11	9.31	1.15
1519.00	9.38	1.20
1518.89	9.28	1.13
1518.78	9.48	1.27
1518.67	9.49	1.24
1518.56	9.40	1.19
1518.44	9.34	1.17
1518.33	9.52	1.27
1518.22	9.41	1.19
1518.11	9.40	1.22
1518.00	9.37	1.20
1517.89	9.50	1.30
1517.78	9.49	1.23
1517.67	9.30	1.21
1517.56	9.24	1.22
1517.44	9.47	1.27
1517.33	9.35	1.22
1517.22	9.16	1.11
1517.11	9.26	1.17
1517.00	9.18	1.10
1516.89	9.22	1.17
1516.78	9.22	1.14
1516.67	9.38	1.22
1516.56	9.33	1.23
1516.44	9.38	1.26
1516.33	9.20	1.19
1516.22	9.30	1.23
1516.11	9.36	1.21
1516.00	9.33	1.16
1515.89	9.54	1.32
1515.78	9.33	1.18
1515.67	9.31	1.18
1515.56	9.33	1.17

1515.44	9.34	1.22
1515.33	9.60	1.34
1515.22	9.34	1.21
1515.11	9.37	1.26
1515.00	9.38	1.23
1514.83	9.26	1.19
1514.67	9.31	1.22
1514.50	9.25	1.18
1514.33	9.28	1.18
1514.17	9.35	1.25
1514.00	9.33	1.26
1513.91	9.40	1.34
1513.82	9.32	1.23
1513.73	9.48	1.35
1513.64	9.39	1.31
1513.55	9.31	1.29
1513.45	9.27	1.23
1513.36	9.44	1.30
1513.27	9.40	1.31
1513.18	9.32	1.20
1513.09	9.23	1.18
1513.00	9.32	1.23
1512.91	9.46	1.31
1512.82	9.42	1.25
1512.73	9.47	1.27
1512.64	9.43	1.26
1512.55	9.37	1.23
1512.45	9.44	1.28
1512.36	9.41	1.27
1512.27	9.36	1.23
1512.18	9.27	1.18
1512.09	9.44	1.29
1512.00	9.29	1.21
1511.89	9.35	1.23
1511.78	9.39	1.28
1511.67	9.44	1.27
1511.56	9.39	1.25
1511.44	9.23	1.23
1511.33	9.33	1.21
1511.22	9.47	1.28
1511.11	9.30	1.22
1511.00	9.54	1.34
1510.89	9.41	1.25
1510.78	9.34	1.23
1510.67	9.43	1.24
1510.56	9.30	1.20

1510.44	9.34	1.18
1510.33	9.37	1.22
1510.22	9.26	1.15
1510.11	9.47	1.28
1510.00	9.51	1.30
1509.90	9.36	1.26
1509.80	9.39	1.31
1509.70	9.35	1.22
1509.60	9.37	1.29
1509.50	9.27	1.20
1509.40	9.33	1.21
1509.30	9.15	1.15
1509.20	9.32	1.18
1509.10	9.36	1.25
1509.00	9.30	1.24
1508.91	9.33	1.23
1508.82	9.34	1.22
1508.64	9.20	1.18
1508.55	9.21	1.15
1508.45	9.18	1.22
1508.36	9.26	1.17
1508.27	9.48	1.37
1508.18	9.38	1.26
1508.09	9.28	1.18
1508.00	9.45	1.29
1507.88	9.36	1.30
1507.75	9.29	1.23
1507.63	9.43	1.29
1507.50	9.35	1.20
1507.38	9.36	1.17
1507.25	9.26	1.17
1507.13	9.26	1.10
1507.00	9.25	1.16
1506.89	9.20	1.14
1506.78	9.37	1.24
1506.67	9.41	1.21
1506.56	9.32	1.22
1506.44	9.25	1.14
1506.33	9.33	1.25
1506.22	9.41	1.28
1506.11	9.28	1.12
1506.00	9.24	1.24
1505.90	9.33	1.28
1505.80	9.32	1.18
1505.70	9.23	1.21
1505.60	9.39	1.23

1505.50	9.29	1.20
1505.40	9.14	1.14
1505.30	9.17	1.14
1505.20	9.24	1.17
1505.10	9.43	1.31
1505.00	9.38	1.24
1504.90	9.51	1.37
1504.80	9.46	1.38
1504.70	9.42	1.31
1504.60	9.27	1.23
1504.50	9.43	1.24
1504.40	9.41	1.26
1504.30	9.49	1.29
1504.20	9.37	1.22
1504.10	9.43	1.20
1504.00	9.38	1.19
1503.89	9.54	1.30
1503.78	9.34	1.23
1503.67	9.30	1.22
1503.56	9.25	1.19
1503.44	9.23	1.17
1503.33	9.45	1.26
1503.22	9.13	1.12
1503.11	9.23	1.17
1503.00	9.39	1.25
1502.86	9.30	1.19
1502.71	9.23	1.12
1502.57	9.25	1.16
1502.43	9.32	1.19
1502.29	9.27	1.15
1502.14	9.31	1.18
1502.00	9.37	1.24
1501.91	9.25	1.29
1501.82	9.40	1.24
1501.73	9.29	1.22
1501.64	9.36	1.21
1501.55	9.33	1.26
1501.45	9.34	1.20
1501.36	9.27	1.14
1501.27	9.37	1.20
1501.18	9.39	1.24
1501.09	9.55	1.28
1501.00	9.40	1.25
1500.88	9.33	1.17
1500.75	9.25	1.20
1500.63	9.53	1.32

1500.50	9.51	1.30
1500.38	9.46	1.26
1500.25	9.45	1.22
1500.13	9.47	1.19
1500.00	9.43	1.26
1499.91	9.42	1.25
1499.82	9.37	1.20
1499.73	9.48	1.29
1499.64	9.45	1.27
1499.55	9.50	1.29
1499.45	9.50	1.28
1499.36	9.39	1.22
1499.27	9.36	1.22
1499.18	9.39	1.27
1499.09	9.33	1.23
1499.00	9.39	1.28
1498.91	9.51	1.25
1498.82	9.34	1.24
1498.73	9.43	1.31
1498.64	9.47	1.31
1498.55	9.37	1.23
1498.45	9.51	1.26
1498.36	9.34	1.23
1498.27	9.53	1.28
1498.18	9.40	1.22
1498.09	9.49	1.27
1498.00	9.39	1.25
1497.91	9.54	1.34
1497.82	9.38	1.22
1497.64	9.30	1.22
1497.55	9.35	1.24
1497.45	9.17	1.16
1497.36	9.24	1.19
1497.27	9.33	1.21
1497.18	9.22	1.14
1497.09	9.27	1.15
1497.00	9.34	1.25
1496.89	9.23	1.18
1496.78	9.49	1.33
1496.67	9.29	1.18
1496.56	9.28	1.22
1496.44	9.25	1.14
1496.33	9.08	1.11
1496.22	9.04	1.10
1496.11	9.32	1.25
1496.00	9.36	1.38

1495.89	9.29	1.26
1495.78	9.33	1.29
1495.67	9.26	1.22
1495.56	9.37	1.29
1495.44	9.36	1.27
1495.33	9.36	1.29
1495.22	9.25	1.20
1495.11	9.19	1.21
1495.00	9.36	1.31
1494.90	9.36	1.32
1494.80	9.25	1.26
1494.70	9.39	1.27
1494.60	9.49	1.39
1494.50	9.42	1.31
1494.40	9.38	1.29
1494.30	9.25	1.23
1494.20	9.18	1.17
1494.10	9.28	1.24
1494.00	9.65	1.52
1493.89	9.35	1.30
1493.78	9.31	1.30
1493.67	9.28	1.23
1493.56	9.36	1.40
1493.44	9.31	1.28
1493.33	9.31	1.23
1493.22	9.31	1.25
1493.11	9.23	1.18
1493.00	9.37	1.29
1492.91	9.25	1.20
1492.82	9.27	1.27
1492.73	9.30	1.29
1492.64	9.27	1.18
1492.55	9.28	1.24
1492.45	9.21	1.19
1492.36	9.27	1.23
1492.27	9.21	1.24
1492.18	9.10	1.11
1492.09	9.20	1.23
1492.00	9.06	1.21
1491.86	9.13	1.20
1491.71	9.14	1.24
1491.57	8.99	1.11
1491.43	9.15	1.17
1491.29	9.13	1.14
1491.14	9.13	1.17
1491.00	9.21	1.28

1490.90	9.31	1.35
1490.80	9.29	1.32
1490.70	9.29	1.31
1490.60	9.18	1.22
1490.50	9.08	1.15
1490.40	9.00	1.16
1490.30	9.12	1.15
1490.20	9.22	1.18
1490.10	9.19	1.16
1490.00	9.24	1.19
1489.90	9.20	1.16
1489.80	9.21	1.18
1489.70	9.32	1.27
1489.60	9.15	1.14
1489.50	9.13	1.21
1489.40	9.13	1.14
1489.30	9.13	1.13
1489.20	9.28	1.17
1489.10	9.21	1.16
1489.00	9.27	1.16
1488.91	9.18	1.14
1488.82	9.15	1.22
1488.73	9.18	1.21
1488.64	9.15	1.15
1488.55	9.17	1.15
1488.45	9.09	1.08
1488.36	9.08	1.12
1488.27	9.05	1.11
1488.18	9.24	1.22
1488.09	9.07	1.16
1488.00	9.11	1.13
1487.90	9.14	1.21
1487.80	9.17	1.19
1487.70	9.10	1.11
1487.60	8.99	1.09
1487.50	9.14	1.14
1487.40	9.16	1.11
1487.30	9.04	1.11
1487.20	9.04	1.09
1487.10	9.12	1.13
1487.00	9.06	1.12
1486.89	9.09	1.17
1486.78	9.13	1.19
1486.67	9.15	1.21
1486.56	9.22	1.18
1486.44	9.08	1.17

1486.33	9.02	1.15
1486.22	9.08	1.17
1486.11	9.05	1.12
1486.00	9.04	1.09
1485.89	9.10	1.12
1485.78	9.22	1.19
1485.67	9.18	1.21
1485.56	9.12	1.16
1485.44	9.11	1.12
1485.33	8.92	1.02
1485.22	9.11	1.13
1485.11	9.19	1.19
1485.00	9.11	1.14
1484.90	9.14	1.15
1484.80	9.03	1.06
1484.70	9.12	1.10
1484.60	9.14	1.12
1484.50	9.03	1.05
1484.40	9.04	1.06
1484.30	8.90	0.98
1484.20	9.05	1.10
1484.10	9.12	1.12
1484.00	9.07	1.11
1483.86	9.29	1.14
1483.71	9.25	1.16
1483.57	9.36	1.18
1483.43	9.17	1.10
1483.29	8.47	1.08
1483.14	9.26	1.16
1483.00	9.56	1.34
1482.86	9.28	1.20
1482.71	9.56	1.34
1482.57	9.51	1.29
1482.43	9.49	1.28
1482.29	9.51	1.24
1482.14	9.25	1.06
1482.00	9.37	1.18
1481.89	9.30	1.11
1481.78	9.32	1.07
1481.67	9.21	1.18
1481.56	9.18	1.15
1481.44	9.24	1.30
1481.33	9.12	1.13
1481.22	8.95	1.01
1481.11	9.19	1.22
1481.00	9.15	1.17

1480.86	9.11	1.11
1480.71	9.16	1.18
1480.57	9.03	1.14
1480.43	9.15	1.19
1480.29	9.08	1.21
1480.14	9.19	1.20
1480.00	9.19	1.19
1479.88	9.10	1.13
1479.75	9.28	1.29
1479.63	9.37	1.11
1479.50	9.59	1.34
1479.38	9.36	1.17
1479.25	9.42	1.24
1479.13	9.28	1.18
1479.00	9.40	1.21
1478.90	9.27	1.19
1478.80	9.39	1.19
1478.70	9.27	1.20
1478.60	9.26	1.16
1478.50	9.30	1.16
1478.40	9.33	1.22
1478.30	9.24	1.17
1478.20	9.30	1.18
1478.10	9.28	1.23
1478.00	9.43	1.29
1477.89	9.40	1.24
1477.78	9.33	1.17
1477.67	9.35	1.23
1477.56	9.37	1.24
1477.44	9.41	1.29
1477.33	9.35	1.27
1477.22	9.34	1.28
1477.11	9.33	1.26
1477.00	9.40	1.23
1476.89	9.34	1.24
1476.78	9.30	1.20
1476.67	9.19	1.11
1476.56	9.31	1.21
1476.44	9.28	1.25
1476.33	9.32	1.23
1476.22	9.33	1.25
1476.11	9.51	1.29
1476.00	9.49	1.34
1475.89	9.51	1.32
1475.78	9.58	1.27
1475.67	9.36	1.21

1475.56	9.27	1.24
1475.44	9.30	1.27
1475.33	9.42	1.30
1475.22	9.29	1.23
1475.11	9.67	1.34
1475.00	9.30	1.27
1474.90	9.52	1.40
1474.80	9.76	1.42
1474.70	9.39	1.27
1474.60	9.44	1.32
1474.50	9.25	1.23
1474.40	9.66	1.38
1474.30	9.40	1.34
1474.20	9.44	1.30
1474.10	9.57	1.40
1474.00	9.40	1.30
1473.90	9.31	1.20
1473.80	9.37	1.16
1473.70	9.26	1.16
1473.60	9.31	1.12
1473.50	9.44	1.25
1473.40	9.45	1.31
1473.30	9.40	1.21
1473.20	9.44	1.20
1473.10	9.56	1.35
1473.00	9.37	1.22
1472.89	9.28	1.17
1472.78	9.41	1.20
1472.67	9.41	1.29
1472.56	9.55	1.29
1472.44	9.39	1.18
1472.33	9.23	1.11
1472.22	9.25	1.15
1472.11	9.36	1.13
1472.00	9.34	1.09
1471.90	9.43	1.22
1471.80	9.49	1.29
1471.70	9.36	1.23
1471.60	9.55	1.36
1471.50	9.34	1.14
1471.40	9.22	1.13
1471.30	9.13	1.14
1471.20	9.17	1.14
1471.10	9.17	1.08
1471.00	9.27	1.11
1470.88	9.16	1.10

1470.75	9.37	1.21
1470.63	9.40	1.16
1470.50	9.24	1.10
1470.38	9.17	1.09
1470.25	9.21	1.08
1470.13	9.33	1.13
1470.00	9.15	1.13
1469.86	9.48	1.12
1469.71	9.49	1.08
1469.57	9.42	1.12
1469.43	9.49	1.13
1469.29	9.65	1.24
1469.14	9.64	1.20
1469.00	9.35	1.27
1468.89	9.31	1.21
1468.78	9.22	1.18
1468.56	9.09	1.05
1468.44	9.26	1.15
1468.33	9.34	1.20
1468.22	9.18	1.18
1468.11	9.08	1.13
1468.00	9.18	1.20
1467.90	9.17	1.27
1467.80	9.23	1.24
1467.70	9.20	1.14
1467.60	9.15	1.13
1467.50	9.51	1.26
1467.40	9.20	1.15
1467.30	9.30	1.18
1467.20	9.13	1.10
1467.10	9.21	1.13
1467.00	9.11	1.10
1466.91	9.10	1.14
1466.82	9.16	1.09
1466.73	9.25	1.19
1466.64	9.29	1.13
1466.55	9.39	1.22
1466.45	9.23	1.12
1466.36	9.17	1.06
1466.27	9.32	1.20
1466.18	9.21	1.06
1466.09	9.20	1.13
1466.00	9.27	1.12
1465.89	9.26	1.14
1465.78	9.35	1.20
1465.67	9.33	1.18

1465.56	9.26	1.18
1465.44	9.25	1.17
1465.33	9.45	1.29
1465.22	9.27	1.14
1465.11	9.28	1.13
1465.00	9.45	1.29
1464.89	9.34	1.23
1464.78	9.31	1.22
1464.67	9.46	1.26
1464.56	9.01	1.08
1464.44	9.54	1.27
1464.33	9.45	1.28
1464.22	9.52	1.30
1464.11	9.50	1.31
1464.00	9.39	1.18
1463.88	9.24	1.11
1463.75	9.23	1.13
1463.63	9.12	1.10
1463.50	9.31	1.19
1456.25	9.48	1.29
1456.00	9.54	1.24
1455.75	9.45	1.27
1455.50	9.23	1.20
1455.25	9.31	1.26
1455.00	9.41	1.20
1454.75	9.37	1.12
1454.50	9.26	1.11
1454.25	9.27	1.16
1454.00	9.25	1.15
1453.75	9.28	1.13
1453.50	9.20	1.02
1453.25	9.44	1.22
1453.00	9.49	1.17
1452.75	9.85	1.35
1452.50	10.09	1.53
1452.25	10.08	1.52
1452.00	9.91	1.35
1451.75	9.70	1.45
1451.50	9.49	1.26
1451.25	9.46	1.15
1451.00	9.28	1.07
1450.67	9.45	1.21
1450.33	9.52	1.13
1450.00	9.37	1.20

1449.86	9.31	1.15
1449.71	9.17	1.10
1449.57	9.23	1.11
1449.43	9.20	1.06
1449.29	9.12	1.03
1449.14	9.29	1.23
1449.00	9.36	1.17
1448.75	9.27	1.10
1448.50	9.18	1.06
1448.25	9.22	1.07
1448.00	9.13	1.06
1447.86	9.24	1.11
1447.71	9.20	1.10
1447.57	9.17	1.10
1447.43	9.43	1.17
1447.29	9.36	1.14
1447.14	9.23	1.07
1447.00	9.16	1.07
1446.83	9.13	1.01
1446.67	9.16	1.02
1446.50	9.25	1.14
1446.33	9.19	1.08
1446.17	9.20	1.07
1446.00	9.33	1.17
1445.86	9.16	1.04
1445.71	9.22	1.16
1445.57	9.24	1.11
1445.43	9.33	1.21
1445.29	9.30	1.17
1445.14	9.25	1.08
1445.00	9.40	1.27
1444.86	9.50	1.29

Year	Sr-U (3yr bins)	Sr-U uncertainty (1σ)
1672	9.16	0.08
1670.5	9.10	0.04
1669	9.07	0.04
1667.5	9.06	0.04
1641	9.09	0.05
1639.5	9.02	0.03
1638	9.01	0.04
1636.5	9.06	0.02

1635	8.98	0.03
1633.5	9.03	0.04
1632	9.10	0.04
1630.5	9.07	0.03
1629	9.10	0.04
1627.5	9.09	0.06
1626	9.02	0.08
1624.5	9.01	0.07
1623	9.07	0.04
1621.5	9.08	0.03
1620	9.07	0.04
1618.5	9.07	0.04
1617	9.11	0.03
1615.5	9.11	0.01
1563	9.07	0.03
1561.5	9.10	0.04
1560	9.12	0.03
1558.5	9.13	0.04
1557	9.11	0.06
1555.5	9.03	0.05
1554	9.05	0.04
1552.5	9.20	0.04
1551	9.23	0.05
1549.5	9.11	0.02
1548	9.11	0.02
1546.5	9.10	0.03
1545	9.16	0.04
1543.5	9.16	0.02
1542	9.15	0.02
1540.5	9.16	0.02
1539	9.17	0.02
1537.5	9.21	0.03
1536	9.23	0.03
1534.5	9.21	0.02
1533	9.18	0.03
1531.5	9.18	0.03
1530	9.21	0.03
1528.5	9.22	0.02
1527	9.23	0.02
1525.5	9.21	0.02
1524	9.18	0.03
1522.5	9.15	0.03
1521	9.14	0.03
1519.5	9.15	0.03
1518	9.19	0.03

1516.5	9.15	0.03
1515	9.20	0.04
1513.5	9.18	0.04
1512	9.13	0.04
1510.5	9.15	0.04
1509	9.16	0.03
1507.5	9.20	0.03
1506	9.20	0.03
1504.5	9.15	0.03
1503	9.18	0.04
1501.5	9.22	0.05
1500	9.23	0.04
1498.5	9.14	0.04
1497	9.14	0.04
1495.5	9.11	0.02
1494	9.13	0.03
1492.5	9.08	0.04
1491	9.07	0.03
1489.5	9.10	0.02
1488	9.08	0.02
1486.5	9.05	0.02
1485	9.07	0.02
1483.5	9.10	0.05
1482	9.10	0.07
1480.5	9.15	0.05
1479	9.18	0.06
1477.5	9.19	0.03
1476	9.10	0.06
1474.5	9.20	0.05
1473	9.27	0.03
1471.5	9.22	0.02
1470	9.25	0.05
1468.5	9.24	0.07
1467	9.18	0.03
1465.5	9.18	0.02
1464	9.16	0.03
1455.5	9.25	0.09
1454	9.25	0.06
1452.5	9.32	0.07
1451	9.29	0.07
1449.5	9.25	0.03
1448	9.23	0.02
1446.5	9.23	0.01

Year	Sr-U (10yr bins)	Sr-U uncertainty (1σ)	Reconstructed SST ($^\circ$C, 10yr bins)
1669.5	9.11	0.03	26.8
1633.5	9.07	0.02	27.2
1628.5	9.07	0.03	27.2
1623.5	9.06	0.03	27.3
1618.5	9.09	0.01	27.0
1557.5	9.09	0.02	27.0
1552.5	9.12	0.02	26.6
1547.5	9.15	0.02	26.3
1542.5	9.15	0.01	26.3
1537.5	9.18	0.01	25.9
1532.5	9.20	0.01	25.7
1527.5	9.20	0.01	25.7
1522.5	9.18	0.02	26.0
1517.5	9.16	0.02	26.2
1512.5	9.17	0.02	26.1
1507.5	9.18	0.02	26.0
1502.5	9.19	0.02	25.8
1497.5	9.19	0.02	25.8
1492.5	9.09	0.01	27.0
1487.5	9.06	0.02	27.4
1482.5	9.09	0.02	27.0
1477.5	9.17	0.02	26.1
1472.5	9.23	0.02	25.4
1467.5	9.21	0.02	25.6
1450	9.25	0.02	25.2

Appendix D

Supplementary data for Chapter 5

D.1 Gulf of Maine *Madrepora*

Collection location: 27 ° N, 89 ° W, 600m water depth

Depth along track (μm)	Sr/Ca (mmol/mol, relative uncertainty 0.9%)	U/Ca (μmol/mol, uncertainty 4.7%)
0	11.69	2.80
125	11.26	2.59
250	11.35	2.52
375	11.02	2.37
500	11.22	2.41
625	11.59	2.67
750	11.52	2.40
875	10.90	1.87
1000	10.79	1.79
1125	10.71	1.78
1250	10.82	1.84
1375	10.61	1.68
1500	10.68	1.72
1625	10.90	1.75
1750	10.99	1.88
1875	11.22	2.09
2000	11.15	2.02
2125	10.98	2.04
2250	11.01	2.00
2375	11.04	1.96
2500	10.87	1.85
2625	10.93	1.71
2750	10.80	1.59
2875	10.75	1.41
3000	10.55	1.40
3125	10.48	1.42
3250	10.68	1.68
3375	11.39	2.45

3500	11.59	2.53
3625	11.39	2.59
3750	11.39	2.53
3875	11.36	2.55
4000	11.05	1.94
4125	10.94	1.85
4250	11.07	1.81
4375	11.25	2.15
4500	11.23	2.15
4625	10.79	1.72
4750	10.58	1.48
4875	10.57	1.24

D.2 Sodwana Bay *Porites sp.*

Collection date: May 1994

Collection location: 27.52 ° N, 32.68 ° E, 16 m water depth

Depth along track (mm)	Year	Sr/Ca (mmol/mol, uncertainty 0.04)	U/Ca (µmol/mol, uncertainty 0.02)
0.4	1968.13	9.07	1.11
1.2	1968.04	9.14	1.15
2.0	1967.96	9.13	1.15
2.8	1967.88	9.14	1.14
3.6	1967.79	9.24	1.24
4.4	1967.71	9.32	1.27
5.2	1967.63	9.37	1.28
6.8	1967.46	9.17	1.20
7.6	1967.38	9.32	1.30
8.4	1967.29	9.18	1.19
9.2	1967.21	9.11	1.14
10.0	1967.13	9.07	1.11
10.8	1967.04	9.09	1.09
11.6	1966.96	9.17	1.20
12.4	1966.88	9.17	1.23
13.2	1966.79	9.29	1.30
14.0	1966.71	9.38	1.34
14.8	1966.63	9.42	1.34
15.6	1966.54	9.33	1.26

16.4	1966.46	9.38	1.31
17.2	1966.38	9.21	1.21
18.0	1966.29	9.14	1.16
18.8	1966.21	9.11	1.13
19.6	1966.13	9.05	1.08
20.4	1966.03	9.11	1.14
21.2	1965.93	9.12	1.17
22.0	1965.83	9.15	1.16
22.8	1965.74	9.29	1.24
23.6	1965.64	9.25	1.21
24.4	1965.54	9.32	1.27
25.2	1965.46	9.25	1.22
26.0	1965.39	9.22	1.19
26.8	1965.31	9.18	1.21
27.6	1965.23	9.15	1.14
28.4	1965.16	9.10	1.11
29.2	1965.05	9.17	1.16
30.0	1964.94	9.14	1.14
30.8	1964.84	9.21	1.20
31.6	1964.73	9.26	1.22
32.4	1964.63	9.43	1.37
33.2	1964.54	9.39	1.38
34.0	1964.46	9.22	1.25
34.8	1964.38	9.18	1.17
35.6	1964.29	9.17	1.15
36.4	1964.21	9.13	1.14
37.2	1964.13	9.08	1.10
38.0	1964.04	9.19	1.18
38.8	1963.96	9.19	1.17
39.6	1963.88	9.18	1.19
40.4	1963.79		
41.2	1963.71	9.30	1.27
42.0	1963.63	9.36	1.29
42.8	1963.50	9.23	1.21
43.6	1963.38	9.18	1.16
44.4	1963.25	9.12	1.09
45.2	1963.13	9.09	1.08
46.0	1963.06	9.11	1.14

46.8	1962.99	9.15	1.15
47.6	1962.92	9.24	1.21
48.4	1962.85	9.34	1.29
49.2	1962.78	9.33	1.28
50.0	1962.71	9.29	1.23
50.8	1962.56	9.39	1.31
51.6	1962.42	9.32	1.27
52.4	1962.27	9.17	1.16
53.2	1962.13	9.12	1.12
54.0	1962.03	9.13	1.13
54.8	1961.93	9.16	1.14
55.6	1961.83	9.20	1.17
56.4	1961.73	9.25	1.22
57.2	1961.63	9.36	1.29
58.0	1961.56	9.24	1.26
58.8	1961.50	9.24	1.22
59.6	1961.44	9.23	1.22
60.4	1961.37	9.23	1.22
61.2	1961.31	9.17	1.17
62.0	1961.25	9.21	1.18
62.8	1961.18	9.08	1.08
63.6	1961.12	9.11	1.10

D.3 Green Island (Taiwan) *Porites sp.*

Collection date: June 2013

Collection location: 22.39 ° N, 121.47 ° E

Depth along track (mm)	Year	Sr/Ca (mmol/mol, uncertainty 0.04)	U/Ca (µmol/mol, uncertainty 0.02)
0.5	2013.45	8.88	1.05
1.5	2013.31	8.94	1.02
2.5	2013.18	9.02	1.11
3.5	2013.04	9.13	1.21
4.5	2012.79	8.97	1.09
5.5	2012.54	8.86	1.03
6.5	2012.37	8.88	1.04
7.5	2012.20	8.96	1.10

8.4	2012.04	9.04	1.15
9.2	2011.91	8.97	1.17
10.05	2011.78	8.84	1.11
11	2011.63	8.82	1.02
11.8	2011.51	8.84	1.10
12.6	2011.39	8.99	1.14
13.55	2011.24	9.04	1.19
14.35	2011.13	9.05	1.15
15.05	2010.99	9.00	1.11
15.95	2010.81	8.89	1.12
16.85	2010.63	8.86	1.06
17.75	2010.50	8.95	1.13
18.75	2010.37	8.93	1.09
19.6	2010.26	8.97	1.02
20.4	2010.15	8.95	1.07
21.2	2010.04	9.19	1.19
22.05	2009.92	9.15	1.22
22.9	2009.79	9.07	1.17
23.75	2009.67	8.92	1.15
24.65	2009.54	8.85	1.06
25.4	2009.38	8.91	1.07
26.15	2009.23	8.91	1.07
27.05	2009.04	9.07	1.12
27.85	2008.94	8.94	1.09
28.75	2008.84	8.90	1.14
29.7	2008.72	9.05	1.21
30.5	2008.63	8.88	1.10
31.25	2008.54	8.87	1.02
32.05	2008.44	8.97	1.03
33.05	2008.32	9.04	1.11
33.95	2008.22	9.06	1.12
34.75	2008.12	9.09	1.13
35.6	2007.93	8.97	1.15
36.5	2007.74	8.98	1.21
37.4	2007.54	8.73	1.13
38.1	2007.45	8.80	1.08
39	2007.34	8.91	1.12
39.95	2007.23	8.96	1.07

40.75	2007.13	8.96	1.09
41.5	2007.04	9.03	1.18

D.4 Bahamas *Siderastrea siderea*

Collection date:
1991
Collection location: 25.84 ° N, 78.62 ° W

Sample	Sr/Ca (mmol/mol)	U/Ca (µmol/mol)
1	9.154216332	1.117693927
2	9.205547825	1.148743433
3	8.974165871	1.179192292
4	9.223048552	1.138641001
5	9.255773307	1.1192798
6	9.259417444	1.228289802
7	9.270918498	1.170179014
8	8.902508255	1.02338386
9	8.965663467	0.999904821
10	9.227587797	1.160132011
11	8.858188193	0.892428618
12	8.923879809	0.832196744
13	8.731755942	0.821261626
14	9.023785775	0.876204835
15	8.722064047	0.800947698
16	8.774824357	0.716222684
17	8.822619699	0.810698151
18	8.820295103	0.853056797
19	8.630418226	0.624633037
20	8.468237515	0.640968801
21	8.632261337	0.688131528
22	8.693421669	0.632068806
23	8.798851425	0.737635492
24	8.965317977	0.807523585
25	8.963815053	0.806416372

26	8.484204445	0.646814142
27	8.807385257	0.779286352
28	8.532183805	0.66028954
29	8.805844833	0.667734175
30	8.54229156	0.577583203
31	8.583764939	0.576445698
32	8.517566145	0.539823847
33	8.577288181	0.664694445
34	8.586028293	1.872856447
35	8.230124954	0.461612812
36	8.450707916	0.560921625
37	8.296833585	0.400147742
38	8.38434886	0.490282639
39	8.184005141	0.435606985
40	8.268138119	0.506515965
41	8.53012901	0.69856866
42	8.679908614	0.988710282
43	9.033074432	1.477683266
44	8.389000091	0.653476036
45	8.482690889	0.560531257
46	8.513956291	1.761924174
47	8.770168332	0.910661581
48	8.440504202	0.557046313
49	8.507689477	0.733476186
50	8.706976426	0.646244709
51	8.621817567	0.743732753
52	9.028636022	1.256769387
53	8.817055563	0.768805749
54	8.507175589	0.719871933
55	8.981521362	1.111029512
56	9.015600217	1.327753172
57	8.947593999	1.054256117
58	9.233056925	2.826680968
59	8.620239896	0.928099527
60	8.670229819	0.761216166
61	8.959089718	0.902988433
62	8.653578871	0.999658211
63	9.214371873	1.589311538

64	9.178927154	1.340592033